THE EFFECT OF ACTIVATED CARBON ON THE ORGANIC AND ELEMENTAL COMPOSITION OF PLANT TISSUE CULTURE MEDIUM

A Dissertation Submitted by

Stephen C. Van Winkle

B.S. Forest Products, Virginia Tech
M.S. Wood Science and Forest Products, Virginia Tech

in partial fulfillment of the requirements of the
Institute of Paper Science and Technology
for the degree of Doctor of Philosophy
Atlanta, Georgia

May, 2000

Advisor:

Gerald S. Pullman, Ph.D., Professor, IPST

Research Committee Members:

Frederick S. Baker, Ph.D., Research Associate, Westvaco Corporation

Jeffrey F.D. Dean, Ph.D., Assistant Professor, Warnell School of Forestry, University of Georgia

Peter H. Promm, Ph.D., Associate Professor, IPST

ABSTRACT

This research was motivated by differences in plant tissue culture success when using growth media with different activated carbons (non-acid washed vs. tissue culture grades). The primary research objective was to correlate the physical or chemical character of activated carbon with its impact on the elemental and hormonal composition of tissue culture medium, and hence with culture success.

A bioassay (Norway spruce initiation) was developed based on a liquid medium containing activated carbon (0.3 g/L). Activated carbon was characterized using standard techniques. Elemental composition of media was quantified by inductively coupled plasma atomic emission spectroscopy and capillary ion electrophoresis. Hormonal composition was measured using UV spectroscopy and high performance liquid chromatography.

Of the mineral elements present in the growth medium, only copper and zinc were adsorbed onto activated carbon, ca. 95% and 50%, respectively. Extent of adsorption was similar for non-acid washed and tissue culture grades of activated carbon. The elemental composition of the medium was more sensitive to the system pH than to differences in activated carbon character, with marked precipitation of elements in response to increased pH (from 5.8 to 6.5): iron (-33%), manganese (-40%), phosphorus (-15%), and zinc (-28%). Precipitation was reversible. Media formulated with reduced levels of Fe, Mn and P gave reduced success of the bioassay (-20%).

In single-hormone adsorption experiments (constant pH 5.8), 6-benzylaminopurine (BAP) adsorbed to twice the level of 2,4-dichlorophenoxyacetic acid (2,4-D). When both hormones were present, BAP adsorption was similar to its single-solute case, while 2,4-D adsorption was greatly reduced. 2,4-D adsorption varied with pH over the normal tissue culture pH range, explained through solubility and pK_a . Hormone adsorption was linearly correlated to activated carbon surface area (BET) and total pore volume with r^2 values exceeding 0.97. On a per-mass basis, at constant pH, total pore volume accounted for approximately 95% of the hormone adsorption for eight different activated carbons.

The bioassay was more sensitive to different hormone levels than to the observed differences in elemental composition. Therefore, the critical material characteristic when using different tissue culture grades of activated carbon is their relative total pore volumes.

TABLE OF CONTENTS

LIST OF FIGURES

I. INTRODUCTION

In the near future the U.S. pulp and paper industry predicts fierce competition within the North American market from foreign producers. This competition will be driven by the ability of other countries to produce fiber more cheaply. David Luke III, chairman of Westvaco, presented these data at the 1994 TAPPI Biological Sciences Symposium:

Table 1. Comparison of growth yields for the U.S. and Brazil (Luke, 1994).

Country	Loblolly Pine*	Eucalypts (Hdwd)*
BRAZIL	8	7-9
U.S.A.	2-3	(0.5-1.1)

*numbers given in dry tons wood growth per acre per year.

In long fiber production (loblolly pine), Brazil was able to produce three to four times what the U.S. produced per acre. For short fiber production (eucalypts and hardwoods), the situation was worse, with Brazil producing up to eighteen times what might be produced per U.S. acre. Countries such as New Zealand, Australia, and others in Asia, South America, Central America and Africa also have favorable growing conditions, which could yield growth rates similar to those reported for Brazil. Cottonwood plantations, a promising development in the U.S., have achieved yields of 7.6 dry tons per acre per year on select sites.

As a result of projected wood fiber scarcity and the decline in land dedicated to forests in the U.S., IPST member companies have singled out improvement in growth rates of commercially important species as their top priority. The general strategy will be the improvement of growth performance coupled with mass replication of superior genotypes. The improvement in growth performance will be achieved using classical plant breeding techniques coupled with newer technologies, such as gene splicing. Additional research will be directed towards producing trees that are more readily pulped.

The most promising technique for replicating a superior genotype is tissue culture. This technique offers the opportunity to replicate a single genotype *ad infinitum*. Tissue

culture eliminates much of the random variability inherent in sexual reproduction, though somaclonal variation in older subcultures has been observed (George, Sherrington 1984). The advent of somatic embryogenesis has significantly changed commercial propagation practices. However, it is an emerging technology with an uneven success record when applied to species important to the pulp and paper industry. Efforts to apply the technique to loblolly pine have been hampered by low success rates in inducing the somatic culture from the zygotic embryo explant. Additionally, immature embryos have been required, which limits initiation experiments to a few weeks per year.

Successful tissue culture media have been developed through largely empirical means, reflecting a lack of knowledge about the specific functions and activities of the individual medium components. Most media are “tailored” to a particular species. One common component of successful media is activated carbon (AC). Little is known for certain about the mechanism of its beneficial role. It has been well established that activated carbon is a superior adsorbent in other applications, for example gas-mask filters and waste water treatment: it is reasonable to expect that the beneficial effect of activated carbon in tissue culture is derived from this sorptive function.

Though a number of articles have been published concerning activated carbon in tissue culture media, much of this work has been driven by the study of a single medium component or single class of compounds. Thus, individual growth regulators have been monitored (Ebert, Taylor, 1990; Fridborg, Ericksson, 1975; Zaghmout, Torello, 1988; Nissen, Sutter, 1990; Johansson et al., 1982). Additionally, it has been suggested that AC sorbs inhibitory metabolic by-products of growth, such as ethylene and phenolic compounds (Menzuali-Sodi et al., 1993; Fridborg et al., 1978; Horner et al., 1977). The possibility that AC might be adsorbing carbohydrates has been dismissed by most researchers, based on articles by Horner et al. (1977) and Weatherhead et al. (1979). However, it has been shown that AC adsorbs the toxic sucrose breakdown component, hydroxymethyl furfural, which is produced upon autoclaving (Weatherhead et al., 1978). The adsorption of mineral nutrients has been suggested (Weatherhead et al., 1978, 1979), and the release of unidentified substances has been speculated (Johansson et al., 1990).

From the diverse range of those previous results, it may be deduced that the effect of adding activated carbon to the medium is multi-faceted. Clearly, more work is needed to develop an adequate understanding of the role of activated carbon in tissue culture media.

Activated carbon-related differences in success have been observed at IPST in experiments with two different tissue culture systems, Douglas-fir and Norway spruce. Variability was related to carbon type, as well as to different production lots of the same type. Haberle-bors (1980) also reported differences in success related to activated carbon type. This variability poses a dilemma for the tissue culturist who must periodically replenish supplies of activated carbon.

This study is an investigation into the impact of different activated carbons on the chemical composition of the medium and whether these differences are significant to culture success.

II. LITERATURE REVIEW

A. Tissue Culture

Definition

Tissue Culture is a collective term referring to all types of *in vitro* plant cultures. The tissue may originate from any plant organ and be differentiated or it may be undifferentiated callus. *Culture* refers to maintenance of metabolizing cells in artificial media, which may be solid, semi-solid, or liquid. Callus cultures arise from disorganized growth, often preceded by de-differentiation of excised plant tissue or organs. Suspension cultures are cultures sustained in an agitated liquid medium. For our purposes, the goal of tissue culture is plant propagation, i.e., growth and division of an embryogenic tissue, development and growth of mature embryos, and germination and production of plantlets having satisfactory vigor. An overview of the process is presented in Figure 2.1.

Tissue culture, in theory, allows the unlimited replication of a particular genotype. This genotype may be naturally occurring or it may be a genotype produced through genetic engineering. Tissue culture offers the prospect of growing an entire forest from somatic embryos genetically engineered for a desired trait, such as a lower degree of lignification (Cairney et al., 1994).

For the purposes of this study, tissue culture of conifers concerns producing viable plantlets after first inducing the formation of somatic embryos. This is a multi-stage process that incorporates different media for the different stages. The first stage involves the *induction* or *initiation* of embryogenic tissue from the explant. This non-pigmented tissue, referred to as embryo-suspensor mass or ESM, has a clear, crystalline appearance and is composed of embryo and suspensor cells. The ESM is collected and transferred to a medium specially formulated to provide maintenance nutrients and also promote multiplication (cell division). A portion of the ESM may be transferred to fresh maintenance media at regular intervals. In this way, a living culture may be sustained over an indefinite period. During this phase of the culture process the embryos are minimally differentiated. Tissue is next transferred to maturation media in one or more stages, where the embryos mature to the point that they resemble somewhat immature

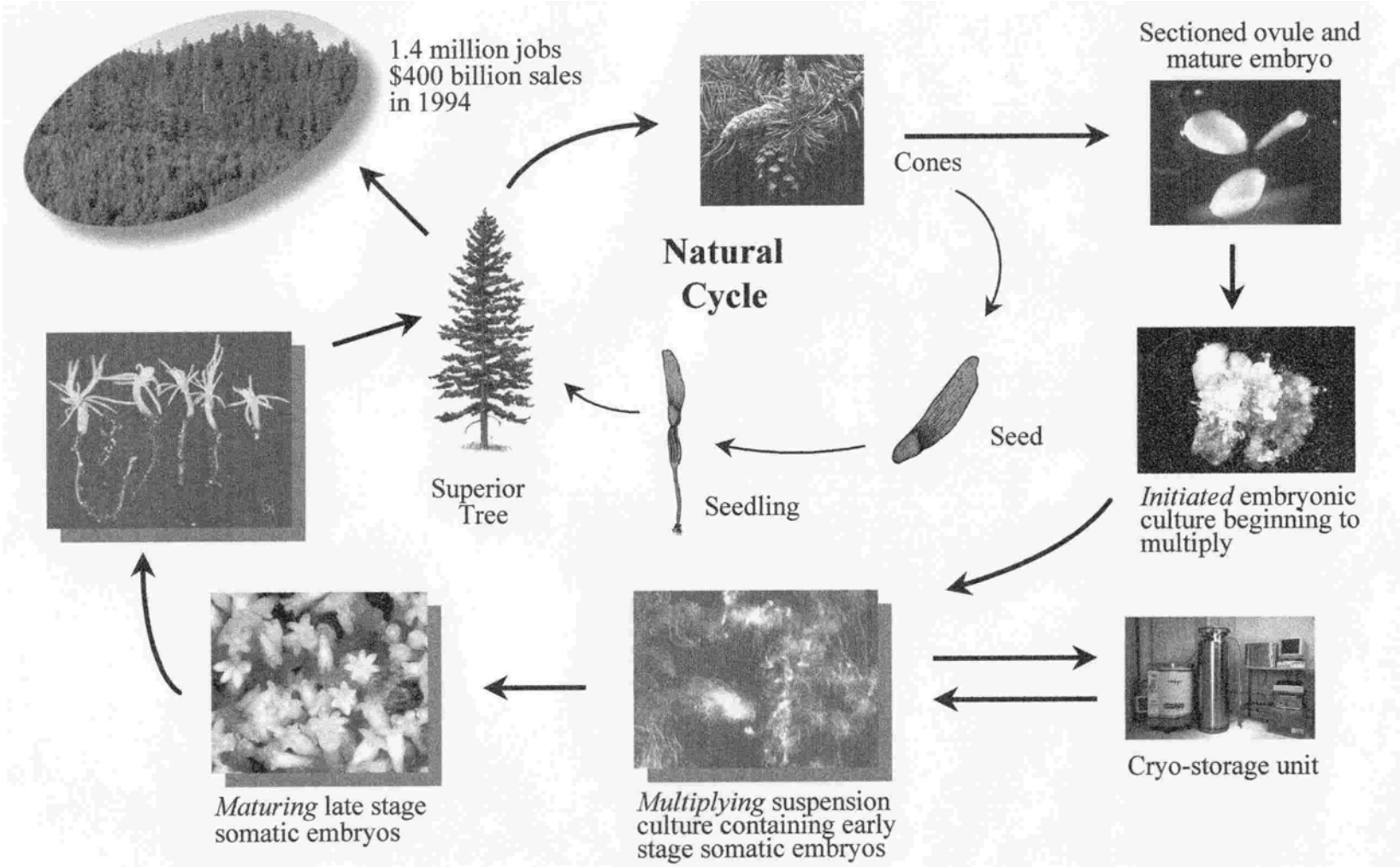

Figure 2.1. Overview of conifer propagation by tissue culture. Schematic is a composite of Norway spruce (sectioned ovule and initiation stages) and other conifer images (Xiu, 1997, with modifications).

natural embryos. Germination of these may then be induced in one or more additional stages. The germinants may then be grown on media until they are viable plantlets. The entire process may require up to six months.

Development

The initial conception by Schleiden and Scwann in the 1830's, that the cell is capable of autonomy and is totipotent (containing all the necessary means to replicate an entire plant), is cited by Gautheret as the birth of the theory that 100 years later led to successful tissue culture of plant callus (Gautheret, 1983). Many researchers contributed to the development of techniques and media that would ultimately allow successful propagation by tissue culture. However, current practice depends heavily upon the discovery and subsequent identification of growth hormones. The auxins control cell growth and elongation, while the cytokinins are associated with cell division and organization (Bonga, 1982; George, Sherington, 1984; Lesham, 1973; Roberts et al., 1988). The first of these to be identified was indoleacetic acid, an auxin, by Wendt (1926). Kinetin a cytokinin, was first identified by Skoog and co-workers in 1956.

Other regulatory plant growth substances have subsequently been identified, including gibberellins, abscisic acid, ethylene, and jasmonic acid derivatives. Gibberellins are thought to stimulate the synthesis of specific enzymes that influence the availability of endogenous auxin. Abscisic acid has been shown to inhibit callus formation and to promote morphogenesis. Ethylene is an endogenous compound that may regulate physiological activity in the plant, particularly callus production, the ripening of fruit or senescence (George, Sherington, 1984). Synthetic analogs of these natural substances have also been formulated. The broader term "growth regulator" is used to distinguish these from the naturally occurring hormones. Naphthalene acetic acid (NAA) and 2,4-dichlorophenoxyacetic acid (2,4-D) are examples of synthetic auxins, while benzylaminopurine (BAP) is an example of a synthetic cytokinin.

Zygotic and Somatic Embryo Development

Somatic embryos may be developed from different vegetative tissues. The term *somatic* is an adjective meaning “of the body”, but is broadly applied to dividing (living) tissue *Embryogenesis* refers to the generation of embryos. Somatic embryogenesis may then be interpreted as the generation of embryos from plant organs or tissue. In common vernacular, somatic embryogenesis is the “cloning” of embryos and refers to dividing tissue. After the initial stages, somatic embryos develop through a sequence of stages that resemble those observed for developing zygotic embryos (embryos derived from sexual reproduction).

In theory, embryogenic tissue may be developed from any plant explant. An explant may be a mature plant organ, such as a root, stem, leaf or bud, or it may be a cell or group of cells. In practice, tissues from the cotyledon, the meristem, or the zygotic embryo are preferred. In the cases of Douglas-fir and loblolly pine, success at IPST has been achieved using the whole, immature embryo.

Zygotic embryo development may be broken down into stages, each characterized by a recognizably different morphology. Researchers at IPST have characterized a series of nine stages for loblolly pine (Pullman, Webb 1994). This work was performed by carefully selecting and sectioning seeds at various stages of development. Similar stages were observed for both Douglas-fir and loblolly pine. The various stages are shown in Figure 2.2.

The initial stage is characterized as having approximately 12 cells total, with a few suspensor cells supporting an indistinct proembryo. The second stage displays the elongation of the suspensor cells, but no radial increase. The developing embryo is still located at the micropylar end of the megagametophyte, but has become distinct and translucent. Stage 3 displays a significantly elongated suspensor which has also increased radially. The elongation of the suspensor coincides with the development of the corrosion cavity and the embryo proper is located towards the chalazal end of the cavity. At this stage the embryo is becoming whitened and opaque. Stage 4 is characterized by the

elongation and expansion of both the suspensor mass and the embryo. The embryo has acquired a characteristic dome shape and is now opaque. Stage 5 resembles stage 4

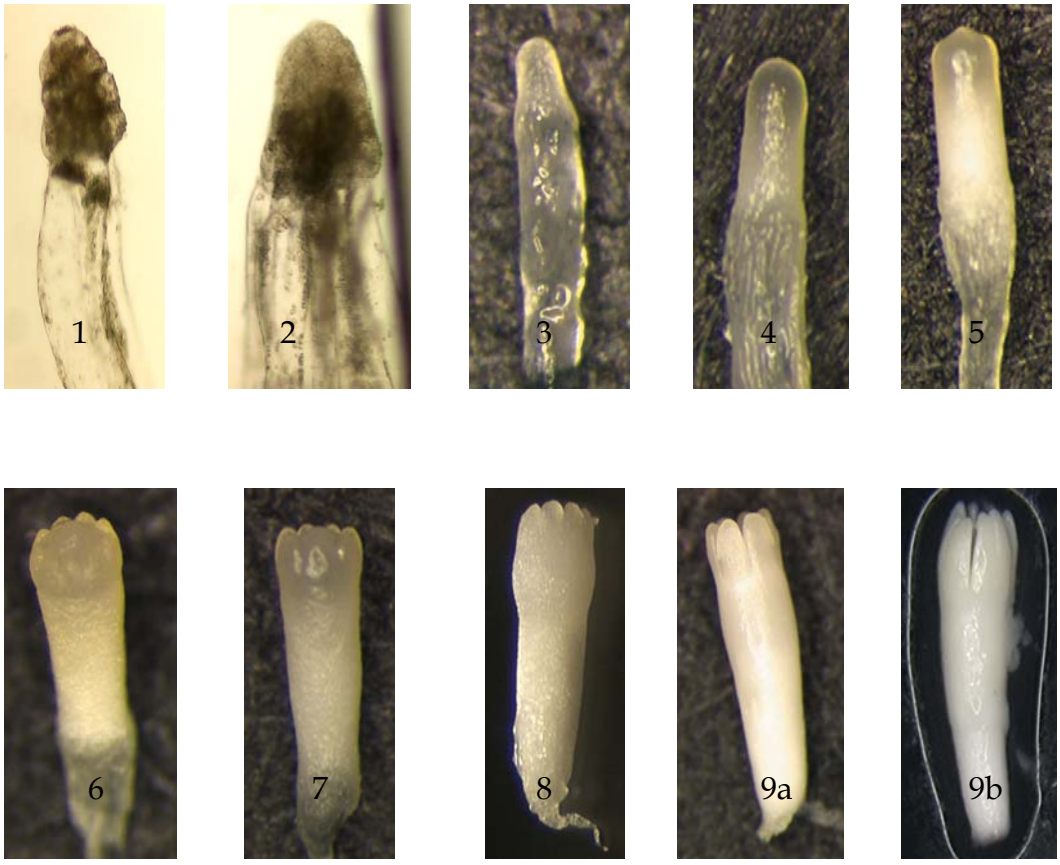

Figure 2.2. Nine stages of embryo development in loblolly pine. Stage 1 is the earliest stage, characterized by sixteen cells in the embryo region and only a few suspensor cells. Stage 9b is the fully mature embryo, suspensor cells not shown. The intermediate stages have been assigned based on characteristic morphological features. Stage 2 features more suspensor cells. Stage 3 is characterized by an increase in opacity due to a significant increase in the number of cells. The embryo develops a characteristic dome shape. Stage 4: more suspensor cells, longer dome, increased opacity. Stage 5: whitening of embryo and tip (apical meristem primordia) on "dome". Stage 6: similar to Stage 5 but with addition of barely discernable cotyledon primordia below apical primordia. Stage 7: More prominent cotyledons. Stage 8: Cotyledons have over-topped the meristem but have not yet fused, suspensor is a translucent thread of cells(tail) to lower right of image. Stage 9a: Cotyledons have over-topped but have not finished developing. (Pullman, Webb 1994).

with the addition of clearly visible apical meristem primordia. Stage 6 follows with the development of barely discernible cotyledon primordia below the apical meristem primordia. Stage 7 is similar to stage 6 except that the cotyledons have elongated but have not yet overtopped the meristem. The cotyledons overtop the meristem in stage 8. In stage 9, the curving cotyledons join at their tips, completely enclosing the meristem. All of this development occurs within the megagametophyte (Figure 2.3).

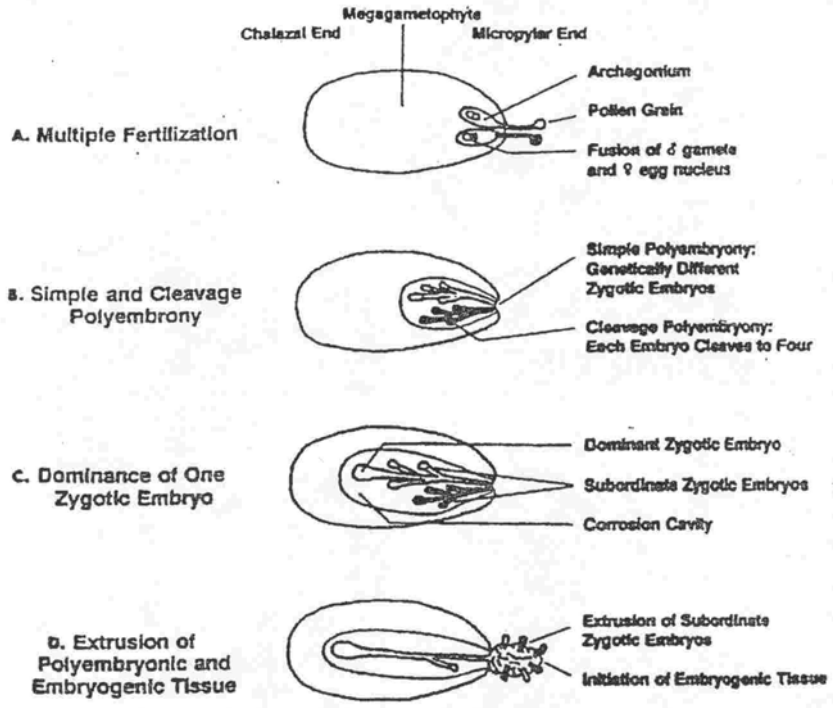

Figure 2.3. Embryo development within the megagametophyte (Becwar, Pullman 1994; reprinted with permission from Kluwer-Plenum). A. Multiple fertilization results when gametophytes from separate pollen grains fuse with separate egg nuclei within the archegonia. B. Multiple and genetically different zygotic embryos develop, simple polyembryony. In addition, each genetically different embryo cleaves to form four individual zygotic embryos, cleavage polyembryony. C. One of the zygotic embryos develops more vigorously becoming the dominant embryo. Elongation of the suspensor cells pushes the embryonal region of the dominant embryo towards the chalazal end of the megagametophyte and a corrosion cavity results. D. Culture of immature megagametophytes at the development stage shown in C results in initiation of embryogenic tissue from extruded zygotic embryos. The growth stage of the zygotic embryo explant has proven to be critical to successful somatic embryogenesis for loblolly pine and Douglas-fir. For Doug-fir, the optimal explant has been found to be the zygotic embryo between stages 4 and 5. This limitation translates to a “window” of opportunity that lasts for about two weeks for any given embryo. For some species, i.e. Norway spruce, somatic embryos have been produced from mature full-term embryos (seeds). Culturing from the mature seed greatly facilitates research, as initiation of somatic embryos from the zygotic embryo may be performed at any time during the year.

Somatic embryos develop from a net-like mass of suspensor cells, with emerging or budding embryos at the nodes. At a later stage, the somatic embryos take on a polar morphology characterized by multiple suspensor cells that support a dome of approximately 100 cells. The suspensor cells are elongated and their numbers have increased in the radial direction. The later stages in development are similar in appearance to zygotic embryos, however, the ninth stage has not been obtained for somatic embryos.

Growth Medium Description

The chemical compounds that comprise tissue culture media are typically classified into several different, broad components. These components include water, a solid or semi-solid support, micronutrients, vitamins, macronutrients, a nutrient carbon source, growth regulators or hormones, amino acids, sorbents, and osmoticants. Each stage in the development of the embryo may require a different mix of these basic ingredients.

Macronutrients are those required in relatively large concentrations, up to several hundred mg/L (ppm). In the case of the carbohydrate, which is the nutrient carbon source, the concentration commonly exceeds 10 g/L. The macronutrients include nitrogen, phosphorus, potassium, calcium, magnesium, carbon (carbohydrate), and sulfur. These nutrients are added in salt form, typically sulfates and chlorides. Nitrogen may be supplied in the forms of nitrate and ammonium salts, as well as amino acids. The balance between nitrate and ammonium ions has a strong pH dependence, which isn't an issue for systems that rely solely on amino acids for their nitrogen source (Verhagen, Wann, 1989).

Micronutrients are required in smaller concentrations, less than approximately 100 μg/L (0.1 ppm). These include iron (in chelated form, typically), and salts of the following: manganese, zinc, boron, copper, molybdenum, and chlorine. Other minerals, which are sometimes added to media include nickel, titanium, beryllium, cobalt, and aluminum.

The most commonly used carbohydrate has been sucrose. Other sugars have been tried with varying degrees of success. The type and concentration of carbohydrate may be optimized for a particular application. Success has been reported using maltose for culturing loblolly pine (Pullman et al., 1994). Inositol is another carbohydrate frequently added to media. However, it is not metabolized; it functions as an osmoticant.

The plant growth regulators that will be considered in this study are cytokinin and auxin. These two regulators are added to initiation media and are critical to achieve high success rates. Chemical structures for common growth regulators are shown in Figure 2.4.

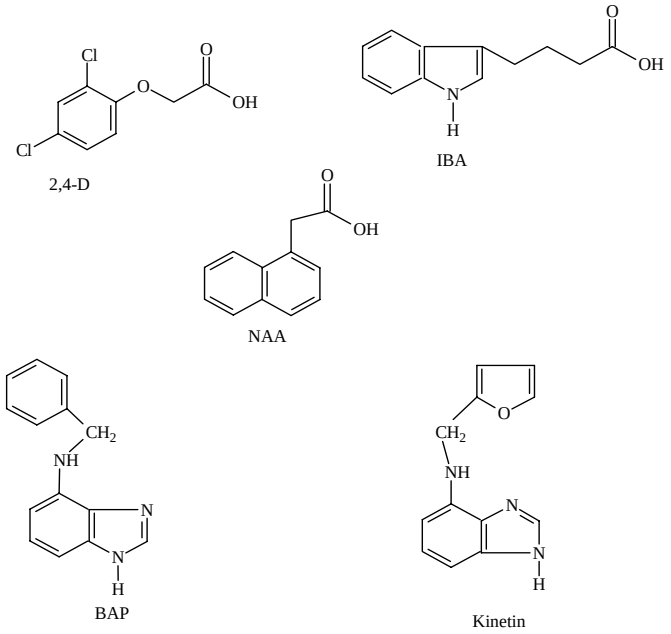

Figure 2.4. Chemical structures for common auxins (2,4 dichlorophenoxyacetic acid, 3-indolebutyric acid, 1-naphthylacetice acid) and cytokinins (6-benzylaminopurine, kinetin)

The interaction, or relative concentration, of auxin and cytokinin has been shown to be critical to growth morphology and rate (George, Sherington 1984). This characterization is presented in Table 2.1.

Table 2.1. Hormone interaction and growth characteristics (after George, Sherington 1984).

Relative Concentration		Resulting growth morphology
Auxin	**Cytokinin**	
High	Low	Root formation
Intermediate	Intermediate	Embryogenesis, callus
Low	High	Shoot formation, proliferation

Support to growing tissue has most commonly been provided by gelling agents such as agar, a polysaccharide from seaweed, and Gelrite. Other means of support have included paper, glass beads, and synthetic fiber matting.

There have been numerous medium compositions reported in the literature. A selection of these has been cataloged (George et al., 1987). Many of these formulations are variations on a medium developed by Murishige and Skoog, who quantified the mineral content in tobacco explants and then formulated a nutrient medium with those measured levels. This basic mineral mix has been augmented with the other ingredients already noted.

Tissue Culture Technique

Successful initiation and plantlet development from somatic embryos by the technique of tissue culture requires that the developing culture be aseptically transferred to fresh media of varying composition at particular growth stages.

The method to be summarized, reported in the patent of Gupta and Pullman (1991) used the basal medium for loblolly pine culture given in Table 2.2. This medium was adapted from the P6 medium developed by Teasdale, et al. (1986). This basal medium composition was modified in various ways for the different stages in the culture process.

Table 2.2. Basal medium for loblolly pine (Pullman, Gupta 1991).

Pinus taeda Basal Medium (Modified ½ P6 Basal Salts*)

Constituent	Concentration, mg/L	Constituent	Conc., mg/L
NH_4NO_3	603.8	Sucrose	30,000
KNO_3	909.9	myo-Inositol	1,000
KH_2PO_4	136.1	Casamino acids	500.0
$Ca(NO_3)_2 * 4H_2O$	236.2	L-Glutamine	1,000
$MgSO_4 * 7H_2O$	246.5	Thiamine HCl	1.0
$Mg(NO_3)_2 * 6H_2O$	256.5	Pyridoxine HCl	0.5
$MgCl_2 * 6H_2O$	50.0	Nicotinic Acid	0.5
		Glycine	2.00
KI	4.15	Agar+	6,000
H_3BO_3	15.5		
$MnSO_4 * H_2O$	10.5	pH	5.7
$ZnSO_4 * 7H_2O$	14.4		
$Na_2MoO_4 * 2H_2O$	0.125		
$CuSO_4 * 5H_2O$	0.125		
$CoCl_2 * 6H_2O$	0.125		
$FeSO_4 * 7H_2O$	6.95		
Na_2EDTA	9.33		

*According to Teasedale, Dawson and Woolhouse (1986) as modified

+ Used if a solid medium is desired

The induction or initiation medium received the fresh explant; in this case the whole ovule containing immature embryos. This medium featured relatively high levels of cytokinin and auxin (Table 2.3).

Table 2.3. Media for different stages (Pullman, Gupta 1991).

Composition of Media for Different Stage Treatments

BM_1 – Induction Medium
BM + 2,4-D (50μm) + KIN (20μm) + BAP (20μm)

BM_2 – Maintenance and Multiplication Medium
BM + 2,4-D (5μm) + KIN (2μm) + BAP (2μm)

BM_3 – Late Proembryo Development Medium
BM_2 + 9000 mg/L myo-inositol

BM_4 – Embryo Development Medium
BM + 4.0 to 8.0 mg/L abscisic acid

BM5 – Germination Medium
BM modified by reducing sucrose to 20,000 mg/L myo-inositol to 100.0 mg/L, glutamine to 200.0 mg/L, and casamino acids to 0.0 mg/L

The initiation phase required about 45 days, after which the embryo-suspensor mass was transferred to maintenance medium having greatly reduced levels of each growth

regulator. The late proembryo development medium was similar to the maintenance medium, but included an elevated osmoticant level. The major patent claim was related to the embryo development medium which featured a high level of abscisic acid in combination with activated carbon. The germination medium featured reduced concentrations of sucrose and inositol. It was found that both multiplication and development could be accelerated by using liquid medium. The process required about 90 days prior to germination, which required an additional 6-8 weeks.

B. Activated Carbon

Definition

Active refers to adsorption activity: a carbon that is *activated* has a high capacity for adsorption. The carbon may be produced from practically any source, including vegetable, animal, petroleum, coal, and peat.

Manufacture

Activated carbon (AC) is manufactured in different ways. The physical and chemical properties of AC depend on the source material and the manufacturing process.

Much of the variability in activated carbons is due to the variety of source materials, which differ profoundly in their structure and chemical composition. Coconut shell, a popular source for the production of AC for gas phase applications, produces a uniformly porous material with a high percentage of micropores. Carbons produced from hardwood are noted for their greater variability in pore size with a larger percentage of mesopores (Mattson, Mark, 1971). Bone char is another popular source of AC. The presence of calcium and phosphate and a relatively low percentage of carbon (10%) give this material unique sorptive properties, due in part to its coarse pore structure and low percentage of carbon (Bonga, 1982). Peat, petroleum and coal have become important sources for AC production, and they too produce AC of unique character. Each of these source materials is highly variable. Therefore, given the same manufacturing technique and the same type of source material there still may be variable performance in the resulting AC (Soffel, 1978).

Various methods have been used to produce activated carbon. These may be classified into two categories: thermal activation which relies on high temperatures (700+ ^{o}C) and employs steam or CO_2; and, chemical systems which dehydrate the feed stock. Chemical activation with phosphoric acid is used to digest sawdust, wood shavings, or peat (Mattson, Mark, 1971; Houghton, Wildman, 1971). Each method has advantages and disadvantages. The chemical techniques give very high yield of an extremely adsorptive material, but the resultant AC requires further treatment to develop sufficient mechanical strength for certain applications (Baker, 1992).

The process variables that impact the physical and chemical properties of the product are the composition of the activation atmosphere, the residence time and temperature of the activation process, and the chemical composition of the atmosphere during cooling (Mattson, Mark, 1971; Houghton, Wildman, 1971). In the case of "soft" coals and certain other feed materials, a pulverizing stage is necessary to obtain desired material properties. With increased burn-off, porosity increases, particularly in the microporous region (Figure 2.5).

A two-stage process may be employed. Typically these procedures are performed in a controlled-atmosphere furnace with a fixed bed. The activation stage may also be performed using a fluidized bed: the result is a more uniform activation. The initial stage is a carbonization step which takes place in an oxygen-starved atmosphere (pyrolysis). This stage is followed by selective oxidation with steam, air, or flue gas. Depending on the raw material and the desired product, the initial stage may be completed at temperatures in the range of 230-700^{o}C. The initial stage removes volatiles and inorganics. The subsequent stage may take place with temperatures ranging from 700-1000^{o}C in the presence of steam, or occasionally, air. The second stage may also be performed at temperatures that exceed 1000^{o}C under a CO_2 atmosphere, resulting in a minimum of surface oxidation and a maximum surface area (Mattson, Mark, 1971; Houghton, Wildman, 1971).

The atmosphere during cooling plays a key role in determining surface properties. This aspect will be discussed with regard to chemical character in the next section.

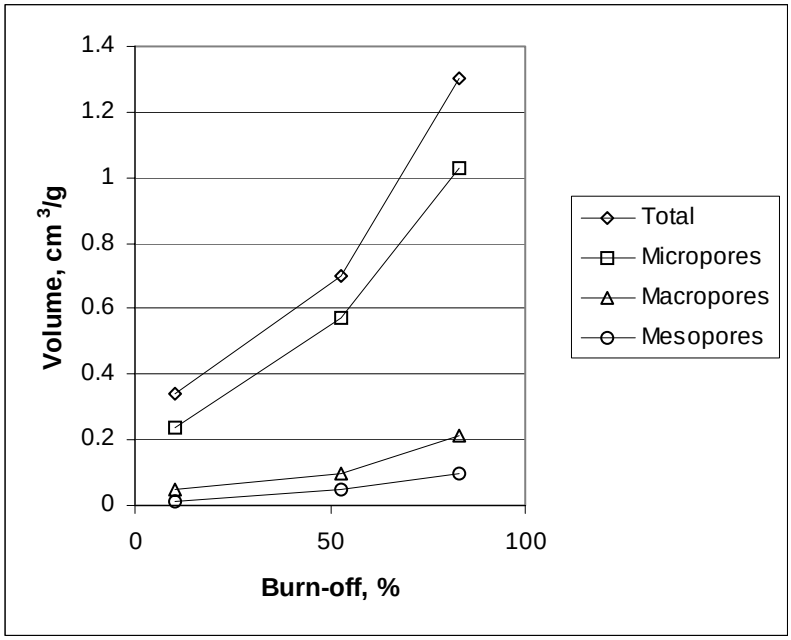

Figure 2.5. Evolution of pore volume with carbon burn-off for a carbon series (adapted from Rodriguez-Reinoso, Linares-Solano, 1989). As the percentage of burn-off increases, the micropore percentage of the total pore volume increases.

Chemical and Physical Character of Activated Carbon

The principal properties for comparison of various activated carbons are the pore-size distribution, surface area, chemical reactivity (surface chemistry), density, and ash content (Soffel, 1978). The determination of porosity and surface area will be presented in a subsequent section.

The structure of activated carbon has been compared to turbostratic graphite, depicted in Figure 2.6, a material that results from the grinding of graphite to particle sizes of less than 0.1μm . Because the graphite crystallites have been reduced in size, three dimensional order typical of natural graphite is not present (Seeley, 1978). The parallel graphene layers are separated by a greater distance in the case of the turbostratic material, 0.344 nm vs. 0.335 nm (Mattson, Mark, 1971). Thus, van der Waals forces between the

layers are expected to be much weaker in the turbostratic material. As with turbostratic graphite, activated carbons are believed to have a higher percentage of broken ring structures than are present in natural graphite, creating holes in the lattice and binding sites for heteroatoms.

Perhaps a more accurate description results from considering materials that either yield or do not yield graphite upon high temperature pyrolysis (3000^{o}C for 2 hours under helium). Carbons that are graphitizable are referred to as “soft”. Those materials that do not yield graphite are known as “hard” carbons and possess a network of crosslinks which effectively prevent graphene layers from crystallizing. Activated carbon would be similar in structure to the nongraphitizing material (Baker et al., 1992).

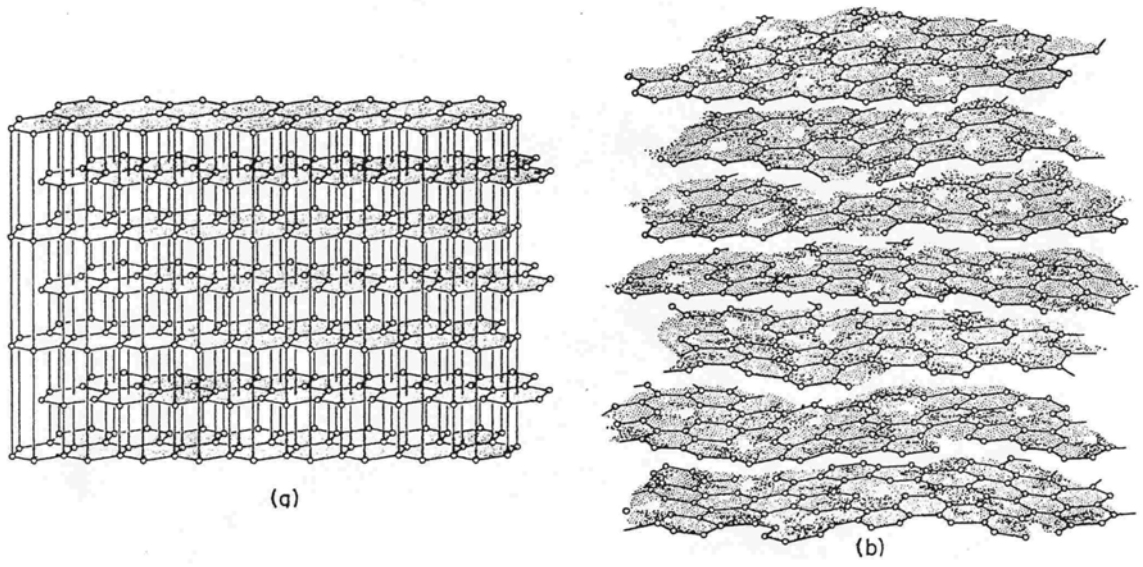

Figure 2.6. Schematic comparison of graphite lattice (a) to turbostratic structure (b) (Bokros 1969, reprinted with permission from Marcel Decker, Inc.). Turbostratic structure results from mechanically stressing graphite. The separation between the graphene layers increases, order is disrupted, and “holes” in the lattice appear.

For AC with high surface area (1000 m^2/g), the microporosity accounts for the largest percentage of the measured surface. Macro- and mesopores may assume greater

importance than suggested by their contribution to surface area in that they may regulate access to a significant portion of the microporosity. Accessibility to the microporosity varies with interconnectedness of pores and tortuosity of the pore network. The activated carbon grain is highly irregular and has been characterized as a fractal surface: for certain activated carbons much of the microporosity may occur in readily accessible regions.

For gas phase applications, AC with average pore widths less than 3 nm is preferred. The diffusion-limited, liquid-phase applications require larger pores (Mattson, Mark, 1971). Surface area may vary from 300 m^2/g to 2500 m^2/g (BET), most commonly falling in the range between 800 and 1200 m^2/g for commercial applications. The sorption behavior is largely determined by the percentage of microporosity. In micropores, the overlap of van der Waals fields from opposing pore surfaces leads to an enhanced adsorption potential, up to 2 to 3 times that of a flat surface (Rodriguez-Reinoso, Linares-Solano, 1989).

The surface chemistry of AC is dominated by oxygen functionality. The affinity of AC for oxygen is quite high, as chemisorption has been demonstrated at temperatures below -40^oC: the resultant oxides could only be removed as CO and CO_2 at temperatures greater than 200^oC (Mattson, Mark, 1971).

Oxygen is preferentially sorbed at edge carbons that are free of the crystalline regions. Many compounds are oxidized by activated carbon and this has been attributed to the presence of oxide ions that are formed when oxygen is irreversibly adsorbed on the carbon surface (Zawadzki, 1989). It has been hypothesized that oxide ions result from π-electron transfer from the aromatic system to the oxygen molecule (Che, Tench, 1983).

It is believed that many different oxygen-based acidic functionalities are present on the surface of activated carbon. These include carboxyl groups, phenolic hydroxyls, quinone-type carbonyls, lactones, carboxylic acid anhydrides, ethers, and cyclic peroxides. Not only do these groups impart various levels of acidity, they also influence possible mechanisms for covalent bonding and surface catalysis (Mattson, Mark, 1971; Hougthon,

Wildman, 1971). Basic oxides are believed to be present in the form of chromene and pyrone groups.

The surface chemistry of AC is greatly influenced by the method of manufacture. As a result, careful control during manufacture offers the opportunity to "normalize" the surface reactivity of AC produced from differing feed stocks. Acidic surface character results from activation over the temperature range of 600-800^{o}C in the presence of oxygen. Basic character may be maximized following pretreatment in the range 750-850K, independent of initial oxygen content, if the cooling is performed in an oxygen-free environment. Subsequent uptake of atmospheric oxygen at room temperature imparts a basic surface. These surfaces may be interconverted through reactivation. The manufacturing temperature of transition from acidic to basic surface character is approximately 750^{o}C. The Steenberg nomenclature is often used: *L* carbons are those that have been produced at low temperature and have acidic character, while *H* carbons are those that have been produced at temperatures above 750^{o}C and have basic character (Mattson, Mark, 1971).

In addition to oxygen and hydrogen, inorganic impurities are present in AC and these may be released in liquid systems. The concentration and composition of the impurities will vary with the source material. Activated carbon for liquid-phase applications may have total ash content of 18% or more, though 10% or less is probably more representative (Soffel, 1978).

Effect of Acid Washing

The activated carbons that are favored for tissue culture applications are marketed as *acid-washed*. Hydrochloric acid is commonly used for this purpose, though the nature of the anion does not influence chemisorption of acid (Leon y Leon et al., 1994). No exact protocol for acid washing could be obtained from the suppliers, but acid washing probably consists of an acidic aqueous treatment, possibly heated, followed by washing with water until no acid is detectable in the rinse (Boehm, 1994).

It is well established that AC contains Bronsted acid and base sites, as well as Lewis base sites. Both oxygen-containing and oxygen-free basic sites are believed to exist on the surface. Therefore, acids and bases will be adsorbed on AC with an accompanying change in AC chemical or physical properties. The hydrochlorides of the basic surface oxides are unstable *in vacuo* and towards hydrolysis. It may be expected that acid washing, followed by water rinsing, either neutralizes or removes basic surface oxides. Chemisorbed HCl may be washed from the surface with water (Leon y Leon et al., 1994).

C. Effects of Activated Carbon on Tissue Culture Medium

Adsorption

The role of activated carbon as an adsorbent has been well established (adsorption theory will be presented in the theory section). Industrially, AC is an increasingly important material for filtering effluent streams and gaseous emissions. The list of potential sorbates present in plant tissue culture media includes: contaminants in agar (Kohlenbach, Wernicke, 1978), mineral nutrients (Weatherhead et al., 1978, 1979), metabolic by-products (Fridborg et al. 1978), ethylene (Menzuali-Sodi, et al. 1993), growth inhibitors and regulators added to the medium (Ebert et al., 1993; Nissen, Sutter, 1990; Gupta, Pullman, 1991), growth hormones (regulators produced by the plant), and other unidentified compounds (Johansson et al., 1990).

pH

It is normal for the pH of the medium to drift. Typically, during tissue culture experiments, pH is adjusted prior to autoclaving to between 5.2 and 5.8. Tissue culture media are poorly buffered and in the presence of developing tissue the pH may go up or down. Figure 2.7 depicts the pH profile of a liquid maintenance medium (no activated carbon present) containing loblolly pine embryogenic tissue. The pH dropped nearly one unit over a period of twelve days, but subsequently increased several tenths of a unit over the ensuing twelve day period. Several different mechanisms for this drift have been suggested, including the excretion of substances by the growing embryo or plantlet, absorption of atmospheric CO_2, and ion transport across the membrane of the tissue

(Bonga, 1982). Drifting pH has been observed for media in the absence of the explant as well (Owen et al., 1991).

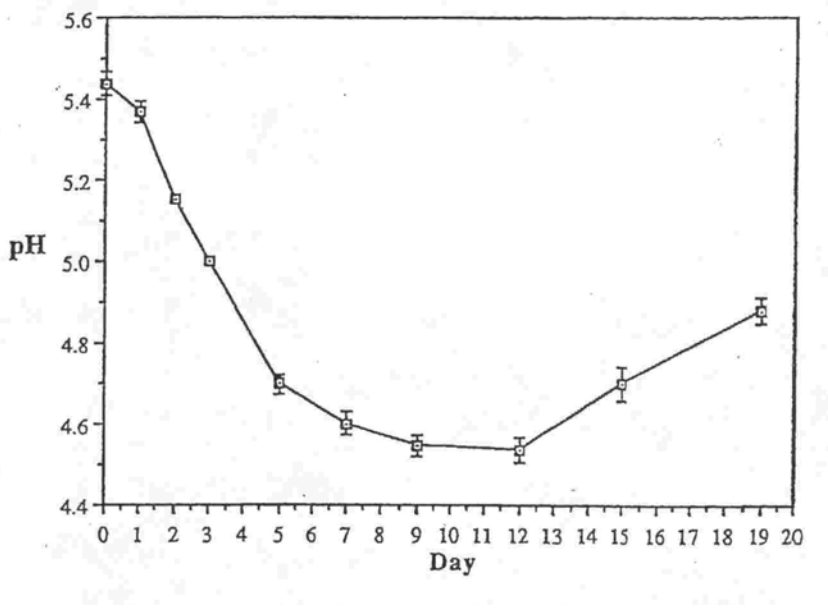

Figure 2.7. A growing culture influences the pH of growth medium. Data are shown for liquid loblolly pine suspension culture (multiplication media), no activated charcoal present.

The effect of medium pH is species-dependent. Successful embryogenesis has been achieved at low pH (between 4 and 4.5) for carrot (Smith, Krikorkian 1992) and daylily (Smith, Krikorkian 1991). However, for soybean, pH of 5.0 was low enough to completely inhibit organogenesis (Lazzeri et al. 1987). Interactive effects between light, auxin, and pH have been noted by Williams et al. (1985) in rooting experiments.

A trend towards increased pH when AC is present has been noted (Johansson et al. 1982). This is in agreement with data collected at IPST for media containing acid-washed AC in the absence of growing tissue (Figure 2.8). The pH of the medium had increased by almost 0.5 pH units in one hour. After eight hours the pH appeared to be reasonably stable. As stated previously, however, AC may have acidic character depending on how it was manufactured.

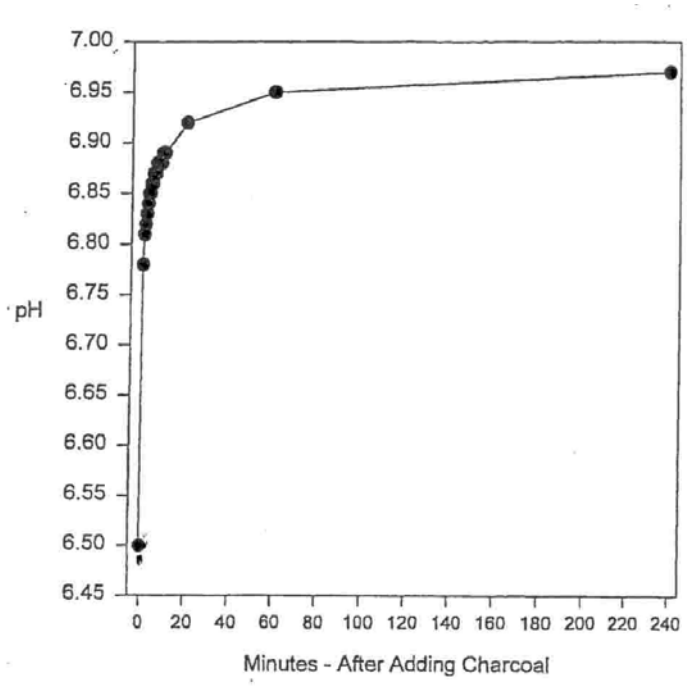

Figure 2.8. The pH of pre-autoclaved medium after adding AC, 2.5 g/L. The addition of activated carbon to a tissue culture medium resulted in an increase in pH. The medium had not been autoclaved. (S. Johnson, previously unpublished results).

Media Darkening

In a short note, Proskauer and Berman (1970) proposed that darkening of the medium may be one benefit of including AC. The darkness of the medium would seem to be irrelevant as the presence of complete nutrients produces pigment-free callus or embryo suspensor mass (esm): growth is not dependent on light being present. In fact, many stages in the example tissue culture process were conducted in the dark (Pullman, Gupta 1991). Other researchers (Nissen, Sutter 1970) found that the auxins IAA and IBA were prone to breakdown when exposed to near UV light (300nm). It is not known if AC impacts this breakdown. Surface catalysis may also impact medium composition.

Release of Substances from Activated Carbon

A comparison of adsorbents revealed AC to be superior to polyvinylpolypyrrolidone (PVPP) for culturing anthers. Further tests revealed that AC was possibly releasing Fe-EDTA or some other trace element not assayed for, but that no organics were being released (Johannson 1983). In this same study it was found that potassium, nitrate, nitrite,

sulfate, and sodium ions were being released to the medium. An unidentified substance was being released by the gelling agent, Gelrite.

Data collected at IPST suggest that nickel and other ions may be released from AC, while copper and zinc are significantly reduced (Table 2.4). It is reasonable to expect that AC will release minerals into the medium as it may have ash percentages exceeding 10%. The level of ash content is expected to vary with AC from different vendors as the source materials may be completely different, i.e. one vendor may supply a petroleum-based product while another supplies a coconut shell carbon.

Table 2.4. Activated carbon affects mineral nutrient composition (Pullman et al. 1995)

	Activated Carbon*			
Element	0 g/L	2.5 g/L	% Change	Significant at 95%
	mg/L:	mg/L:		
K	454	550	21	yes
Ca	404	307	-24	yes
Na	65.7	67.2	2.4	no
Mg	50.0	49.3	-0.44	no
Mn	6.91	6.43	-6.9	yes
Fe	2.05	2.02	-1.5	no
Zn	1.53	0.78	-49	yes
	μg/L:	μg/L:		
B	361	379	5.0	no
Co	51.4	101	97	no
Cu	36.9	3.62	-90	yes
Ni	1.67	135	8900	yes

* Average values for three replications

D. Literature Summary

For the purpose of this study, the importance of tissue culture stems from its potential to regenerate forests with improved genotypes, which will help ensure a plentiful fiber supply for the forest products industry. Somatic embryogenesis is an emerging science and two commercially important species, Douglas-fir and loblolly pine, have proven difficult to culture from mature seeds. The bottleneck for loblolly pine occurs at the initiation stage, which has been characterized by low success rates. In contrast, Norway spruce is a conifer that may be reliably cultured from mature seed.

Activated carbon is often included in tissue culture media with documented benefits in culture growth. Activated carbon is well known for its adsorbent properties and it is expected that it is these properties which benefit the growing culture. Different activated carbons may yield different tissue culture responses. Few studies have investigated the impact of different activated carbons on the chemical composition of tissue culture media. Though there are good reasons to investigate the adsorption of any of the medium components or growth metabolites, the adsorption of medium components known to be critical to success, i.e. the mineral elements and hormones, has not been adequately addressed in prior studies.

III. DISSERTATION OBJECTIVES

The primary objective of this thesis was to correlate AC character with sorptive performance and relate this to tissue culture performance. Initiation of embryogenic tissue was chosen as a tissue culture performance indicator, or *bioassay*. A secondary objective of this thesis was to quantify and understand the impact of different activated carbons on the concentrations of the mineral nutrients and growth regulators in a successful somatic embryo initiation medium.

Three hypotheses directed this research. For media which use different activated carbons:

1. The difference in initiation success is due to the release of soluble ionic material;
2. The difference in initiation success is due to a difference in sorption of growth regulators;
3. The difference in initiation success is due to different adsorption of ions.

IV. BACKGROUND THEORY: PARTITIONING, ADSORPTION

The literature concerning adsorption and partitioning phenomena is extensive. Entire textbooks have been written on the topics to be summarized. The purpose of this summary is to provide adequate background, it is not intended as an exhaustive review. The treatment presented here is largely based on the excellent text by Schwarzenbach et al. (1993), and augmented by additional references: Shaw (1992), Adamson (1967) and Weber et al. (1991).

A. General Thermodynamics: Chemical Potential, Fugacity, Activity

The relative energy status of atoms or molecules within a given phase (i.e. liquid, solid, gas) is dependent upon their internal energy (*intra*-molecular interactions) and external energy (*inter*-molecular interactions). The sum of these energies for all of the molecular species present in a system is the total free energy of the system, or *Gibbs free energy*. The change in energy which results from the incremental addition or removal of component *i*, at constant temperature (T), pressure (P), and composition ($n_{j\neq i}$) is referred to as the *chemical potential of i*, designated, μ_i:

$$\left(\frac{\partial G}{\partial n_i}\right)_{T,P,n_{j\neq i}} \equiv \mu_i \qquad (4.1)$$

where G is the Gibbs free energy (kJ) and n_i is the number of moles of species *i*. The total free energy is expressed by:

$$G_{(P,T,n_1,n_2,\ldots,n_i)} = \sum_i n_i \mu_i \qquad (4.2)$$

However, the chemical potential can not be directly measured. Instead, *relative* chemical potentials are used. For an *ideal* gas, this relative chemical potential varies as the natural log of the ratio of the corresponding vapor pressures:

$$\mu_i - \mu_i^o = RT \ln\left[\frac{P_i}{P_i^o}\right] \qquad (4.3)$$

where superscript *o* refers to an arbitrary standard state (typically the pure compound, or the compound in solution at infinite dilution at 25°C and 1 atm). For *real* gases a similar expression gives:

$$\mu_i - \mu_i^o = RT \ln\left[\frac{f_i}{f_i^o}\right] \tag{4.4}$$

where *f* designates the fugacity of the compound. Fugacity is simply the "fleeing" tendency of a compound and accounts for nonideality due to molecular interactions:

$$f_i = \theta_i P_i \tag{4.5}$$

where θ_i is refered to as the *fugacity coefficient*.

For liquids, equation (4.4) takes a similar form:

$$\mu_i - \mu_i^o = RT \ln\left[\frac{f_i}{f_{reference}}\right] \tag{4.6}$$

but the ratio $f_i / f_{reference}$ is defined differently:

$$\frac{f_i}{f_{refernce}} = \gamma_i x_i = a_i \tag{4.7}$$

where γ_i is the *activity coeficient* of solute *i*, x_i is the molar fraction, and a_i is the activity, hence:

$$\mu_i - \mu_i^o = RT \ln a_i \tag{4.8}$$

Under dilute aqueous conditions, the activity coefficient is close to a value of 1. The activity is then taken to be approximately equal to the molar fraction, which may be converted to concentration. This result indicates, that for dilute solutions, the chemical potential of a compound varies with its concentration in solution.

B. Partitioning phenomena

Partitioning processes involve the movement and distribution of a chemical species between two phases. This movement occurs in both directions, i.e. for a liquid/vapor system, molecules move from vapor to liquid and also from liquid to vapor. Equilibrium is attained when the rates of movement from each phase are equal. Alternately, equilibrium may be considered in terms of chemical potential. As the solute concentration (partial pressure) in one phase declines, so does its chemical potential (activity, fugacity) in that phase. At equilibrium, the chemical potentials in both phases will be equal.

Nonpolar solutes which are incapable of forming hydrogen bonds are very poorly soluble in water. The water molecules which surround such solutes become “locked” into position. Adjacent layers of water molecules also become more structured. This structured region has been compared with ice. The entropy of the system increases when water molecules are freed from the “solvent shell” surrounding a solute molecule. This entropic force of exclusion is refered to as *hydrophobic* force and gives rise to *hydrophobic bonding*. The positive entropy results in a decrease in free energy (negative *dG*):

$$dG = dH - TdS \tag{4.9}$$

where *dG* represents the partial molar free energy (constant *T*), *H* is the enthalpy (the sum of internal energy and work), *S* is the entropy. A decrease in *G* indicates that a process is thermodynamically favored. A solute molecule in bulk solution must first travel to the interface before it may partition to the vapor phase. This transport occurs through bulk fluid currents and Brownian motion.

For aqueous systems, a neutral solute will partition from solution into the air above the solution. For a closed system, an equilibrium is attained between molecules fleeing each phase. Over the concentration range below saturation, the partitioning is constant and may be expressed as:

$$K_H = \frac{P_i}{C_w} \tag{4.10}$$

where K_H is known as the Henry's Law constant, P_i is the equilibrium vapor pressure of solute *i*, and C_w is the equilibrium aqueous concentration. Dissolved compounds with higher activity in the aqueous phase exhibit higher vapor pressures and greater K_H.

The partitioning concept may be extended to the partitioning of a dissolved neutral solute between immiscible fluids, typically water and an organic solvent. For most liquid/liquid systems involving water, it is the activity in water which determines the degree of partitioning to the organic phase. Thus, K_H may be a suitable predictor for ranking the solvent/water partitioning behavior of a group of compounds. The equilibrium solvent/water distribution coefficient is given by the ratio of concentrations in each phase:

$$K_{sw} = \frac{C_s}{C_w} = \frac{\gamma_w}{\gamma_s} \cdot \frac{V_w}{V_s} \tag{4.11}$$

where C_s is the concentration (moles per liter) in the organic solvent, C_w is the molar concentration in the water, V is the molar volume and γ is the activity coefficient.

A large number of organic compounds with biological activity have been characterized for their octanol-water partitioning. The *octanol-water partitioning coefficient, K_{ow},* correlates well with the partitioning of neutral organic compounds into biological lipid phases and with aqueous solubility. Systematic means for approximating K_{ow} for solutes of known chemical structure have been developed based on chemical structure-energy relationships (Schwarzenbach et al., 1993).

C. Liquid/vapor adsorption

The interfacial region between a liquid and vapor may be treated as a two-dimensional boundary, or the region may be considered as a third phase with its own associated volume. The Gibbs treatment assumes an interphase; i.e. the vapor-to-liquid transition requires several molecular diameters. The free energy relationships must be modified to allow for the presence of the interphase.

Guggenheim and Hill redefined enthalpy to include work performed in creating surface (interface):

$$H = U + PV - \gamma A \tag{4.12a}$$

$$dU = TdS - PdV + \gamma dA + \sum_i \mu_i dn_i \tag{4.12b}$$

where U is the internal energy (defined in equation 4.12b), PV and γA are the work of occupying volume and creating interface, respectively. Using this enthalpy term, and substituting for U, the free energy may be derived as (Jaycock, Parfitt, 1986):

$$dG = -SdT + VdP - Ad\gamma + \sum_i \mu_i dn_i \tag{4.13}$$

The molar Gibbs energy is also the sum of the chemical potentials for each of the chemical species present.

$$G = \sum \mu_i n_i \tag{4.14}$$

Differentiating G,

$$dG = \sum_i \mu_i n_i + \sum_i n_i \mu_i \tag{4.15}$$

and substituting into equation (4.13) gives the Gibbs-Duhem relation:

$$SdT - VdP + Ad\gamma + \sum_i n_i d\mu_i = 0 \tag{4.16}$$

Under conditions of constant pressure and temperature, the Gibbs-Duhem relation reduces to:

$$-Ad\gamma = \sum_i n_i d\mu_i \tag{4.17}$$

Dividing by A gives the quantity n_i / A, known as the *surface excess*, Γ_i. The definition of Γ depends on the designation of a dividing surface. The location of the dividing surface is commonly chosen such that the surface excess of the solvent, Γ_1, is equal to zero. For a single solute system, this technique leads to equations (4.18) and (4.19):

$$d\gamma = -\Gamma_2 d\mu_2 \tag{4.18}$$

$$\Gamma_2 = -\frac{d\gamma}{d\mu_2} \tag{4.19}$$

where the subscripts 1 and 2 designate the solvent and solute phases, respectively. At low concentration the chemical potential may be expressed in terms of concentration:

$$\mu_2 = RT \ln C_2 \tag{4.20}$$

Substituting into equation (4.19) gives the Gibbs adsorption isotherm:

$$\Gamma_2 = \frac{-d\gamma}{RTd\left(\ln C_2\right)} = -\frac{C_2}{RT}\frac{d\gamma}{dC_2} \tag{4.21}$$

This result indicates that the surface excess and the change in interfacial tension have an inverse relationship. This prediction has been confirmed directly for liquid/vapor systems (Shaw 1989).

D. Solid Phase Adsorption

Adsorption to a solid phase is more complex than solvent/water or air/solution partitioning. The surface of the sorbent is expected to be heterogeneous and may react with the sorbate to form a chemical bond (*chemisorption*). The heterogeneity gives rise to different sorption sites characterized by different adsorption energies. Functional groups

on the sorbent may comprise sites which are selective for one sorbate over another. Additionally, the spatial arrangement of surface features may create selective sites. Sorption may occur as a single *monolayer* or as multiple layers. As the surface becomes loaded, adjacent sorbate molecules may interact and adjust their orientation. Precipitation from solution or condensation from the gas phase may occur within the sorption volume. Sorption from solution is further complicated by the presence of competing solvent molecules. For certain systems, adsorption may be regarded as a non-equilibrium (irreversible) process. However, the theory of adsorption is largely based on thermodynamic or kinetic equilibria.

Adsorption occurs at an interface or interphase and is confined to a relatively small volume, whereas partitioning is treated as a bulk-phase phenomenon. To a first approximation, the adsorption of neutral solute molecules onto a solid sorbent may be treated as a 2-dimensional analog of partitioning processes already discussed (physisorption). The concepts of chemical potential and fugacity may be extended to adsorbed molecules in equilibrium with the bulk phase. A partitioning coefficient may be defined, in this case for an aqueous system:

$$K_d = \frac{C_s}{C_w} \tag{4.22}$$

where C_s is the solid phase concentration (mol/kg), and C_w is the equilibrium aqueous phase concentration (mol/L).

Over the broad concentration range of interest, many systems do not obey the implicit linear relationship that defines the distribution coefficient. A curvilinear relationship is far more common:

$$C_s = K \cdot C_w^{1/n} \tag{4.23}$$

where n > 1. This equation is of the same form as the Freundlich adsorption isotherm, to be discussed subsequently.

Adsorption is often classified into three types: physical adsorption or physisorption, electrostatic adsorption and chemical adsorption (chemisorption). Of these types of interactions, physisorption is the weakest, having forces of interaction of about 2 kg/mol. Physisorption arises through dipole-dipole, dipole-induced dipole, and instantaneous dipole (London forces) interactions. These forces vary in strength as the inverse distance of atomic separation raised to the sixth power (third power in the case of dipole-dipole interaction). Electrostatic bonds result from ion-ion or ion-induced dipole interactions. These vary inversely as the distance of separation (second power in the case of ion-induced dipole). Chemical adsorption is characterized by covalent bonding (strongest energy of interaction, several hundred kJ/mol) and hydrogen bonding (two or three times the energy level of physical adsorption). Covalent bonding may require a significant energy input (high energy of activation) and is therefore less likely to occur in systems at room temperature. Chemisorption is expected to be slow relative to physisorption. The orders of magnitude for these different bonds are included in Table 4.1 (Chang, 1981). Adsorption from solution is believed to be generally limited to physical adsorption, though chemical adsorption has been observed in a few systems (Leon y Leon, 1994).

Table 4.1. Forces for different types of chemical interactions (Chang, 1981).

Type of Interaction	Energy of Interaction	Example	Order of Magnitude (kJ/mol)
Covalent bond	No simple expression	H – H	200 – 800
Ion – ion	$\frac{e^2}{\varepsilon r}$	Na+ Cl-	40 – 400
Ion – dipole	$\frac{e\mu}{\varepsilon r^2}$	Na+ $(H_2O)_n$	4 – 40
Dipole – dipole	$\frac{2}{3}\frac{\mu_1^2\mu_2^2}{\varepsilon r^6 kT}$	SO_2 SO_2	0.4 – 4
Dipole – induced dipole	$\frac{\alpha\mu^2}{\varepsilon r^6}$	HCl C_6H_6	0.4 – 4
Ion – induced dipole	$\frac{1}{2}\frac{\alpha e^2}{\varepsilon r^4}$	Na+ C_6H_6	0.4 – 4
Dispersion	$\frac{3}{4}\frac{I\alpha^2}{r^6}$	He He	4 – 40
Hydrogen bond	No simple expression	H_2O H_2O	4 – 40

Where *e* is the charge on an electron, μ is the dipole moment, ε is the dielectric constant, *r* is the ionic radius, α is the polarizability, and *I* is the first ionization potential of the atom or molecule.

Many related phenomena influence adsorption from solution. These include concentration gradients, the relative affinities between solute, solvent, and sorbent, the

relative size of sorption sites (pores), and the physical properties of the system and its components. For multi-solute systems and systems where the solvent has a high affinity for the sorbent, competition for sorption sites may also be a significant factor.

Equilibrium data from sorption experiments are usually presented in the form of an "isotherm", which graphically displays the ratio of sorbed to non-sorbed solute per mass of sorbent at a constant temperature. Figure 4.1 presents two isotherms that are representative of isotherms for liquid systems.

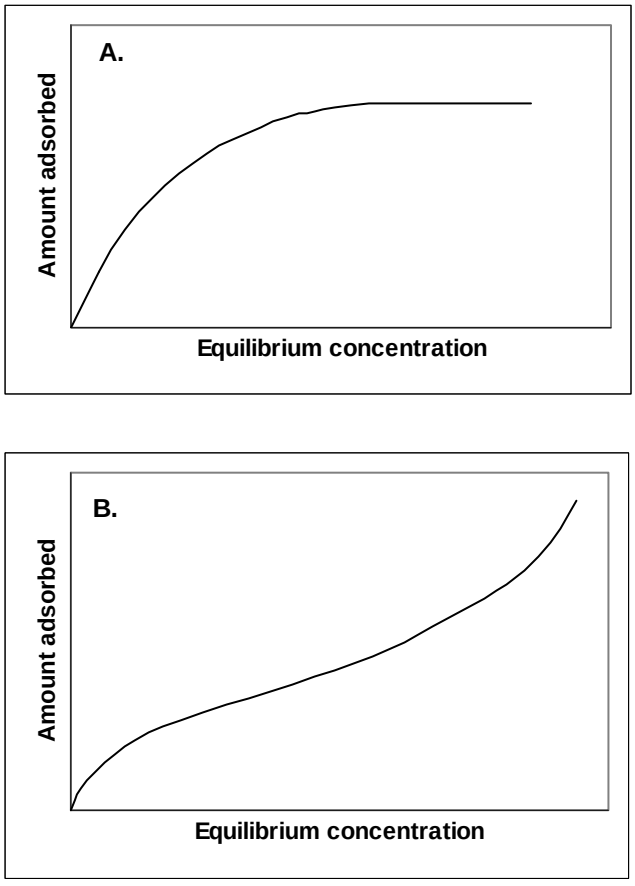

Figure 4.1. Common isotherm shapes for sorption from solution (adapted from Mattson, Mark, 1971). A. Adsorption of solid solutes from solution (*Type 1* isotherm by Brunauer's classification, Shaw 1992). B. Adsorption of poorly miscible liquids (*Type 2* isotherm).

For a particular system, the isotherm profile reveals information about the nature of the adsorption process. When the force of interaction between solute molecules is great

relative to that between solute and sorbent, an *S*-shaped isotherm results. In this case, multilayers of solute may form on the sorbent. If adsorbed molecules have negligible interaction, then the activation energy will be independent of coverage and an *L* or *H* isotherm will result. An isotherm classification is reproduced in Figure 4.2 (Giles et al., 1974). The four different classifications, *S* (S-shaped), *L* (Langmuir), *H* (high affinity) and *C* (constant partition) were based on the initial slope of the isotherm.

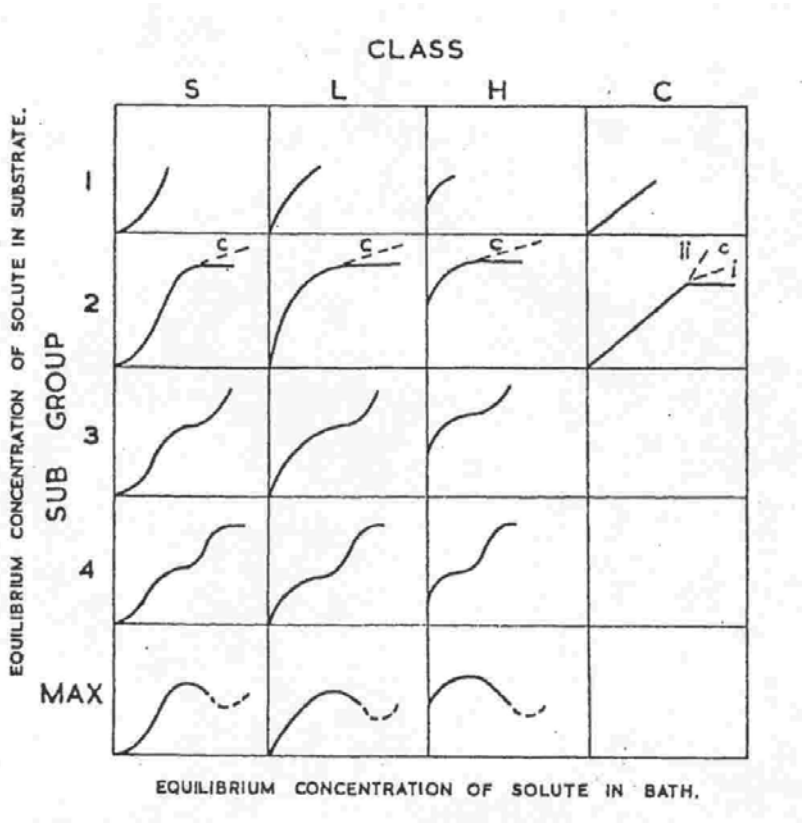

Figure 4.2. Classification of isotherm shapes (Giles et al. 1974, reproduced with permission from Academic Press).

The shape of the isotherm may indicate the type of porosity present. A sharp "knee" and horizontal plateau region have been noted for highly microporous carbons; a less sharp knee and nearly horizontal plateau were observed for carbons with larger micropores; while, a round knee and sloping plateau region were associated with a wide distribution of microporosity with a contribution from mesoporosity (Molina-Sabio et al. 1985).

Isotherms with *Class C* behavior have been produced by microporous sorbents. To produce a *Class C* isotherm, adsorption of solute exposes or creates new sites, hence the number of sorption sites remains the same or perhaps increases. The creation of new sorption sites with adsorption has been observed in studies of water sorption onto activated carbon. This phenomenon has been explained as an initially low affinity between water and charcoal followed by hydrogen bonding between sorbed and free waters. The *c* variation on Subgroup 2 indicates that the slope of the "plateau" region may vary.

For liquid systems at low solute concentrations, type *L* isotherms are commonly observed. For higher solute concentrations the *S* type is more likely.

The Polanyi Potential Theory of Adsorption

The Gibbs treatment of the liquid/vapor interface provides the foundation for what is commonly referred to as the Polanyi potential theory.

Gas phase

The original idea has been credited to Saussure (Brunauer, 1945): the adsorbent exerts a strong attractive force upon the gas in its vicinity, a force great enough to result in the sorption of several layers. These layers are under compression analogous to the compression of the earth's atmosphere. Polanyi defined the adsorption potential at a point near the adsorbent as the work done by the adsorption forces in bringing a molecule from the gas phase to that point. This work of adsorption was treated as a work of compression and mathematically its value is given by:

$$\varepsilon_i = \int_{\delta}^{\delta_s} V dP \qquad (4.24)$$

ε_i is the adsorption potential at a point where the density of the adsorbed substance is δ_S, δ is the density in the gas phase, and $V=M/\delta$, where M is the molecular weight of the adsorbate (molar volume). To evaluate this integral one must be able to express the molar

volume V, or the density δ, as a function of the pressure both in the gas phase and in the adsorbed phase. The equation of state of the adsorbed gas is unknown, but Polanyi assumed that the gas obeys the same equation of state in the adsorbed phase as in the bulk phase. A cross-section of the adsorbed phase as it is pictured by the potential theory is presented in Figure 4.3.

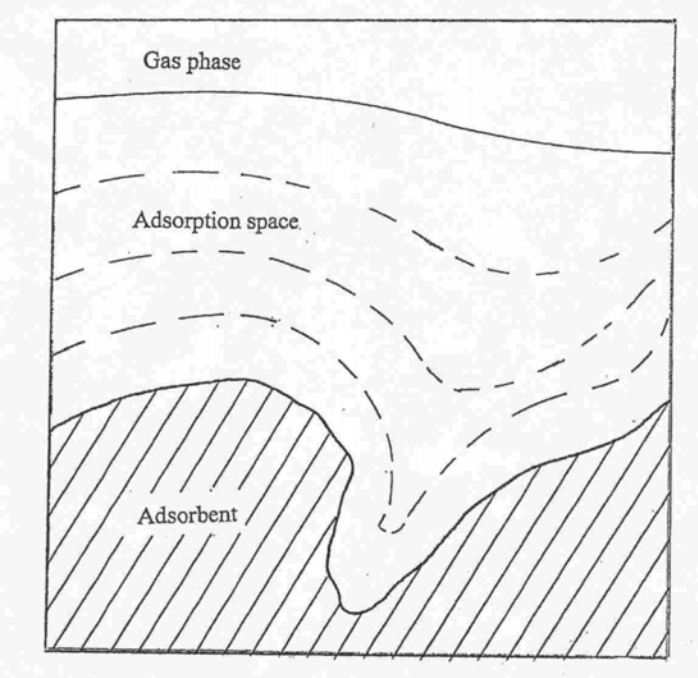

Figure 4.3. A cross-section of the adsorbed phase according to the Polanyi theory (adapted from Brunauer, 1945). The shaded region represents the cross-section of the adsorbent, the full line is the boundary surface between the gas phase and the adsorbed phase, and the dotted lines are equipotential surfaces. The potential along the surface of the adsorbent is ε_0; the potentials along the consecutive potential surfaces are ε_1, ε_2, ..., ε_i, ..., etc. It is assumed that the adsorption potential is similar to the gravitational potential, i.e., along the i-th surface its value is always ε_i, regardless of the number and kind of molecules that are located between the i-th surface and either the adsorbent or the gas phase.

The shaded region represents the cross-section of the adsorbent, the full line is the boundary surface between the gas phase and the adsorbed phase, and the dotted lines are equipotential surfaces. The potential along the surface of the adsorbent is ε_0, the potentials along the consecutive potential surfaces are ε_1, ε_2, ..., ε_i, ..., etc. It is assumed that the adsorption potential is similar to the gravitational potential, i.e., along the i-th surface its value is always ε_i, regardless of the number and kind of molecules that are located between the i-th surface and either the adsorbent or the gas phase.

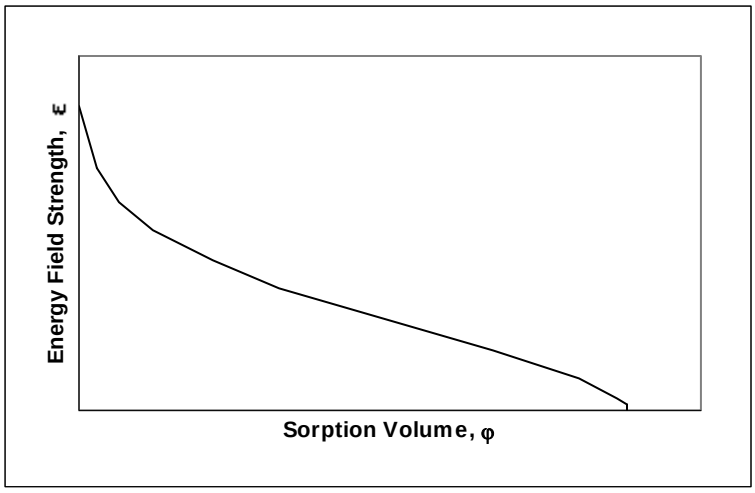

Figure 4.4. An example of a characteristic curve for adsorption of carbon dioxide on charcoal (adapted from Ruthven 1997). The energy field strength declines to zero ($\varepsilon = 0$), coinciding with the maximum sorption volume (φ = maximum). ε_{max} occurs at solid surface, coinciding with φ_{min}.

Each of the potential surfaces together with the surface of the adsorbent encloses a volume (Figure 4.3). These volumes are labeled φ_1, φ_2, ..., φ_i, ..., etc. The volume enclosed by the adsorbent surface and the boundary surface between the gas phase and the adsorbed phase is φ_{max}, the volume of the entire adsorption space. The potential along the outermost surface is zero. At the surface of the adsorbent, where $\varphi = 0$, the potential has its maximum value, ε_0. Between these two limits the shape of the curve $\varepsilon = f(\varphi)$ is shown in Figure 4.4.

The potential theory assumes that the adsorption potential does not change with the temperature, from which it follows that the associated volumes do not change either. The curve is constant for all temperatures and is therefore referred to as the *characteristic curve*.

The only test of validity is that of temperature dependence of the equation.

The calculation of the characteristic curve from an isotherm considerably below the critical temperature is the simplest case. In the first approximation the potential is calculated on the basis of two assumptions: (1) the vapor in the gas phase obeys the ideal

gas laws; (2) the liquid in the adsorbed phase is incompressible. Thus ε_i is the work of compressing an ideal gas isothermally from P the pressure existing in the gas phase to P_s, the vapor pressure of the liquid (saturation pressure). In this case, equation 4.24 becomes

$$\varepsilon_i = RT \ln \frac{P_s}{P} \tag{4.25}$$

The work of creating a liquid surface has been neglected in this expression.

Since the liquid is assumed incompressible, the value of φ_i corresponding to ε_i, is given simply as

$$\varphi_i = \frac{x}{\delta_T} \tag{4.26}$$

where x is the weight of the adsorbed vapor, and δ_T is the density of the liquid at temperature T. To each pair of values of x and P_X, i.e., a point on the isotherm, there corresponds a pair of values φ and ε, i.e., a point on the characteristic curve. These may be calculated given an estimate of the sorbed phase density.

The approximation may be improved by correcting for the density of the liquid at the gas/liquid interface: the liquid is presumed to be in an expanded state analogous to a liquid near the boiling point.

Liquid phase

Adsorption from liquid solution complicates the analysis. Two primary concerns are (1) the role of the solvent which must be displaced by the sorbate and (2) the density of the sorbed phase.

Adsorption of solutes is assumed to be analogous to the precipitation of solids. The first approximation is to simply substitute C_s/C for P_s/P in equation 4.25, where C_s is the saturated concentration and C is the equilibrium (observed) concentration. Polanyi recognized that this approach failed to take into account the displacement of the solvent. He therefore redefined the equation setting $RTln(C_s/C)$ equal to the *difference* between

solute and solvent adsorption potentials corrected for their relative molar volumes (Manes, Hofer, 1969):

$$RT \ln \frac{C_s}{C} \equiv \varepsilon_{sl} = \varepsilon_s - \varepsilon_l \frac{V_s}{V_l} \tag{4.27}$$

The ε subscripts, *s* and *l* ,designate the solid solute and liquid solvent, respectively. From this equation, Polanyi concluded that solute sorption would be weakest from solutions with high ε / V values. Since the solvents were expected to vary only slightly in their ε / V values, he expected that the more important aspect would be the relative solubility for a given solute.

Equation 4.27 may be expressed this way:

$$\frac{\varepsilon_{sl}(V)}{V_s} = \frac{\varepsilon_s(V)}{V_s} - \frac{\varepsilon_l(V)}{V_l} \tag{4.28}$$

where the notation $\varepsilon(V)$ designates a function. Manes and Hofer (1969) rewrote this equation for economy as:

$$\alpha_{sl} = \alpha_s - \alpha_l \tag{4.29}$$

where each α is the corresponding ε / V.

The characteristic curve is then simply a plot of volume filled by sorbate per mass AC vs. $RT\ln(C_s / C)/V_s$. According to the theory, as presented by Manes and Hofer, all such curves should collapse to a single curve by application of a single abscissa scale factor, which is likely to be different for different adsorbates. The magnitude of this scale factor indicates the extent to which the adsorption potential deviates from proportionality to the molar volume.

A plot for a pure hypothetical solute, pure solvents and the solute in solution is reproduced from Manes and Hofer (1969) in Figure 4.5. The pure solute displays higher volume at a given energy level or conversely, higher energy at constant volume than

either of the solvents considered. Benzene should displace heptane. A solution of the solute in benzene is expected to show lower sorptive potential for the solute than the similar solution in heptane.

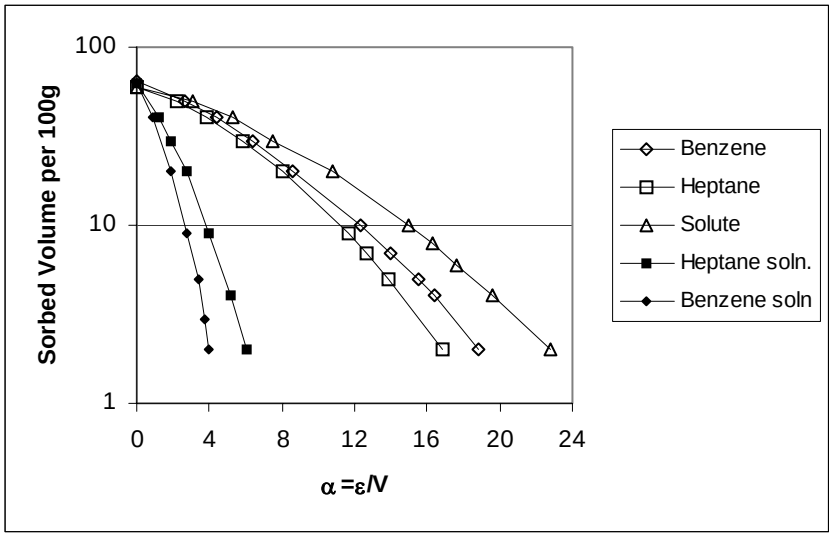

Figure 4.5. Schematic Polanyi plot of the sorption volume occupied (cm^3) per solute adsorbed from two different solvents (adapted from Manes, Hofer 1969. The figure illustrates the calculation, $\alpha_{sl} = \alpha_s - \alpha_1$, for adsorption from heptane solution. Subscripts *sl*, *s*, and *l* designate solution, solute and solvent, respectively.

Langmuir and Freundlich Adsorption Isotherm Equations

At concentrations well below saturation, solute adsorption from liquid to solid is believed to be limited to monolayer coverage. This monolayer limit is due to the rapid decay of the surface forces involved: the forces of attraction are not expected to extend more than one molecular diameter away from the solid surface. Therefore, it is believed that solute is present in bulk concentration adjacent to the first sorbed monolayer; i.e. the transition to bulk phase is abrupt. One notable exception to the monolayer "rule" is the orientation of amphiphilic solutes at the interface, which may lead to multi-layer or hemimicelle formation.

The Langmuir adsorption isotherm equation, which assumes monolayer coverage, was originally derived for gas adsorption onto uniform solid surfaces. Its derivation was based on a consideration of occupied sites and total sites available for adsorption, and may be

derived from mass action, kinetic or statistical thermodynamic approaches. The equation may be expressed in this form:

$$V = \frac{V_m bp}{1 + bp} \tag{4.30}$$

where V is the surface volume occupied by sorbed molecules, V_m is the volume occupied when all surface sites are filled (the subscript m designates a monolayer volume), p designates pressure, and b is a constant related to the energy of solid/solute interaction, or the enthalpy of adsorption. At very low pressure the Langmuir equation reduces to Henry's Law:

$$\frac{1}{b} = \frac{p}{V/V_m} \tag{4.31}$$

where $1/b$ is a constant and V/V_m is equivalent to concentration. At high pressure the Langmuir equation implies a limiting adsorption or asymptote. At high pressure the equation is no longer a function of pressure, and at low pressure it is a function of pressure to the first power. Therefore, at intermediate pressures V may be thought of as a function of p raised to a fractional power ($1/n$):

$$V = bp^{1/n} \tag{4.32}$$

which is the Freundlich isotherm equation (again). The Freundlich equation is an empirically derived equation which pre-dates the Langmuir derivation. Though it has been shown to apply to certain heterogeneous surfaces as the summation of Langmuir-type adsorption onto different sites, it is primarily used as a convenient analytic expression for fitting isotherm data. The Freundlich equation does not define a limiting volume nor is it thermodynamically consistent as it doesn't reduce to Henry's Law at low concentration. The meaning of b has changed to reflect sorption capacity instead of intensity, which is now given by n.

The Langmuir model was developed using a set of assumptions, which are probably violated by real systems:

1. Physisorption of a single monolayer
2. Ideal behavior
3. No migration of solutes along the solid surface
4. Uniform distribution of sites with constant energy
5. No interactions between adsorbed molecules

Sorption from liquid solution to solid phase often produces a relationship that may be fit by either the Langmuir or Freundlich isotherm equations. The Langmuir equation for this case may be expressed as:

$$q_e = Q^o \frac{bC_e}{1 + bC_e} \tag{4.33}$$

where q_e is the specific adsorption of the solute (mass of solute per mass of sorbent), Q^o designates the limiting adsorption, and C_e designates the equilibrium solution concentration. The Freundlich equation takes this form:

$$q_e = K_F C_e^{1/n} \tag{4.34}$$

Adsorption from solution is not the same process as that from the gas phase, for which the Langmuir model was originally derived: competition with solvent molecules complicates the analysis. Therefore, the interpretation of the constants b and Q^o , K_F and n is not straightforward. Also, the heterogeneity of common adsorbents, such as activated carbon, violates the assumptions of the Langmuir analysis. However, these constants are generally treated as representing similar qualities as the respective constants for gas phase adsorption (Weber et al., 1991).

Polar Solutes

The adsorption of polar solutes (organic or inorganic) to solid surfaces is further complicated by the role of surface/solute charge interactions. Typically, the species involved are treated as point charges. When solid particles are dispersed in aqueous systems, a net electrostatic charge is present at the interface. This charge may be the result of functionality such as dissociated carboxyl or hydroxyl groups. These groups

may be present as covalently bound groups or they may be in the form of oxidized impurities, such as trace metal oxides. The charged solute will then either be attracted to or repulsed from the charged solid/water interface depending on whether the charges are opposite or similar. The distribution of surface charges varies with the pH of the solution, i.e. surface groups dissociate as a function of pH.

The oppositely charged ions from solution, which are directly adjacent to the charged particle surface, are tightly bound (Figure 4.6).

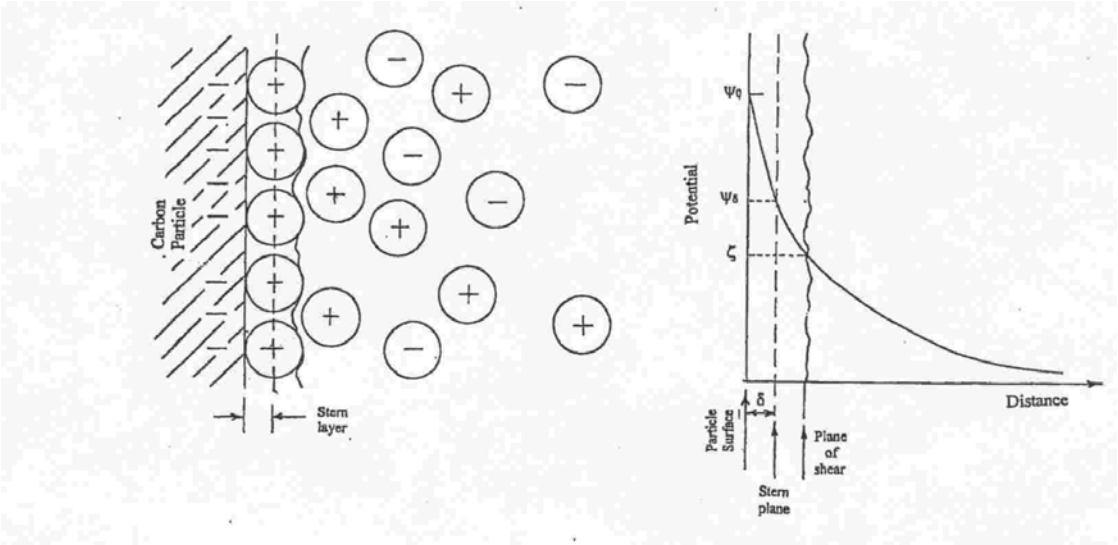

Figure 4.6. Electrical double layer (adapted from Schwarzenbach et al. 1993, Shaw 1992). Surface charge is negative. Tightly bound ions are positively charged, define the outer boundary of the Stern layer. The diffuse layer is defined by the gradual decline in ionic concentration to bulk fluid levels. The charge measured in electrophoretic techniques is the charge at the plane of shear, or zeta potential.

These closely bound counterions, along with bound water molecules, define a layer known as the Stern layer. In measurements based on electrophoretic mobility the shear plane occurs just outside the Stern layer. For such measurements, the effective charge or zeta potential on the hydrated particle, is therefore determined by the tightly bound counterions. The aqueous region adjacent to the Stern layer is populated by counter ions and co-ions. This diffuse region ensures electrical neutrality. The concentration of these

ions gradually declines with distance until bulk concentrations are achieved. This region is referred to as the Gouy-Chapman region. The thickness of the Gouy-Chapman layer varies inversely with the ionic strength of the solution, and may range up to about 30nm from the surface. Over half of the ions in the G-C layer are expected to be within 10 nm of the particle surface. This region (1 to 10nm) includes the "solvent shell" of structured water. Together, the Stern and Gouy-Chapman layers define a region known as the *electrical double layer*.

In addition to the electrostatic interactions, transition metal ions may also be subject to surface complexation. These types of interactions involve surface species with free electron pairs, i.e. oxygen and nitrogen. The spatial arrangement of more than one heteroatom may result in multiple electron pairs participating in the complexation, which is then analogous to chelation.

Complexes are expected to be more stable than simple electrostatic interactions due to ligand-field stabilization. The transition metal species contain incomplete d-orbitals. The complexing ligands possess electron fields which influence the splitting of the d-electrons between different energy levels. Splitting patterns depend on the number of electrons in the d-shell, which depends on the atomic number. Certain splitting patterns result in a more stable distribution of electron density.

Data from the adsorption of ions to solid surfaces may often be fit by either the Langmuir or Freundlich isotherm equations. Therefore, analysis has commonly involved the effort to quantify and characterize the polar sites of the substrate. The Langmuir treatment logically follows by considering the proportion of occupied and unoccupied *polar* sites.

E. Competitive adsorption: Polanyi and IAST

Polanyi Theory

The Polanyi theory may be extended to the situation involving competing solutes. At the postulated equipotential line where solid and solution are at equilibrium, i.e. where the

adsorption potential approaches zero on Figure 4.5, the following relationship has been suggested (Manes, Rosene 1976):

$$\varepsilon \geq RT \ln \frac{C_s}{C} \tag{4.35}$$

For regions within the adsorption space an excess energy is present, expressed as:

$$-\Delta G_i = \varepsilon_i - RT \ln\left(\frac{C_s}{C}\right)_i \tag{4.36}$$

In the situation where more than one solute is adsorbing, Rosene and Manes (1976) assume that the individual solutes are mutually insoluble as solids and, therefore, as adsorbates. The adsorption space is then expected to be the sum of volume elements, each occupied by a quantity of only one solute. Displacement of one solute by another is expected to occur with no distortion of the sorption volume; e.g., for the adsorption of dn_i moles of solid *i* and the displacement of dn_j moles of solid *j*,

$$V_i dn_i + V_j dn_j = 0 \tag{4.37}$$

$$dn_j = -(V_i / V_j) dn_i \tag{4.38}$$

Then for the process where two solutes compete for an element of sorption volume, the net energy change must be negative:

$$dG = \Delta G_i dn_i + \Delta G_j dn_j \leq 0 \tag{4.39}$$

Substitution from equations 4.38 and 4.36 leads to the equation:

$$\frac{dG}{dn_i} = \left(\frac{\varepsilon_j}{V_j} - \frac{RT}{V_j}\ln\frac{C_{js}}{C_j}\right) - \left(\frac{\varepsilon_i}{V_i} - \frac{RT}{V_i}\ln\frac{C_{is}}{C_i}\right) \leq 0 \tag{4.40}$$

as the criterion for the displacement of component *j* by component *i*. If, however, $dG/dn_i > 0$, then component *j* will displace component *i* (or be adsorbed in preference to component *i*). For any element of volume in the adsorption space, equation 4.40 leads to the expectation that the adsorbed solid will be the one with the highest value of $-\Delta G/V$. (Note: the saturated concentrations now refer to saturation in a solution containing the competing sorbate.)

Rosene and Manes (1976) gave sample calculations (graphical) for two situations. In the first example one component was present at saturation concentration; the second example considered the situation where the solution was not saturated with either component. Only the second calculation will be considered here.

The case where neither component is saturated is presented in Figure 4.7.

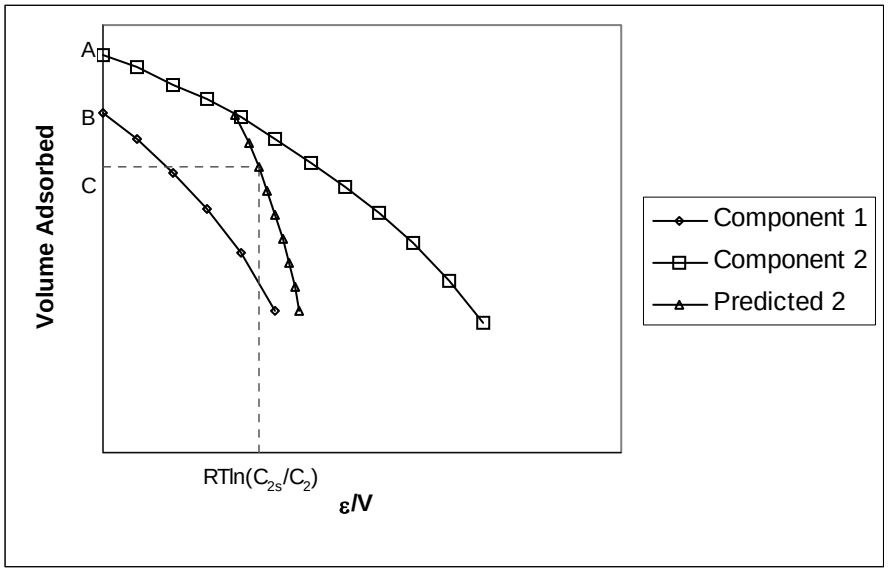

Figure 4.7. The competitive adsorption case where neither component is saturated (Rosene, Manes 1976). The correlation curve on the right is for component 2. Component 2 is depicted as having the higher sorption potential per molar volume and so its curve appears to the right of component 1. The correlation curve for component one has been shifted to the left by an amount equal to $(RT/V_1)ln\ (C_{1s}/C_1)$ as prescribed by equation 4.40. Equation 4.40 further indicates that the resulting curve, ε_1/V_1, is subtracted from ε_2/V_2, resulting in the dotted curve. To find the adsorption of both components at equilibrium concentrations C_1 and C_2 we enter the abscissa with the value of $(RT/V_2)ln(C_{2s}/C_2)$. The corresponding volume, at point C is the volume of component 2 adsorbed. If B>C, the volume of component 1 adsorbed is B-C,. If C>B, then only component 2 will be adsorbed.

The correlation curve on the right is for component 2. Component 2 is depicted as having the higher sorption potential per molar volume and so its curve appears to the right of component 1. The correlation curve for component one has been shifted to the left by an amount equal to $(RT/V_1)ln\ (C_{1s}/C_1)$ as prescribed by equation 4.40. Equation 4.40 further indicates that the resulting curve, ε_1/V_1, is subtracted from ε_2/V_2, resulting in the dotted curve depicted in Figure 4.8. To find the adsorption of both components at equilibrium

concentrations C_1 and C_2, we enter the abscissa with the value of $(RT/V_2)ln(C_{2s}/C_2)$. Referring to Figure 4.7, the corresponding volume, at point C is the volume of component 2 adsorbed. If B>C, the volume of component 1 adsorbed is B-C,. If C>B, then only component 2 will be adsorbed.

Rosene and Manes (1977) subsequently went on to consider the situation where three sorbates compete for the adsorption space. They indicated that the same equation (eqn. 4.40) held for multicomponent adsorption, but presented it in a slightly different fashion:

$$\frac{RT}{V_k}\ln\left(\frac{C_s}{C}\right)_k \leq \frac{\varepsilon_k}{V_k} - \frac{\varepsilon_j}{V_j} + \frac{RT}{V_j}\ln\left(\frac{C_s}{C}\right)_j \qquad (4.41)$$

where the *k*-th component is the component with the highest $-\Delta G/V$ at any element in the adsorption space, and the *j*-th component is the one with the next highest value of $-\Delta G/V$. For a given set of concentrations, the rank of $-\Delta G/V$ may change over the adsorption space, depending on the relative values of ε/V.

The Ideal Adsorbed Solution Theory, IAST

Radke and Prausnitz (1972) developed a model for competitive sorption from solution which has become known as the ideal adsorbed solution theory (IAST). They based the theoretical development of the model on the concept that the adsorbed phase forms an ideal solution. An ideal solution is one in which the fugacity and spreading pressure of each solute is proportional to its mole fraction. The spreading pressure is the difference in interfacial tension between the pure solvent-sorbent interface and that of the solution-sorbent interface. This pressure cannot be directly measured; however, it may be derived, as a function of the area under the isotherm. The model is based on data gathered from single solute isotherms.

There are three concentrations (*mmol/L*) to keep in mind as one reviews these equations:

$\mathbf{C_{e,i}}$ is the *actual* solution phase equilibrium concentration for solute *i* which results when the mixture is adsorbed onto AC,

$C_{o,i}$ is the initial concentration of solute *i* present in the mixture for which a prediction is desired,

$C_{s,i}$ is the solution phase equilibrium concentration from the single solute isotherm for solute *i* which gives the same spreading pressure as the overall spreading pressure for the mixture.

There are two different sorbed quantities (*mmol/g*):

$q_{e,i}$ which is the actual amount of solute *i* sorbed from the mixture,

$q_{s,i}$ which is the amount sorbed from single solute solution at a spreading pressure equal to that of the mixture.

The spreading pressure relationship derives from the Gibbs equation, and has been presented in the following form (Sorial et al., 1993):

$$\pi = \frac{RT}{A}\int_{0}^{C_{s,i}}\left(\frac{q_{s,i}}{C_{s,i}}\right)dC \qquad (4.42)$$

where π is the spreading pressure, *A* is the interfacial area of the sorbent, *R* is the gas constant, and *T* is the absolute temperature. The integral refers to the area under the sorption isotherm and may be solved given an analytic expression, such as the Freundlich or Langmuir isotherm equations. For all of the solutes of interest, π is constant and the upper limit of integration is unknown. Solution of the integral results in a relationship between equilibrium concentration and spreading pressure. In applying the IAST, a spreading pressure is typically assumed and then the remaining equations evaluated for convergence: solution requires a series of iterations. A variety of methods have been reported in the literature for solving these equations.

In their development of the theory, Radke and Prausnitz (1972) determined that the equilibrium concentration from mixture was related to the single solute concentration (at constant spreading pressure) through the sorbed mole fraction:

$$C_{e,i} = (C_{s,i})\frac{q_{e,i}}{\sum_{i=1}^{i=N} q_{e,i}} \qquad (4.43)$$

Treating the sorbed phase as an ideal solution leads to this equation (Sorial 1993):

$$\sum_{i=1}^{i=N} \frac{q_{e,i}}{q_{s,i}} = \sum_{i=1}^{i=N} \frac{C_{e,i}}{C_{s,i}} = 1 \tag{4.44}$$

The mass balance equation includes the initial concentrations for the solutes of interest,

$$q_{e,i} = \frac{(C_{o,i} - C_{e,i})*V}{m} \tag{4.45}$$

where *V/m* is the ratio of solution volume to sorbent mass.

Again, noting that π is constant, this set of equations may be solved given initial solute concentrations and *V/m*. An example of the application of the IAST is reproduced in Figure 4.8. The prediction appears to be better at lower solute concentrations.

The IAST model has been modified to account for non-ideal competition due to unequal accessibility and irreversible sorption (Yonge, Keinath, 1986). It has also recently been analyzed for the effects of unequal adsorbent sizes and heterogeneity (Sircar, 1995) when applied to gas phase adsorption.

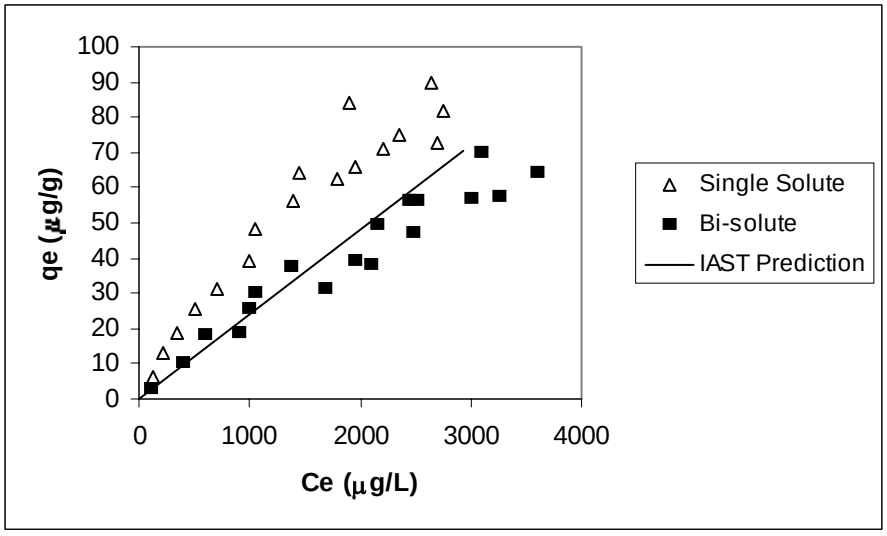

Figure 4.8. Single-solute and bi-solute equilibrium data and IAST model prediction for sorption of tetrachloroethylene on Ann Arbor I soil in the presence of dichlorobenzene in a continuously mixed batch reactor (adapted from Weber et al. 1991).

V. BACKGROUND THEORY: SURFACE AREA, POROSITY

A. Surface Area

BET Equation

The BET (Brunauer, Emmet, Teller) equation was originally derived as an extension of the Langmuir isotherm for physical adsorption onto a nonporous solid surface. It was motivated by a need to describe type II (sigmoidal) isotherms in which multilayer formation was suspected: the Langmuir derivation only applies to monolayer formation. It was derived by equilibrating rates of evaporation and condensation for adjacent layers of adsorbate. This phase/transport equilibrium was coupled with the assumption that the heat of liquifaction applies for every layer except the first, which is the only layer subject to a characteristic heat of adsorption. The derivation is presented elsewhere (Brunauer 1945; Jaycock, Parfitt, 1986), only the resulting equation will be presented here:

$$\frac{P/P_o}{V[1-(P/P_o)]} = \frac{1}{(V_m C)} + \frac{(C-1)}{(V_m C)} * (P/P_o) \qquad (5.1)$$

which may be linearized by plotting:

$$\frac{(P/P_o)}{V[1-(P/P_o)]} \quad \text{vs. } (P/P_o), \qquad (5.2)$$

where V is the volume adsorbed at pressure P, V_m is the monolayer volume, P_o is the saturation pressure of the adsorbing gas, and C is a constant.

The monolayer volume V_m and constant C may be calculated from the slope and intercept of the best linear fit to equation (5.2). In practice, it is common to fit adsorption data for three or more points over the relative pressures from 5 to 25% to derive values for V_m and C. For most systems, C is found to be much greater than 1, and $P/P_o >> 1/C$. This allows the BET equation to be simplified to:

$$S = (V) * [1-(P/P_o)] \qquad (5.3)$$

where S is the surface area. This equation allows approximation of the surface area based on a single point measurement with a gas of approximately 30% N_2 in a carrier of helium.

Surface area may then be derived from conversion of V using Avogadro's number and the cross-sectional area of a single adsorbed nitrogen molecule (0.162 nm^2).

B. Pore Volume and Pore Size Distribution

Barrett-Joyner-Halenda Method

The traditional method for determining pore size distribution (PSD) is based on the stepwise application of the Kelvin equation (Barrett et al. 1951) or a modified version:

$$RT\ ln(P_r/\ P_o\ ) = 2\gamma V_m / r \qquad (5.4)$$

where r designates the radius of curvature at a fluid/vapor interface, and γ is the surface tension of the fluid in a cylindrical-shaped pore (Shaw, 1992). The adsorption demonstrates a hysteresis effect and analysis is usually performed on the desorption leg of the isotherm.

Barrett et al. (1951) refined the analysis by accounting for the reduction in pore radius resulting from nitrogen, which had condensed on the pore wall. Additionally, they allowed for thinning of the condensed layer in response to increased temperature. They found that very little error was introduced by treating the thickness of the layer as a constant percentage of the pore radius (Sutherland 1967).

Though the Kelvin equation is adequate for characterizing porosity down to the mesoporous range, it fails to predict observed behavior for materials with significant porosity below 7 nm. The concept of surface tension begins to lose meaning due to the low number of molecules required to span the pore diameter for pores smaller than about 7.5nm. The result is an underestimation of pore sizes, or an overestimation of the pressure required to fill small pores (Lastoskie et al., 1993). An additional drawback is the assumption of cylindrical pores: slit-shaped pores are more representative of the activated carbon surface.

Density Functional Theory

Techniques based in statistical mechanics have proven to be more consistent than traditional Kelvin-equation based methods for fitting isotherm data, particularly in the low pressure range where incomplete surface coverage occurs. These methods are not limited by "macro" thermodynamic concepts such as surface tension; therefore they may be extended to any minimum pore size. They have been enabled by the advent of high speed computing technology and are not readily amenable to "back-of-the-envelope" calculations. The basic ideas for the technique will be introduced here (Lastoskie et al. 1993; Lastoskie et al. 1994; Gubbins 1997).

For this research, the pore size distributions were derived from experimental nitrogen adsorption data. These data were combined with theoretical sorption isotherms for a range of pore sizes to solve the adsorption integral for an equivalent pore size distribution.

The adsorption integral is given as:

$$N(P) = \int_{H\,min}^{H\,max} \rho(P,H)\, f(H)\, dH \qquad (5.5)$$

where $N(P)$ is the actual adsorption data, $\rho(P,H)$ is the density profile of the adsorbate at pressure P across a model pore of width (H) or the isotherm for the individual model pore, and $f(H)$ is the size distribution, to be determined.

The adsorption integral is a form known as a Fredholm integral of the first kind. Solutions tend to be unstable: slight variations cause large differences in the expression. The solution to the adsorption integral is an "effective pore size distribution (PSD)"; that is, the carbon *behaves as if* it had a certain size distribution of ideal pores. Because they offer a more realistic description of porosity in activated carbons, slit-shaped pores have been chosen in preference to cylindrical pores.

For the purposes of this work, density functional theory concerns the generation of theoretical isotherms for theoretical pores, in which the "adsorption" is expressed as fluid density for a given pore dimension as a function of relative pressure. The density profile within a given pore size, expressed in terms of adsorbate diameters, is generated by minimizing the grand canonical potential (free energy of the ensemble) for the system. This potential is built from fluid-fluid and fluid-solid interactions (solid refers to the pore wall material) at the atomic scale, as derived from consideration of attractive and repulsive components. The fluid density is a function of location within the sorption space. The Lennard-Jones 12-6 potential is utilized for fluid-fluid interactions; whereas, the Steele 10-4-3 potential is used to describe solid-fluid interactions.

Lennard-Jones:

$$\phi_{NN}(r) = 4\varepsilon_{NN}\left[\left(\frac{\sigma_{NN}}{r}\right)^{12} - \left(\frac{\sigma_{NN}}{r}\right)^{6}\right] \tag{5.6}$$

where ϕ_{NN} designates the nitrogen pair interaction potential at a separation distance r, and ε_{NN} and σ_{NN} designate the bulk nitrogen well depth from the potential curve and molecular diameter, respectively.

Steele:

$$\phi_{CN}(z) = 2\pi\varepsilon_{CN}\rho_C\sigma_{CN}^2\Delta\frac{2}{5}\left[\left(\frac{\sigma_{CN}}{z}\right)^{10} - \left(\frac{\sigma_{CN}}{z}\right)^{4} - \left(\frac{\sigma_{CN}^4}{3\Delta(z+0.61)^3}\right)\right] \tag{5.7}$$

where ϕ_{CN} designates the potential between the nitrogen molecule and the graphite slab, z is the separation distance from the surface, ρ_C is the graphite density, and ε_{CN} and σ_{CN} are the nitrogen/carbon-well depth and effective diameter, respectively.

In a slit-shaped pore, the nitrogen molecule will experience interactions from both walls, expressed as the sum of : $\phi_{CN}(z)$ and $\phi_{CN}(H\text{-}z)$, and designated $V_{ext}(z)$, where H is the pore width.

The grand potential function, Ω, takes the following form when the mean field approximation is applied to the fluid-fluid interaction energy:

$$\Omega[\rho L(r)] = \tfrac{1}{2}\iint dr dr' \rho_L(r)\rho_L(r')\phi_{att}(|r-r'|) + kT\int dr \rho_L(r)[ln(\Lambda^3\rho_L(r)) - 1]$$
$$+ kT\int dr \rho_L(r) fex[\rho(r); d] - \int dr \rho_L(r)[\mu - V_{ext}(r)] \qquad (5.8)$$

where ρ_L is the local fluid density at position r; Λ is the thermal wavelength of nitrogen; ϕ_{att} is the attractive part of the fluid-fluid potential; and f_{ex} is the Helmholtz free energy per molecule for a hard sphere fluid of diameter d.

The minimization of Ω (an iterative process) results in the pore density profile as a function of pore width H and chemical potential (reduced pressure P/P_o).

A variant of DFT doesn't consider fluid density, but instead models the theoretical pores based on the energy field profile or adsorption energy distribution (Jagiello, Tolles, 1998). This variation, coupled with regularization of the PSD fit to the actual data using B-splines, results in a more stable solution to the adsorption integral (Jagiello, 1994). For the carbons considered here, the results from either method are expected to be interchangeable (Baker, 1999).

Two different forms of density functional theory have commonly been reported in the literature. One involves the local density approximation. This variant does not account for effects due to neighboring molecules or atoms. The other form is referred to as non-local theory. The Tarazona variation of non-local theory makes use of a power series expansion to account for the effects of neighboring species. This is the version of DFT most commonly applied to the problem of characterizing activated carbon PSD.

For activated carbon, the pores are best described by a slit-shaped geometry. Therefore, the theoretical pores have been modeled as parallel planes of a given separation distance. The pore walls have been modeled as being chemically uniform and infinite in area.

These simplifications avoid the difficult characterizations of the heterogeneity and interconnectedness of carbon porosity.

The actual pores are thought to vary in size in a continuous fashion. Therefore, a distribution function was used to fit the model isotherms to the actual isotherm. The theoretical isotherms were fit to the actual isotherms using numerical techniques and interpolating between sizes of theoretical pores. For this application, the log-normal and the gamma functions have been found to be equivalent (Gubbins, 1997).

An example of an N_2 isotherm fit using DFT is given in Figure 5.1. As can be seen from the figure, the fit is consistent across five orders in relative pressure. The cumulative pore distribution for this sample is given in Table 5.1

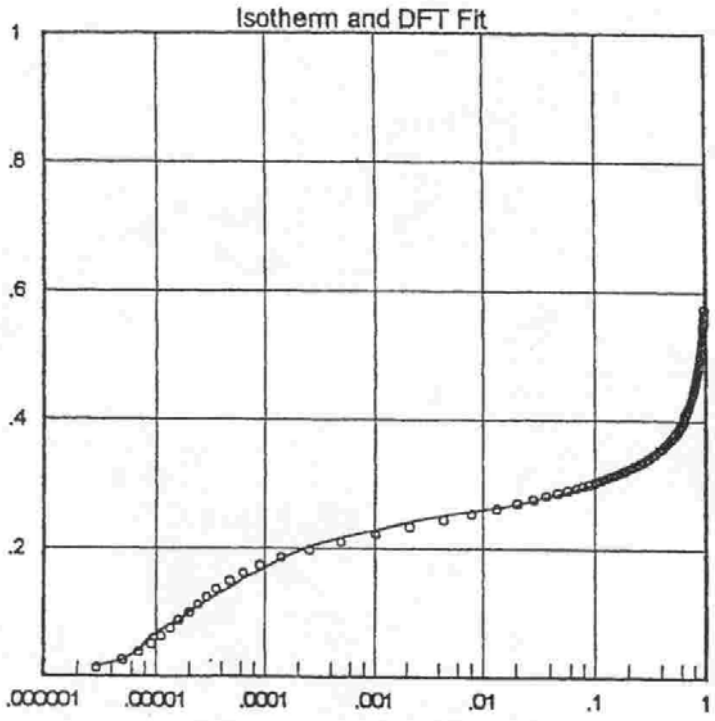

Figure 5.1 Density functional theory applied to N_2 adsorption isotherm data for the activated carbon type designated N1 (Sigma C5260 Lot # 124563).

Table 5.1 Cumulative pore volume and surface area based on isotherm data in Figure 5.1.

Range (nm)	Volume (cc/g)	Area (m2/g)
0.7	0.066	212
1	0.2056	555
1.5	0.2299	595
2	0.2505	620
3	0.2723	636
4	0.3018	653
8	0.3933	686
160	0.4779	701
320	0.5397	707
	BET Area	702

VI. EXPERIMENTAL MATERIALS and METHODS

A. Materials

Water and Reagents

Reverse osmosis (Nanopure) water was used throughout the experimental work, except as noted. Except for sucrose (J.T. Baker) and casamino acids (Difco), all other reagents were obtained from Sigma and were of ACS grade or better purity and were used without further purification.

Activated Carbon

Powdered activated carbon was obtained from three different suppliers (Table 6.1). Sigma supplied untreated powder (C-5260, 400 mesh), designated as "N" type, and acid-washed, tissue culture tested (C-9157) designated as "T" type. Two different production lots of T and N were used, designated as "T1", "T2", "N1", and "N2". Three AC types were supplied through J.T. Baker: Norit Sx2, Norit Sx4 and Darco G60, designated Sx2, Sx4 and G60. Merck AC was supplied through EM, referred to as "Merck".

Table 6.1. Activated carbon designation codes.

Activated Carbon	Lot Number	Designation
Sigma C-5260	124563	N1
	124677	N2
Sigma C-9157	1723656	T1
	672894	T2
Norit Sx2	1739890	Sx2
Norit Sx4	2873499	Sx4
Darco G60	35789	G60
Merck	536782	Merck

Activated Carbon Characterization

Particle appearance, size

Carbon powder was gently blown across double-sided conductive carbon tape affixed to a standard sample stub using a plastic pipet. SEM images were produced using a Jeol JSM 6400. Electron micrographs of activated carbons, N1 and T1, are shown in Figure 6.1. The images revealed irregularly shaped particles of variable size, ranging up to tens of

microns. The majority of the observed particles were less than 20μm, with an estimated median size on the order of 10μm.

A.

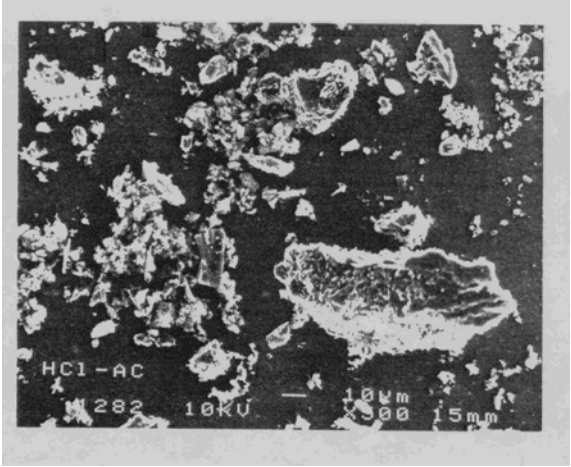

B.

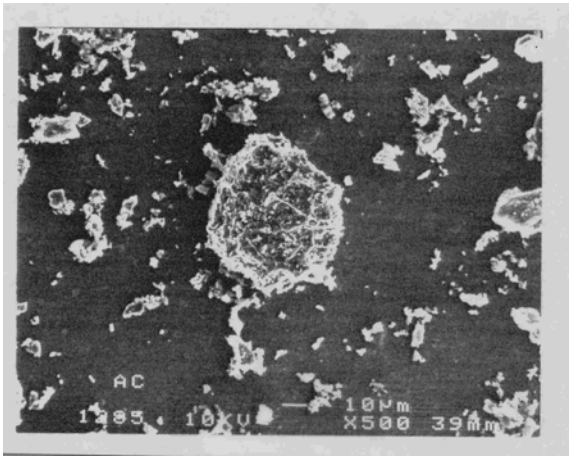

Figure 6.1. SEM micrographs of activated carbon particles. A. T1, B. N1.

Moisture content and apparent density

Moisture content (Table 6.2) was determined for each carbon type by drying replicate samples for twelve hours in an oven set to 150^{o}C. Apparent density was determined according to ASTM D2854 at Westvaco, Charleston, South Carolina. The range in densities measured was in good agreement with the range reported for wood based liquid-

application carbons, 0.25 g/mL minimum (Soffel 1978). In comparison, the minimum for lignite coal was given as 0.48 g/mL

Table 6.2. AC character: moisture content and apparent density

AC Type:	N1	N2	Sx4	T1	T2	Merck	G60	Sx2
Moisture content (%)*	7.4	5.6	8.2	8.3	8.4	5.6	7.8	3.7
Apparent density, g/cc	0.31	0.30	0.33	0.22	0.24	0.27	0.28	0.27

* Moisture content, average of two values, was determined by oven drying at 150^{o}C for 12hrs and is expressed as a percentage of the wet weight; apparent density was determined according to ASTM D2854

Ash analyses

Ash content was determined gravimetrically by combusting AC (2 g) at 650^{o}C within a covered crucible using a muffle furnace. The muffle furnace was programmed to ramp up to 400^{o}, and hold for ten minutes, and then ramp to 650^{o}. The temperature was held at 650^{o} for two hours before ramping down to 105^{o}C. The samples were cooled in a desiccator prior to weighing. The ash levels were significantly higher for the non-acid washed carbons, two to three times the ash levels for the tissue-culture grade carbons (Table 6.3). Ash content in carbons may range from 1 to 20 % by weight, commonly less than 10% for most grades (Baker et al. 1992).

Unsuccessful attempts were made to completely dissolve the ash in nitric, hydrochloric, and phosphoric acids in preparation for ICP-AES analysis. The ash was qualitatively analyzed using the SEM x-ray dispersive feature (Link eXL). These results are shown in Figure 6.2. It may be seen that the ash from both carbons was similar in atomic species, with silica giving a strong signal. Sodium, potassium, and chloride were present in each carbon type to a similar extent. The remaining elements, Mg, Al, P, S, Ca, and Fe gave stronger relative signals in the ash for the non-acid-washed carbons. The presence of clay is a plausible explanation for the presence of these elements.

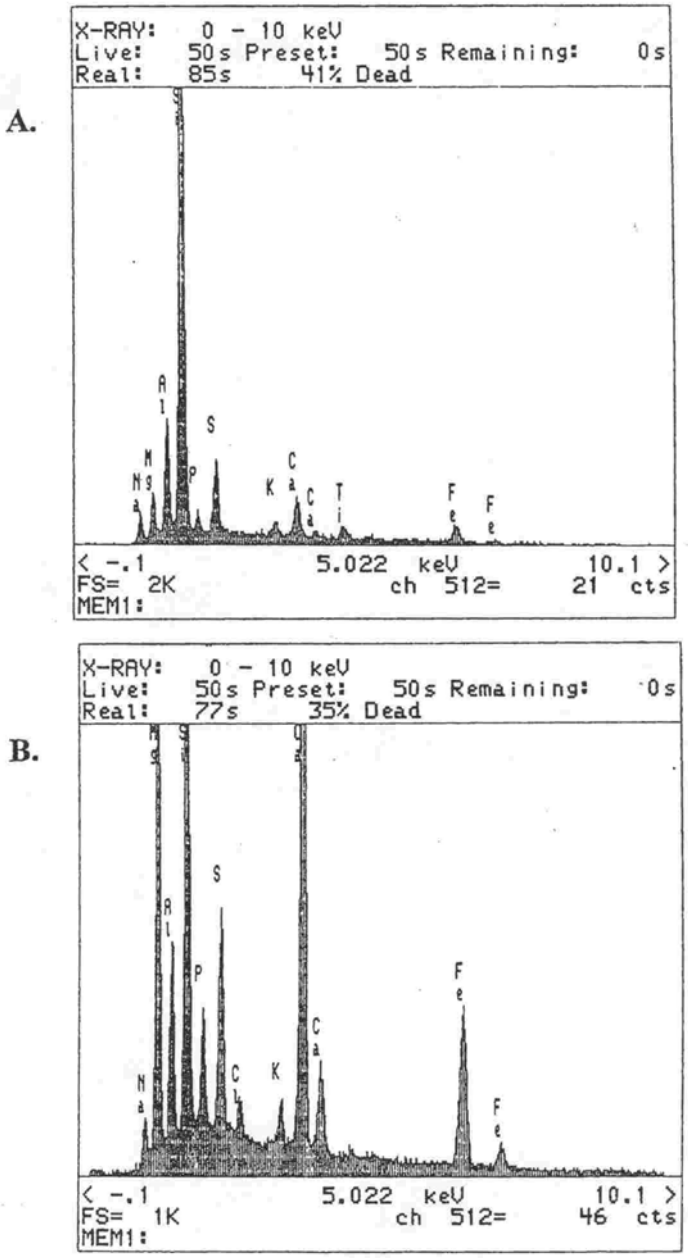

Figure 6.2. Dispersive x-ray spectra (EDS) from SEM scans of the ash of two activated carbons, A. T1; B. N1.

CHNSO analysis

Four carbons (T1, T2, N1, N2) were submitted to the Center for Applied Energy Resources (CAER) at the University of Kentucky in Lexington for ultimate analysis, often referred to as *oxygen-by-difference*. An *ultimate analysis* is a technique which

utilizes a chromatographic separation of gases evolved upon combustion (S, N, and C species), leaving ash, with oygen being calculated by difference (100%, less the sum of the other quantities). The methods referenced by CAER were: ASTM D5142 (proximate analysis), ASTM D5373-93 (CHN analyses) and ASTM D 4239-C (S analysis).

Table 6.3. Ultimate analysis (%) of activated carbon, oxygen by difference*

Sample		C	H	N	S	O	Sum	Ash, mean	Ash, IPST
T1	a	90.4	1.0	1.9	0.2	3.4	96.9	3.1	2.8
	b	86.7	1.1	1.1	0.2	7.8	96.9		
T2	a	89.6	1.1	1.7	0.1	5.1	97.6	2.2	2.6
	b	87.8	1.2	1.1	0.2	7.7	97.9		
N1	a	89.2	1.2	1.6	0.2	2.0	94.2	5.6	5.8
	b	86.3	1.1	1.1	0.2	5.9	94.6		
N2	a	85.4	0.8	1.4	0.2	3.4	91.2	8.6	8.7
	b	85.5	0.8	1.2	0.3	4.1	91.7		

* The analyses were performed at the Center for Applied Energy Research (CAER), at the University of Kentucky using a LECO CHN 600 instrument.

The results of the ultimate analysis are given in Table 6.3 for two separate replications, labeled *a* and *b*, of the four carbon samples (T1, T2, N1, and N2). The range in oxygen content from 3.4% to 7.7% was in good agreement with published data for Norit carbons oxidized to varying degrees: Biniak and co-workers reported a range from 0.42 to 10.28 % by weight (Biniak et al. 1990). Leon y Leon et al. (1992) reported values of 4.18 and 3.08 % for two polymer-derived microporous carbons.

However, a significant variation between trials was displayed, particularly for carbon and oxygen content. The level of variation was great enough that the relative ranking of the carbons with respect to oxygen content was different for the two trials. The ash data from CAER and IPST (average of two samples) were in acceptable agreement, indicating that the variation in the elemental composition was not due to insufficient combustion. This result indicated that several replications were required when using this technique to establish a statistically valid ranking.

FTIR spectroscopy

Measurements were made using a Nicolet Magna 550 with microscope attachment. Carbon was extracted with ether using a soxhlet extractor. Carbon was then dried overnight in a vacuum oven set to 110^{o}C. Oven-dry samples were prepared for FTIR scans in four common modes: KBr pellet (transmittance, 1:500 AC:KBr); DRIFTS (diffuse reflectance); ATR (attenuated total reflectance); and microscope slide (reflectance). Additionally, the KBr pellets were dried overnight in an oven set at 105^{o}C, and spectra were produced from 500 scans at 4cm^{-1} resolution. None of those resulted in spectra that could be used for quantitative characterization purposes, due to the strong, uniform absorbance (high opacity, high extinction coefficient) of the carbon. Spectra for the two carbons are shown in Figure 6.3.

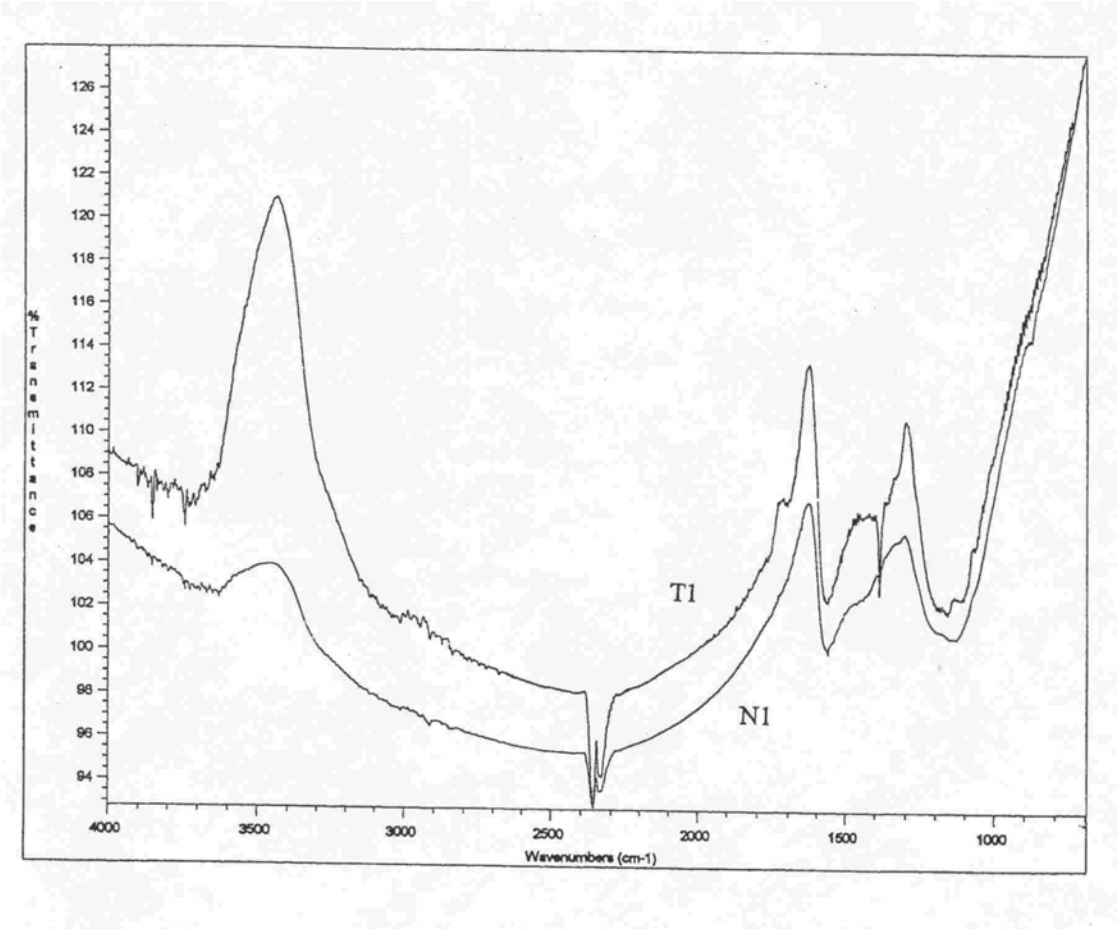

Figure 6.3. FTIR spectra for two different activated carbons, T1 and N1. Carbons were extracted with ether prior to drying. Spectra were obtained from KBr pellets with a ratio of KBr to AC of 500:1.

Peaks have been previously assigned for AC (Kinoshita, 1988; Zawadzki, 1989). Referring to Figure 6.5, the overlapping peaks in the range of 1100 cm^{-1} may be assigned to various vibration modes for C-O bonds as well as phenoxy linkages. The sharp peak near 1400 cm^{-1} may be assigned to phenol. The carboxyl C=O stretch absorbs over the range from 1500 to 1670 cm^{-1} which overlaps the same spectral region attributed to aromatic structures, 1590 cm^{-1}. Peaks in the 1700 to 1760 cm^{1} range may be attributed to carboxyl and lactone carbonyl stretching. The peaks near 2350 cm^{1} are CO_2 artifacts and have no diagnostic value. The 3000 cm^{1} and up range has less diagnostic value, being associated with hydrogen bonding and CH absorption. Overall, the spectra for these two activated carbons were most notable for their similarities rather than differences.

Boehm titration

Solutions of three bases, NaOH, Na_2CO_3, and $NaHCO_3$, were formulated to 0.05M. Activated carbon (1 g) was weighed into a 40 mL vial, and base (35 mL) was added. The vials were sonicated for five minutes, and after 3 days the samples were filtered. The residual base in the filtrate was titrated to the first end point using a back titration method. That is, excess HCl was added (0.1M, 10 mL), the filtrate was then boiled and cooled, and the remaining HCl titrated with NaOH (0.1M).

Data for four different AC's are given in Table 6.4. The results from a Boehm titration are generally interpreted in terms of neutralization of acid groups of decreasing strength, i.e. $NaHCO_3$ neutralizes only the strongest acids (carboxyls); Na_2CO_3 neutralizes the strongest and next weakest (carboxyls plus phenolics); and, NaOH neutralizes all of the acid groups.

Table 6.4. Boehm titration data* for four different activated carbons.

	NaOH	**COV, %**	**Na_2CO_3**	**COV, %**	**$NaHCO_3$**	**COV, %**
T1	32	7.4	36	49.7	19	36.5
T2	26.4	13.8	35	15	8	71
N1	22.7	12.1	33	30.2	n/a	n/a
N2	25.7	12.8	28	38.8	n/a	n/a

* Data are given in milli-equivalents of base per 100 gram of AC. One gram of AC was equilibrated over more than three days with 40 mL of base (all bases were 0.05M). A back titration technique against degassed filtrate was employed. Data are presented for three or more replications..

Though the mean values were in general agreement with other published data (Noh and Schwarz 1990 reported NaOH neutralization ranging from 4 to 60 meq per g), the high coefficient of variation for each base was confounding. Additionally, the non-acid washed carbons did not neutralize any $NaHCO_3$. The interpretation of these data was further confounded by the impact of base concentration: the level of neutralization varied directly with base concentration (Figure 6.4), suggesting kinetic effects.

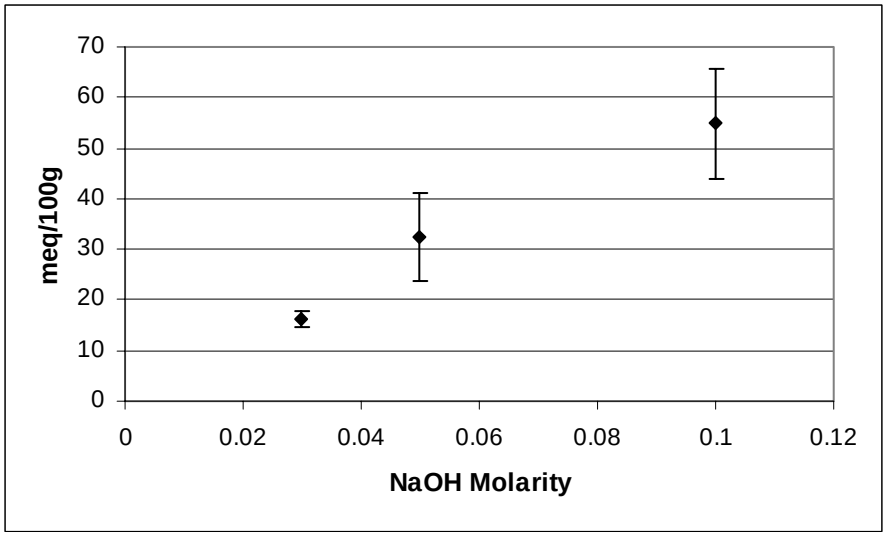

Figure 6.4. Concentration dependence of Boehm titration. NaOH (40 mL) was added to vials containing AC (T1). The carbon was dispersed in an ultrasonic bath and equilibrated 24 hours at room temperature prior to analysis. Filtrate was back titrated using HCl and NaOH (each 0.1M). Error bars depict the 90% confidence interval.

Direct HCl titration

Water (100mL), was degassed by boiling, then poured into a glass bomb. Activated carbon (0.25g) was added to the bomb. Argon was bubbled into the bomb to displace oxygen and CO_2 prior to sealing and autoclaving.

After autoclaving, the slurry was transferred to a beaker (200mL). The titrant (0.01N HCl) was metered to the beaker using a Metrohm Dosimat 665 set at a flow rate of 0.1 mL/min at room temperature (approx 21^{o}C). The beaker, titrant dispensing wand, and glass pH probe were sealed with parafilm and a nitrogen sparge applied to the head space. The slurry was monitored by a pH probe and recorded on a strip chart recorder.

Subsequently, the data were digitized manually and entered into a spreadsheet (MS Excel). The data were analyzed by Jacek Jagiello at Westvaco using a numerical technique, SAIEUS (Jagiello et al. 1995), which is a numerical solution to the adsorption integral equation based on the assumption of a continuous distribution of acidic constants. Those researchers applied SAIEUS to data from NaOH (0.1M) titrations.

Example titration curves for two activated carbons, T1 and N1, are shown in Figure 6.5. The slope of the trace at any given point is a measure of buffering strength. Primary interest was in the region near pH 5.8 where it can be seen that the acid consumption and slopes were significantly different for these two carbons. The buffering strength values for the four carbons are given in Table 6.5.

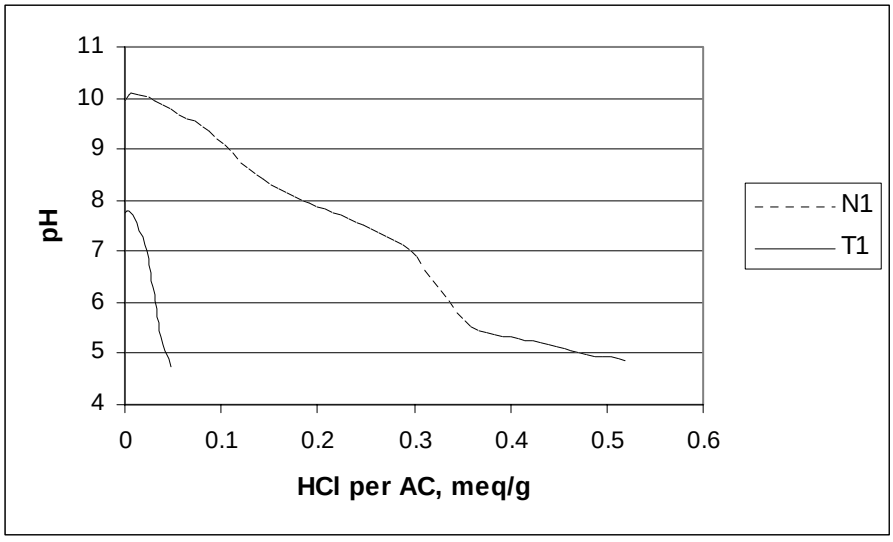

Figure 6.5. Acid titration curves for N1 and T1. Acid (HCl 0.01N) was dispensed at 0.1mL/min into AC slurry (0.25g per 100mL degassed, nanopure H_2O). Headspace was sparged with nitrogen during titration.

Table 6.5. Buffering strength for four activated carbons at pH 5.8.
(from titration data).

	N1	N2	T1	T2
Buffering strength per g AC (ΔpH/meq H+)	-24.2	-23.1	-138	-138

The non-acid-washed carbons, N1 and N2, were nearly equal and displayed six times the buffering strength of T1 or T2 at pH 5.8. At pH 5.3 the non-acid washed carbons had thirty-nine times the buffering strength of T1 or T2.

The titration data of Figure 6.5 were first translated into a proton binding isotherm format (mmol vs. pH) and then analyzed with SAIEUS, a numerical technique (Jagiello et al. 1995). SAEIUS produces a stable solution to the adsorption integral equation using a regularization technique. The results are shown in Figure 6.6.

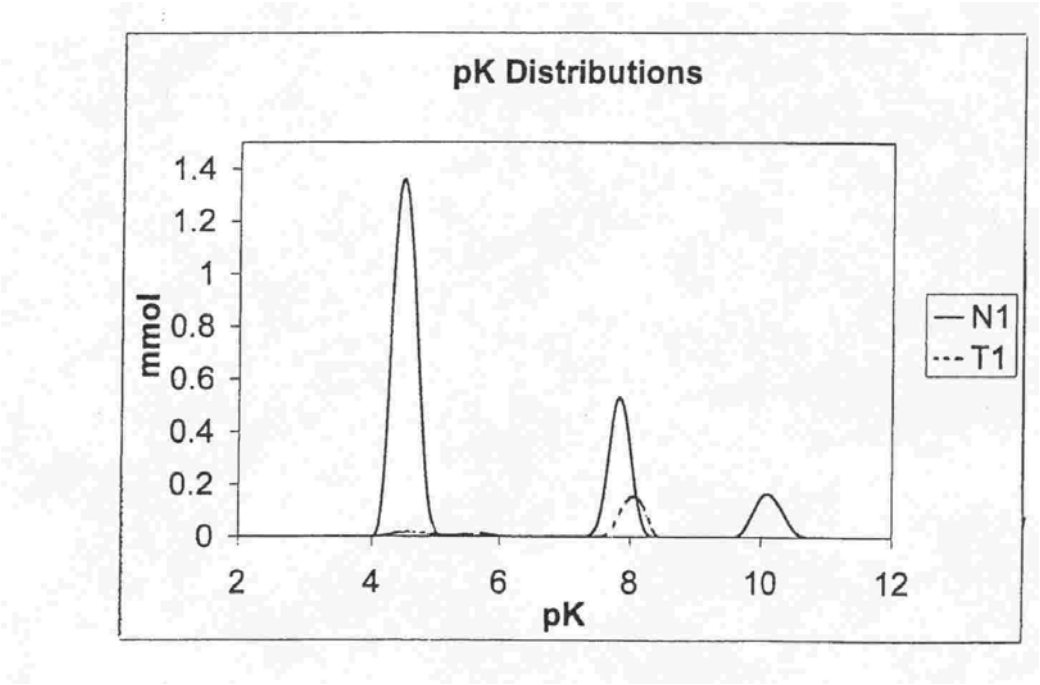

Figure 6.6. Distribution of acid dissociation constants based on acid titration data. A numerical technique, SAIEUS, was applied to the adsorption integral equation to fit the titration data (Jagiello et al. 1995; Jagiello 1994). Analysis courtesy of Westvaco.

The calculated isotherms that result from the distributions of dissociation constants are compared with the actual data in Figure 6.7. As with the density functional theory, the fit was excellent. The distributions of the dissociation constants were similar for the two different carbons; however, the number of sites was much greater for the non-acid washed carbon.

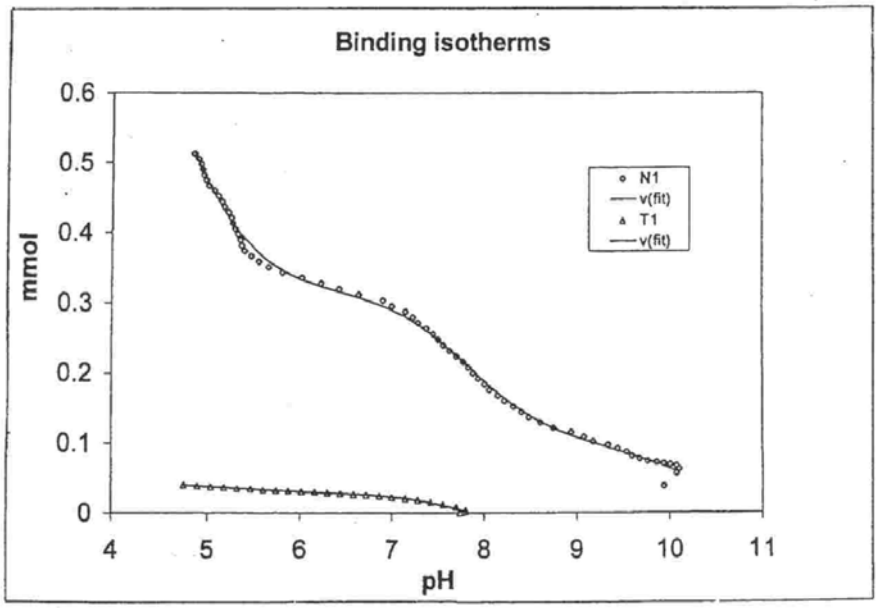

Figure 6.7. Proton binding isotherm data compared with calculated isotherm based on the distribution of dissociation constants shown in Figure 6.6.

Zeta potential

Zeta potential was measured manually using a Zeta-meter, an electrophoresis instrument consisting of a flow cell, dc voltage source with integral timer, and a calibrated, dual microscope. Voltage was also monitored using a separate digital multi-meter. Prior to making measurements on a sample, a calibration check was performed using a colloidal silica standard.

Water was degassed by boiling. Carbon (0.01 g) was added to the degassed nanopure water (200 mL), dispersed with ultrasonic bath, and equilibrated 24 hours prior to measurements. Typically, 200V were applied and a group of particles were tracked and timed across three divisions in the ocular grid. A further series of groups was measured until ten divisions had been traversed. The total elapsed time was about 40 seconds. After each individual measurement the slurry was remixed. Two measurements were performed on each sample. Three samples were measured for each replication and three or more replications were performed.

The estimate of isoelectric point (IEP) is generally carried out by measuring EM for particles over a range of pH levels which bracket the IEP, then extrapolating to zero mobility. An EM of zero indicates that the positive and negative charges on the outer perimeter of the hydrated particles are in balance, i.e. the net zeta potential is zero.

The velocity, or electrophoretic mobility, of the particles in a slurry varies with the applied voltage. Zeta potential may be calculated from EM using the Helmholz-Smulokowski equation:

$$EM = ZPxD_t / (4\pi V_t), \tag{6.1}$$

where *EM* is the electrophoretic mobility of the particle(s) in cm/sec per esu volt per cm; *ZP* is zeta potential (esu); D_t is the dielectric constant of the suspending liquid; and V_t is the viscosity of the suspending liquid in poise.

Dilute suspensions of activated carbon in nanopure water (0.05 g/L) were analyzed for zeta potential and these data are given in Table 6.6.

Table 6.6. Zeta potentials for four AC's from dilute aqueous suspensions.

	T1	**T2**	**N1**	**N2**
No. of replicates	3	5	3	3
pH	5.8	5.0	6.1	6.2
Zeta potential (mV)	45.3	37.5	62.8	59.6
Std dev.	2.1	2.5	3.7	3.9

Carbon (0.01 g) was added to degassed nanopure water (200 mL), dispersed with ultrasonic bath and equilibrated 24 hours prior to measurements. The mean value for each replicate was determined on six samples, i.e. the mean ZP for T1 resulted from eighteen separate measurements.

Attempts to extend the technique to the approximation of the IEP were confounded by the slow-moving carbon particles that tumbled and fell out of the focal plane. Increasing the voltage to compensate resulted in heating of the fluid, undesirable, as zeta potential varies with temperature. If the flow cell were heated enough, the carbon particles assumed a spiral trajectory. This phenomenon was particularly apparent for the attempted IEP

characterization, which required a fairly high, constant ionic background over a pH range near the IEP (low EM).

The positive EM for all of the carbons tested was consistent with materials suspended at pH below their IEP.

Point of zero charge (pzc)

Activated carbon (1g/L to 62 g/L) was added to water (40 mL) within sealed polystyrene bottles and dispersed by shaking on a shaker table. After two days the water was decanted by pipet to a plastic test tube and the pH measured (Orion 410a with combination electrode Orion 9106). The asymptotic limit was estimated from the resulting plot.

The point of zero charge represents an equivalence of positive and negative charges. The point of zero charge differs from the IEP in that it is a static measurement and accounts for the *total* surface rather than just the outer perimeter of the hydrated particle. The PZC may be approximated using mass titration, a simple technique where activated carbon is added to water until a pH asymptote is approached (Noh, Schwarz 1990).

For these carbons, the pH value at 62.5 g/L was used as an estimate of the PZC. The plots for N1 and T2 are shown in Figure 6.8. The data have been tabulated for four carbons in Table 6.7.

Table 6.7. Point of zero charge for four carbons.

	PZC	**Std dev**
T1	8.5	0.4
T2	10	0.11
N1	10.7	0.05
N2	11	0.06

Numbers based on five replications; see note for Figure 6.8.

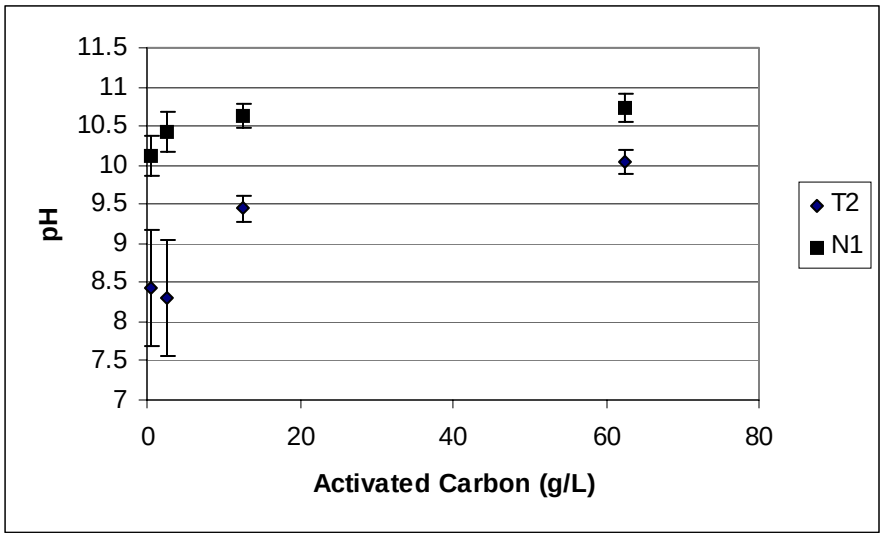

Figure 6.8. Point of zero charge (pzc) approximation. Carbon (0.5, 2.5, 12.5, 62.5 g/L) was added to water (40 mL). Measurements were made after three days. Error bars represent the 90% confidence interval based on five replications. Error bars depict the 90% confidence interval.

Porosity

The activated carbons were characterized for BET surface area and pore volume distribution at Westvaco, Charleston, S.C. (nitrogen adsorption at 77 K, Coulter Omnisorp 100). Prior to analysis, samples were dried at 420 K and outgassed under vacuum for several hours at 520 K to attain an indicated pressure below $5x10^{-6}$ torr. Cumulative pore volume distributions were produced from the nitrogen sorption data using density functional theory (Jagiello, Tolles 1998).

Four carbons were analyzed for BET surface area at IPST using a Micromeretics Flowsorb 2300 instrument (single point approximation, N_2 @ 22% relative pressure). Prior to analysis, samples were dried overnight under vacuum at 495 K and then outgassed on the instrument under nitrogen at 673 K. The calibration on the Flowsorb was found to be 4.4% low. The adjusted data, along with the Westvaco data are compared in Table 6.8.

The pore volume distribution for eight different activated carbons was generated at Westvaco by applying density functional theory to nitrogen adsorption data over five orders of magnitude in relative pressure. (See Figure 5.1 for an example DFT plot). The

cumulative pore volume data for the eight carbons are given in Table 6.9. The micropore volume is highlighted on bold, and represents cumulative volume to pores of 2 nm in size. The total pore volume was taken as the last value given, cumulative volume to 32 nm.

Table 6.8. BET Surface area comparison*.

	N1	N2	T1	T2
Westvaco	702	753	1105	949
IPST	681	741	1100	986
Std dev.	67	44	85	24
No. of samples	6	3	3	3

Values are given in m^2/g.

Table 6.9. Cumulative pore volume (cm^3/g) from nitrogen adsorption, fitted using density functional theory. Samples analyzed at Westvaco, Charleston, South Carolina.

Range, nm	N1	N2	Sx4	T1	T2	Merck	G60	Sx2
0.7	0.066	0.072	0.079	0.075	0.070	0.067	0.067	0.060
1	0.206	0.223	0.207	0.259	0.242	0.236	0.250	0.215
1.5	0.230	0.260	0.231	0.334	0.299	0.281	0.305	0.248
2	**0.251**	**0.286**	**0.249**	**0.391**	**0.341**	**0.315**	**0.344**	**0.272**
3	0.272	0.308	0.270	0.431	0.374	0.341	0.373	0.291
4	0.302	0.329	0.295	0.470	0.405	0.373	0.402	0.319
8	0.393	0.385	0.364	0.566	0.501	0.461	0.483	0.384
16	0.478	0.435	0.413	0.698	0.618	0.568	0.578	0.468
32	0.540	0.482	0.442	0.833	0.730	0.645	0.679	0.535

Summary, AC Characterization

The most difficult aspect of characterizing the activated carbons proved to be quantifying oxygen content and identifying oxygen functionality. The FTIR results were inconclusive. The Boehm titration results were found to vary with the concentration of the titrant. The oxygen-by-difference analysis (CHNSO) gave a high level of variability. None of these techniques satisfied the objective of identifying a meaningful, reliable parameter. A better technique is needed.

The translation of acid titration data to an equivalent distribution of dissociation constants is a promising technique that avoids the pitfalls of classifying carbons on the basis of

classical organic chemistry and oxygen functionality. The titration is a standard technique. The mathematical algorithms may be programmed.

The attempt to characterize carbons for isoelectric point was confounded by factors elaborated previously. The point of zero charge approximation through mass titration was adequate, simpler to apply, and gave a low standard deviation. A major advantage of the pzc is that it uses a significant mass (1g per 40 mL) and therefore approaches a bulk quantity.

The most developed techniques for characterizing activated carbon are those based on the interpretation of gas-phase isotherm data.

Selected characterization data are summarized in Table 6.10.

Table 6.10. AC Chemical and Physical Characteristics

	Ash	**PZC**	**ZP**	**Buffering at pH 5.8**
	(%)	(pH)	(mV)	(ΔpH/meq H+)
T1	2.8	8.5	45.3	-138
T2	2.6	10	37.5	-138
N1	5.8	10.7	62.8	-24.2
N2	8.7	11	59.6	-23.1

	N1	**N2**	**Sx4**	**T1**	**T2**	**Merck**	**G60**	**Sx2**
Moisture content[1], %	7	6	8	8	8	6	8	4
Apparent density[2], g/cm^3	0.313	0.301	0.334	0.224	0.238	0.273	0.28	0.272
BET*, m^2/g	702	753	668	1105	949	872	931	736
Micropore Volume*, cm^3/g	0.251	0.286	0.249	0.391	0.341	0.315	0.344	0.272
Total Pore Volume*, cm^3/g	0.540	0.482	0.442	0.833	0.730	0.645	0.679	0.535
Ratio of Micro to total, %	46	59	56	47	47	49	51	51

* Data generated by Westvaco.
1. Weight %, wet basis
2. Dry basis

Tissue Culture Medium

The growth medium for the tissue culture experiments and the sorption experiments was based on a one-half strength Brown and Lawrence formulation (Amerson et al. 1985), ½ BLG. This was essentially the same formulation as that reported by Wann and Verhagen

(1988), the major difference being omission of the gelling agent. The same medium has been referenced as 'MSG' media (Tautorus et al. 1991). Compositions for standard media without AC and modified media containing AC (1.25 g/L) are included in Table 6.11.

Table 6.11. Medium composition (mg/L)

½ BLG Macro Salts	½ BLG ("Standard")	Modified for AC
KCl	372.5	372.5
KNO_3	50	50
KH_2PO_4	85	85
$MgSO_4 * 7H_2O$	160	160
$CaCl_2 * 2H_2O$	220	220

1/2 MS Micro Salts	½ BLG ("Standard")	Modified for AC
KI	0.415	0.415
H_3BO_3	3.1	3.1
$MnSO_4 * H_2O$	8.45	8.45
$ZnSO_4 * 7H_2O$	4.3	8.6
$Na_2MoO_4 * 2H_2O$	0.125	0.125
$CuSO_4 * 5H_2O$	0.0125	0.25
$CoCl_2 * 6H_2O$	0.0125	0.0125
$FeSO_4 * 7H_2O$	13.9	13.9
Na_2EDTA	18.65	18.65

Organic Components	½ BLG ("Standard")	Modified for AC
Sucrose	10,000	10,000
myo-Inositol	50	50
Casamino acids	500	500
L-Glutamine	750	750
Thiamine HCl	0.05	0.15
Pyridoxine HCl	0.05	0.15
Nicotinic Acid	0.25	0.75
L-Asparagine	50	50
2,4-D	2	varying
BAP	1	varying
pH	5.8	5.8

The media were prepared by pipetting from stock solutions of higher concentration with the exceptions of casamino acids and sucrose, which were dissolved in the media as dry reagents. A beaker was filled with nanopure water to approximately half of the final volume. The volume of medium varied with the experiments, but in every case a volumetric flask was used to achieve the target volume. After the media had been

formulated and brought to volume, activated carbon was added and the pH of the medium adjusted using HCl or KOH, each at concentrations of 1N, 0.1N and 0.01N.

Media were sterilized using an autoclave (Amsco, Laboratory model). The autoclave cycle was the same for all of the tissue culture and adsorption experiments. Approximately 3 minutes were required to ramp up to pressure and temperature (saturated, 121^{o}C).

Media were then autoclaved for 22 minutes. Approximately 4 minutes were required to ramp down at the end of the cycle. Media were promptly removed from the autoclave after atmospheric pressure had been reached.

All subsequent manipulations of the media were carried out aseptically, within a laminar flow hood. Glutamine, which is known to break down under autoclave conditions, was filter sterilized and added to media after autoclaving.

B. Methods

All pH measurements were performed using a glass gel-filled electrode (Orion). Measurements were typically performed on filtered samples.

Chemical Analyses

Elemental analysis, ICP

Each experimental treatment was replicated two or more times. Media were prepared in bulk per each replication. For these experiments, the hormone levels were 90 ppm BAP and 100 ppm 2,4-D. Activated carbon (0.125g/100 mL or 1.25g/L) was weighed into individual flasks (Ehrlenmeyer 250 mL). A flask without activated carbon served as the control. Media, 100 mL, were poured into the flasks and pH adjusted prior to autoclaving. The media were equilibrated two days on a shaker table at 21^{o}C. Samples (10 mL) were collected using sterile, disposable syringes, and were filtered through syringe filters (Acrodisc Tuffrin membrane, 0.22μm pores, 25mm diameter, Gelman) which had been pre-rinsed with water. The first few mL of filtrate were discarded. The remaining 7mL

were collected and acidified with concentrated HNO_3 (2 drops). The samples were analyzed for 30 cations using inductively coupled plasma – atomic emission spectroscopy (ICP-AES, Perkin Elmer Optima 3000DV). Each individual sample was measured three times and the three values were averaged.

Anion (Cl^-, NO_3^-) analysis, CIE

Tissue culture media were prepared (500 mL) with hormone levels of 100 ppm 2,4-D and 90 ppm BAP. Activated carbon, 0.125g T1, was weighed into each of three flasks (250 mL). Medium was (100mL) poured into each of the four flasks, three with AC and one control (no activated carbon). Media were pH adjusted to 5.8 prior to autoclaving, then shaken on a rotary shaker for 24 hours prior to sampling. Samples were filtered as for cation analyses but no acid was added.

Capillary ion electrophoresis (CIE) was performed using a Waters Capillary Ion Analyzer with fused silica capillary and 1.8mM OFM high mobility electrolyte. The electrolyte was prepared by passing 100 mMolar TTAB (tetradecyltrimethylammonium bromide), 1.8 mL, through an anion exchange cartridge attached to a 20 cc syringe (Alltech maxi-clean IC/OH PLUS, prerinsed with two 10 mL aliquots of reagent water). The cartridge was rinsed with water (two 10 mL aliquots) after eluting TTAB. The rinsate and conditioned TTAB were combined in a 100 mL flask. To this flask were added 100 mM sodium chromate tetrahydrate (5 mL), and 100 mM CHES (2-[N-cyclohexylamino]-ethane sulfonate), 10 mL. The solution was brought to volume with reagent-grade water. Each capillary was preconditioned by rinsing for 10 minutes with 0.5N NaOH, followed by ten minutes of water rinse.

Hormone analysis

Media were prepared in bulk for each experimental replication, as for cation analysis. Treatments were replicated three times unless otherwise noted. The media were equilibrated 2.5 days on a shaker table set at 100 rpm at 21^{o}C. Samples (10 mL) were collected using sterile, disposable syringes and were filtered through sterile syringe filters as for cation analyses.

The separations were performed using a Hewlitt Packard 1090 Liquid Chromatograph equipped with an autosampler. Samples were refrigerated in sealed vials if they weren't analyzed the same day they were prepared. The reversed phase separation (C-18 column packing, 5μm Aldrich, with guard column) was isocratic, using a 50/50 methanol/ aqueous buffer mobile phase containing KOH-acetate buffer (0.01M) adjusted to pH 6.0, flowing at the rate of 0.5 mL/min. Under these conditions, 2,4-D eluted within 9.3 minutes and BAP required approximately 24 minutes. The UV-diode array detector was set to monitor three wavelengths: 284nm, 270nm, and 230nm.

HPLC Calibration

The calibration curve for 2,4-D was constructed using solutions of a calibration-standard grade powder obtained from Chem Service of Westchester, Pennsylvania. A calibration standard was not available for BAP: its calibration was based on the grade supplied through Sigma (B-3408), described as "better than 98% pure". The calibration solutions were formulated by dilution of stock solutions (1 g/L), which were formulated with the aid of KOH (1 N) in the case of 2,4-D, and HCl (1 N) in the case of BAP. Calibration samples were pH adjusted to pH 5.8 and filtered through Acrodisc Syringe filters (Gelman, 0.22 μm) prior to analysis. The filters were found to have no impact on the measurements as compared to centrifuged and decanted samples.

For each hormone, over the concentration range studied, a linear calibration was adequate. For 2,4-D, UV absorbance at 230 nm was most often used, though occasionally UV_{284} was used due to an interference that became significant at concentrations below 0.7 ppm. For BAP, UV_{270} was used throughout. Peak identity was confirmed using the UV spectrum produced by the diode array detector.

Bioassay Procedures

Media

Media were generally stored one day prior to dispensing to petri plates. However, for the tissue culture experiments with media containing 0.3 g/L AC, 2.5 days were allowed for

media equilibration prior to dispensing. Liquid growth media (10 mL) were aseptically dispensed within a laminar flow hood into 15 mL disposable polystyrene petri plates. Support for the cultured cells was provided by a filter/pad combination (Ahlstrom #8613-0425, 47mm filter black cellulosic) and polyester padding (Poly-fil batting, Fairfield Processing Corp.) The filter and pad combinations were rinsed three times and autoclaved prior to use. Explants (see seed preparation section, below) were transferred to the culture plates the same day that the media were dispensed.

Seed preparation

Mature Norway spruce seeds (*Picea abies* L.S.) were obtained from the F.W. Schumacher Company, Inc., Sandwich Massachusetts. The seeds were stored frozen. For each experimental replication, approximately 20% more than the required number of seeds were rinsed under tap water for 30 minutes prior to soaking overnight. The next day the seeds were surface sterilized.

The sterilization procedure involved agitating the seeds for ten minutes in a solution of detergent (10% Liquinox) and Tween 20 (0.15%) followed by rinsing with tap water (30 min). The seeds were then sterilized with 20% H_2O_2 (approx. 150 mL, 10 min). The seeds were rinsed five times with five volumes (approx. 150 mL each) of water (10 min per volume), under asceptic conditions.

On the same day they were surface sterilized, the seeds were asceptically dissected. The hard seed coat and interior integuments were removed. The remaining gametophyte was sectioned carefully to remove the embryo without damaging it, though the suspensor cells were severed. Each embryo, and its gametophyte sections, was then transferred to a petri plate containing the liquid growth medium and filter pad support (described below). The plates were wrapped in parafilm and incubated at 21^{o}C, and 50% relative humidity using a sixteen hour photoperiod.

Each experiment was monitored for nine weeks. A “success” was scored when a culture produced one or more somatic embryos as determined from visual morphological features, observed using an optical dissecting stereo microscope.

Imaging

Cultures were imaged using a stereoscope (Zeis Axioplan 2) and digital video camera (Sony DKC-5000). Images were processed using Photoshop software.

Fluorescein diacetate staining procedure

Tissues suspected of being embryo suspensor mass (ESM) from a live culture were gently dispersed in a test tube with water (a few milliliters) using a glass stirring rod. Fluorescein diacetate stain (20μL, Sigma-Aldrich) was added to the suspension (Haugland 1992). The tube was gently swirled to promote mixing. Cells were transferred to the inverted lid of a disposable polystyrene petri plate (15mL). The bottom part of the plate was then gently placed into the lid, in effect acting as a cover slip. This mounted tissue was then imaged using a fluorescing microscope (Zeis Axioplan 2) and digital video camera (Sony DKC-5000).

VII. MEDIUM COMPOSITION: MINERAL ELEMENTS

A. Results

AC Characterization

The four carbons (T1, T2, N1 and N2) were characterized for BET surface area, pH at the point of zero charge (PZC), ash content (Table 7.1), and buffering strength at pH 5.8.

It can be seen that N1 and T1 were substantially different in all four categories, with the surface area for N1 being about half that for T1, the ash percentage being about double, and the PZC differing by several units. The buffering strength also differed by a factor of more than 2.5. The ash from each carbon was subsequently scanned for heavy metal species using SEM-EDS. The atomic species were similar for both AC types with evidence for the presence of clay, sulfates, and silicates, i.e., atomic species included aluminum, silicon, magnesium, calcium, and sulfur.

Table 7.1. Activated carbon character summary.

AC Sample	Ash %	PZC, pH	BET m^2/g	Buffering Strength per g AC (ΔpH/meq H+)
T1	2.8	8.5	1105	-138
T2	2.6	10	949	-138
N1	5.8	10.7	702	-24.2
N2	8.7	11	753	-23.1

"T1" and “T2” designate acid-washed, tissue culture tested, Sigma #C 9157 AC from two different production lots; “N1” and “N2” designate two different production lots of untreated powder, 100-400 mesh, Sigma #C 5260.

Data for the second production lot for each type of activated carbon, designated N2 and T2, are also included in Table 7.1. Except for the buffering strength values, the parameters were significantly different for the two different production lots of each type of carbon. However, the differences between the types were of greater magnitude.

From Table 7.1, it may be seen that the extremes in two properties were represented by T1 and N1. Additionally, tissue culture experiments had been performed earlier at IPST using these carbons. Therefore, these two carbons were chosen for further study.

The ash from these carbons proved to be only partially soluble in nitric acid. An SEM-EDX scan revealed that the primary elements were the same for both carbons: calcium, magnesium, aluminum, and silica.

Medium pH

The pH of the medium was adjusted to pH 5.8 after AC addition and just prior to autoclaving. Data depicted in Figure 7.1 show the pH of a medium two days after autoclaving, a typical timeframe prior to introduction of a culture. The data show that media with significantly different pH resulted from use of two different activated carbons, T1 and N1. Further, the pH of the resulting medium varied depending on how much time was allowed for pH adjustment prior to autoclaving. This trend was demonstrated by each activated carbon, but was more pronounced for N1.

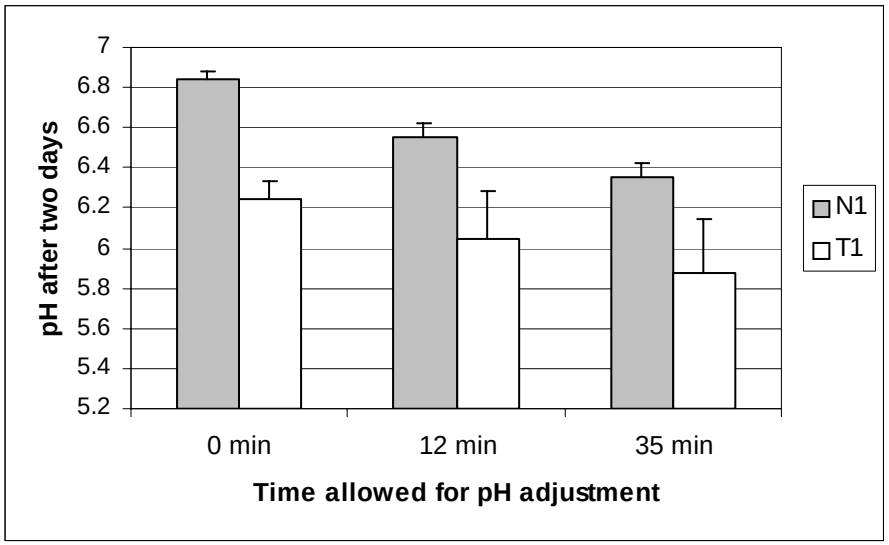

Figure 7.1. Medium pH varied with preparation. Media were adjusted to pH 5.8 prior to addition of AC. After the AC (1.25 g/L) was added, 0, 12, or 35 minutes were allowed for further pH adjustment prior to autoclaving. The pH measurements were taken after the media had equilibrated two days.

As shown by the PZC data, these carbons were basic in nature. Even the acid-washed carbon, T1, retained a slightly basic nature. Thus, pH adjustment prior to autoclaving neutralized more of this alkalinity as more time was allowed. The buffering strength data (Table 7.1) revealed a large difference between the two carbons.

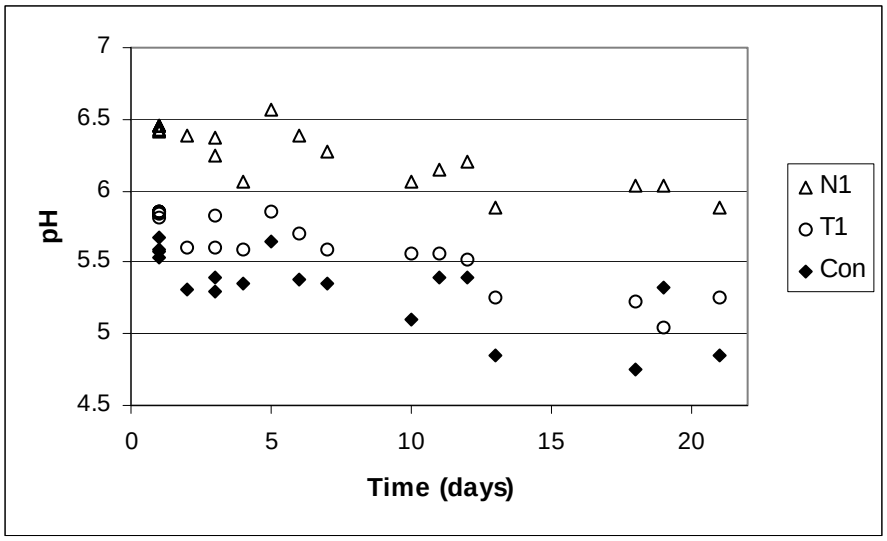

Figure 7.2. Growing culture decreased medium pH. Data were collected from media prepared using support membranes (mixed cellulose esters) which were found to be nearly pH neutral and have insignificant buffering effect. Each data point represents a single culture plate (destructive measurement). Activated carbon was added to media at 1.25 g/L. The control media contained no activated carbon.

After autoclaving, the media with N1 routinely exceeded pH 6.5, media with T1 gave pH 5.8, and control media were near pH 5.6. It is well documented that the pH of the tissue culture medium is altered by growing cultures (Minocha 1987). Norway spruce cultures were found to drive the medium to pH 4.8 over a period of about twenty days (Figure 7.2). Therefore, media containing the two different activated carbons were studied over the range from pH 4.8 to pH 6.5.

Acid titration curves for two activated carbon samples slurried in water were shown previously in Figure 6.5. The differences in slope (buffering strength) between the two carbons were significantly greater in the titration zones above pH 7 and below pH 5.5. A prominent end-point drift was also observed for N1 (not shown): within fifty-five minutes of reaching pH 4.8 the pH had drifted beyond pH 5.5. An additional milliliter of titrant was required to again reach the end point of pH 4.8. This drift in end point was mirrored by the difficulty in attaining a stable target pH level for growth media containing N1. Autoclaving accelerated this drift in pH.

Mineral Nutrient Composition: Allowing for AC

The culture medium for these experiments was based on modifications to the Brown and Lawrence formulation (Verhagen, Wann 1988). The ionic composition of the growth medium was derived from ½ Murashige and Skoog micronutrients and ½ BLG macronutrient composition. Based on the prior findings of Pullman et al. (1995), the zinc and copper levels were increased by 2x and 20x, respectively, to correct for depletion by AC. The media formulations were compared in Table 6.11. Successful initiation of Norway spruce somatic embryos was observed for the control medium and for media modified to accommodate AC at the level of 1.25 g/L. These modifications are given in the second column of the table and simply allow for known adsorption by AC.

Elemental Composition: Cu, Zn, Fe

The elemental composition of the medium was found to change at a very slow rate after the initial two days; therefore, measurements at two days were treated as equilibrium data. The cations displaying the most dramatic behavior in response to either AC or pH were Fe, Mn, Zn, and Cu. Copper, zinc and iron will be considered first.

The available concentration (ppm) of each element was determined from the solution phase at different pH levels. The resulting data are presented as a function of medium pH at the time of filtration for each carbon type, N1 and T1, in Figures 7.3, 7.4 and 7.5.

The control samples, labeled "Con", were media without activated carbon, but with elevated copper and zinc levels, as well as elevated hormones (Table 6.11, right column). Standard media, "Std", did not contain activated carbon and were formulated with normal hormone, copper, and zinc levels (Table 6.11, left column). The calculated value appears as a dotted line across the figure and is based on the non-AC medium composition (Table 6.11, left column).

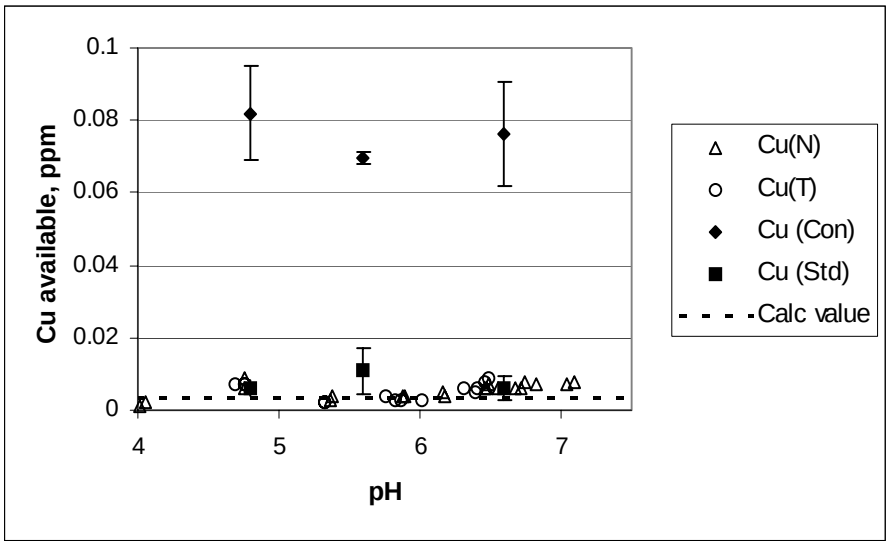

Figure 7.3. Available copper vs. carbon type and pH. Data are presented for media with both AC types (N1, T1, 1.25 g/L) and two controls. "Std" refers to media with normal Cu and Zn levels, "Con" refers to media with the same Cu and Zn as the AC-containing media (20x and 2x Std levels, respectively). Error bars for Con and Std treatments depict the 90% confidence interval based on three replications.

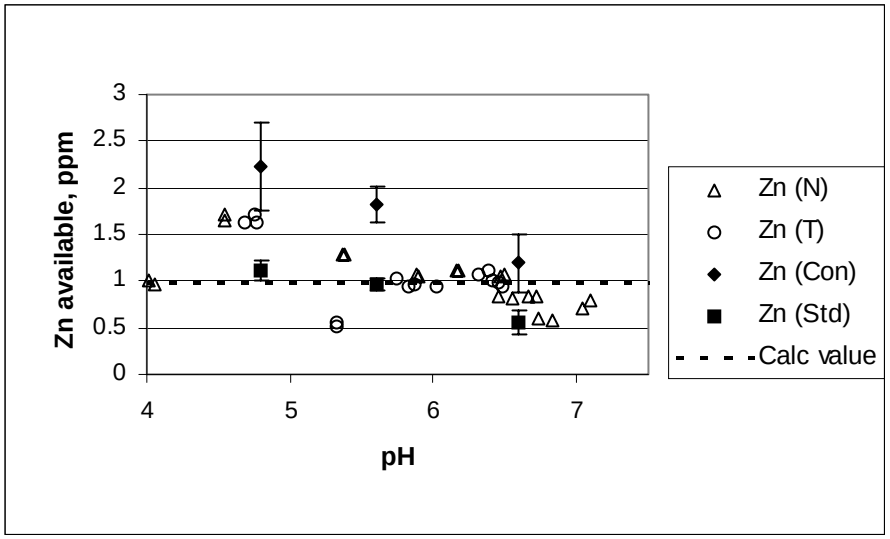

Figure 7.4. Available zinc vs. carbon type and pH. Data are presented for media with both AC types (N1, T1, 1.25 g/L) and two controls. "Std" refers to media with normal Cu and Zn levels, "Con" refers to media with the same Cu and Zn as the AC-containing media (20x and 2x Std levels, respectively). Error bars for Con and Std treatments depict the 90% confidence interval based on three replications.

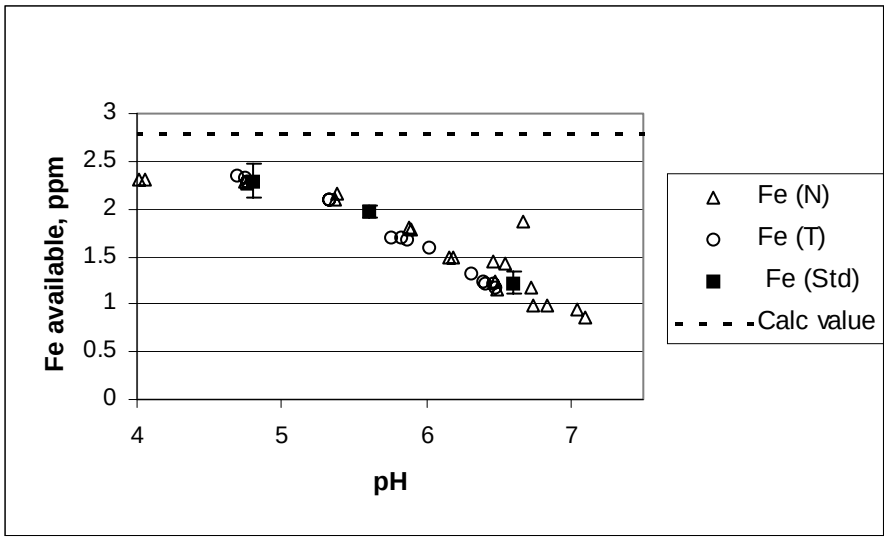

Figure 7.5. Available iron vs. carbon type and pH. Data are presented for media with both AC types (N1, T1, 1.25 g/L) and the standard media without AC (Std). "Std" refers to media with normal Cu and Zn levels; AC media contained elevated copper and zinc (20x and 2x Std levels, respectively). Error bars for Std treatment depict the 90% confidence interval based on three replications.

The variability in Figures 7.3, 7.4, and 7.5 is expected to represent what may be encountered in standard practice. Each data marker represents a single observation but most conditions were replicated at least twice and the experiments were performed over a period of months using different stock solutions to formulate the media. Many of the markers for the replicates overlapped as the difference (range) was generally less than 3% of the mean value. However, the variability of the copper data was greater than this level, with the range sometimes exceeding 10% of the mean. The higher variability for copper was attributed to the lower levels present and hence a greater impact due to impurities introduced during sample preparation prior to analysis, and instrument variability.

Copper and zinc (Figures 7.3 and 7.4) were the only mineral elements present in the medium to demonstrate adsorption onto activated carbon. It is expected that cobalt was also adsorbed, but the concentrations of cobalt were below the detection threshold of the instrument. Cobalt adsorption onto AC has been documented (Howard, 1988). However, cobalt complexes have lower stability constants than those for copper and zinc (Morel, Hering, 1993); thus, cobalt adsorption was not expected to significantly impact the

adsorption of the other two ions. Cobalt is not considered to be an essential nutrient (Minocha, 1987), and so its probable depletion is not a critical concern.

As shown in Figure 7.3, approximately 95% of the copper was adsorbed (compare control media, Con, with AC-containing media, T or N). It may also be seen that nearly 50% of the zinc was adsorbed for media below pH 5.8. Compensating for adsorption by doubling the initial concentration of zinc and increasing copper twenty fold, resulted in copper and zinc levels which were in good agreement with those for media without activated carbon (compare "Std" to "T", "N " data), confirming prior results (Pullman et al., 1995). Note that the present data do not indicate significant differences based on AC type.

Zinc and copper differed in pH response. For control media without AC (Con), zinc declined in concentration as pH increased. For the standard media (Std) a pH response was indicated at pH 6.5. For media with N1 and T1 the data were inconclusive; however, if the data points at pH 4.0 are neglected, a pH response was indicated for N1. Copper, showed no pH trends for the control (Con) or standard (Std) media, but showed increased availability with increased pH for the media containing activated carbon. Differences in copper levels were insignificant for the media with the different AC's.

Data are presented for iron in Figure 7.5. Notice that at no pH did the available iron level approach the calculated amount. The iron level demonstrated strong pH dependence, decreasing more than 50% over the range from pH 4.8 to pH 6.8. The pH response was very similar to that noted for zinc. It may be seen that the media with activated carbon were in very good agreement with standard (Std) media and with each other (Figure 7.5): no adsorption was indicated. Data for experiments where iron was left out of the medium indicated that iron was not introduced into the medium by either of the activated carbons (not shown).

Elemental Compositon: Mn

Data for manganese vs. pH are shown in Figure 7.6. It is apparent that Mn declined in response to pH changes to a degree that exceeded iron (Fe^{3+}) losses, and over a narrower pH range. The control medium responded in a similar manner to media containing AC: no adsorption of manganese was indicated. The data were similar for media with the different AC types. Manganese exceeded target levels below pH 5.4.

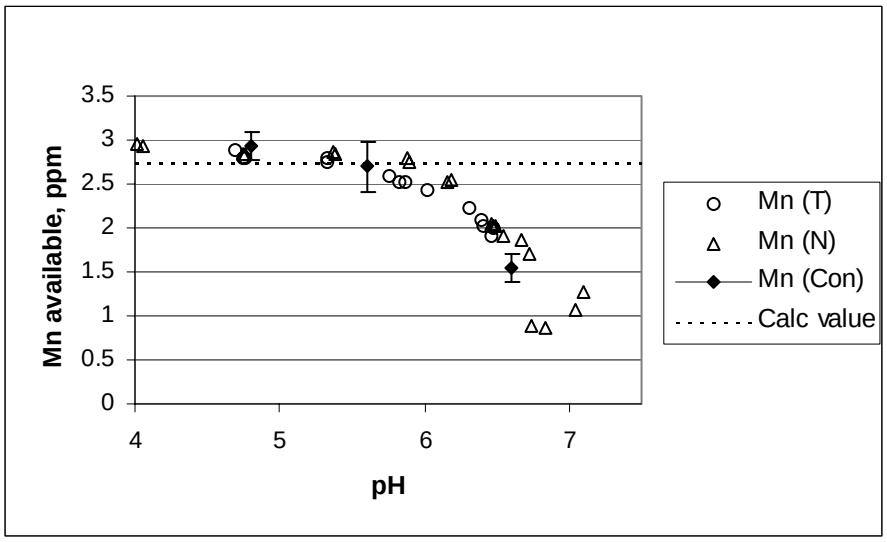

Figure 7.6. Available manganese vs. carbon type and pH. Data are presented for media with both AC types (N1, T1, 1.25 g/L) and the control media without AC (Con). "Con" and AC media contained elevated copper and zinc (20x and 2x Std levels, respectively). Error bars for Con treatment depict the 90% confidence interval based on three replications.

Remaining Elements

Of the remaining nutrients, boron (as boric acid), sulfur (present as sulfate), and potassium showed no dependence on either AC or pH. Phosphorus and calcium, however, showed a pH dependence above pH 6.5 with decreased availability of about 20% and 15%, respectively (Figures 7.7 and 7.8). Data for the anions, Cl^- and NO_3^-, were collected using capillary ion electrophoresis. Neither anion was adsorbed onto AC.

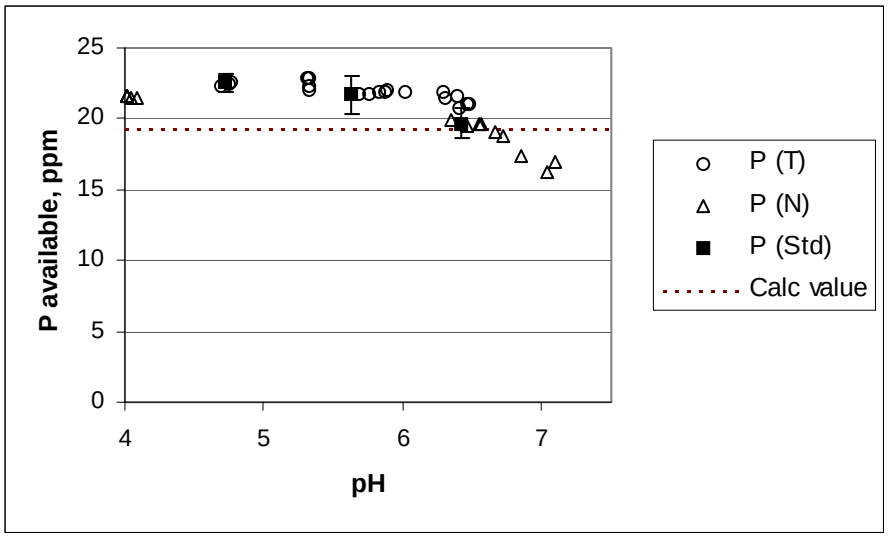

Figure 7.7. Available phosphorus vs. carbon type and pH. Data are presented for media with both AC types (N1, T1, 1.25 g/L) and the standard media without AC (Std). "Std" refers to media with normal Cu and Zn levels; AC media contained elevated copper and zinc (20x and 2x Std levels, respectively). Error bars for Std treatment depict the 90% confidence interval based on three replications.

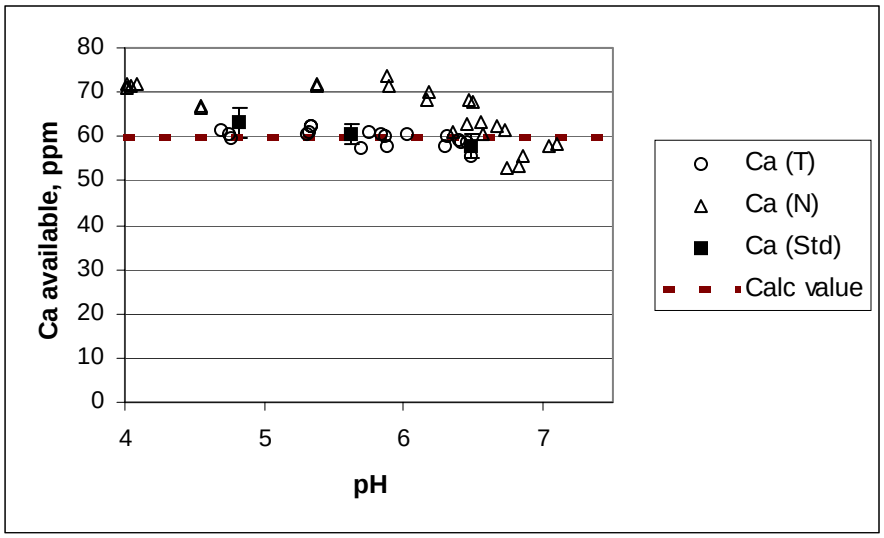

Figure 7.8. Available calcium vs. carbon type and pH. Data are presented for media with both AC types (N1, T1, 1.25 g/L) and the standard media without AC (Std). "Std" refers to media with normal Cu and Zn levels; AC media contained elevated copper and zinc (20x and 2x Std levels, respectively). Error bars for Std treatment depict the 90% confidence interval based on three replications.

For media containing N1, both calcium and magnesium were released into the medium at pH 5.8, resulting in 10% and 65% increases, respectively. Increased pH led to a decline in available magnesium of 20% (Figure 7.9). The difference in calcium concentration was

insignificant above pH 6.5, perhaps indicating that a solubility product had been achieved. Other than Ca, Mg and possibly Si, no other ionic impurities were detected. All of the above ions exceeded the calculated levels. Molybdenum appeared to be depleted through precipitation to about 60% of the calculated level independent of pH or the presence of activated carbon.

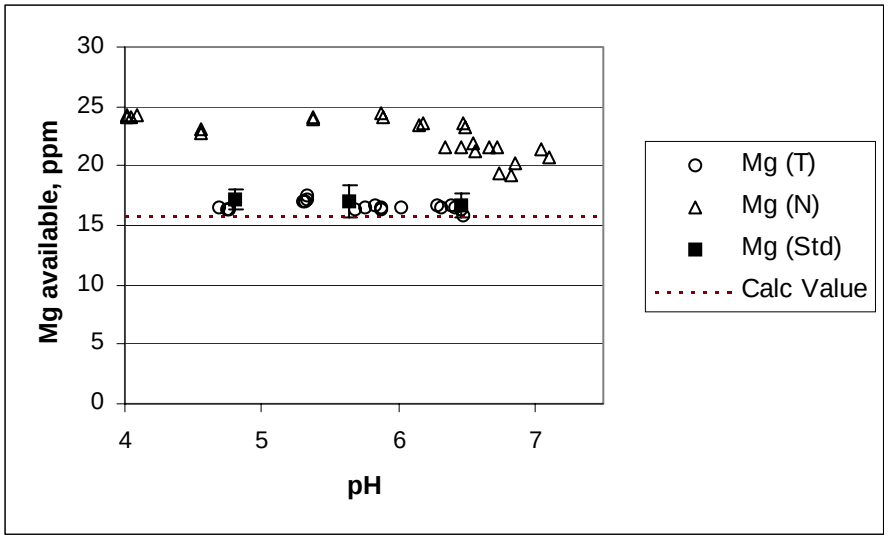

Figure 7.9. Available magnesium vs. carbon type and pH. Data are presented for media with both AC types (N1, T1, 1.25 g/L) and the standard media without AC (Std). "Std" refers to media with normal Cu and Zn levels; AC media contained elevated copper and zinc (20x and 2x Std levels, respectively). Error bars for Std treatment depict the 90% confidence interval based on three replications.

The pH-dependent precipitate was isolated and analyzed; its composition in molar percentage is presented in Figure 7.10. The percentage of calcium was marked, and the flocc-like appearance of the precipitate and its pronounced onset at pH 6.5 suggested the formation of hydroxide species that probably incorporated phosphorus (Elliott 1994).

Reversibility of Precipitation

As stated previously, the growing culture caused a decline in the pH of the medium. It was observed that a precipitate was present in media at pH 5.8 after autoclaving.

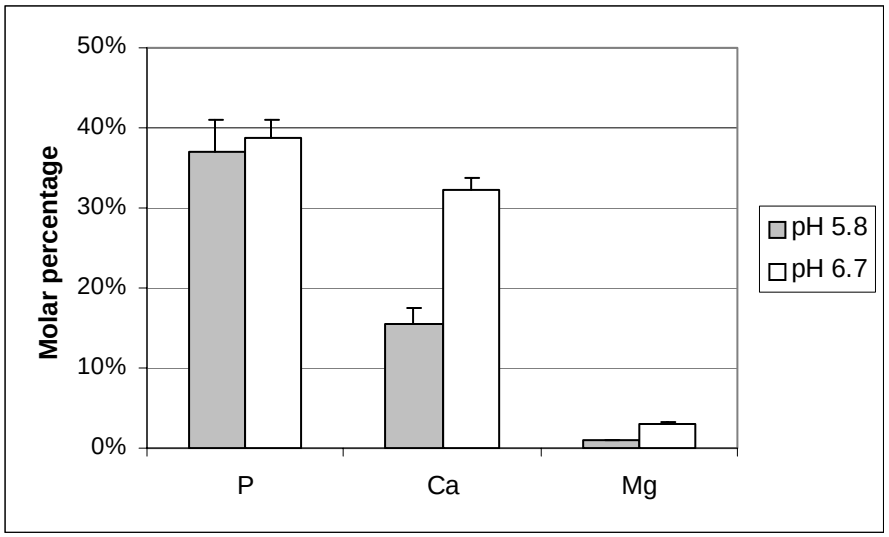

Figure 7.10. Analysis of precipitate collected from autoclaved media formulated to different pH levels. The precipitate was redissolved in nitric acid and analyzed by ICP.

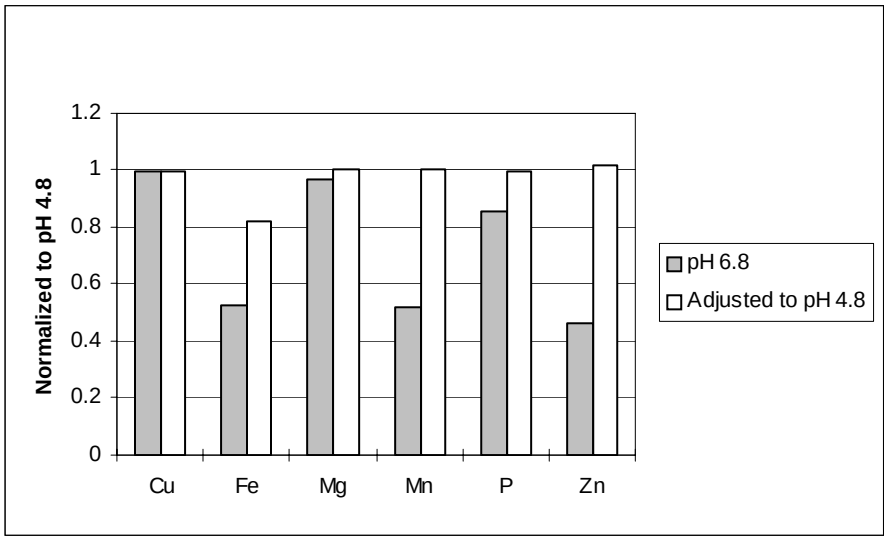

Figure 7.11. Reversibility of precipitation. Media were prepared to pH 6.8 and autoclaved. Samples were taken after a day and then the media were readjusted to pH 4.8 and allowed to equilibrate overnight. The values are the average of two replications and have been normalized to those obtained previously for media at pH 4.8. Precipitation was complete reversible except for iron.

To test whether this precipitation was reversible, media without AC were formulated, adjusted to pH 6.8 and autoclaved. After autoclaving, the media were readjusted to pH 4.8 and allowed to equilibrate at room temperature overnight. The data were normalized to the values measured for control samples formulated and autoclaved at pH 4.8. Refering to Figure 7.11, the left bar for each ion represents the medium at pH 6.8; the right bar

represents the same media after adjustment to pH 4.8. The data at pH 6.8 show that Fe, Mg, Mn, P, and Zn decreased relative to the pH 4.8 control, but there was no difference for copper. After adjustment of the medium to pH 4.8, Mg, Mn, P, and Zn were completely recovered. Only a percentage of the iron (18%) remained insoluble.

A summary of the elemental composition of media with the two different carbons is presented in Table 7.2 below. The composition of media with N1 reflects the elevated pH, as well as the release of ions (Mg, Si). The impact on culture success of these different ionic compositions will be considered in Section IX.

Table 7.2. Available elemental composition of media with AC

Ion	N1, pH 6.5*	T1, pH 5.8*
Cu	0.003	0.004
Zn	0.8	0.95
Fe	1.1	2.25
Mn	1.6	2.7
B	0.67	0.67
S	26.6	26.6
K	330	330
P	18	21.8
Ca	58	60
Mg	21.3	17
Co	n/a	n/a
Mo	0.03	0.03
Si	1.8	1.05

*Values are given in ppm; initial Cu, Zn elevated by 20x and 2x to compensate for AC adsorption.

Strategies to Counter the Precipitation of Fe

As shown in the previous results and summarized in Table 7.2, manganese and iron were depleted by more than 50% in response to increased pH. The detrimental effects of iron deficiency are well documented. Additionally, a fundamental difficulty in studying the pH response of a tissue culture system is that the medium composition changes with pH: the observed effects on culture success may be related to [H+], or they may be related to the nutrient composition, or both. The ideal experiment would be one in which the media were identical at several different pH levels. The following work explored several approaches for maintaining high iron concentrations at elevated pH.

Four different strategies for correcting for iron depletion were applied: 1) doubling the EDTA level while leaving the iron at the original level; 2) increasing Fe-EDTA by a factor of 2.5 times; 3) filter sterilizing as opposed to autoclaving; and, 4) including citrate at the level of 10μM. The media were sampled at two days and thirty days. None of the samples included AC and the control for this experiment was the standard medium (column 1 from Table 6.11).

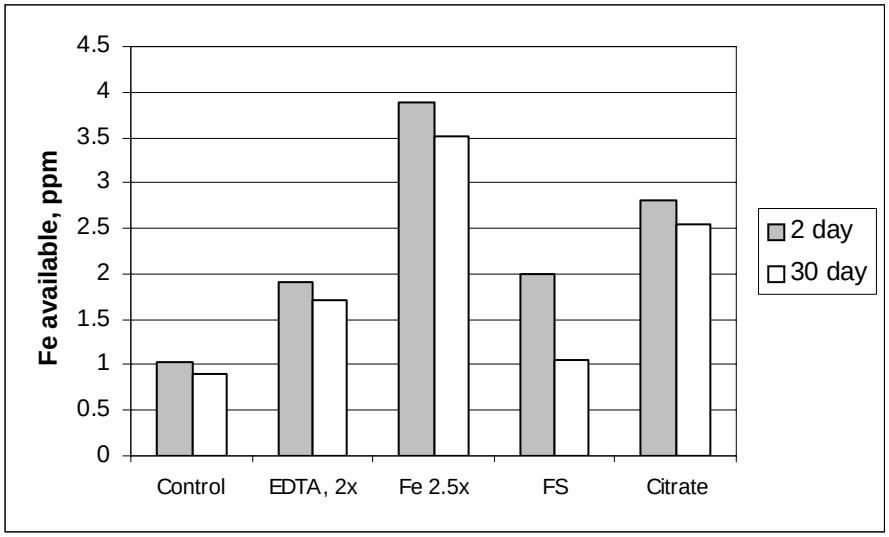

Figure 7.12. Comparison of different treatments to increase Fe levels at pH 6.5. Media were formulated with standard levels of copper and zinc. Each value represents the average of two replications. Treatments included standard media (control), doubling of EDTA, increasing Fe-EDTA by a factor of 2.5, filter sterilizing (FS) standard media, and adding K-citrate (10μm).

The resulting data are shown in Figure 7.12. For every treatment the thirty day level was lower than the two day level. The control gave the lowest level of Fe, as expected. Filter sterilizing resulted in a doubling of Fe at the two day sampling, but at the thirty day sampling Fe declined to a level which was close to the level of the standard medium. Doubling of EDTA led to a significant increase in available Fe at each sampling. The greatest increase in available Fe occurred simply through increasing the initial level of Fe. Compared to the calculated level of 7.0 ppm, about 40% precipitated within two days, increasing to about 50% by the thirty day sampling (probably iron had dropped to this level within fourteen days, Dalton et al. 1983). The addition of citrate had significant impact on the available Fe, resulting in a level which matched the calculated value. After

thirty days the Fe level remained high for the citrate treatment, which was also the medium with the highest pH (approaching pH 7.0).

Each of the four treatments had a different overall impact on the medium. Data for Mn vs. the strategies for compensating Fe are shown in Figure 7.13. Increasing Fe by a factor of 2.5 had no impact on the Mn concentration, but the other three treatments resulted in increased Mn. Over time three of the treatments showed an increase in Mn while two showed a decrease. The highest value for available Mn was recorded for the citrate treatment, which exceeded the calculated level.

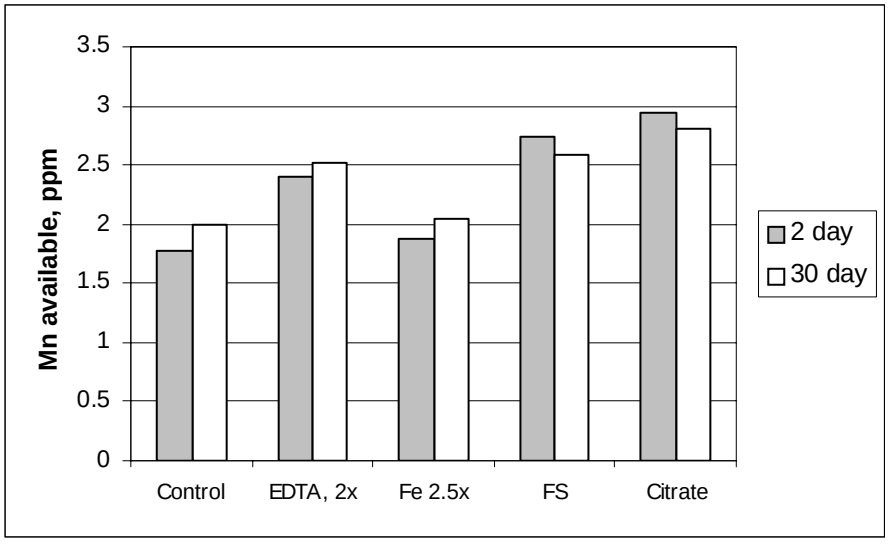

Figure 7.13. Available Mn also increased with treatments. Media were formulated at pH 6.5 with standard levels of copper and zinc. Each value represents the average of two replications. Treatments included standard media (control), doubling of EDTA, increasing Fe-EDTA by a factor of 2.5, filter sterilizing (FS) standard media, and adding K-citrate (10μm).

B. Discussion

Adsorption

The adsorption of various ions onto AC, including cadmium, copper, zinc (Ferro-Garcia et al. 1988; Rubin, Mercer 1987; Chang, Ku 1994, 1995), nickel, lead (Corapcioglu, Huang 1987; Wilczal, Keinath 1993; Reed, Nonavinakere 1992) cobalt (Howard 1988), chromium (Bautista-Toledo et al. 1994), Fe-EDTA (Johansson et al. 1990), cyanide (Adams 1991; Kongolo et al. 1997; Petersen, Van Deventer 1997) and others have been reported in the literature. Both anions and cations adsorb onto AC. Anions are thought to be *specifically* adsorbed, that is, adsorbed within the Stern layer, directly adjacent to the positively charged surface species of the AC. Anions are believed to be particularly prone to this type of adsorption due to their weaker affinity for water molecules. Accordingly, positively charged counter ions are adsorbed in the diffuse region of the double layer to ensure electrical neutrality (Scwarzenbach et al., 1993).

Specifically adsorbed ions are retained by the AC and contribute to its apparent surface charge or zeta potential. At pH below the pzc, activated carbon will display a surplus of protonated groups and a positive charge. However, a percentage of the acid groups will remain dissociated. These negatively charged groups are expected to be partially neutralized by *specifically* adsorbed cations, contributing to the positive zeta potential. Cations are also present in the diffuse layer. These diffuse cations do not travel with the AC during electrophoretic measurements and do not contribute to the zeta potential.

Based on the electrical double layer described above, it would be expected that the various cations in the culture medium would compete for the same adsorption sites. The majority of the hydrated cations in the growth medium carry a charge of +2. Thus, it was expected that the ions present at the highest relative concentrations would outcompete the remaining ions. From the composition of the medium, calcium and magnesium should

have been adsorbed to a high degree. However, copper and zinc were the only ions to adsorb.

For media without AC, the precipitation of medium components from Murishige and Skoog-based media is a well-known phenomenon that has been primarily attributed to the precipitation of iron as ferric phosphate. Teasdale (1987) suggested this mechanism: Fe precipitates as phosphate and the liberated EDTA then titrates Cu, Zn, Co, Mn and Ca in sequence, based on their EDTA stability constants (Table 7.3).

Table 7.3. Stability Constants (Morel, Hering 1993)

Ion	EDTA	log value
Na^{+}	NaL	2.5
K^{+}	KL	1.7
Ca^{2+}	CaL	12.4
Mg^{2+}	MgL	10.6
Fe^{3+}	FeL	27.7
Mn^{2+}	MnL	15.6
Co^{2+}	CoL	18.1
Cu^{2+}	CuL	20.5
Zn^{2+}	ZnL	18.3

The stability constants, or formation constants, are equilibrium constants which relate the activity (concentration for dilute solutions), of the ligated ion (products) to the dissociated precursors (reactants). This sequence conforms to the empirically derived sequence for the stability of transition metal complexes which is known as the Irving-Williams series (Gerloch, Constable 1994): $Mn^{2+} < Fe^{2+} < Co^{2+} < Ni^{2+} < Cu^{2+} > Zn^{2+}$. However, iron is oxidized to Fe^{3+} in aqueous solution exposed to atmospheric oxygen, and complexes with Fe^{3+} have much higher stability constants than complexes of the +2 transition ions. Complexes with the alkaline earths, Ca^{2+} and Mg^{2+}, are less stable than those with Mn^{2+}.

Iron (Fe^{3+}) may be displaced from EDTA even though it has a much higher stability constant than the displacing ion(s). This is possible when the concentration of the displacing ion is in great excess. The Fe^{3+} concentration will be pushed to near zero due to the exceedingly low solubility product of ferric phosphate, which is expected to form

upon dissociation of Fe^{3+} from EDTA. This displacement phenomenon has been documented for the Ca^{2+}/Fe^{3+}/EDTA system (Xue et al. 1995). The dissociation of iron from EDTA, believed to occur through an adjunctive mechanism (analogous to an S_n2 mechanism), was found to be rate-limiting. In the tissue culture system there are several divalent ions, including copper and zinc. The combined concentration of these ions exceeds that of hydrated Fe^{3+} by orders of magnitude. The mechanism proposed by Xue et al. should apply to the medium used here; however, it could be significantly slower due to the high levels of amino acids present which could complex with free ions. The data in Figure 7.12 are consistent with this mechanism: increasing Fe or EDTA or adding another complexing agent (citrate) resulted in increased levels of Fe remaining available.

A discrepancy was noted between the obtained data and the proposed mechanism of Teasdale. Though no adsorption from the complete medium with AC was observed for iron (Fe-EDTA), it was found that Fe-EDTA was almost completely removed (adsorbed) when the organic components of the medium were omitted. Spectroscopic data (absorbance at UV 284 and UV 270) confirmed that EDTA was also adsorbed. It is worth noting that adsorption of Fe^{3+} has been reported previously (Xue et al. 1995). The adsorption of Cu-EDTA has also been noted (Chang, Ku 1995), with AC actually demonstrating a higher affinity for the chelated form as opposed to the free copper ion (Cu^{2+}) in their system. In chelated form the complexes could be negatively charged as EDTA may have four dissociated acid groups. Chang and Ku proposed an electrostatic mechanism to account for the adsorption of copper. In the present study, the other chelated divalent cations would carry the same (-2) charge as Cu-EDTA.

Solubility and partitioning behavior have been used as predictors for the relative sorption of organic compounds onto soils (Sangster 1997). According to this conception, the driving forces for adsorption include hydrophobicity and van derWaals forces between the surface and the sorbate. The hormones are the least soluble component in the medium and are readily adsorbed (Weatherhead et al.1978, 1979). The next least soluble compounds are the vitamins and amino acids. It is expected that these organic anions would outcompete the chelated ions. Omitting the organic components therefore reduced

competition for sorptive sites on the surface of the activated carbon, allowing the adsorption of chelated iron. However, in this study, the adsorption of inorganic anions was not indicated (Table 7.4).

These observations taken together suggest that other compounds present in the complete medium, such as the hormones, the vitamins, or the amino acids, outcompeted or perhaps displaced the chelated ions.

Table 7.4. Data for anions and elements present as anions, showing no adsorption by activated carbon.

	Calc. Target	Control	T1	N1
S*	24.6	26.9	26.6	27.5
P	19.3	21.4	21.9	20.6
Mo	0.05	0.029	0.029	0.03
Cl^-	284	294	293	n/a
NO_3^-	30.6	26.5	27.3	n/a

* S (sulfate), P (phosphate), Mo (molybdic acid) were measured by ICP-AES; Cl^- and NO_3^- were measured as anions directly, through capillary ion electrophoresis.

One half hour after mixing the control media (no activated carbon present) without autoclaving, 25% of the available iron in solution was depleted (2.1 ppm vs. calculated value of 2.8 ppm). On a molar basis this left 12.5 μmoles of EDTA available to chelate the copper and zinc. Though this total agrees fairly well with the molar total of zinc and copper not adsorbed from media containing activated carbon (10.3 μmoles), if all of the copper were chelated, then only a very small percentage of it should have been adsorbed. If copper and zinc were chelated to a significant percentage but adsorbed as free ions, then leaving out the EDTA should have resulted in much greater adsorption. Contrary to expectation, it was found that omitting the Fe-EDTA from the medium had insignificant impact on the adsorption of copper or zinc. The implication was that the copper and zinc weren't chelated as proposed.

Based on the preceding discussion, it is suggested that copper and zinc ions were adsorbed as non-chelated species. It is hypothesized that copper and zinc were adsorbed through a surface complexation mechanism with high selectivity. Carbon surfaces are physically and energetically heterogeneous. This heterogeneity derives from microporosity and from oxygen functionality.

Metal ion selectivity has been noted for the adsorption of nickel and cadmium onto activated carbon (Reed, Nonavinakere 1992). Though both metals were adsorbed, the increased presence of one metal did not affect the adsorption of the other: they were adsorbed selectively onto different sites. An increased initial level of cadmium led to an increase in cadmium adsorption, which the authors attributed to a non-selective adsorption mechanism (adsorption in the diffuse layer) analogous to the adsorption of hydrophobic organic compounds: cadmium was adsorbing to two different types of sites. In free energy terms, the idea of sorptive selectivity is similar to stating that the free energy of adsorption is composed of an electrostatic component and a chemical component. The chemical component varies with each compound and is always present regardless of any electrostatic forces.

$$\Delta G_{adsorption} = \Delta G_{chemical} + \Delta G_{electrostatic}$$

The thermal response for the adsorption of copper and zinc from aqueous solution onto different activated carbons was reported by Garcia at al. (1988). They reported that the adsorption of copper was endothermic, whereas the adsorption of zinc was exothermic, indicating different adsorption mechanisms. A lower ΔG_{chem} (more negative) was indicated for copper which they attributed to a greater energy of interaction (increased H-bonding or increased covalent bonding). The observation that copper and zinc were adsorbing differently agrees with our results which showed a greater percentage adsorption for copper. They reported that the addition of EDTA reduced adsorption, though other complexing agents actually increased the adsorption of copper and zinc. Autoclaving may also play an important role, as the adsorption of copper onto activated carbon was found by Garcia et al. to be endothermic. The present data showed that copper adsorption increased with autoclaving (Figure 7.14), in agreement with an

endothermic process. Data are shown after 0.5 hours. After 3.5 hours the non-autoclaved treatment had declined in copper concentration to 0.006 ppm, much closer to the levels present for autoclaved media (0.003 ppm in this experiment) indicating that the autoclave effect was rate-related. Adsorptive selectivity could result from a particular spatial arrangement of surface features or heteroatoms such as oxygen or nitrogen.
One could imagine an arrangement which might produce a highly selective site for copper, analogous with plant enzymes and protein catalysts. Zinc may have had special properties due to its uniform electron distribution in the ionized state, yielding a polarizable electron cloud and also giving a covalent character to bonding.

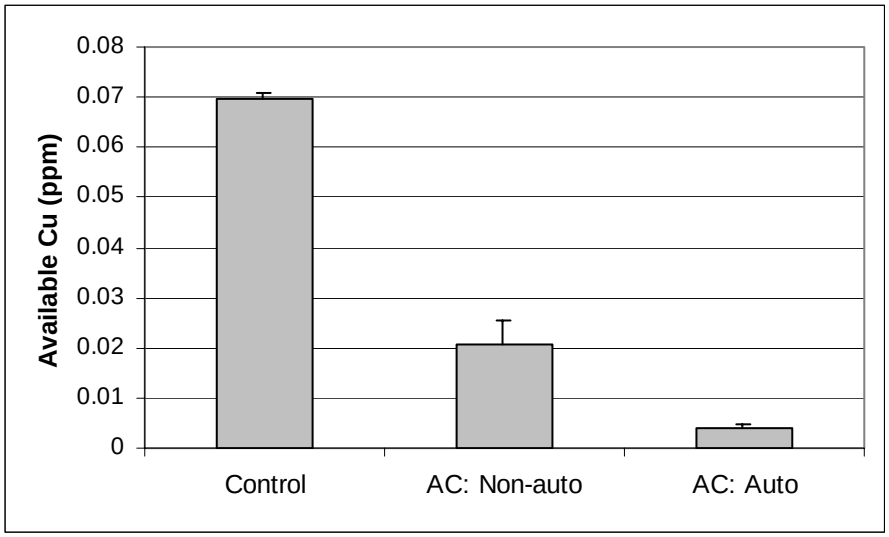

Figure 7.14. Copper available after 0.5 hours for control media (elevated copper) and the same media with AC (T1, 1.25 g/L).

Manganese demonstrated anomalous behavior. With regard to adsorption, manganese behaved as an alkaline earth metal (Ca^{2+}, Mg^{2+}), but with respect to precipitation it was similar to Fe^{3+} or Zn^{2+}. It is unclear why manganese wasn't adsorbed. It has electronic structure (uniform electron distribution in the d-orbitals) which, according to ligand field theory (Gerloch, Constable 1994), should result in properties similar to Zn^{2+}. If it were chelated, it wouldn't precipitate. However, the ligand field theory does predict lower complexation energy for Mn compared to copper, zinc or cobalt. Hard/soft acid theory

also leads to the conclusion that zinc and manganese should behave similarly (Figure 7.15). Kinetic arguments based on dewatering as the rate-limiting step for complexation also indicate that zinc and manganese should behave similarly (Table 7.5).

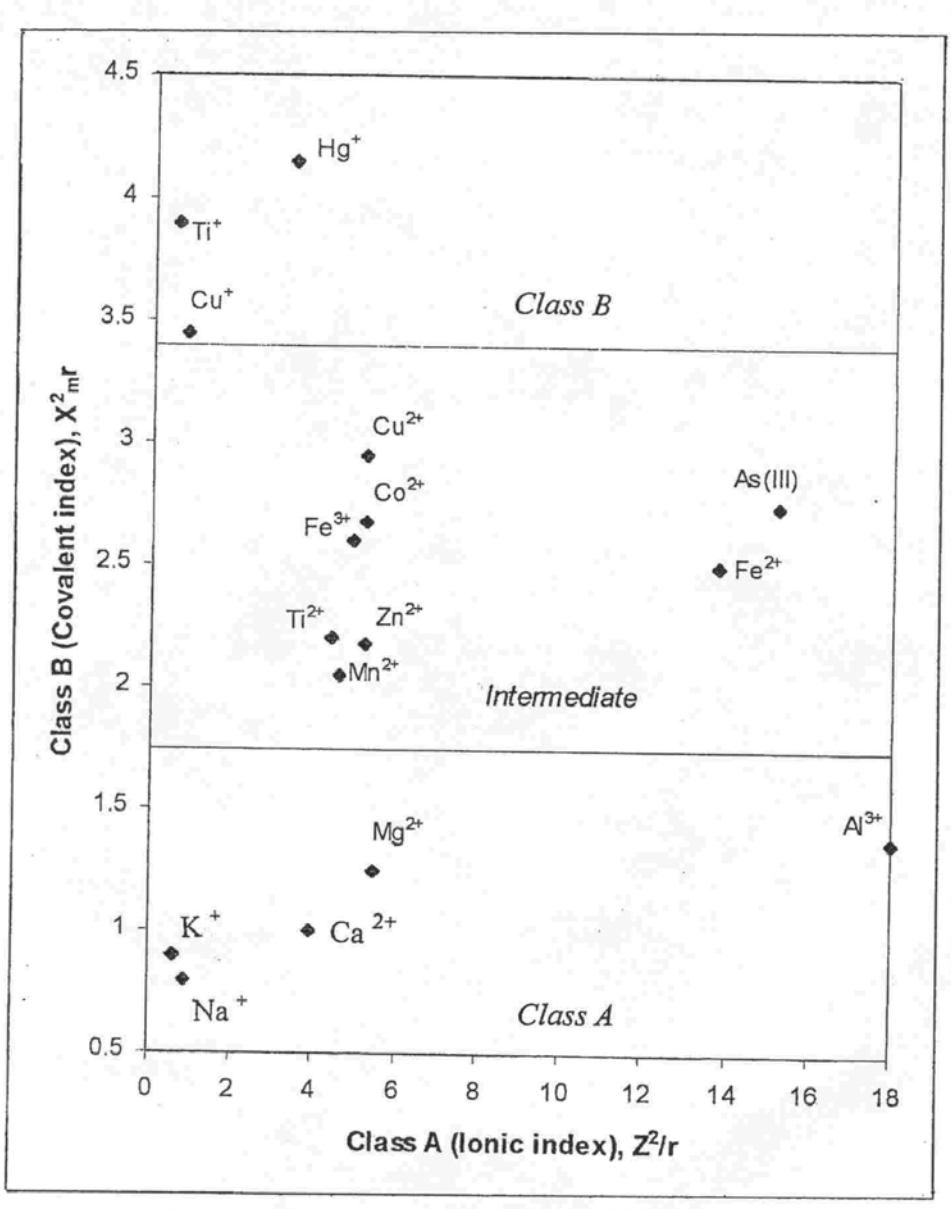

Figure 7.15. Classification of ions based on bonding tendency. Covalent character increases along the y-axis. Xm is the metal-ion electronegativity, r its ionic radius, and Z its formal charge. (Adapted from Stumm, Morgan 1996 and references within).

Table 7.5. Rate Constants for Water Exchange (Stumm, Morgan 1996).

Metal Ion	k_{-w} (s^{-1})
Cu^{2+}	1×10^{9}
Ca^{2+}	6×10^{8}
Zn^{2+}	7×10^{7}
Mn^{2+}	3×10^{7}
Co^{2+}	2×10^{6}
Mg^{2+}	3×10^{5}
Fe^{3+}	2×10^{2}

Stumm and Morgan (1981) considered the acidic character of hydrated ions (aquo ions), that is the propensity of hydrated ions to donate a proton. They defined a dissociation constant:

$$*K_1 = \{MOH^{(z-1)+}\}\{H^+\}/\{M^{z+}\}$$

where M is the metal ion. A partial ranking of pertinent ions is given here:
$Fe^{3+}>>Cu^{2+}>Zn^{2+}>Fe^{2+}>Co^{2+}>Ni^{2+}>Mn^{2+}>Mg^{2+}>Ca^{2+}>>Na^{+}>K^{+}$.
The log $*K_1$ for Fe^{3+}, Cu^{2+}, Zn^{2+}, and Mn^{2+} were -2.1, -8.2, -9.1, and -11.6, respectively. The lower relative acidity of aquo Mn^{2+} may be a plausible explanation for its lack of adsorption if it is assumed that adsorption occurred onto basic sites.

pH and Precipitation

Considered in total, the data indicated that the ionic composition was influenced to a greater extent by the pH of the medium than by adsorption onto AC. Precipitation increased with pH. Iron and manganese were the ions depleted the most in response to increased pH, each being depleted by over 50% over the pH range from 4.8 to 6.5. This depletion may be attributed to precipitation primarily as phosphates, with hydroxide species becoming more important as pH increased. Calcium and possibly zinc precipitation increased markedly at pH 6.5, which coincided with expected increases in hydroxide precipitates. Phosphate decreased about 17% as pH increased. The phosphorus which precipitated was completely redissolved as pH declined. This reversibility, coupled with the fact that a portion of the iron precipitation was irreversible, supports the hypothesis that ferric hydroxide species were being formed. Thus, the influence of AC on

the pH of the medium was more important to the overall ionic composition than was its adsorption of inorganic species.

The non acid-washed carbon, N1, was more basic as shown by its PZC value, and it displayed much greater buffering strength than the acid washed carbon, T1. For N1, the typical pH adjustment procedure prior to autoclaving was insufficient to guarantee that target pH levels would result following autoclaving. In addition, N1 displayed a time-dependent pH drift as noted with respect to the titration data. The titration samples were prepared with degassed, nanopure water, and the titrations were carried out under a nitrogen blanket. The end-point drift was much more pronounced for N1 than for T1, indicating that the phenomenon was related to the carbon type rather than the titration conditions. Therefore, it is not believed that dissolved carbonate species were responsible for the time-dependent consumption of acid.

Different explanations for the slow consumption of acid by activated carbon have been proposed in the literature. Diffusion of protons is not believed to be limiting as protons are transported through aqueous media extremely rapidly, perhaps through a very rapid transfer mechanism whereby protons are “exchanged” between adjacent water molecules. One possible explanation is that the anion, Cl^- in this case, is adsorbed and the proton accompanies it to maintain charge neutrality (Mattson, Mark 1971). Accordingly, the adsorption rate would be limited by the diffusion of hydrated Cl^-. Leon Y Leon et al. (1992) have suggested that the resistance to Cl^- diffusion arises from the charge repulsion at pore entrances and also from the diffusion through accessible pores.

Alternatively, the hydrolysis of oxidized metal species may be responsible for the drift. Following activation, it is expected that much of the ionic content of the AC exists in an oxidized state. The hydrolysis of these oxides results in the formation of hydroxide species (Cotton, Wilkinson 1976). These are basic compounds which dissociate to neutralize protons. In this case, the slow hydrolysis could be explained by slow dissolution. For media with N1, the increase in magnesium and calcium would be consistent with this mechanism.

A third possibility is that the acid consumption was related to the slow consumption of dissolved oxygen by the AC surface, which may result in the creation of OH-. Accordingly, AC acts as an oxygen electrode (Mattson, Mark 1971). Bound oxygen might have been present on the carbon surface, though this possibility was unlikely, given that the samples were degassed and autoclaved prior to titration.

None of these suggested mechanisms excludes the others. The slow consumption of acid is plausibly the result of different simultaneous phenomena.

Autoclave Effects

Medium pH after autoclaving was found to be approximately pH 5.8 when using T1 and greater than pH 6.5 when using N1. The pH varied, depending on how much time was spent adjusting pH prior to autoclaving. The growing Norway spruce cultures drove the pH down to pH 4.8 for media with T1, but did not drop as low with N1, remaining near pH 6.0.

Autoclaving resulted in lower copper levels, essentially accelerating the depletion of this ion (Figure 7.14). At pH above 5.8, autoclaving accelerated iron depletion and resulted in slight increase in available zinc. At pH below 5.3, iron was unaffected by autoclaving and zinc decreased slightly. With time, iron was further depleted; however, the concentration of zinc actually increased slightly at both pH levels (Figure 7.16).

This slight increase was seen in four experimental replications. This increase in zinc concentration may have been due to displacement from the surface of the activated carbon. Such phenomena have been suggested for the displacement of H^+ by adsorbing organic species (Mattson, Mark 1971). Alternately, a metastable precipitate may have formed in the autoclave with its formation promoted on the surface of AC. Such phenomena have been reported previously for systems at somewhat higher pH (Gabaldon, et al. 1996).

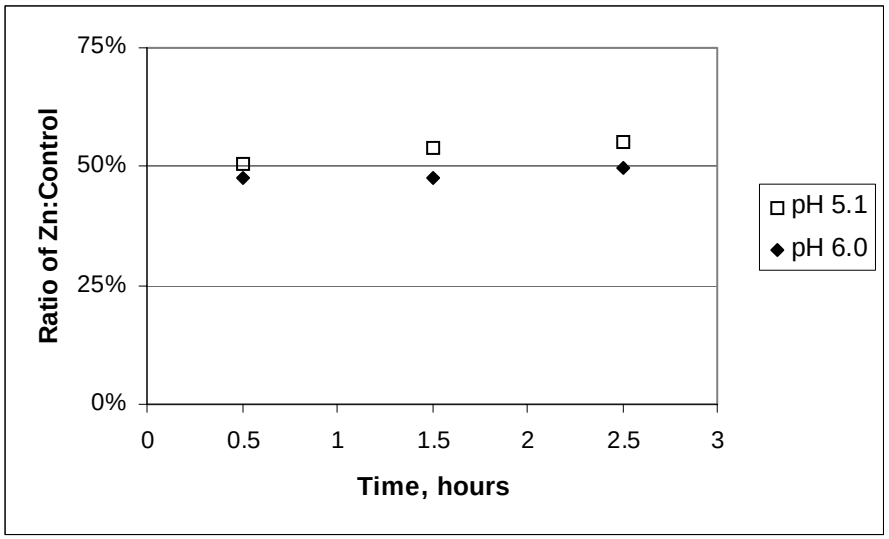

Figure 7.16. Available zinc vs. time, media with AC relative to control. Each data point represents the average of two samples with the range/mean being less than 2.8%.

The observed precipitation behavior of iron was in very good agreement with previous research by Dalton et al. (1983). However, there were a couple of important experimental distinctions. The previous researchers filter-sterilized their media, and two weeks were allowed for equilibration. Measurements here were taken after two days, and autoclaving appeared to accelerate equilibration. Dalton's medium contained the full MS ionic composition, or twice as much iron as was used in the Norway spruce medium. These differences didn't significantly affect the agreement between results. The finding that phosphorus was completely recovered (iron was expected to precipitate as ferric phosphate) in response to lowering the pH while a portion of the iron remained unavailable suggests that a portion of the iron precipitate involved other species, perhaps OH^-. Ferric hydroxide species are known to form at pH 5.0 (Dalton 1983) and are insoluble.

Compensating for Iron Precipitation

The experiments designed to compensate for the precipitation of iron revealed time-dependent behavior. The time dependency for the filter-sterilized sample indicated a loss in Mn, as well as a loss in Fe. The three samples which increased in Mn concentration

with time were autoclaved (Figure 7.13); the ligand exchange reaction which would have resulted in more available Mn didn't appear to occur to the same level with the filter-sterilized samples.

Based on this observation, the same explanation as was used for the zinc response could be applied; a metastable precipitate formed during autoclaving, and subsequently redissolved. No precipitate was visible initially for the filter-sterilized sample, but a fine precipitate did appear over time. This granular precipitate was quite different in appearance from the flocc-like precipitate in the autoclaved samples. No precipitate at all was observed in the citrate sample. It is expected that the precipitate did not form in the case of the citrate medium due to nearly complete complexation of all divalent ions.

Each of the iron strategies has drawbacks. EDTA is known to become toxic at higher levels (Teasdale 1987). Increasing the initial concentration of iron could result in toxicity; the precipitate formed at elevated pH would redissolve as the growing culture forced the pH downward. At constant pH, filter-sterilizing would not prevent losses over time. Citrate may also have inhibitory effects associated at levels as low as 1mM (Kato-Naguchi 1997) and, in addition, leads to an increase by a factor of four in the potassium concentration due to KOH added to exceed pH 6.5 (the target level for this experiment). The buffering effect of the citrate would be an additional consideration.

C. Conclusions

Different elemental compositions may result when using different activated carbons in tissue culture media. However, the elemental composition of the tissue culture medium is primarily determined by the pH of the medium, rather than by different levels of adsorption of inorganic elements onto the different activated carbons. Hence, the main concern when using common tissue-culture grade carbons is their impact on the pH of the medium.

Of the mineral elements in the growth medium, only copper and zinc were adsorbed onto activated carbon (93-95% and 50%, respectively). The data suggest that these ions did

not adsorb as chelated species. The levels of copper and zinc adsorption were similar for two carbons that were significantly different in physical and chemical character. The adsorption was attributed to selective complexation.

Non acid-washed activated carbons may introduce impurities into the medium. The non-acid-washed AC, N1, introduced about 15% more calcium, 50% more magnesium, and 30% more Si into the medium.

Increased zinc levels led to more iron precipitation. This was attributed to ligand exchange with Fe-EDTA, which resulted in more free Fe^{3+} precipitating in phosphate form (in accordance with the mechanism proposed by Teasdale). Autoclaving media catalyzed adsorption of Cu. Adsorption of Zn increased with autoclaving below pH 5.3 but decreaed with autoclaving above pH5.8. Autoclaving increased precipitation of Fe above pH 5.8 but led to slight increases at pH below 5.3. The trade-off between iron and zinc was consistent with the mechanism proposed by Teasdale. In media without activated carbon, autoclaving also changed the morphology of the precipitate, which became more floc-like as pH increased. This pH-dependent precipitation was in agreement with the formation of hydroxide species, including calcium, iron, and zinc.

Four different strategies for increasing the iron levels at elevated pH were applied: increasing Fe, increasing EDTA, filter-sterilization, and the addition of citrate. All four strategies resulted in increased [Fe]. The filter-sterilized media, however, displayed a slow loss of available Fe, attaining control levels in less than thirty days. This slow equilibration was in agreement with the mechanism suggested by Teasdale. The samples which included citrate were the only ones in the entire study to attain the targeted Fe concentrations.

VIII. HORMONE ADSORPTION

A. Method Development

HPLC Chromatogram

An HPLC chromatogram for complete growth medium is presented in Figure 8.1. The retention time is given along the x-axis The y-axis is given in milli-absorbance units, referring to the UV absorption at three wavelengths depicted (230, 270 and 284nm). The absorption peaks in the initial region of the chromatogram, retention time less than eight minutes, were attributed to absorption by casamino acids, EDTA, and three vitamins (pyridoxine, nicotinic acid, and thiamine) as these other compounds demonstrated UV absorbance. For the purposes of this study, this region was not of interest.

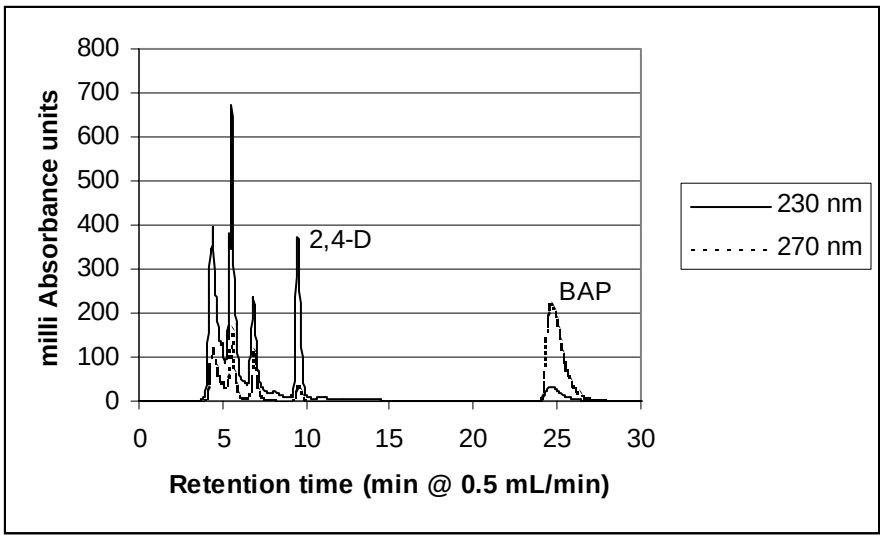

Figure 8.1. HPLC Chromatogram for complete tissue culture growth media. A separation of the hormones was achieved using reversed phase (Sigma-Aldrich Spherisorb ODS-2 5µm, 250mm x 4.6mm) and isocratic elution. Traces presented for two wavelengths (230nm, 270nm). 2,4-D eluted near 9.3 minutes; BAP eluted near 24 minutes.

The diode array detector, DAD, produced a complete UV spectrum for a given peak and was used in addition to retention times to confirm the identity of a compound. Figure 8.2 is a comparison between the diode array detector response for the peak at 9.3 min and the UV spectrum for 2,4-D in water, generated using a spectrophotometer. The y-axis has been normalized in order to bring the two traces to the same scale. The slight discrepancies in the regions of 250 nm and 220 nm may have been due to trace impurities

present from the synthesis of 2,4-D (Sigma listed this reagent as 95+% pure, catalog #D-2128). When compared to calibration-grade 2,4-D (99+% purity, Chem Service), Sigma #D-2128 was found to be 2% less pure, based on UV spectra. For BAP, there were no discrepancies between spectra from the DAD and the spectrophotometer.

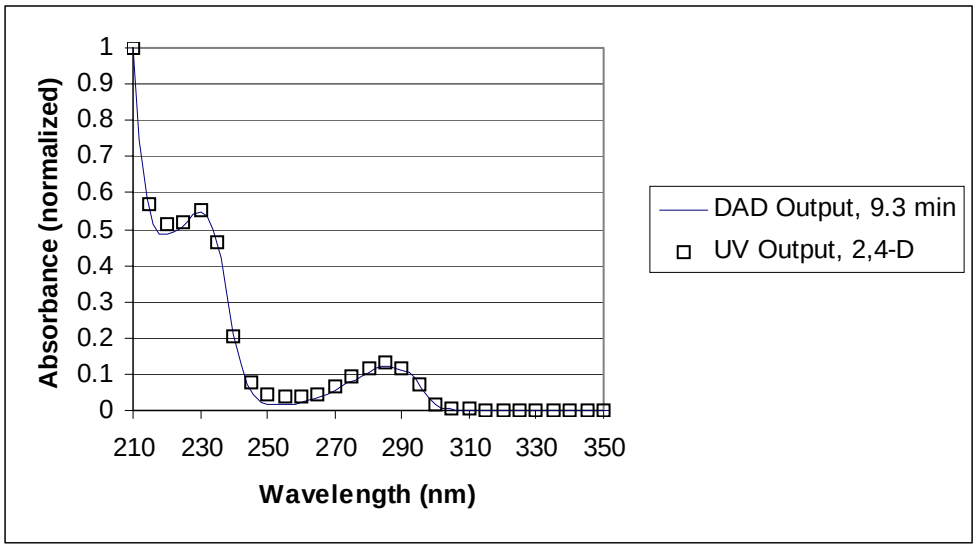

Figure 8.2. HPLC diode array detector response for the peak at 9.3 minutes (Figure 8.1) compared with spectrophotometer output for 2,4-D (UV Output, 2,4-D). Data have been normalized.

Precision

Based on a set of ten repeated measurements of a particular sample (approximately 1 ppm BAP and 2 ppm 2,4-D), and omitting the extreme measurement, a 95% confidence interval was calculated for each hormone. Expressed as a percentage of the mean this interval was found to be ± 5.5% for BAP and ± 12.3 % for 2,4-D.

Number of Samples

Experiments were typically replicated three times. The reported standard deviation or confidence interval for each experiment was calculated from the three replications.

Precision, three replications

The precision for three replications of an adsorption experiment may be represented as a confidence interval:

$$\text{½ Confidence interval} = (\text{COV})(\text{t-value})/(\text{sample size})^{1/2} \qquad (8.1)$$

An estimate for the coefficient of variation is needed in order to apply Formula 8.1. The data for two different activated carbons are collected in Table 8.1 below. Neglecting the lowest value for the combination of 2,4-D and T1, the average COV was 23%.

Table 8.1. Hormone availability data from HPLC analysis for two activated carbons.

	T1 (15 samples)		**Sx4 (7 samples)**	
	BAP	2,4-D	BAP	2,4-D
Mean, ppm	1.00	1.97	1.15	2.27
Standard dev.	0.23	0.27	0.24	0.46
COV	22 %	13 %	24 %	23 %

Adsorption data collected after 2.5 days from complete media containing activated carbon (0.3 g/L). Media were formulated with initial hormone levels of 65:12 and 32:8, BAP:2,4-D for T1 and Sx4, respectively.

Precision at $p = 0.05$ for three values was approximately ± 58 %. At the $p = 0.1$ level the precision was approximated as ± 39 %. Data for the hormones are presented throughout this section with error bars representing ± 1.69 standard deviations, the 90% confidence interval, based on three replicated experiments. It should be noted that when comparing mean values, the confidence level of 90% is conservative: the data from the different treatments may be pooled per experiment to increase the statistical power and hence the confidence level.

Experimental Parameters

Sampling period

The decline in hormone availability with time (days) is illustrated in Figure 8.3. These data were generated for media containing carbon T1 (0.3 g/L) with calculated initial hormone levels of 65 ppm BAP and 12 ppm 2,4-D. Reading from left to right, the first data point from the origin was generated for samples taken six hours after sterilization

(autoclaving). Subsequent sampling occurred at 2.5, 7, 15, and 36 days. The major proportion of adsorption occurred within six hours.

A.

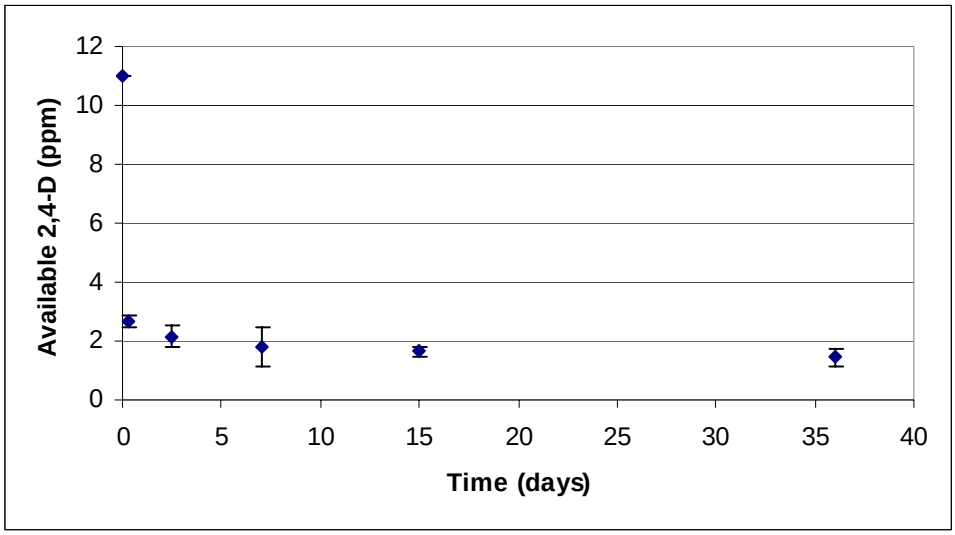

B.

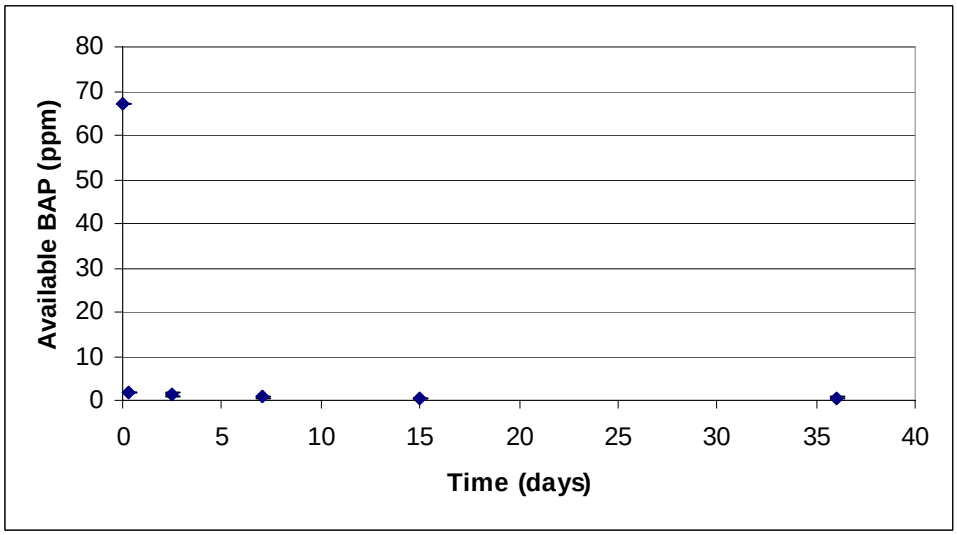

Figure 8.3. Hormone adsorption vs. time, A: 2,4-D, B: BAP.
Tissue culture growth media were formulated with 65 ppm BAP and 12 ppm 2,4-D and 0.3 g/L AC (Sigma C-9157 Lot 1723656, designated *T1*, 7.2% moisture content). Data points at time zero indicate control samples (media without AC) after autoclaving. Error bars represent the 90% confidence interval (± 1.69 standard deviations) based on three replications.

The data are presented again in Figure 8.4, but omitting the initial concentration at time zero. It may be seen more clearly that adsorption was still occurring after six hours. The hormone concentrations continued to decline slowly to the last measurement at 36 days.

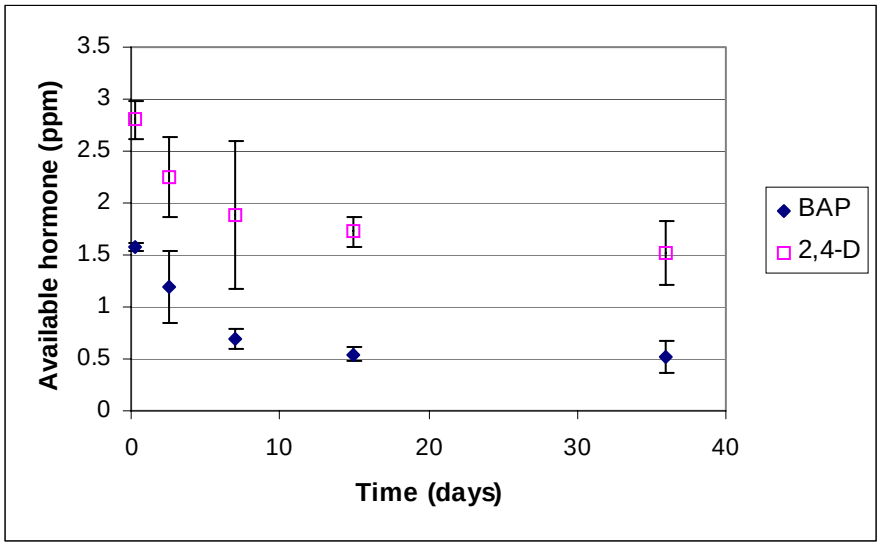

Figure 8.4. Adsorption of hormones onto T1 from six hours to thirty-six days, replot of data from Figure 8.3.

Based on the slow rate of hormone decline, the best compromise between equilibration time and expediency was seven days of equilibration. However, in tissue culture practice, media with activated carbon are generally not stored that long prior to use, one or two days being more typical. The possible degradation of nutrients in the medium, thiamine for example (Merck, 1989), is a good reason for not storing media for more than a few days. The data which follow are therefore based on a pre-sampling equilibration period of about 2.5 days (media were prepared in the evening and sampled 2.5 days later).

In Figure 8.5, the same data are plotted in terms of specific adsorption (mg hormone per gram AC), normalized to adsorption at 36 days. The data for BAP revealed that relatively small changes in specific adsorption could result in potentially significant differences in the level of hormone remaining available to a growing culture.

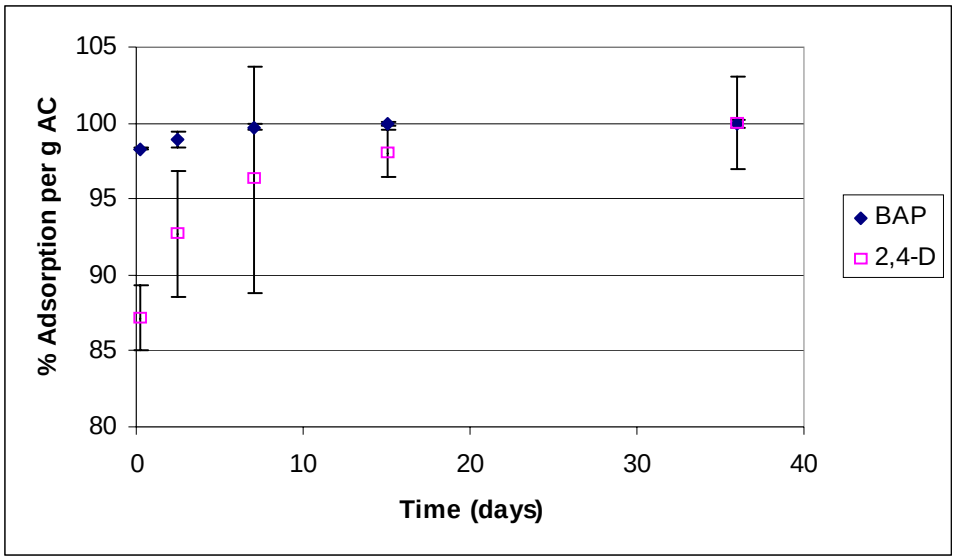

Figure 8.5 Adsorption vs. time as a percentage of adsorption after 36 days, replot of data from Figure 8.3.

Rate of mixing

To optimize experimental conditions, hormone levels were measured in media shaken at different speeds (0, 100, 120 and 185 rpm) and in different vessels (250 mL flask with 100mL media, and 40 mL vials completely full).

The different shaker speed settings were chosen in response to differences in how the carbon suspension behaved. With the shaker speed set at 100 rpm, the activated carbon settled to the bottom and moved with the flask. This combination of shaker speed and flask geometry (approximately half filled) was representative of common tissue culture practice. Increasing the shaker speed to 120 rpm resulted in activated carbon moving independently of the flask, i.e. the carbon was moving with the fluid but remained positioned near the flask bottom. At the 185 rpm setting mixing was vigorous with a deep vortex present and the carbon dispersed throughout the fluid volume.

Data comparing the response of the hormones to different shaker settings are presented in Figure 8.6. Comparing the hormones, BAP appeared to be more sensitive to shaker speed. A statistically insignificant increase in BAP adsorption resulted when increasing the shaker speed to 120rpm. A trend is indicated, however, by the more pronounced

increase in adsorption when the shaker speed was increased to 185 rpm. Therefore, it is expected

that there was a minor difference in adsorption, when the shaker speed was increased from 100 to 120 rpm. The 2,4-D data were insensitive to shaking.

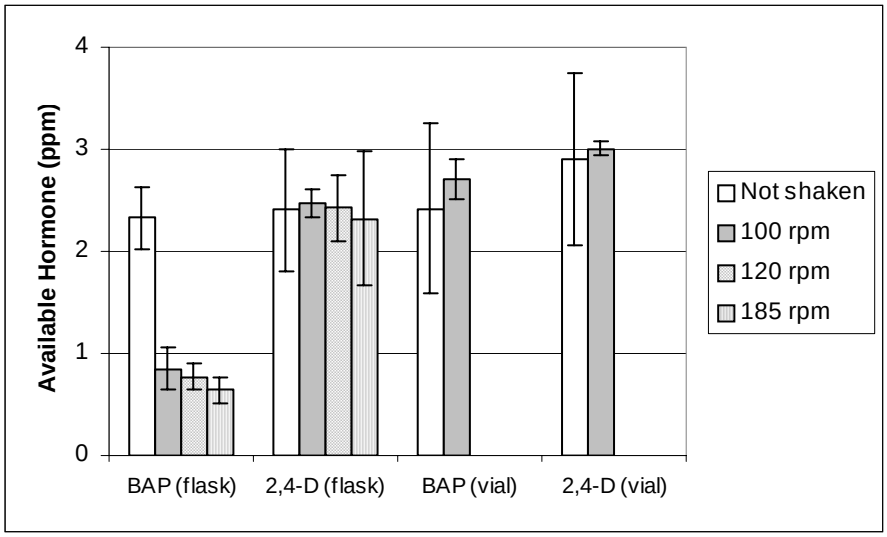

Figure 8.6 Effect of shaker speed settings and vessel type (flask vs. vial). No data were collected for samples in vials shaken at 120 or 185 rpm. Tissue culture growth media were formulated with initial hormone levels of 65 ppm BAP and 12 ppm 2,4-D with AC (T1, 0.3 g/L @ 7.2% moisture content). Samples were collected after 2.5 days. Error bars indicate the 90% confidence interval based on three replications.

Based on these data, and a desire for data to be relevant to standard tissue culture practice, a shaker speed near 100 rpm was chosen and used throughout this study.

Vessel geometry: vials vs. flasks

Due to the large number of samples formulated for this study, there were practical incentives to use smaller vessels. Figure 9.6 presents data for identical media dispensed to flasks and vials (250 and 40 mL capacity, respectively) and shaken at the same speed. It may be seen that less adsorption occurred within the vials. An increase in shaker speed from 100 to 120 rpm for the vials resulted in a minor, statistically insignificant increase in adsorption for both BAP and 2,4-D.

Ultrasound has been used industrially for the dispersion of particles in fluids (Shoh1988). Treatment of tissue culture media in an ultrasonic bath led to a uniform dispersion of the activated carbon. The agglomerated carbon particles appeared to separate, resulting in an

ink-like suspension. When compared with a control sample, ultrasonic treatment of the vials resulted in approximately 30% less available hormone. The BET surface area of the activated carbon was measured as 702 m^2/g before and 698 m^2/g after ultrasonic treatment. The increase in adsorption, which resulted from ultrasonic treatment, was therefore not related to changes in the surface area of the AC.

An experiment in which a drop of food coloring was added to a flask and a second drop was added to a vial (both vessels were placed on the same shaker table) revealed that the mixing was much more rapid in the flask. For the flask, ten minutes were required for the dye to disperse uniformly, whereas, five *days* were required for uniform dispersion within the vial. This difference was attributed to bulk fluid currents present to a greater degree in the flask due to the wave-like motion of the fluid. Therefore, to ensure adequate mixing, flasks were chosen for the experiments.

Temperature effect

Tissue culture media are commonly stored at ambient temperatures (ca. 21^oC) and may be subject to fluctuations of two degrees or more. The effect of an exaggerated difference in temperature is depicted in Figure 8.7. The axes have been inverted from standard practice to emphasize that it is the hormone remaining in solution that is of primary concern. These data were collected in separate experiments for each hormone from otherwise complete media.

An increase in temperature of nine degrees resulted in less adsorption (1.6% on average) and hence more available hormone (increase of 26% on average). If a linear relationship between temperature and sorption equilibrium were assumed, then the two degree temperature fluctuation would result in ca. 10% change in available hormone. The equilibrium constant for adsorption/ desorption may vary exponentially with temperature (Schwarzenbach et al. 1993) and the magnitude of fluctuation would then be closer to 5%. This level of fluctuation in available hormone is not expected to impact culture success. Considered in terms of specific adsorption, this would give a fluctuation on the order of 0.5%.

A.

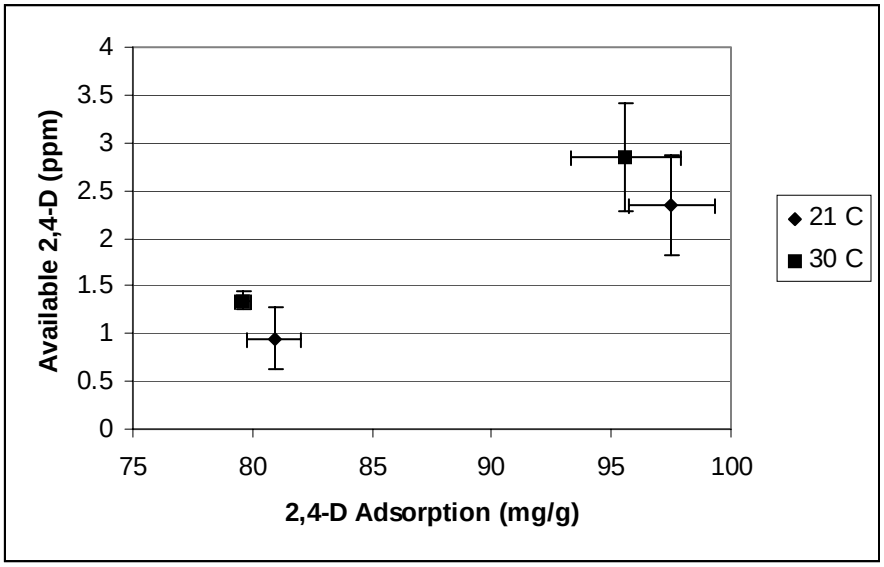

B.

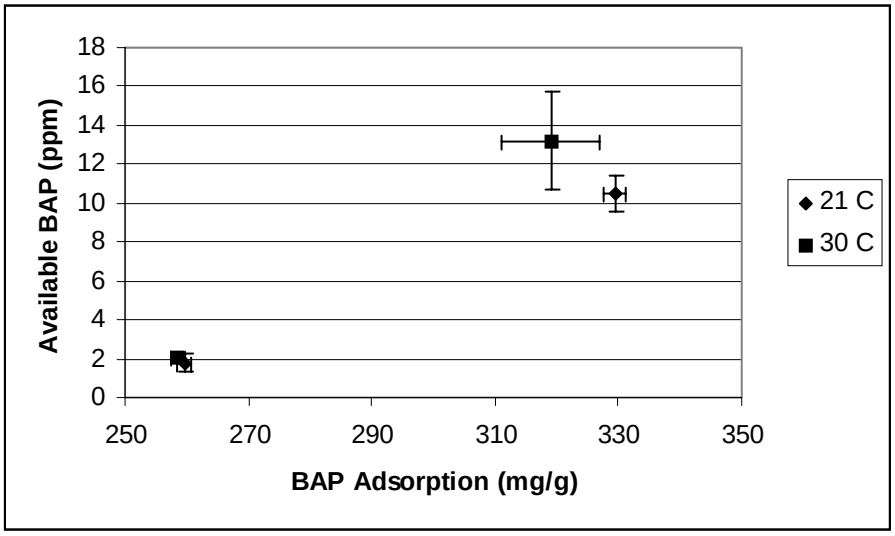

Figure 8.7. Temperature effect on adsorption, A: 2,4-D; B: BAP. Separate media with AC (T1, 0.3g/L, 7.2% MC) were prepared for each hormone. For 2,4-D data, the media were formulated with initial hormone levels of 20ppm and 25ppm. For BAP data, initial hormone levels were 75 and 100ppm. Measurements were taken after 2.5 days.

Autoclave effect

The mean evaporative loss due to autoclaving was approximately 4.5% (measured volumetrically on solutions at room temperature). The available BAP level tended to be higher when media were autoclaved for a duration of fifteen minutes as compared to

longer durations (Figure 8.8). The 2,4-D level was insensitive to differences in autoclave duration. Our lab practice is to sterilize for 22 minutes. The primary concern was whether slight differences in autoclaving time near 22 minutes would lead to significantly different hormone levels. Though there may have been significant differences initially, these were not present when media were sampled, after 2.5 days. The magnitude of the variability in adsorption due to differences in autoclaving was expected to be less than the variability due to other sources and was therefore considered to be insignificant.

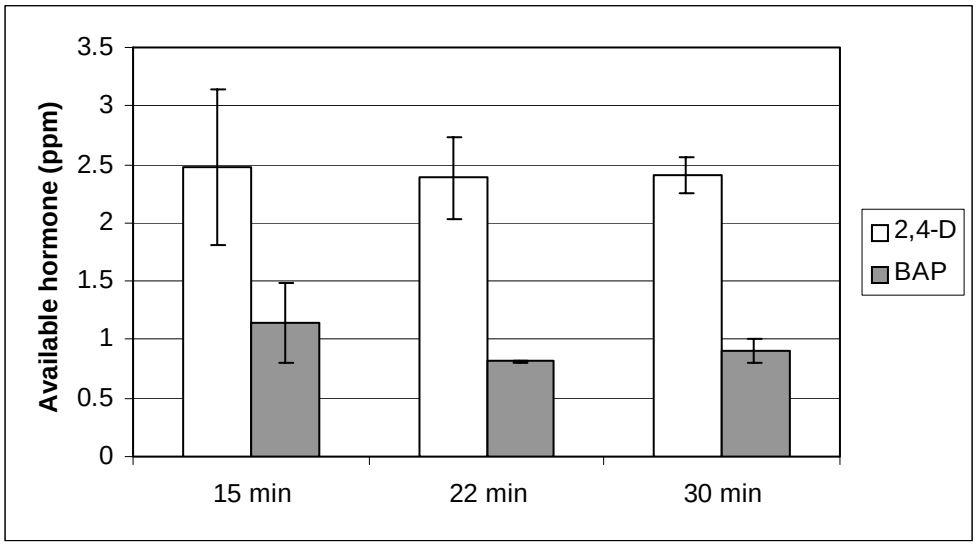

Figure 8.8. Effect of increasing the duration of autoclaving.
Tissue culture media were formulated with AC (T1, 0.3 g/L, 7.2% MC) and both hormones (2,4-D 12 ppm, BAP 65 ppm) autoclaved for 15, 22, or 30 minutes. Samples were collected after 2.5 days. Error bars represent the 90% confidence interval based on three replications (± 1.69 standard deviations).

Summary of Method

Based on the findings above, the media were prepared in flasks, autoclaved for 22 minutes at 121^{o}C and promptly removed to a shaker table in a thermostated room (21^{o}C). The shaker table was set at 100 rpm. Samples were taken after 2.5 days.

B. Results

Initial Results

A liquid growth medium based on a semisolid medium (1/2 BLG, Table 6.11) for Norway spruce initiation that had been previously developed at IPST (unpublished results), was modified to accommodate activated carbon at a significant level (1.25 g/L), but gave low tissue culture success (less than 20%). This medium, in comparison with the control medium (liquid media without AC), included elevated hormone levels: 2,4-D 100 ppm, and BAP at 90 ppm initially; elevated copper and zinc (20 times and 2 times the control levels, respectively, Pullman et al. 1995); and three times the control levels for the vitamins thiamine, nicotinic acid and pyridoxine.

The AC-containing medium became the basis for an experiment using a set of eight different activated carbons. The BET surface area of the eight carbons was distributed over the range from 665 m^2/g to 1105 m^2/g (these will be detailed in a later section). The results for each hormone from this adsorption experiment are shown in Figure 8.9. The results show that for media with AC, the BAP levels were significantly lower than for the control media. The 2,4-D levels, however, were close to the desired level (2 ppm) for three carbons. Five of the carbon-containing media were significantly different from the 2 ppm target, with four being significantly greater than the control and one being lower.

Single-hormone Isotherms (Apparent)

A liquid-solid adsorption isotherm is a graphical depiction of a mass balance for a compound removed from bulk solution to the solid/liquid interface. It is commonly depicted as specific adsorption (e.g. mg sorbate per g sorbent) as a function of bulk phase equilibrium concentration (relative pressure in the case of gas phase adsorption). "Adsorption isotherm" is a term that is generally reserved for systems under thermodynamic equilibrium.

A.

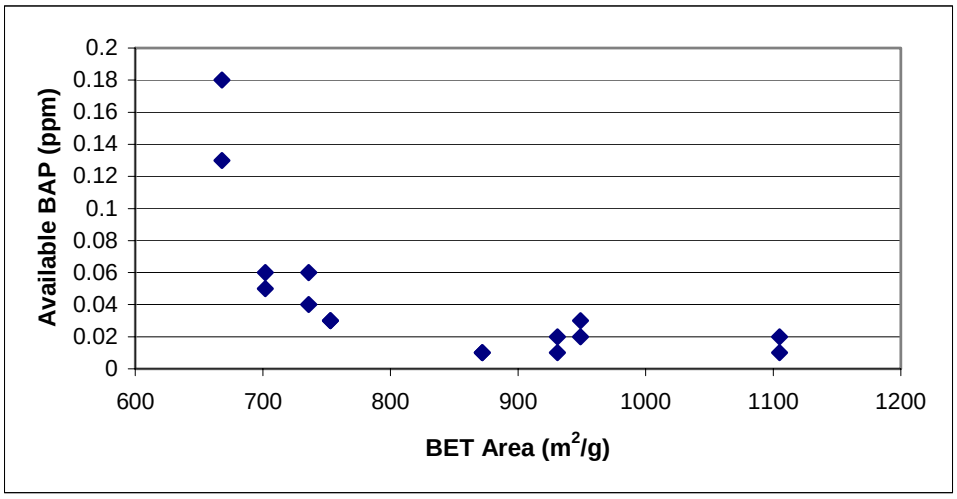

B.

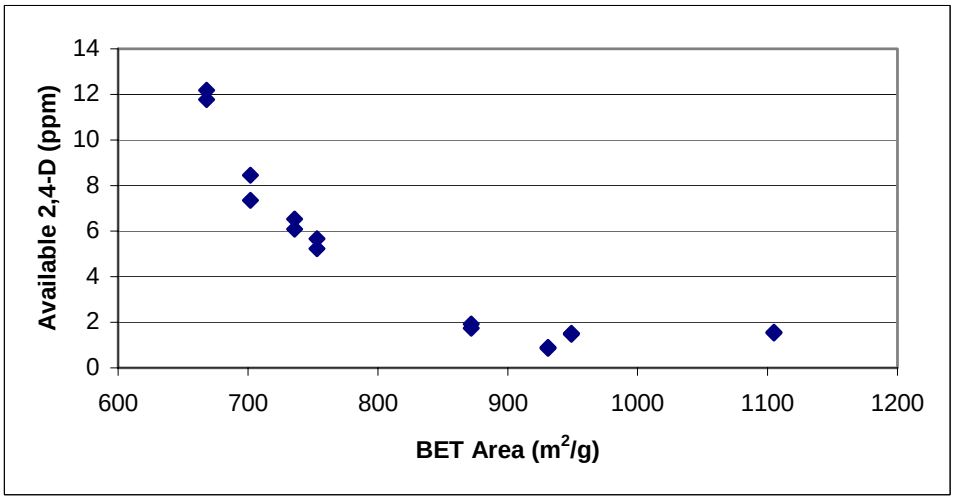

Figure 8.9 Available hormone vs. AC surface area, A. BAP; B. 2,4-D.
Tissue culture media were formulated with 100 ppm 2,4-D and 90 ppm BAP and eight different activated carbons (1.25 g/L) which spanned the depicted range in BET surface area. Samples were collected after 2.5 days and analyzed by HPLC. Each data point represents a single replication.

As shown by the data in Figure 8.3, a true equilibrium state was not achieved within the 2.5-day time frame. However, the rate of adsorption had slowed to such an extent that sufficient hormone would be available to the growing culture if the control hormone levels were present after 2.5 days. The term *apparent isotherm* will be applied to the data presented here.

The collected data from a large group of experiments suggest that 2,4-D was depleted from control media (media without AC) over the 2.5 day timeframe (Table 8.2). Based on data from twenty-nine separate replications measured after 2.5 days, the 2,4-D concentration in control media was 2.3% lower on average than the dispensed value, with a standard deviation of 3.9% (based on actual medium composition, allowing for 2% impurity for the tissue culture-grade reagent vs. the calibration grade). The mean 2,4-D levels after 2.5 days were about 4.5% lower than for media just after autoclaving, but the data displayed a large variability.

Table 8.2. Comparison of hormone levels in control media (% of initial, dispensed level), after autoclaving and after 2.5 days.

	# of Samples	Mean (%)	Stdv. (%)	90% Conf Interval
Autoclave volume loss [1]	7	4.5	0.29	4.0 to 5.0
Post autoclave concentration [1]				
BAP increase	5	+1.7	1.8	(-)1.3 to 4.7
2,4-D increase	5	+ 4.1	1.8	1.1 to 7.1
2.5 day control [2]				
BAP	22	+ 0.5	1.8	(-) 2.5 to 3.5
2,4-D	29	(-) 2.3	3.9	(-) 8.7 to 1.6

1. Compared to non-autoclaved media.
2. Compared to calculated (dispensed) hormone levels in non-autoclaved media.

For BAP, the mean value on 22 replications was 0.5% greater than the calculated level with a standard deviation of 1.8%. The BAP data were consistent with increases due to autoclaving.

The sorption values for media with AC were calculated by subtracting the amount remaining in solution from the post-autoclave control concentration and dividing by the mass of carbon present. For the purposes of this study, it was assumed that all of the BAP and 2,4-D were accounted for by the sum of the adsorbed mass and the mass remaining in solution. On a per-liter-basis this sorption was expressed as sorbed mass (mg) per carbon mass (g).

Growth medium is a complex mixture of inorganic salts and organic solutes, with each potentially affecting the adsorption of the hormones. Some of these solutes would be expected to increase adsorption of the hormones by impacting hormone solubility; whereas competitive effects could be exhibited by a few of the compounds present and possibly decrease the adsorption of hormones. Therefore, adsorption measurements were made using nearly complete growth medium, when possible, as it could not be assumed that adsorption from pure aqueous solutions would be representative of actual medium response.

Most of the hormone data were collected from nearly complete tissue culture media, adjusted to pH 5.8 before autoclaving, and equilibrated 2.5 days at 21^{o}C. Glutamine was usually omitted, based on the standard lab practice of adding glutamine just prior to culturing, after adsorption had already proceeded one or more days.

Single-hormone isotherm data were collected from growth media without glutamine. Apparent isotherms for BAP and 2,4-D adsorption onto three different activated carbons are presented in Figure 8.10. For BAP, the isotherm was based on six data points per trace, whereas for 2,4-D five data points defined each apparent isotherm. Generally, more points are required to completely define an adsorption isotherm. However, successful tissue culture media for somatic embryogenesis typically include hormones at levels below 5ppm: the region in Figure 8.10 below the available hormone level of 10 ppm is of primary interest.

The HPLC data for 2,4-D were in very good agreement with previous data generated using UV measurements on partial media (Figure 8.11). Below 5 ppm, the isotherm may be treated as a linear relationship. The data points above the 10 ppm level help to define the knee (bend) in the isotherm, which is important for fitting an isotherm equation to actual data. The data in Figure 8.10 are fitted using the Freundlich isotherm equation, considered in the next section.

A.

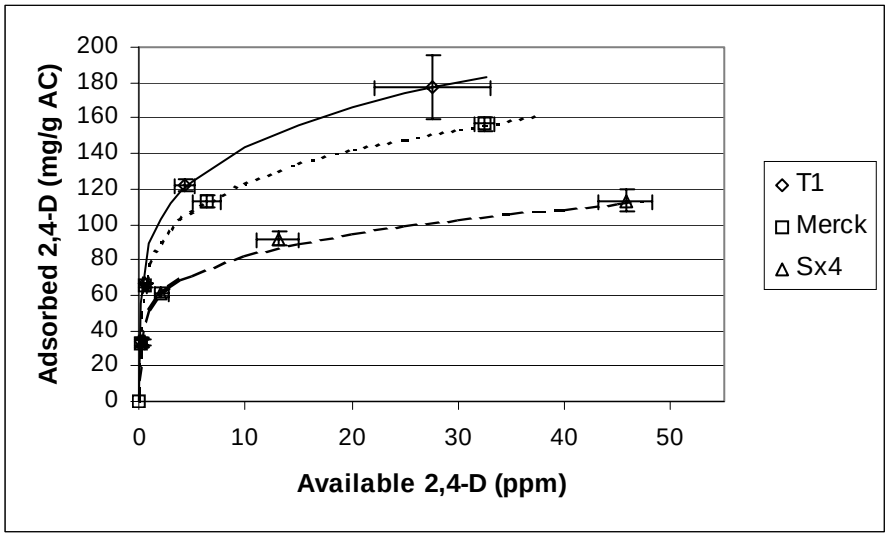

B.

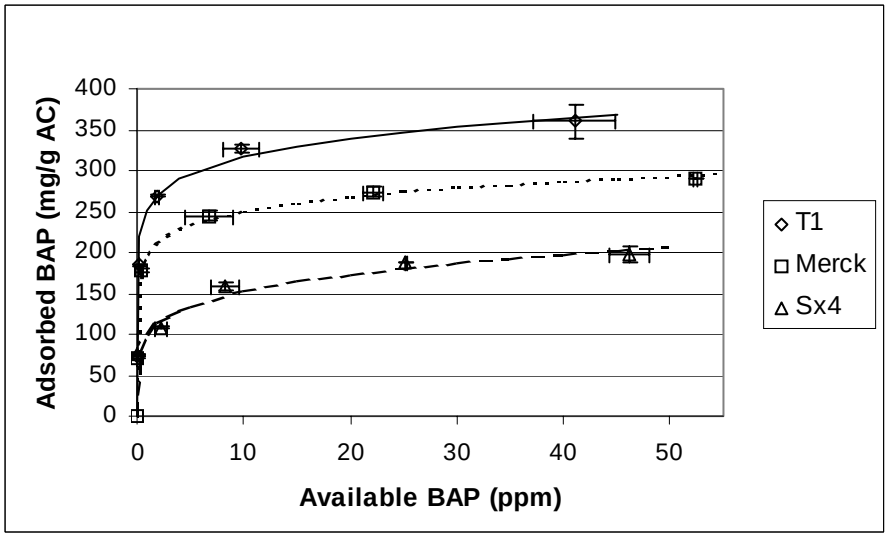

Figure 8.10. Apparent adsorption isotherms for each hormone onto three different activated carbons, A: 2,4-D; B: BAP. The data were generated from separate trials with media containing a single hormone with an equilibration period of 2.5 days. The 2,4-D data were generated from initial concentrations of 10, 20, 40, 80 ppm and AC, 0.3g/L. The BAP data were generated from solutions of 10, 50, 75, and 100, for each carbon (0.3 g/L). Additional BAP sorption points were generated from solutions at 100 ppm and 0.2 g/L Merck and T1, and 30 ppm with 0.3 g/L Sx4. Error bars represent the 90% confidence interval based on three replications. The data have been fitted using the Freundlich isotherm equation. Note that the y-axes are drawn to different scales and that all traces converge to a non-zero point along the y-axis (five data points per apparent isotherm for 2,4-D; six points for BAP).

Comparing the y-axis scales from Figure 8.10, it is apparent that BAP was adsorbed to a level of about twice that of 2,4-D at any level of available hormone, for each activated carbon.

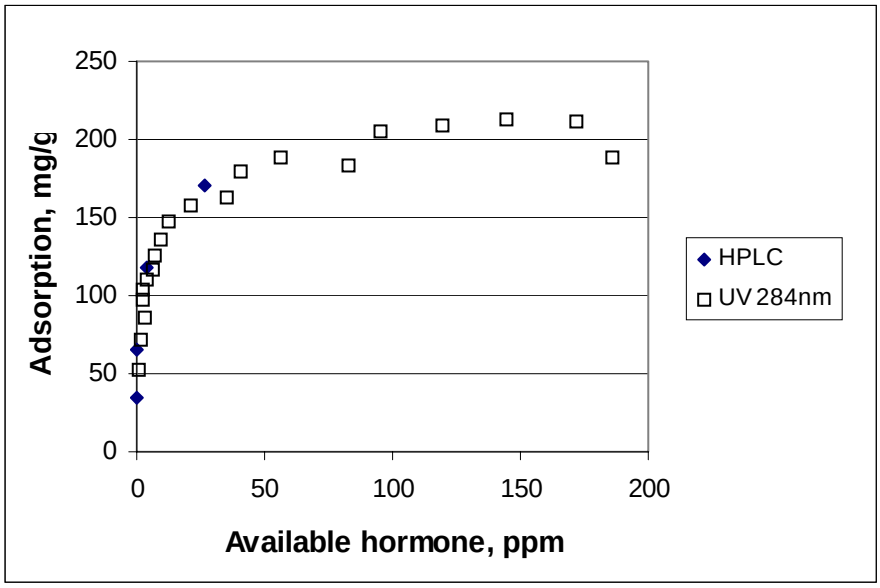

Figure 8.11. Apparent isotherm data for adsorption of 2,4-D onto T1. HPLC data compared with data from a UV technique. The UV data were generated from filter-sterilized, partial media (Fe-EDTA, casamino acids, vitamins were omitted and sucrose solutions were filter-sterilized) that ensured the UV signal would be due to the hormone only.

Freundlich Isotherm Equation

The Freundlich equation is an empirical model that has been found to work well for fitting data for many different systems (see Section IV). The equation is given as (Shaw 1992):

$$x/m = k_F c^{\frac{1}{n}} \qquad (8.2)$$

where *x/m* is the adsorption of solute per gram of activated carbon and k_F and *n* are empirically derived constants related to sorptive capacity and strength of adsorption, respectively. They may be derived from the logarithmic version of the equation, where the slope is equal to *log(1/n)* and the intercept is *log* k_F. These have been tabulated for the adsorption of each hormone onto the three carbons (Table 8.3).

The trend observed from Figure 8.10 was reflected in the magnitude and ordering for the constants, k_F *:* T1 adsorbed more than Merck, which adsorbed more than Sx4. The affinity between the activated carbon and the hormones, as interpreted by constant *n*, was lower for 2,4-D than BAP for each carbon type. Carbon T1 demonstrated higher affinity for BAP than the others, but lower affinity for 2,4-D (compare *n* values).

Table 8.3. Results from Freundlich Curve Fitting of Apparent Isotherm Data

Freundlich Constants				
Carbon type	**BAP**		**2,4-D**	
	n	k_F	n	k_F
Sx4	5.4	100	4.9	52
Merck	9.9	198	5.6	78
T1	10	252	4.8	89

The Freundlich constants are defined by equation 8.2: n is associated with affinity and k_f is associated with sorptive capacity.

Competitive Adsorption

The sorption behavior changed markedly, however, when each hormone was present in excess of the carbon's adsorption capacity. The data for a competitive adsorption experiment are shown in Figure 8.12.

The first sets of tick marks, radiating from the origin, one set for each hormone, result from the initial conditions of 75 ppm (nominal) of each hormone and 0.2 g/L of activated carbon T1. The second sets of marks, again radiating from the origin, result from initial concentrations of 200 ppm for 2,4-D and 100 ppm for BAP with T1 present at 0.3 g/L. Each set of conditions was replicated twice. The presence of 2,4-D at twice the initial level of BAP had insignificant impact on the adsorption of BAP compared to the data generated when they were both present initially at 75 ppm. The deviation of 2,4-D data from the single-hormone isotherm was pronounced. As shown in Figure 8.12, these data were well fit by a linear regression through the origin.

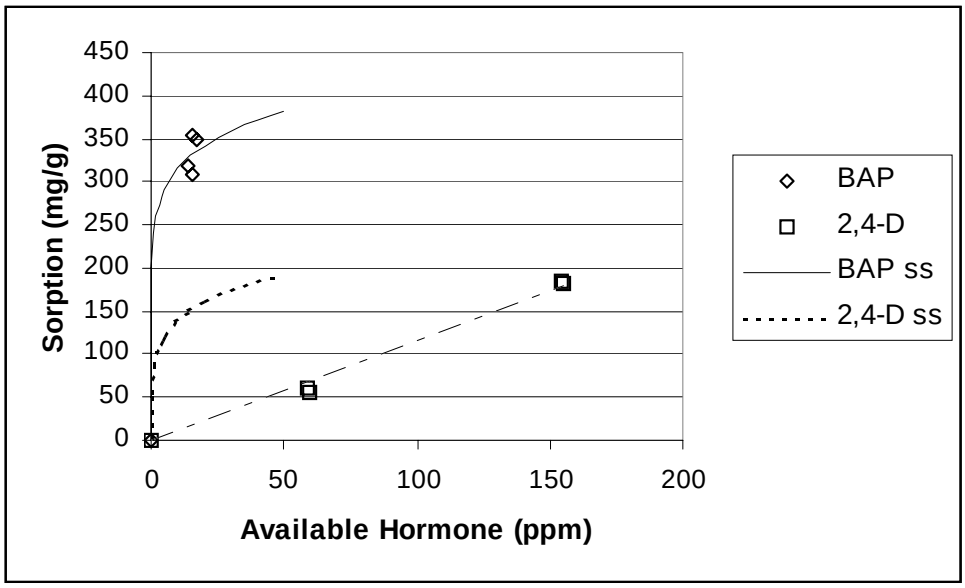

Figure 8.12. Competitive adsorption.
Complete media were formulated with AC and both hormones. Samples were measured after 2.5 days. Radiating from the origin, the first data point for each hormone resulted from the initial concentrations of 75ppm BAP and 100ppm 2,4-D and 0.3g/L AC. The second data points resulted from initial hormone levels of 100ppm BAP and 200ppm 2,4-D and 0.2 g/L AC. The single-solute (*ss*) isotherms for adsorption of 2,4-D and BAP onto T1 (Figure 8.11), are superimposed for the purpose of comparison.

Achieving Target Hormone Levels (2 ppm 2,4-D; 1 ppm BAP)

It was expected that hormone levels in media without AC which gave high culture success could also result in high success rates in media with AC . Target hormone levels were therefore chosen based on the levels which gave high success rates for control media (media without AC): 1 ppm BAP, and 2 ppm 2,4-D.

Referring again to the apparent isotherm data in Figure 8.10, the BAP trace for carbon T1 indicates that, to achieve an available level of 1ppm, 225 ppm would be adsorbed per gram of activated carbon on a per-liter basis. Typical tissue culture practice involves activated carbon levels of 1.25 g/L or 2.5 g/L. An estimate of the BAP concentration necessary to accommodate 1.25 g for carbon T1 would be 1.25 x 225 ppm or 281 ppm, plus the 1 ppm remaining available, for a total of 282 ppm. Similarly, a level of 2.5 g/L would require approximately 564 ppm.

An experiment in which the pH of BAP stock solution (1g/L, BAP with HCl) was increased from pH 3 to pH 5.8 resulted in the precipitation of BAP. The BAP

concentration remaining in solution was approximated (using UV_{270} absorbance) as 165 ppm. Based on the BAP isotherm for T1, this solubility limit for BAP imposed a mass ceiling for activated carbon T1 of about 0.66 g/L. The solubility for 2,4-D exceeded 1 g/L across the pH range of interest and was therefore not a limitation.

Further study was performed using media with a reduced level of activated carbon, 0.3g/L. This level was expected to be low enough to avoid solubility issues and yet was still high enough to have a definite impact on tissue culture growth. Tissue culture results suggested that inhibitory nutrient shortages were present in control media when carbon was added at levels of 0.1 g/L (see Section XI). The moisture content of the activated carbon was measured as 7.2% (e.g. 0.3 g/L T1 “nominal” is equivalent to 0.28g/L oven dry). Nominal, or moist, values will be referred to throughout this study except where noted.

Approximation from BAP Isotherm

Using a carbon level of 0.3 g/L, an initial attempt was made to achieve target hormone levels. Based on the findings with respect to the relative levels of adsorption between BAP and 2,4-D, the first approximation was made by assuming that there was no competition between the hormones, i.e. the entire sorption volume was occupied by BAP. At an available hormone level of 1ppm, the adsorption level for BAP was approximated visually from the apparent isotherm data as 225 mg/g. Multiplying by 0.3g/L of activated carbon gave 67.5ppm. Adding one ppm for the ppm remaining available in the medium gave 68.5 ppm. It was expected that this level would prove to be too high based on the competition effect, so the initial BAP level was reduced to 68 ppm. The initial concentration of 2,4-D (2ppm) was determined by assuming that no adsorption would occur. The results from this trial and two others are depicted in Figure 8.13.

The data in Figure 8.13 are presented in a way that allows both hormone levels to be observed: a functional relationship between the axes is not intended. The first trial involved initial BAP and 2,4-D levels of 68 and 2 ppm, respectively. The "target " on this plot is the intersection defined by 1 ppm BAP and 2 ppm 2,4-D. The initial effort resulted

in levels which were close to the target, giving an *average* for the two trials of about 3.25 ppm BAP and 0.6 ppm 2,4-D.

The next attempt was based on a careful study of the isotherm for BAP and the slope in the region of the first attempt. This happened to agree well with the observation that the initial attempt missed the target by about 3 ppm. Therefore the second attempt incorporated BAP at 65ppm. The next 2,4-D level to be tried was unpredictable based on the single-solute isotherm and so a couple of tries were made before the one depicted in Figure 8.13 with BAP at 65ppm and 2,4-D at 10ppm. This produced available hormone levels of about 0.75ppm for BAP and 1.25 ppm 2,4-D. This was an encouraging result but still too far away from the target.

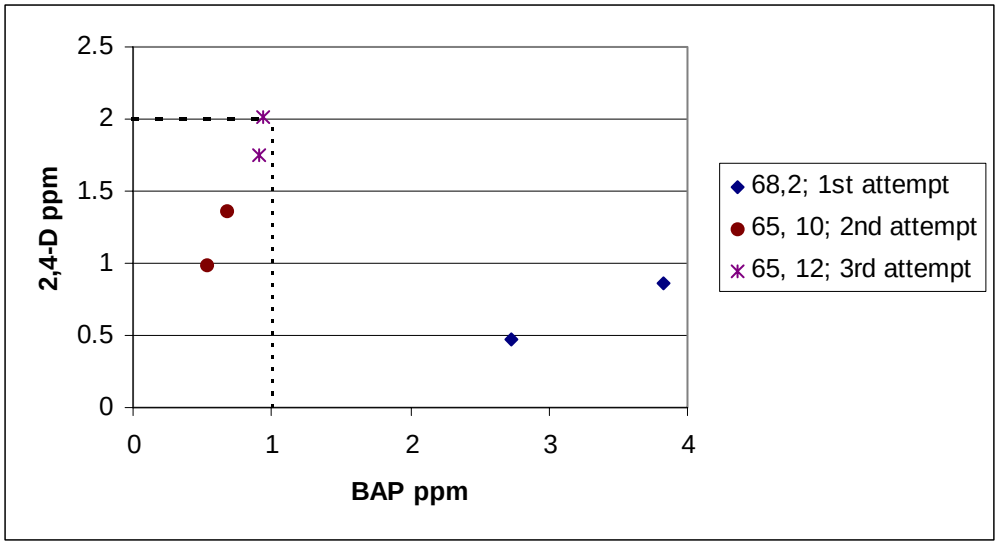

Figure 8.13. Achieving target hormone levels.
Trials were conducted using complete media with AC (0.3 g/L). Media were formulated with initial concentrations of 68 and 65 ppm for BAP and 2, 10, and 12 ppm for 2,4-D. Measurements were made after 2.5 days. The target levels were chosen as 1ppm BAP and 2ppm 2,4-D based on successful media without AC. Each data point represents a single replication. The axes indicate available hormone, adsorption is not depicted: a functional relationship between the axes is not intended. The axes indicate available hormone. The data points summarize an effort that actually required five iterations.

The final effort involved initial hormone levels of 65ppm and 12 ppm for BAP and 2,4-D, respectively. This effort resulted in available hormone levels (average) after 2.5 days of 0.93 ppm BAP and 1.85 ppm 2,4-D. These levels were considered to be acceptably close

to the target levels. Notice that increasing the 2,4-D level from 10 ppm to 12 ppm had a minor effect on the adsorption of BAP.

The data points for the successful combination of initial BAP to 2,4-D of 65ppm:12ppm, along with a few other combinations, have been plotted in Figure 8.14 for each hormone. The data are compared to the limiting cases for each hormone, the "single solute" Freundlich curves (designated *ss*) and competitive isotherms (straight lines) in Figures 8.14 and 8.15. For BAP the low levels of 2,4-D present did not shift the system towards the competitive case: there was good agreement with the BAP single solute data. However, for 2,4-D the presence of BAP caused the data to fall closer to the competitive case. A decrease in initial BAP of 15 ppm, from 65 ppm to 50 ppm, resulted in higher adsorption of 2,4-D.

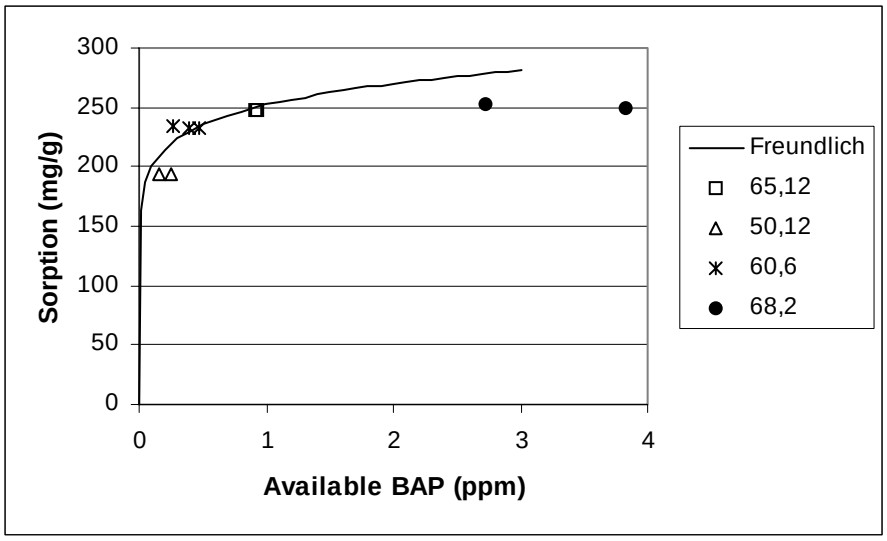

Figure 8.14. Comparison of results for BAP adsorption
The data from Figure 8.13 have been replotted in the manner of isotherm data. The initial hormone levels depicted for four iterations were BAP: 65, 50, 60, and 68ppm with 2,4-D levels of 12, 12, 6 and 2ppm, respectively. The single-solute Freundlich isotherm for adsorption of BAP onto T1 (Figure 8.10) is superimposed for comparison.

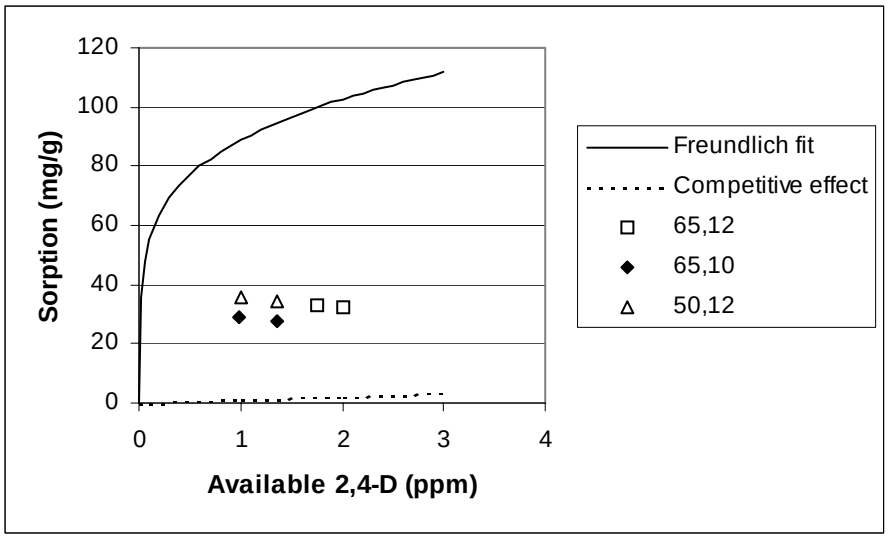

Figure 8.15. Replot of 2,4-D data from Figure 8.14 in isotherm format.
The single-solute Freundlich fit for 2,4-D adsorption onto T1 (Figure 8.10) is superimposed, as is the straight-line relationship depicting the adsorption of 2,4-D when competing with excess BAP (Figure 8.12).

Target levels were achieved with two other activated carbons following a similar procedure. The successful combinations are presented in Table 8.4.

Table 8.4. Hormone levels and resultant adsorption (AC: 0.3g/L)

	Sx4	**Merck**	**T1**
AC + water (g/L)	0.3	0.3	0.3
Solids (%)	91.8	94.6	92.8
AC, dry (g/L)	0.275	0.284	0.278
BAP initial (ppm)	32	55	65
BAP control*	32.5	54.4	65.9
BAP adsorbed (ppm)	31.5	53.4	64.9
BAP adsorbed (mg/g)	114	188	234
2,4-D initial (ppm)	8	10	12
2,4-D control*	7.6	9.5	11.6
2,4-D adsorbed (ppm)	5.6	7.5	9.6
2,4-D adsorbed (mg/g)	19.4	26.4	34.9

*Control media (non-AC). Measurements were made after 2.5 days.
2,4-D losses for controls compared to initial were not due to autoclaving.

The sorption data have been corrected to reflect the 2.5 day hormone levels actually measured in the control sample. These were about the same as the initial value in the case

of BAP and about 5% lower than initial for 2,4-D, on average. The mass of AC was also corrected for moisture content which ranged from 4.5 to 8%.

Correlation Between Porosity and Adsorption of Hormones

The corrected sorption data have been plotted in Figures 8.16 and 8.17 as a function of total pore volume and BET surface area (DFT). An excellent correlation was indicated between adsorption and porosity, when adsorbing to the same apparent equilibrium. Though both parameters fit the data well, the fit was better for BAP using total pore volume and better for 2,4-D using the BET area.

Extending the Correlation with Porosity

It was shown in the previous section that target hormone levels may be achieved using different activated carbons. The applied method however, would be cumbersome given a new set of carbons and a set of different target levels.

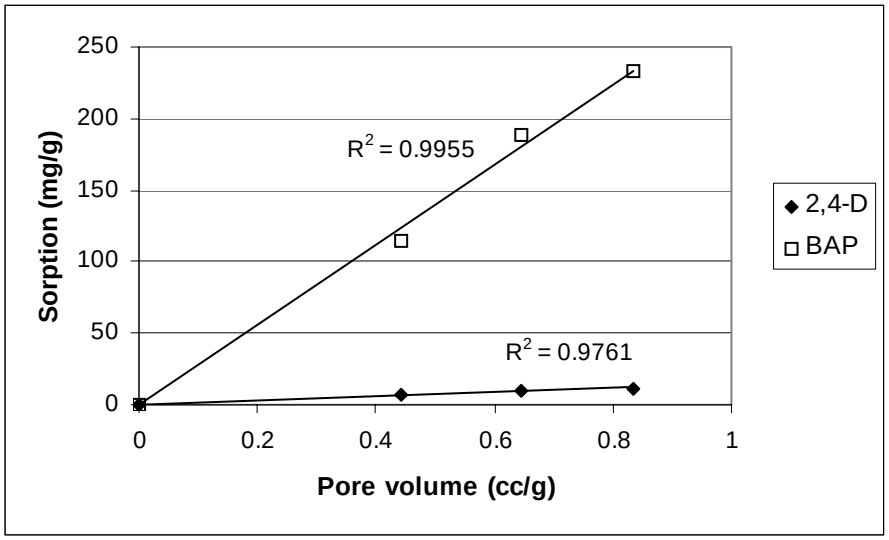

Figure 8.16 Correlation between sorption and total pore volume.
Mean data are shown for the adsorption of each hormone onto three activated carbons (0.3 g/L, T1, Merck, Sx4) that differed in porosity over the depicted range in pore volume. The data depict the amount of hormone adsorbed per gram of carbon to attain target levels of available hormone (i.e. apparent equilibrium levels of 1ppm BAP and 2ppm 2,4-D after 2.5 days from media with initial hormone levels as given in Table 8.4).

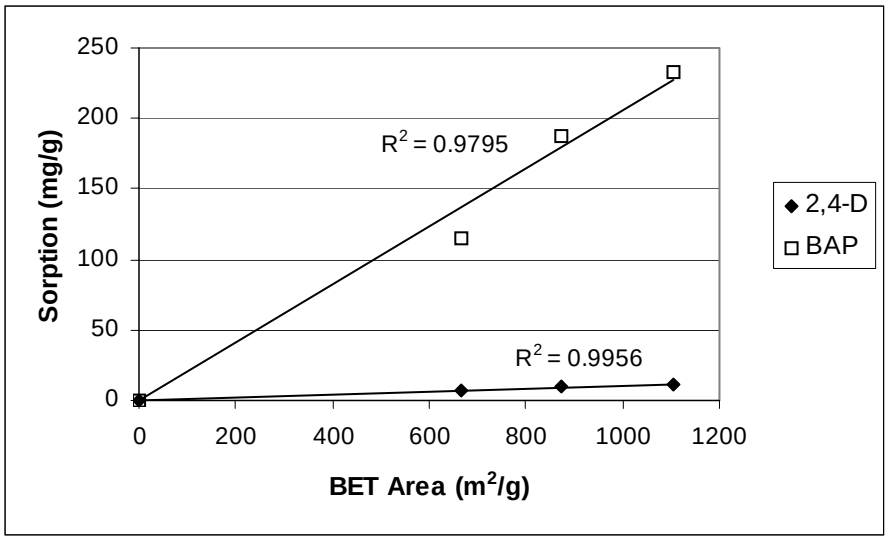

Figure 8.17 Correlation between sorption and BET surface area.
Mean data are shown for the adsorption of each hormone onto three activated carbons (T1, Merck, Norit Sx4) that differed in BET surface area over the depicted range. The data depict the amount of hormone adsorbed per gram of carbon to attain target levels of available hormone (i.e. apparent equilibrium levels of 1ppm BAP and 2ppm 2,4-D after 2.5 days from media with initial hormone levels as given in Table 8.4.).

The sorption vs. porosity data suggest that the mass of the carbon could be adjusted on the basis of relative BET area or total pore volume for each new carbon rather than keeping carbon mass constant and adjusting the initial hormone levels.

The correlation between sorption and porosity, depicted in Figures 8.16 and 8.17, was explored further using a set of eight different activated carbons. Except for the Sigma C-5260 (N1 and N2) carbons, these carbons were chosen based on references in the plant tissue culture literature. Each of the eight different activated carbons was characterized using DFT analysis applied to nitrogen adsorption data. The cumulative pore volume, micropore volume, and the BET surface areas for each of the eight carbons are presented in Table 8.5.

The carbons spanned a range in BET area from 665 m^2/g for Norit Sx4 to 1105 m^2/g for Sigma C-9157 (T1). It can be seen that there were significant differences between production lots for each of the two different carbon types from Sigma. This level of variation is typical for certain grades from commercial sources. The range in BET area

was normal for carbons used for water treatment. Carbons for vapor phase adsorption

generally have much higher BET area, often exceeding 2000 m^2/g (Baker et al. 1992). The cumulative pore volume gave a different ranking for the lower surface area carbons.

Table 8.5. Porosity Summary for Eight Activated Carbons from Nitrogen Sorption Data*

	BET Surface Area (m^2/g)	**Micropore Volume (mL/g)**	**Total Pore Volume (mL/g)**
Norit Sx4	665	0.249	0.442
Sigma C-5260 lot #1 (N1)	702	0.250	0.540
Norit Sx2	730	0.272	0.534
Sigma C-5260 lot #2 (N2)	753	0.2861	0.482
Merck	866	0.314	0.645
Darco G60	938	0.344	0.679
Sigma C-9157 lot #2 (T2)	949	0.341	0.730
Sigma C-9157 lot #1 (T1)	1105	0.391	0.833

* Analyses performed by Westvaco

The ratios of the porosity values for each carbon to the corresponding values for T1 are presented in Table 8.6. It may be seen that for a few of the carbons the ratios based on BET surface area were significantly different from those based on total pore volume or micropore volume. Using these ratios, the mass of each carbon was adjusted to give the pore volume or surface area equivalent to 0.3 g/L of T1. The ratios, which resulted in acceptable agreement with the target hormone levels, are given in the final column of the table. Ash data were collected for four of the carbons, N1, N2, T1, and T2 (mean of IPST and CAER values from Table 6.3). Adjusting for ash improved the agreement for carbons N1 and N2 between the TPV ratio and actual ratio: 1.58:1 vs. 1.65:1, and 1.84:1 vs. 1.8:1 (est.), respectively. The TPV ratio for T2 decreased, however, from 1.14:1 to 1.13:1. More data are needed, but these results suggest that an improved fit could result from applying an ash correction to the mass of activated carbon, indicating that adsorption is directly related to carbon content.

Table 8.6. Ratio to T1 mass for BET, total pore volume (TPV), and micropore volume (μPV) equivalence, compared to the successful ratio.

	BET	TPV	μPV	Actual ratio
Sx4	1.59	1.89	1.57	1.88
N1	1.58	1.54	1.56	1.65
N2	1.45	1.73	1.37	1.8 (est.)
Sx2	1.44	1.56	1.44	1.58 (est.)
Merck	1.22	1.29	1.24	1.3
T2	1.15	1.14	1.15	1.14
G60	1.13	1.23	1.14	1.16
T1	1	1	1	1

Example: If the original system had 1 g/L T1, then the same system with G60 would require 1.13g to have the same adsorptive potential towards the hormones. The measured ratio which resulted in similar hormone levels was 1.16.

The resultant sorption data are presented in Figure 8.18. Overall, the results were quite good, showing that target hormone levels could be achieved for different activated carbons simply by careful adjustment of the initial activated carbon mass. Two carbons stood out as producing relatively high 2,4-D levels: N2 and Sx2.

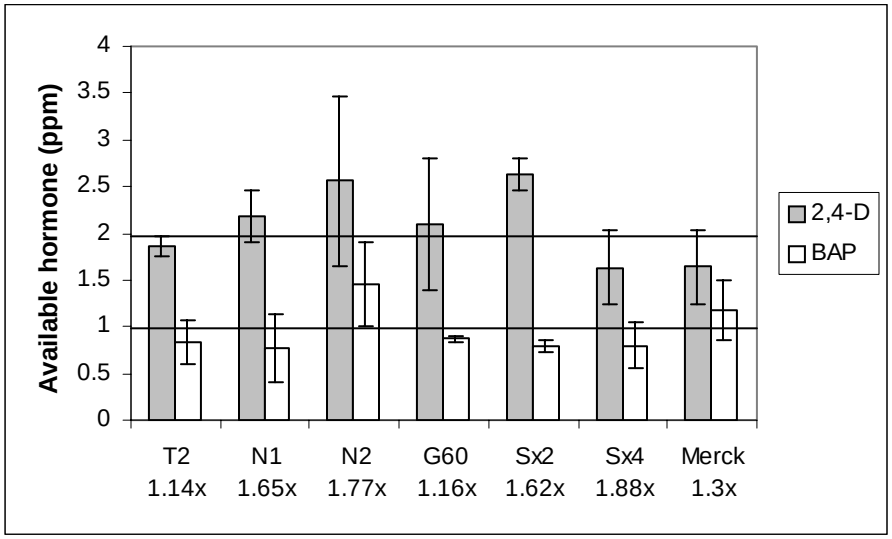

Figure 8.18. Achieving target hormones with seven activated carbons from media formulated for T1. Initial hormone levels were 65ppm and 12ppm for BAP and 2,4-D, respectively. The mass of AC in each case was adjusted by a factor based on the ratio of pore volume to that of T1 (e.g. the mass of T2 was 1.14 times that of T1). Measurements were taken after 2.5 days. Error bars depict the 90% confidence interval based on three replications. The target levels were 1 ppm BAP and 2 ppm 2,4-D.

It was assumed that a slight increase in mass for N2 would result in better agreement with target levels. This level was estimated to be 0.54 g/L, a factor of 1.8 when compared with 0.3 g/L T1, and is the value which appears in Table 8.6.

The Sx2 trials resulted in an elevated pH level of 6.3, significantly higher than the others which averaged pH 5.5. The pH effect on the available hormone levels will be discussed in the next section. Correcting for the elevated pH resulted in 2,4-D levels for Sx2 which were below the others, falling near 1.6 ppm. BAP levels were unaffected by this pH difference. It is expected that a slight reduction in Sx2 mass would result in a ratio very well predicted by the total pore volume ratio: the *Actual Ratio* value for Sx2 in Table 8.6 has been reduced to reflect this.

It can be seen from the table that the mass ratios based on TPV were more consistently near the actual values. The largest difference between the predicted value based on total pore volume and the actual value was 6.7% for N1. The other predictions based on TPV were within 5% of the actual values. Interpreted another way, these data indicate that 95% of the adsorption was accounted for based on the relative pore volume of the different activated carbons.

Increasing the Activated Carbon Level

The 0.3 g/L level for activated carbon was quite low relative to current tissue culture practice. The higher levels used commonly (1.25 g/L, 2.5 g/L) suggest that there are benefits to increasing the level of activated carbon. An experiment was conducted using elevated carbon levels (0.5g/L each, T1 and Sx4) with hormone levels elevated in proportion, but still below the solubility limit for BAP. These data are compared with data pooled from several experiments using 0.3g/L of activated carbon in Figure 8.19.

For each carbon, the mean available hormone levels at 0.5 g/L were greater than the mean values for 0.3g/L levels. The mean hormone values at the higher AC level fell within the 90% confidence limits for three treatments, however. The 2,4-D value for T1 appeared to

be significantly different. More data are needed to firmly establish a mass effect, but the indication from the trend is that hormone levels will likely be higher if AC is increased together with proportionate increases in initial hormone levels.

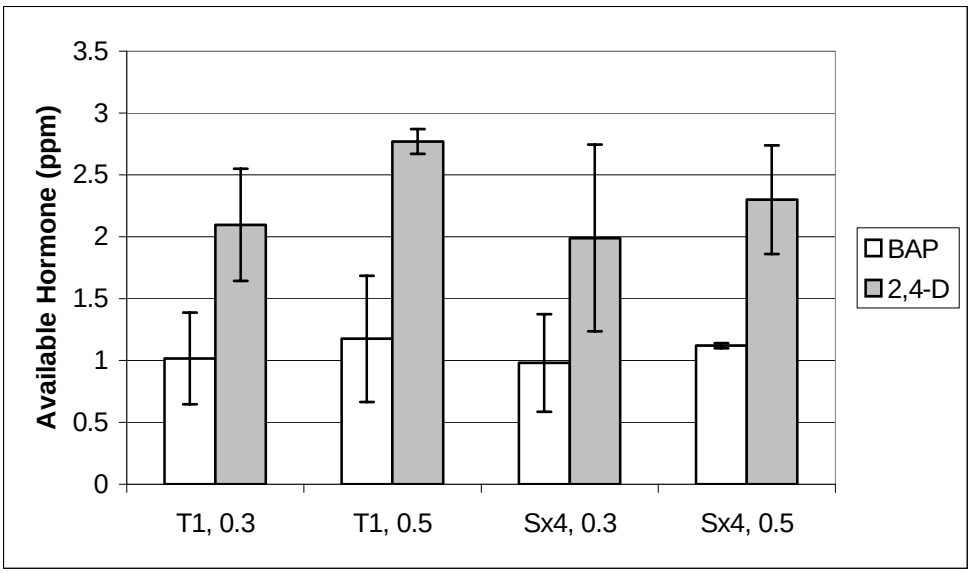

Figure 8.19. The mass of AC in the medium was increased to 0.5 g/L (from 0.3 g/L previously) and initial hormone levels were increased proportionately (by a factor of 1.67). Measurements were made after 2.5 days.

Preloading AC with BAP

If the adsorption of BAP could be prevented or minimized, then its solubility limit would no longer be a constraint on the level of AC in the medium. An alternative approach to the problem of achieving hormone targets would therefore be to minimize the adsorptive capacity of the AC for BAP.

An experiment was conducted in which activated carbons (T1, Sx4) were preloaded with BAP at pH 5.8 with sufficient BAP (100ppm per 0.3 g/L AC) to greatly exceed the target hormone level (1ppm). After 2.5 days, the carbon was filtered from the medium and rinsed into media with control hormone levels (1ppm BAP; 2ppm 2,4-D). These media were then autoclaved and shaken in flasks for 2+ days. The results are shown in Figure 8.20.

The concentration of BAP (Figure 8.20) actually increased relative to the control value, measured as slightly more than 1ppm. This result indicates that a portion of the adsorbed hormone was adsorbed reversibly. Note that the effect was present for both T1 and Sx4. However, one-third to one-half of the initial 2,4-D was adsorbed.

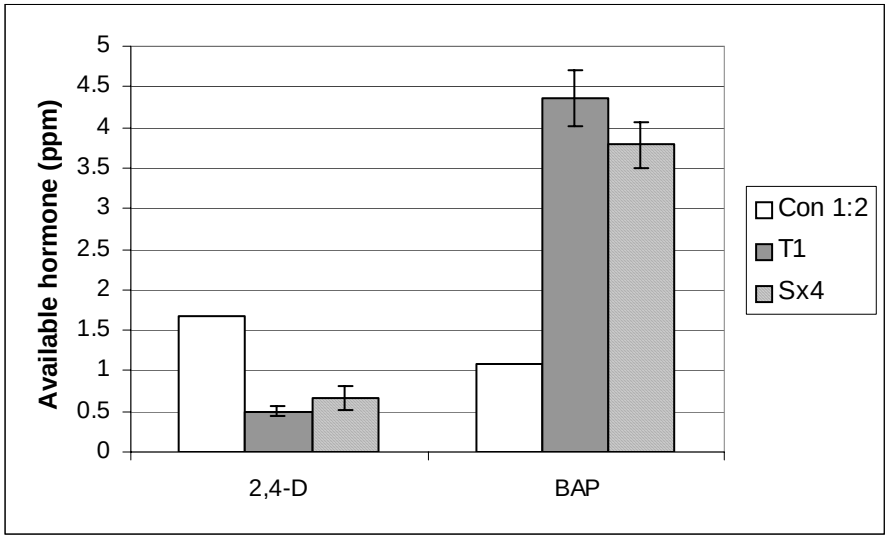

Figure 8.20. Preloading AC with BAP.
BAP was pre-adsorbed onto T1 and SX4 from aqueous solution with excess BAP (100ppm BAP and 0.3g/L AC). After 2.5 days, the AC was filtered off and transferred to non-AC media formulated with 1 ppm BAP and 2 ppm 2,4-D. Measurements were made after an additional 2.5 days. Error bars are given for the 90% confidence interval based on three replications.

The second plot, Figure 8.21, shows the effect when the receiving media hormone levels were elevated to 10 ppm. Under these conditions, the 2,4-D again was adsorbed, nearly by the same percentage as it was for the lower levels. The sorption of BAP was unanticipated. This complex behavior will require further study before it can be predicted: preloading of AC with BAP may prove to be an impractical strategy.

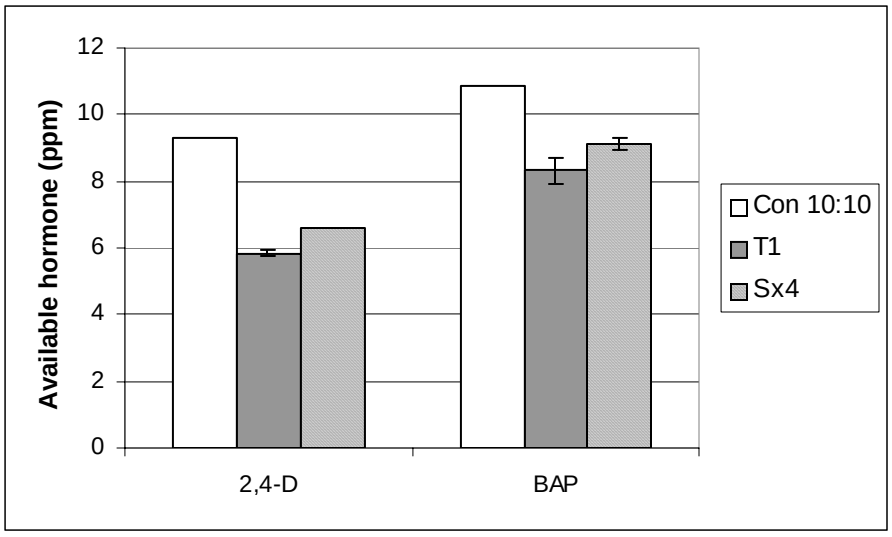

Figure 8.21. Preloading experiment #2.
The procedure was identical to that for Figure 8.20, except that the medium which received the BAP-loaded AC was formulated with 10 ppm of each hormone. Error bars are given for the 90% confidence interval based on three replications. As a percentage of the initial concentration, the adsorption of 2,4-D was similar to Figure 8.20.

Medium Composition Effects

Effect of pH

The pH of the media was adjusted to 5.8 prior to autoclaving, but it dropped to about pH 5.6 after autoclaving. This drop has been attributed to the hydrolysis of sucrose (Druart, Wulf 1993). The growing Norway spruce culture caused a further decline in pH, to approximately 4.8 within 21 days. The acid-washed carbons had minor impact on this behavior. However, the untreated activated carbons in this study (Sigma C-5260) were difficult to neutralize and retained an alkaline character after autoclaving, which continued to influence pH over time. The pH of the N1-containing medium was generally near 6.5 after autoclaving.

The effect of formulating media to different pH levels over the range of 4.8 to 6.7 for media containing two different activated carbons is shown in Figure 8.22. It can be seen from the figure that BAP levels were insensitive to pH changes over this range, whereas 2,4-D levels varied significantly. For T1, the average fell by two thirds from the target level. An instantaneous decrease in pH, from 5.8 to 4.8, resulted in a similar decrease in

available 2,4-D with no impact on available BAP (Figure 8.23), indicating that the decline in pH due to growing tissue will decrease the 2,4-D levels in media containing activated carbon.

Conversely, increasing the pH from 5.2 to 5.8 or 6.5 resulted in the release of sorbed 2,4-D (Figure 8.24), resulting in hormone levels similar to those depicted in Figure 8.22. It should be noted that the level of adsorbed 2,4-D was different in these two figures: the data in Figure 8.22 were collected from complete media with initial hormone levels of 65 ppm BAP and 12 ppm 2,4-D; whereas, the data in Figure 24 were collected from aqueous 2,4-D at an initial level of 42 ppm. For each experiment activated carbon was included at 0.3 g/L.

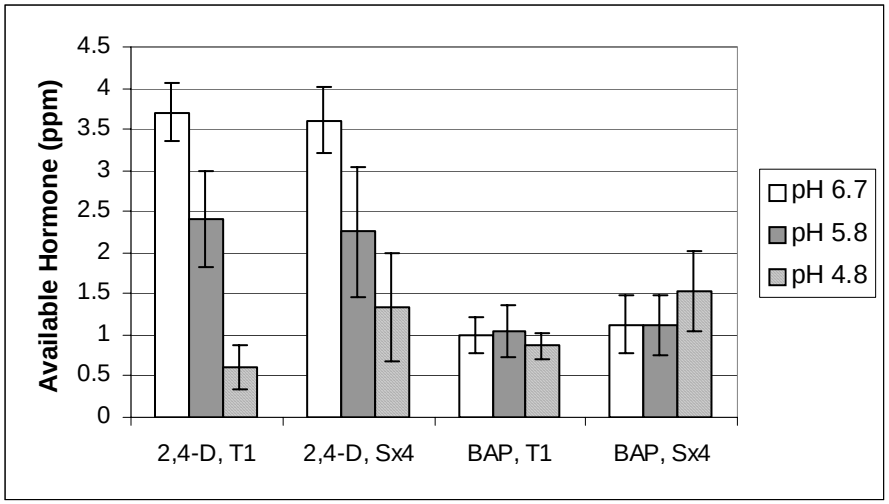

Figure 8.22 pH Effect on hormone adsorption.
Media were formulated with 0.3 g/L AC (T1 and Sx4) to three different pH levels. For T1 media, the initial hormone levels were 65ppm and 12 ppm and for Sx4 media the levels were 32 and 8ppm for BAP and 2,4-D, respectively. Measurements were made after 2.5 days. Error bars depict the 90% confidence interval based on three replications.

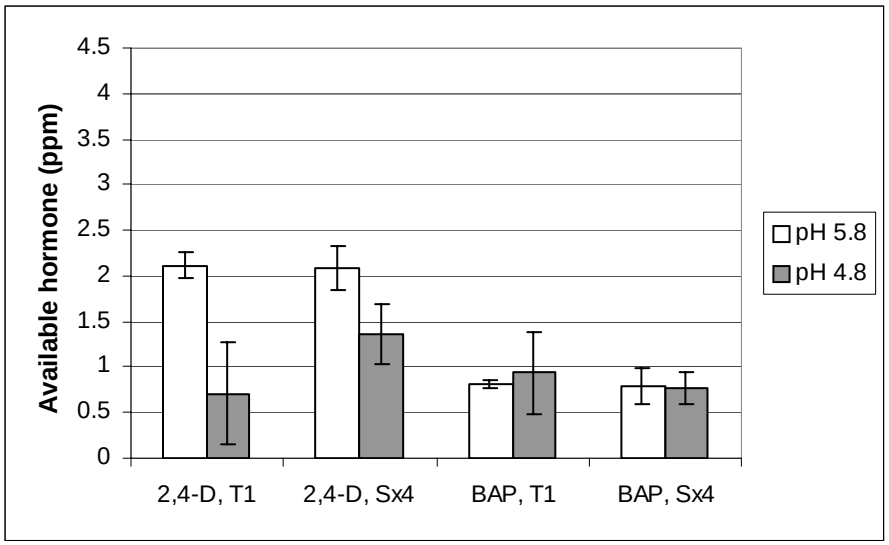

Figure 8.23. Media were formulated to pH 5.8. After 2.5 days the pH was adjusted to 4.8. Measurements were made after six additional hours. Data are depicted for two activated carbons, T1 and Sx4. Error bars depict the 90% confidence interval based on three replications.

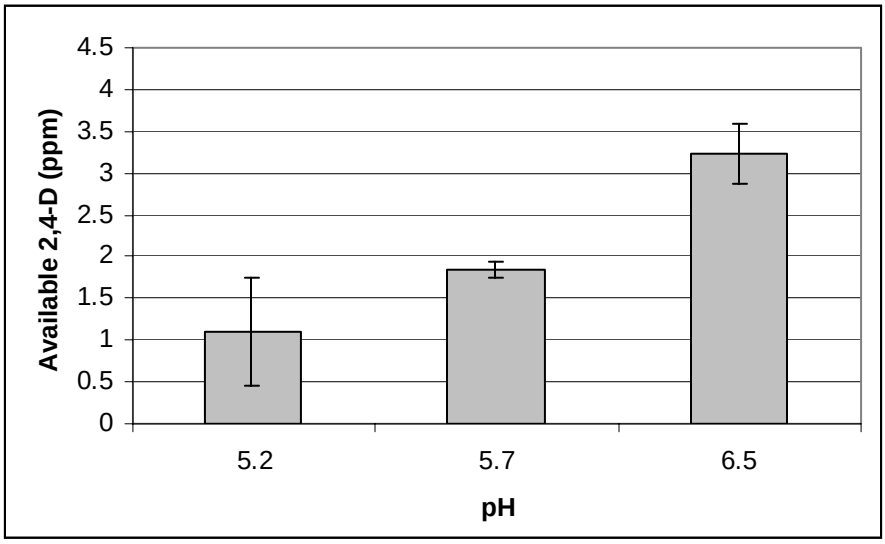

Figure 8.24. 2,4-D was adsorbed onto AC from aqueous buffer (0.02N KH_2PO_4, KOH, HCl) at pH 5.2. After 2.5 days two samples were taken and adjusted to either pH 5.7 or pH 6.5. Measurements were taken at UV_{284}. The initial hormone level was 42 ppm and AC (T1) was present at 0.3 g/L. Error bars depict the 90% confidence interval based on three replications.

Glutamine effect

It is common practice to add glutamine just prior to dispensing media. The elapsed period of time may vary from just after autoclaving to several days after autoclaving. Depending on when it is added to the medium, glutamine addition may result in an increase or a

decrease in available hormone levels. For the system with T1, which yielded target hormone levels of 1 ppm BAP and 2 ppm 2,4-D, the addition of glutamine at 2.5 days resulted in a decrease in available hormone (Figure 8.25). The immediate decrease was sustained over the extended period to 7.5 days. The addition of glutamine resulted in a decrease in pH from 5.6 to about 5.4; and the decrease in 2,4-D level was consistent with this decline in pH.

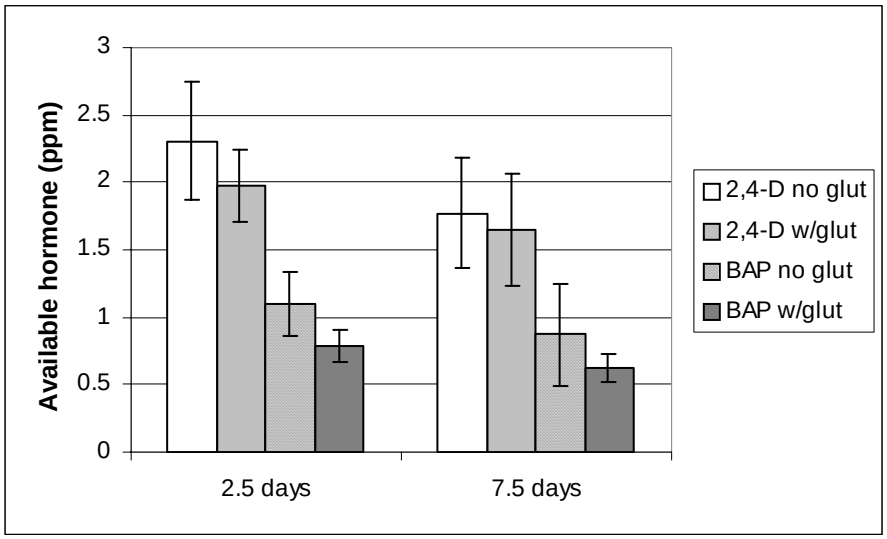

Figure 8.25. The addition of glutamine to media with AC increased the hormone adsorption. Glutamine was added after 2.5 days to growth media containing T1 (0.3g/L) with initial hormone levels of 65 and 12 ppm for BAP and 2,4-D, respectively. For the measurements at 2.5 days, media were sampled within hours of adding glutamine. The same media were sampled again after an additional 5 days. Error bars depict the 90% confidence interval based on three replications.

However, when glutamine was added immediately after autoclaving and the media were allowed to equilibrate 2.5 days prior to measurement, available 2,4-D levels increased significantly whereas BAP levels were unaffected.

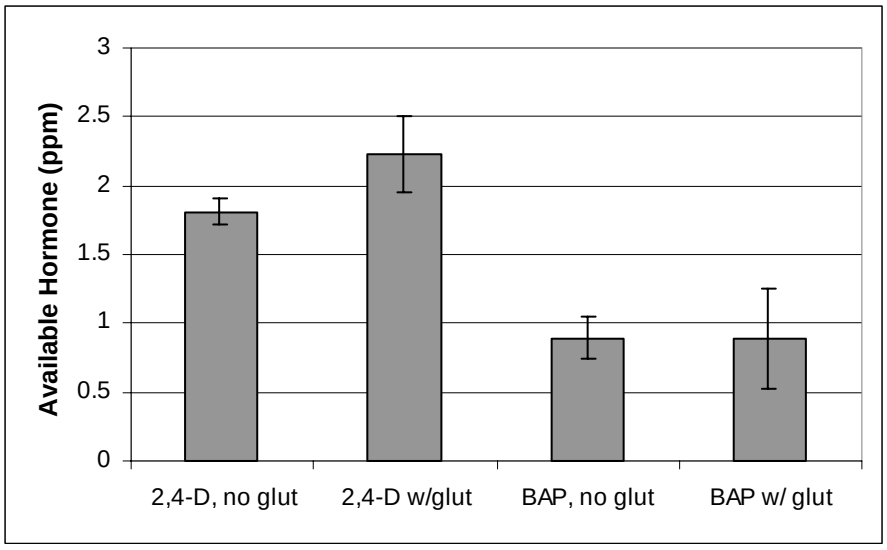

Figure 8.26. Glutamine was added to media with AC immediately after autoclaving. Media contained T1 (0.3g/L) with initial hormone levels of 65 and 12 ppm for BAP and 2,4-D, respectively. Measurements at 2.5 days. Error bars depict the 90% confidence interval based on three replications.

Sucrose effect

Of the medium components, the carbohydrate source is typically present in growth media in the largest concentration. Sucrose, included in media at concentrations ranging from 10 to 40 g/L, is the most commonly used carbohydrate. Data are presented for available hormone vs. time for adsorption onto T1 in Figure 8.27 and Figure 8.28.

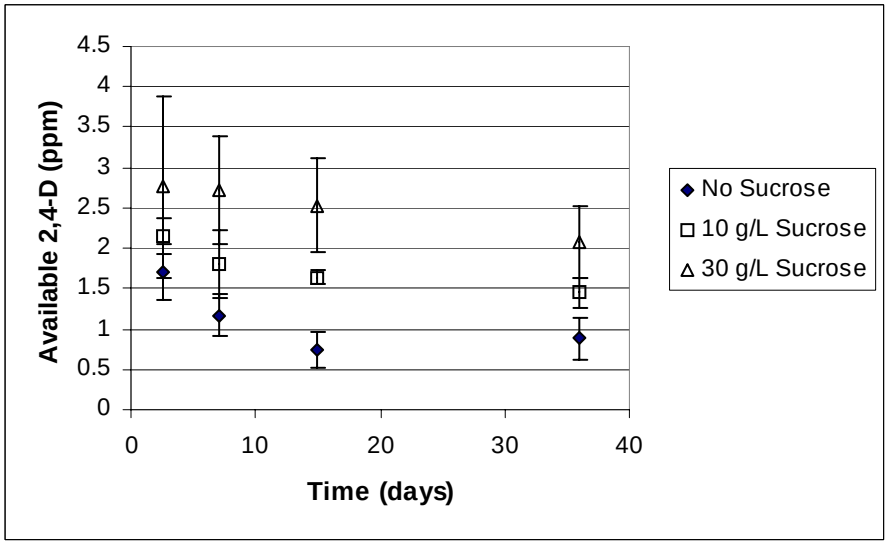

Figure 8.27. The impact of sucrose on 2,4-D adsorption.
Media were formulated as before with T1 (0.3g/L, 65ppm BAP, 12ppm 2,4-D) but with varying concentrations of sucrose. Error bars depict the 90% confidence interval based on three replications.

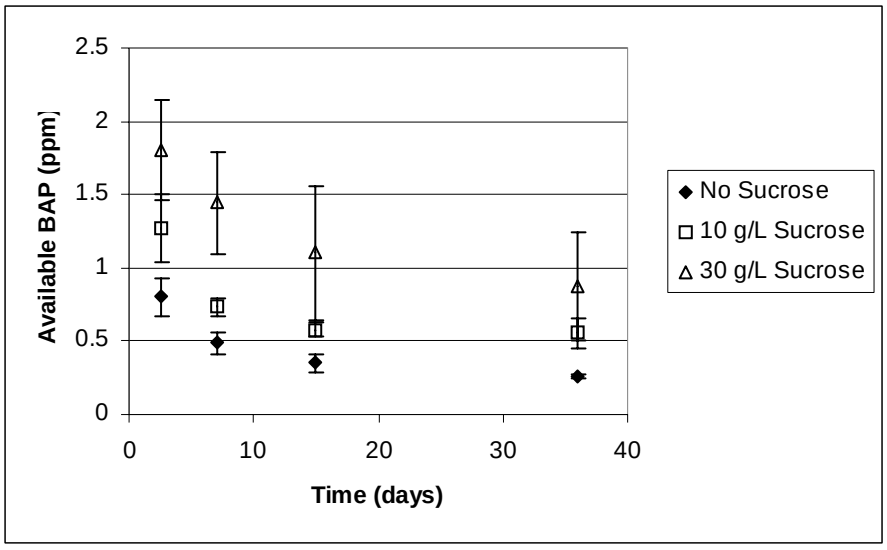

Figure 8.28. The impact of sucrose on BAP adsorption.
Media were formulated with T1 (0.3g/L, 65ppm BAP, 12ppm 2,4-D) and different sucrose levels. Error bars depict the 90% confidence interval based on three replications.

Over the extended period shown (36 days), more hormone remained available as the initial sucrose concentration was increased. The rate of decline for the treatments with no sucrose and 10 g/L was faster than that for the 30 g/L samples during the first seven days. However, beyond ten days, the 30 g/L samples continued to decline at a more uniform rate. Increases in protein solubility have been noted for aqueous solutions upon addition of sucrose (Antipova, Semenova, 1995). A plausible explanation for both observations may be a reduction in the hydrophobic exclusion forces when sucrose is present (see Theory section).

The sucrose effect may also have been due to competitive adsorption. It may be seen from Figure 8.29 that sucrose is adsorbed onto AC in the absence of competing sorbates.

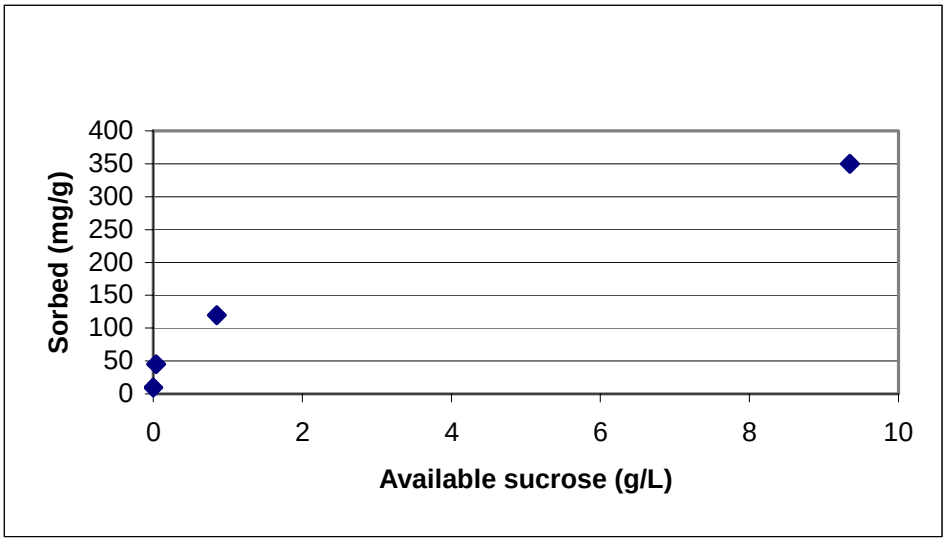

Figure 8.29. Adsorption of sucrose onto AC (T1).
Aqueous sucrose solutions (10g/L, 1g/L, 0.1g/L, 0.01g/L, filter sterilized) were treated with AC (1.25g/L), sampled after 1 day. Analysis was performed on filtrate using HPLC (Biorad Aminex HPX-87P 300 x 7.8 mm, degassed, Nanopure H_2O mobile phase, 0.6mL/min, 85^{o}C, refractive index detection, meso-erythritol as internal standard).

Though it is expected that sucrose is weakly adsorbed, it is present at such a large excess relative to the hormones that it is greatly favored statistically to occupy sites on the surface of the carbon. The adsorption of 2,4-D appeared to be more affected by sucrose than was the adsorption of BAP. This effect may also be related to the solubility of 2,4-D: an additional 18% dissolved in water when sucrose was present. Sucrose in solution is hydrated to the extent that intramolecular hydrogen bonding is absent (Engelsen, Perez 1997). This may result in a hydrophobic micro domain: protein/sucrose complexes and co-solubility have been noted in the literature (Antipova, Semenova 1995; Immel, Lichtenthaler 1995; Engelsen, Perez 1997).

Table 8.7. Summary: Impact of TC medium variables on hormone adsorption

TC Medium Variable	Available Hormone*	
	BAP	2,4-D
Sucrose increase	+	+
Glutamine addition, timing		
post autoclave	n/c	(-)
2.5 days	(-)	(-)
pH Decrease	n/c	(-)
Temperature increase	+	+
Increased shaker speed	(-)	n/c

* n/c designates no change

C. Discussion

Surface Coverage by Hormones

For the eight carbons of this study, BAP was adsorbed to a greater extent than 2,4-D. For each of the three carbons depicted in Figure 8.10 the isotherm data show that about twice as much BAP was adsorbed as 2,4-D at any given hormone availability (apparent equilibrium). For the following calculation, monolayer coverage of the activated carbon was assumed.

The monolayer coverage of BAP was approximated from the plateau region of each apparent isotherm depicted in Figure 8.10b. This was expected to be a reliable estimate due to the significant apparent equilibrium level of BAP (in terms of reduced concentration, the apparent equilibrium level represented a significant percentage of the solubility limit for BAP). It should be noted that these analyses were based on BAP concentration but a more rigorous treatment would be based on activity.

Chromatographic data for 2,4-D adsorption were collected at a low level of available 2,4-D relative to its solubility (ca. 3500 ppm in dissociated form) limit. Therefore it was felt that monolayer coverage for 2,4-D could not be accurately approximated from just the isotherm data in Figure 8.10a. Data over a wider range in available hormone concentration were available from sorption experiments with T1 (UV data in Figure 8.11).

From Figure 8.11, the monolayer coverage for 2,4-D onto T1 was approximated as 221 mg/g. The adsorption onto the other two carbons was approximated from the ratio of 2,4-D sorption to that for T1 at 30 ppm available hormone (Figure 8.10a). This ratio was then multiplied by the level of adsorption for 2,4-D onto T1, 221 ppm from the UV data in Figure 8.11. From the calculated hormone adsorption, an occupied surface area was calculated using Avogadro's number, assuming that 100% of the BET surface was available for sorption. A second calculation considered the possibility that the portion of the surface represented by pores of 0.7 nm or smaller was unavailable for adsorption (the

diameter of a benzene ring was approximated as being close to 0.7 nm). These data appear in Table 8.8. Note the excellent consistency of the calculations between the different carbons. The cumulative surface area data from the density functional theory analysis appear in Table 8.9.

Table 8.8. Surface Coverage by Each Hormone for Three Activated Carbons.

	2,4-D*			BAP*		
	Ads. (mg/g)	100% of BET	Less 0.7nm pores	Ads. (mg/g)	100% of BET	Less 0.7nm pores
T1	221	1.8	1.2	365	1.1	0.8
Merck	192	1.7	1.3	290	1.1	0.85
SX4	129	1.9	1.4	190	1.3	0.89
	mean:	1.8	1.3	**mean:**	1.2	0.8

Adsorption of 2,4-D was calculated from Figures 8.11 and 8.10a, see text. Adsorption of BAP was calculated from Figure 8.10b.
* Surface coverage expressed in nm^2/molecule. The accessible surface area for the "Less 0.7nm pores" case was calculated from data in Table 8.9.

Table 8.9. Cumulative DFT data for T1

Range, nm	T1	Merck	Sx4
0.7	237	212	258
1	688	625	575
1.5	809	699	614
2	877	739	636
3	908	760	651
4	931	778	666
8	965	809	690
16	988	828	699
32	1001	836	702
BET avg	1105	865	665

Cumulative data are shown for the pore size distribution of T1. A portion of the volume below 0.7 nm could be inaccessible to the hormones.

The levels of adsorption for 2,4-D and BAP onto T1 (BET area of 1105 m^2/g) were approximately 1mmole and 1.6 mmole per gram of carbon. In comparison, activated carbon with a surface area of 1092 m^2/g (BET, N_2) adsorbed approximately 3.5 mmoles of p-nitro phenol per gram (Molina-Sabio et al. 1985), and Biniak et al. (1990) reported adsorption of phenol of less than 2 mmoles per gram for activated carbon of 970 m^2/g

BET. The levels of adsorption reported here for 2,4-D and BAP were therefore considered to be of normal magnitude.

The cross sectional areas for 2,4-D and BAP molecules were estimated from bond lengths and angles as 0.42 nm^2 and 0.64 nm^2, respectively. These values were in acceptable agreement with the mean area for pyridine (0.24 nm^2) reported by Rahman and Ghosh (1979), as 2,4-D would be nearly equivalent to two pyridine molecules, while BAP would be equivalent to about three. However, the estimates were low relative to the value used for p-nitrophenol calculated from sorbed data, 0.525 nm^2, reported by Molina-Sabio and coworkers (1985), as 2,4-D would be somewhat larger than p-nitrophenol (PNP), while BAP would be equivalent to between 1.5 and 2 p-nitophenol molecules. The bond length calculations also resulted in lower levels than accepted for the sorbed area of benzene, reported as 0.4 nm^2 (Lowell, Shields 1991). Using the adsorbed benzene molecular size as a guideline, the 2,4-D was approximated as 2 benzene rings, while the BAP molecule was closer to 3 benzene rings, giving a sorbed area of 0.8 and 1.2 nm^2 per molecule, respectively.

The cumulative pore distribution data for T1, from the DFT analysis are reproduced in Table 8.9. It may be seen from the table that if BAP were unable to access pores of 0.7 nm or smaller then the remaining surface area available for adsorption would be 868 nm^2/g (1105 less 237 nm^2). This level of adsorption results in a small sorbed area per molecule of BAP (0.8 nm^2/molecule) compared with the benzene-based estimate of 1.2 nm^2/ molecule. This may be an indication of multilayer formation. Alternately, the data may be interpreted as showing that the total surface available to the nitrogen molecule in the DFT analysis was also available to the BAP which occupied 1.2 nm^2/molecule. The BAP molecule is much larger than nitrogen (0.16 nm^2/molecule, Lowell, Shields 1991). If it is assumed that only a monolayer were present, and BAP was equivalent to 1.2 nm^2/ molecule, then the entire surface available to nitrogen was also available to BAP. This would be possible given a planar conformation of BAP on the surface of the activated carbon and slit-shaped pore geometry.

Though 2,4-D was a physically smaller molecule, much less was adsorbed by the AC (at pH 5.8). The molecular area calculation produced large values even given a pore cut-off of 0.7 nm. This phenomenon was attributed to packing effects due to the dissociated acid group.

Under competitive adsorption conditions, when the two hormones were adsorbed at pH 3.0, similar adsorption for each hormone was indicated (Figure 8.30), approximately 1mM per gram of AC. The increased adsorption of 2,4-D in response to pH changes was previously noted by Ebert and Taylor (1990). Assuming completely accessible BET area, the combined coverage was 0.9 nm^2 per molecule. This was significantly lower than the value of 1.2 nm^2 assigned to BAP based on comparison with benzene: multilayer formation may be indicated. At pH 3.0, ca. 50% of each sorbate is charged. The opposite charges would attract. This analysis suggests that at pH 5.8 the mechanisms of adsorption for BAP and 2,4-D were different, probably involving different sites (to be discussed).

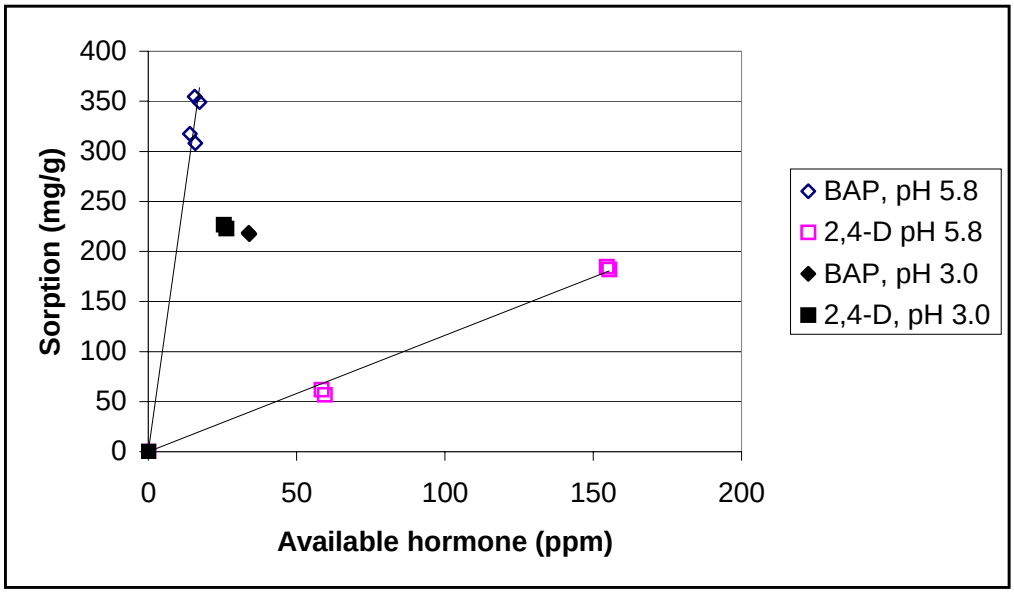

Figure 8.30. Adsorption of the hormones at pH 3.0, near their pKa.
Complete media were formulated with AC (T1, 0.3g/L) and both hormones (initial concentrations of 75ppm each, BAP and 2,4-D); pH was adjusted to 3.0. Samples were measured after 2.5 days. Data from Figure 8.3 are included for comparison.

Adsorption and Shaker Table Response

An individual AC particle has often been modeled as having a readily accessible outer sorptive region and a second region, which is not as accessible. Each zone is expected to have a different resistance to mass transport. Possible diffusive pathways are illustrated in Figure 8.31.

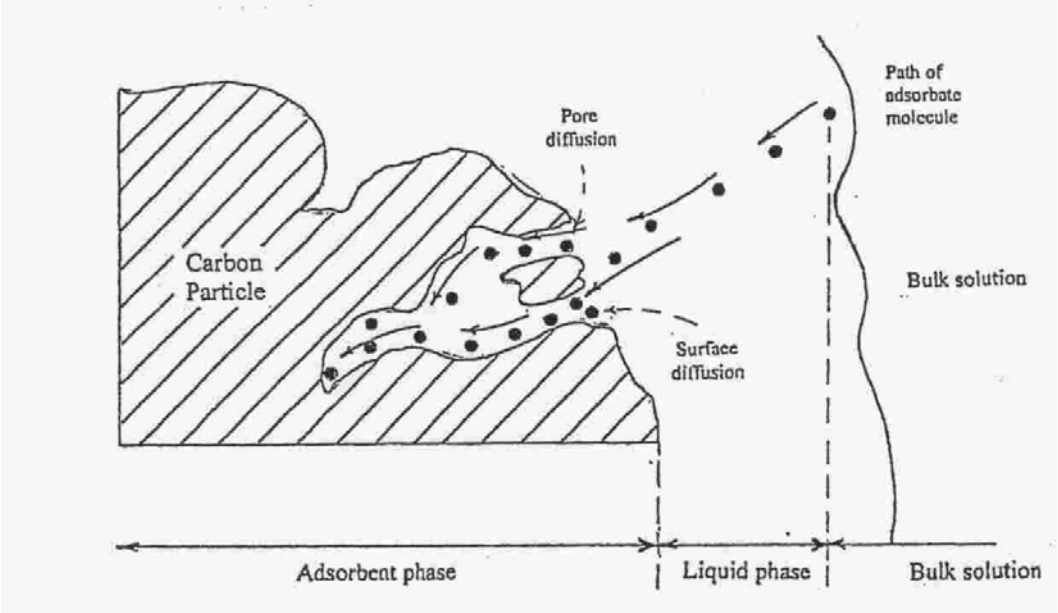

Figure 8.31. Diffusive pathways which may regulate the movement of mass within the pore (adapted from Montgomery 1985).

Constrictions and tortuosity within the sorption space, particularly for micropores (pores comparable in diameter to the size of the sorbate molecules), are thought to account for the slow adsorption phase (Schwarzenbach et al. 1993; Weber et al. 1991). Bottle-shaped pores may account for sorption/desorption hysteresis in nitrogen adsorption experiments and may also help to explain the extent of adsorption that can occur during the slower phase of adsorption from solution (Figure 8.32).

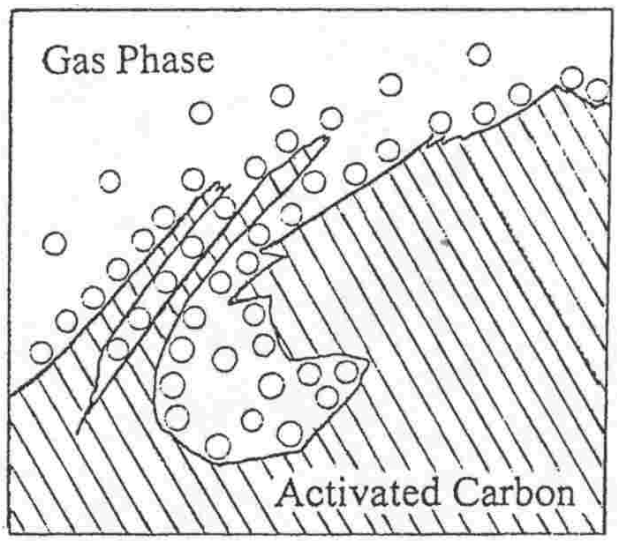

Figure 8.32. Schematic representation of a bottle-shaped pore. Constricted entrance to larger volume limits the rate of adsorption.

Sorptive behavior that is characterized by a very rapid initial adsorption phase followed by much slower adsorption, has been well established for organic compounds adsorbing onto activated carbon (Mattson, Mark 1971). Ebert and Taylor (1990) and Ebert et al. (1993) reported similar findings regarding the adsorption of 2,4-D and BAP. They additionally showed that for 2,4-D, the adsorption from liquid medium reached a "steady-state" much sooner than from gelled media. For semi-solid media, a higher temperature resulted in significantly increased rates of adsorption for 2,4-D: the authors attributed the slow rate of adsorption for semi-solid media to diffusion-controlled transport. The adsorption of BAP was insensitive to the presence of the gel agent: the authors attributed this to the low BAP-to-AC ratio, suggesting that equilibrium had been reached during mixing.

Diffusion within microporous solids is conceptually separated into two different types: pore diffusion and surface diffusion. Surface diffusion is thought to be the more important mechanism for transport within pores of molecular dimensions (Montgomery 1985). As with bulk and pore diffusion, surface diffusion is concentration-driven. It

results from the breaking and reforming of bonds between the organic solute and the pore wall sorption interface. Hence, surface diffusion is an activated process that depends on

sufficient energy levels in the system to break the bond at the pore-wall surface, and it has been analyzed in a manner analogous to Arrhenius activated complex theory. The effective surface diffusion coefficient may be several orders of magnitude lower than the bulk diffusion coefficient for a given sorbate (Schwarzenbach et al. 1993).

In the tissue culture medium system, the major percentage of the total adsorption occurred for each hormone within six hours of sterilization (Figure 8.3). The shaker-table results (Figure 8.6) support the hypothesis that *intra*particle mass transfer was rate limiting after two days, as the rates of adsorption showed a minimal response to changes in mixing. The shaker table experiment was additionally complicated by autoclaving of the media, performed as per standard tissue culture practice. Considering the carbon surface as being populated with polar and nonpolar sites may offer a partial explanation for the increased adsorption of BAP in response to shaking, as opposed to 2,4-D which was unaffected. Mattson and Mark (1971) noted that activation of carbon is not uniform: the outer perimeter and surfaces are hypothesized to possess a higher proportion of oxygen functional groups than do the interior surfaces, resulting in a more polar character towards the outer radius of the particle. However, the CHNSO analysis revealed a small percentage of oxygen relative to carbon: a much greater percentage of the surface is nonpolar in character. Access to this outer sorptive region would be unhindered relative to the interior sorption volume.

Formulating media, adding activated carbon and pH adjusting prior to autoclaving required from 15 minutes to half an hour, during which time adsorption occurred. Higher temperatures were shown to result in less adsorption for each hormone: the autoclave treatment probably impeded, perhaps reversed adsorption. Adsorption to the nonpolar sites is driven largely by hydrophobic forces. However, the adsorption of 2,4-D to the polar sites, also incorporates longer-range coulombic forces. These charged sites and their location on the carbon perimeter, combined with the relatively low BAP concentration (assuming rapid initial adsorption) and hence reduced adsorption rate, could promote a faster re-equilibration for 2,4-D following autoclaving. Note that polar organic molecules

are known to outcompete other charged species, probably as a result of the additional hydrophobic forces (Scwarzenbach et al. 1993).

Solvent-Water Partitioning

The partitioning behavior of these two hormones gives a partial explanation of the observed differences in adsorption. The partitioning of organic molecules from water into organic phases is largely related to their aqueous solubility or activity. Thus, a hexane-water partitioning coefficient may be very nearly the same as an octanol-water coefficient for a given compound under similar aqueous conditions: partitioning is driven by the aqueous interactions (Schwarzenbach et al. 1993).

The octanol-water partitioning concept helps to explain the observed temperature response (Figure 8.7): the hormones were more soluble in warmer water. The temperature difference resulted in approximately one-third to one-half more available hormone in the lower adsorption range of the isotherm. Similarly, the concept may be applied to other factors which affected the aqueous solubility of the hormones. Thus, an increase in the ionic background is expected to decrease the solubility of the hormones due to structuring of water in the vicinity of the ions: hydrophobic exclusion increases with ionic concentration resulting in greater adsorption. Similar trends were reported by Ebert et al. 1993.

Lower adsorption could be attributed to either an increase in solubility, as with the sucrose effect, or to the competitive adsorption of another compound. Depending on when it was added, glutamine (750 ppm) was found to either increase or decrease the adsorption of the hormones. As it is poorly soluble, it had a competitive effect towards 2,4-D when added soon after the media were autoclaved. However, BAP sorption was unaffected by glutamine added just after autoclaving. This may have been related to the high rate of BAP adsorption driven by its lower solubility, or it may be further indication of competition with 2,4-D for charged sites. When glutamine was added later, after the carbon had become loaded, sorption of *both* hormones increased, presumably through

solubility effects due to water structuring as well as pH effects. The addition of glutamine resulted in a decrease in pH from approximately 5.6 to 5.4.

The aqueous solubility of organic molecules is often determined by whether or not they carry a charge: acids dissociate (give up a proton) to become more soluble, whereas bases gain a proton to become more soluble. The pH of the aqueous phase relative to the pK_a of the particular organic compound determines the percentage of the compound present in the charged state (Henderson-Haselbach or *H-H* equation):

$$pH = pK_a + \log_{10} \frac{[A^-]}{[HA]} \qquad (9.3)$$

where HA refers to the nondissociated acid and A^- is the dissociated, ionic species (Garret, Grisham 1995).

According to the H-H relationship, an acid will be 99% dissociated when the pH is two units *above* its pK_a. A basic compound will be 99% charged at two pH units *below* its pK_a. The pK_a of 2,4-D has been found to be 2.8 (Rubery 1980) and for BAP the pK_a has been reported as 3.3 (Shafer 1990). At the normal tissue culture pH of 5.8, 2,4-D is negatively charged and BAP is neutral. Figure 8.33 presents the molecular and charged forms of 2,4-D and BAP.

The data in Table 8.10 indicate that at pH 5.8, BAP should partition to a greater extent than 2,4-D, perhaps to ten times the level (log K_p of 1.56 vs. 0.65). Aqueous solubility is an exceedingly complex topic and partitioning behavior is only one indicator, but in this case, as predicted, BAP is less soluble than 2,4-D.

A. 2,4-D

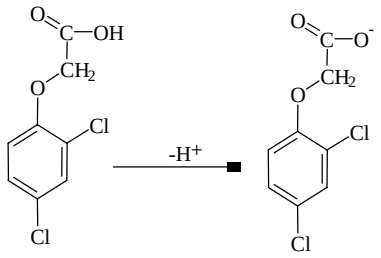

B. BAP

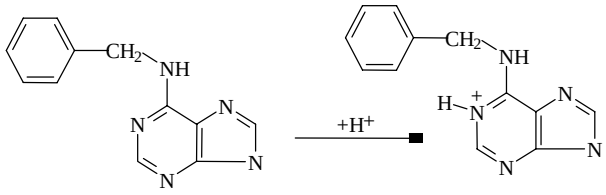

Figure 8.33. Chemical structures for neutral and charged forms of A. 2,4-D (2,4-dichlorophenoxyacetic acid, pKa 2.8, Rubery 1980) and B. BAP (6-benzyladenine, pKa 3.3, Shafer 1990).

Table 8.10. Partitioning coefficients for molecular and dissociated hormones.

	Log K_p, Partition Coefficients		
	Molecular	**Ionized**	**Ref:**
BAP	1.56	1.08*	Shafer 1990
2,4-D	2.81	0.65**	Hansch et al. 1995

* Value measured at pH 3.0 which, based on the pK_a of 3.3, is therefore a mixture of ionic and molecular forms.
**Value obtained from the amine salt form.

At pH equal to its pK_a, a molecule will be 50% dissociated. A log K_p of 2.5 may be estimated for 2,4-D at pH 3.0. If hydrophobicity were the primary force influencing adsorption, then it would be expected that at pH 3.0 the relative adsorption of BAP and 2,4-D would shift. As predicted, the sorption of 2,4-D exceeded that of BAP at pH 3.0 (Figure 8.30).

However, since the K_p for 2,4-D at pH 3.0 was estimated to be significantly greater than that of BAP it was expected that the reversal would have been more pronounced. As already noted, an experiment in which 2,4-D was dissolved in a sucrose solution and

compared to dissolution in water (no base added) revealed that 2,4-D was over 18% more soluble in the sucrose solution. This increase in solubility may help to explain the lower-than-expected adsorption and may be related to disruption of the hydration shell that would otherwise form around 2,4-D . Owing to its hydroxyl groups, sucrose is able to hydrogen bond more readily than 2,4-D .

A more significant factor may have been the surface charge of the activated carbon. The presence of dissociated acid groups on the surface of the AC could account for the lower than expected 2,4-D sorption at pH 3.0: dissociated acid sites would repel 50% of the 2,4-D and attract preferentially the positively charged BAP. In another experiment the single-hormone adsorption of 2,4-D increased with [H+] over the pH range from 4.8 to 6.5 (Figure 8.34). This increase in sorption could not be attributed to changes in the ionization of 2,4-D as the H-H equation predicted that 2,4-D was already 99% dissociated at pH 5.0. However, the observed increase in adsorption could be attributed to a decrease in sites on the AC surface carrying the same charge as the 2,4-D.

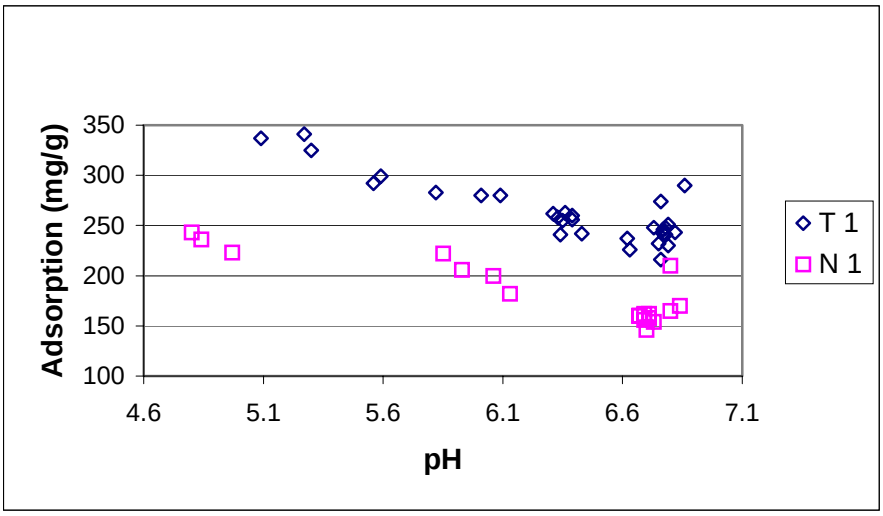

Figure 8.34. Effect of pH on the adsorption of 2,4-D.
Data were generated from buffered aqueous solution using UV_{284}. Measurements were made after five days. Elevated hormone (2,4-D 200 ppm) and reduced AC levels (T1, 0.125 g/L) were used, which resulted in a high level of adsorption, in the plateau region of the 2,4-D isotherm (refer to Figure 8.12).

The dissociated-acid concept may be extended to explain the *difference* in the single-hormone sorption isotherms at pH 5.8. Three types of sorption sites were expected to be

present: basic, acidic, and neutral. The acidic sites were dissociated and carried a negative charge. The basic sites were positively charged. The neutral sites carried no charge. The BAP was unaffected by charged sites, as it was neutral at pH 5.8, whereas the 2,4-D experienced electrostatic attraction or repulsion. The net charge on the carbon was positive for solution pH below the point of zero charge (all of the carbons in this study were basic, that is, the pzc exceeded pH 7).

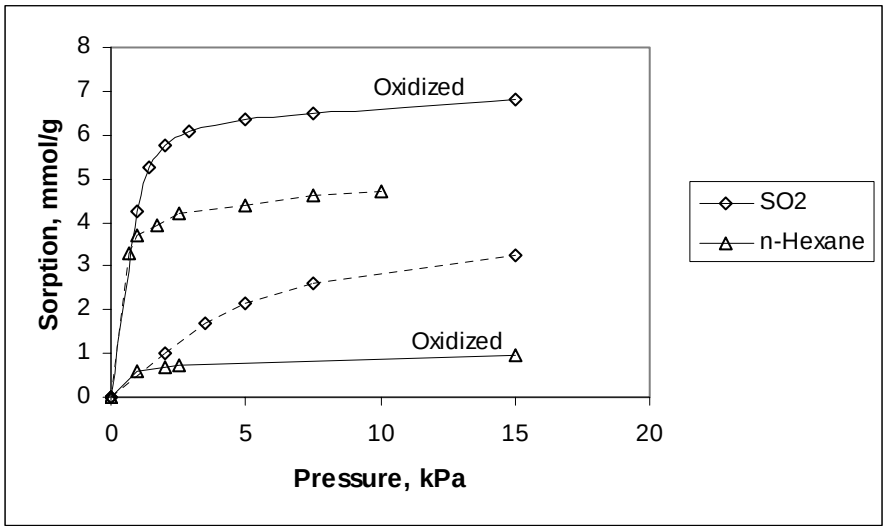

Figure 8.35. Surface polarity influences adsorption (adapted from Ruthven 1997).
Equilibrium isotherms for adsorption onto activated carbon at 298K show the effect of surface modification: solid line designates SO_2; dashed line designates *n*-hexane. The more polar sorbate, SO_2, adsorbs to a greater extent on the more highly oxidized surface; conversely, the nonpolar sorbate, *n*-hexane, adsorbs to a greater extent on the less oxidized AC.

Adsorption from solution requires a displacement of the solvent molecules from the sorption volume. For aqueous systems, the less polar the sorbent, the more readily organic solutes will displace water molecules from the sorption volume. The surface of activated carbon may range from polar to nonpolar. As depicted in Figure 8.35 (reproduced from Ruthven, 1997), the level of adsorption varies with the interaction between the sorbate and the carbon surface: the polar sorbate (SO_2) preferred the oxidized surface and the nonpolar sorbate (n-hexane) preferred the untreated surface. These data were obtained from gas phase experiments but they illustrate the principle.

Though the carbon may exhibit a *net* positive charge, the carbon could also possess acidic, dissociated, and hence, negatively charged sites. The net charge results from the sum of the positive and negative charges. The charged sites consist of a range of different chemistries giving a distribution of dissociation constants. The negatively charged sites have been attributed to functional groups such as phenolic hydroxyls, lactones, carboxyls, etc… Weak positive charges have been attributed to the basal planes of the carbon lattice (Leon Y Leon et al. 1992) and stronger positive charges have been attributed to oxygen functional groups, such as chromene and pyrone structures (Leon-y-Leon, Radovic 1994). The weaker charges would have little impact on the adsorption of 2,4-D as these would result from the aromatic planes that also have a hydrophobic character. They would be occupied by BAP. The stronger basic sites, however, would have interacted strongly with the dissociated 2,4-D. The 2,4-D, therefore, outcompeted or displaced BAP on such sites. Müller et al. (1985) reported that surface charge was undiminished by the adsorption of organic solutes. Accordingly the neutral sites were occupied by the less soluble, neutral, BAP. A schematic representation of the dynamic site interactions with sorbate molecules is presented in Figure 8.36.

Figure 8.36 has been drawn to reflect the relative bond distances predicted for the different types of surface interactions: hydrophobic interactions are expected to result in adsorption onto the surface within the Stern layer, while ionic interactions may occur over a longer range. Additionally, hydrophobic interactions are potentially the strongest of the “weak” bonding interactions (Table 8.11).

Table 8.11. Relative bond strengths for non-covalent bonding (Garrett, Grisham 1995).

Force	**Stength (kJ/mol)**	**Distance (nm)**
Van der Waals interactions	0.4-4.0	0.2
Hydrogen bonds	12 to 30	0.3
Ionic bonds	20	0.25
Hydrophobic interactions	< 40	n/a

The pH data reinforce the multi-site concept: the impact on the available 2,4-D due to pH changes was the same (Figures 8.22, 8.23, 8.24), regardless of how much 2,4-D was

adsorbed, indicating that only a fraction of the sorption sites were charged and responded to pH changes. The fact that 2,4-D response was similar in the presence of BAP suggests that on these polar sites 2,4-D out-competed BAP. The pH reversibility data also suggest that 2,4-D adsorbed by two different mechanisms. The primary, hydrophobic mechanism resulted in high levels of adsorption in the absence of BAP, but when BAP was present it outcompeted 2,4-D for the nonpolar and negatively charged sites. Thus, to attain the target level of 2 ppm 2,4-D, an initial 2,4-D concentration of 42 ppm was required in the absence of BAP.

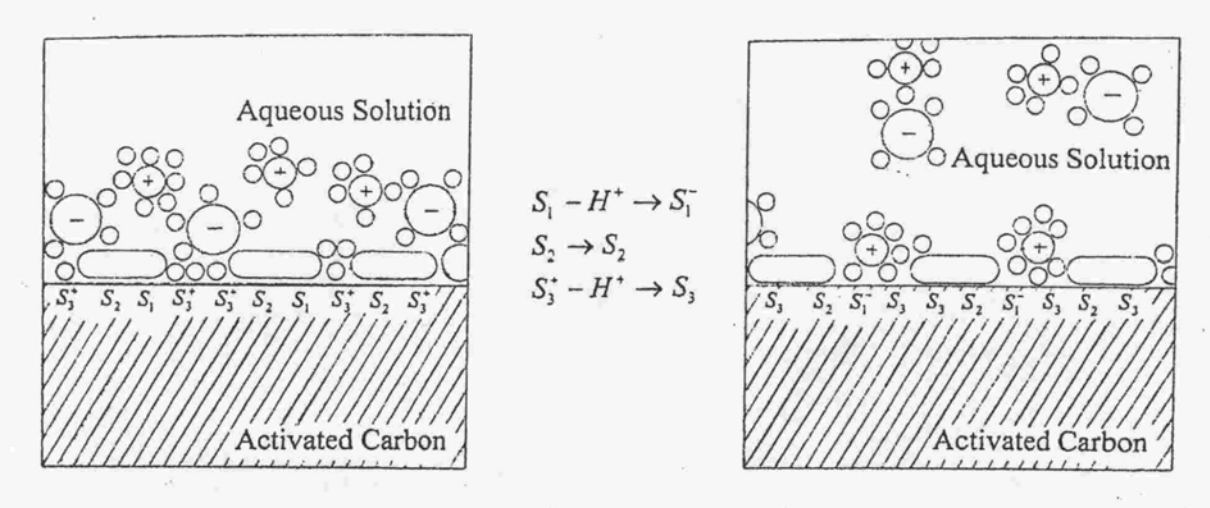

Figure 8.36. Schematic representation showing the impact of a pH change on the surface charge, resulting in repulsion of dissociated organic anions, e.g. 2,4-D. Small circles represent waters of hydration, drawn arbitrarily. Ovals represent nonpolar sorbate molecules, e.g. BAP.

Competitive Adsorption

Partitioning and solubility

Figure 8.28 displays an apparent sorption isotherm for sucrose on activated carbon from aqueous solution. Sucrose, despite its complete aqueous miscibility and insolubility in

organic media, was adsorbed onto AC. By extension, it is expected that any of the components in the medium could be adsorbed in the absence of competing adsorbates. The partitioning and solubility concepts presented in the previous section may be extended to the remaining components of the medium (Table 8.12). It may be concluded that the other components in the medium are unlikely to compete with the hormones for adsorption. If these components were present at very high concentrations relative to the hormones, then a kinetic effect could be expected, but *equilibrium* hormone adsorption would be unaffected.

For *physical* adsorption, selectivity of one component over another is an *equilibrium* process rather than a *kinetic* one. However, kinetic selectivity can result from size differences between the various sorbates (Montgomery 1985). The difference in molecular size between 2,4-D and BAP is minor: the difference in adsorption was not kinetically influenced. Instead, the slower equilibration of 2,4-D (Figure 8.5) may have been due to adsorption to different sites with the displacement of anionic compounds retarded due to a higher energy of activation. Such displacement by poorly soluble organic acids has been noted previously (Mattson, Mark 1971).

Table 8.12. Solubility/partitioning character of major growth medium components

Chemical species		**Log K_{ow} [a]**	**Aqueous Solubility [b]**	**Organic Solubility [b]**
Asparagine		n/a	3.5g/100g	insoluble
Glutamine		n/a	1g/20.8 mL	insoluble in ether,benzene
Inositol		n/a	14g/100 mL	insoluble
Sucrose		(-) 3.67	1g/0.5 mL	1g/170mL alcohol
Casamino acid components [c]	wt %			
Leucine	9.9	(-) 1.79	24.3g/ L	insoluble in ether
Lysine	6.7	(-) 2.82	freely soluble	practically insol. in ether
Phenylalanine	4	(-) 1.43	29.6g/ L	slight solubility in ethanol
Valine	7.2	(-) 1.26	83.4 g/L	almost insoluble in ether
Vitamin components				
Nicotinic acid		n/a	1g/60 mL	insoluble in ether
Pyridoxine*HCl		n/a	1g/4.5 mL	insoluble in ether, chloroform
Thiamine*HCl		n/a	1g/ mL	insoluble in ether, benzene

a. From Leo, Hansch, and Elkins 1971.
b. From the Merck Index 1989.
c. A representative portion of the components tabulated from Difco Manual 1953 and personal communication, Schoenlein 1957.

Ideal Adsorbed Solution Theory, IAST

An attempt was made to fit the data for the successful combinations of initial hormone levels and AC mass using two competitive sorption models, the ideal adsorbed solution theory, IAST (Radke, Prausnitz 1972), and the Polanyi Potential theory (Manes, Hofer 1969, Rosene, Manes 1976, 1977). Each of these models requires only the single-solute isotherms of the competing sorbates. However, each assumes an equilibrium state. The "apparent isotherm" data which were collected after 2.5 days clearly hadn't reached a true equilibrium. These models have also been developed with the assumption that the only competing sorbate in the single-solute isotherms is the solvent. In this research the apparent isotherms were generated against a background of ionic and organic compounds. Despite violating the theoretical underpinnings of each theory, it was believed that there was value in attempting to fit a very complex system to relatively simple models.

According to the IAST, the areas under the single solute isotherms (the spreading pressures) should be equal at an equilibrium point. At the target levels of available hormone, i.e. 1 ppm BAP and 2 ppm 2,4-D, it is clear from the isotherm data that the areas under the single-hormone adsorption curves are not equal (Figure 8.37). The integrated areas were 170 units and 216 units for BAP and 2,4-D, respectively.

The IAST has been shown to be ineffective in situations where one solute is sorbed more strongly than another and in situations of high surface coverage. Charged solutes have also been shown to be troublesome for the IAST (Müller et al. 1985). The IAST is based on the unifying concept of spreading pressure, which is probably best applied to smooth, homogeneous surfaces. In contrast, microporous activated carbons are noted for surface and energetic heterogeneity. One would expect the relative spreading pressures for a charged vs. neutral molecule to vary, depending on the character of the surface at any given point.

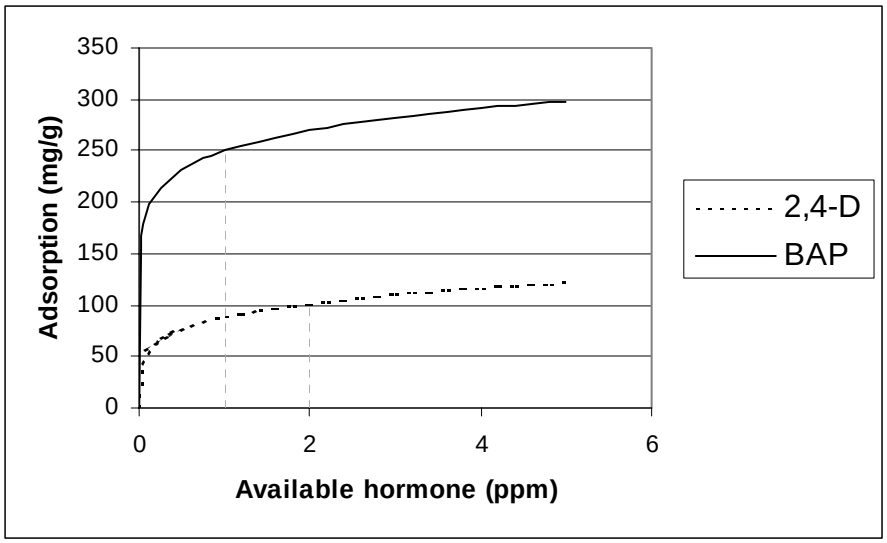

Figure 8.37. IAST analysis based on Freundlich curves for 2,4-D and BAP onto T1. The IAST requires that the area defined by the isotherm up to the equilibrium adsorption (target hormone level) be equal for both hormones. Using the Freundlich curves, the integrated areas were calculated for BAP to 1ppm available: 170; and 2,4-D to 2ppm available: 216.

Polanyi model

The Polanyi theory is based on the concept of filling sorption volumes of differing interaction energies. This energy of interaction varies with the individual sorbate and the local surface character. The Polanyi conception is that adsorption involves a phase change (condensation or precipitation). Therefore, the extent of adsorption is regulated by the sorbate concentration relative to its solubility limit.

In order to apply the Polanyi model, an estimate was needed for the total sorption volume and the density of the sorbed solid solute. According to the Polanyi theory, this volume should be characteristic of the material and should not differ with the sorptive phase. The total pore volume from the DFT data for T1 (0.833 cc/g) provided a reliable estimate of the total sorption volume. The saturated BAP level was taken as 165ppm and the saturated 2,4-D level was taken from the Merck Index value for the sodium salt form, 3.5% or approximately 35 g/L. The sorbed density of each was approximated as 1.2 g/cm^3 based on values given by Rosene and Manes (1976) for a series of similar sorbates.

The sorption data for 2,4-D and BAP onto T1 were transformed to Polanyi coordinates as detailed in the theory section and are presented in Figure 8.38. The curve for BAP was generated from the Freundlich isotherm equation (Figure 8.10), whereas the 2,4-D data were taken from the isotherm shown in Figure 8.11. According to the theory, as applied by Rosene and Manes (1976) to competitive adsorption, if the sorbate with the greater sorptive potential is present at equilibrium at a higher level then competing adsorbates, then the sorption volume will be completely filled with this sorbate and the other competitors will not be adsorbed. The figure includes two points, ordinates B and C, which correspond to the equilibrium available concentrations of 1ppm and 2ppm for BAP and 2,4-D, respectively. It may be seen that the volume will be filled with BAP (ordinate B greatly exceeds ordinate C). According to Figure 8.38, in order for 2,4-D to compete against BAP it would have to initially occupy about four times the adsorbed volume depicted at an equilibrium level of 2ppm, or conversely, BAP would have to be depleted to a level below 0.2 ppm.

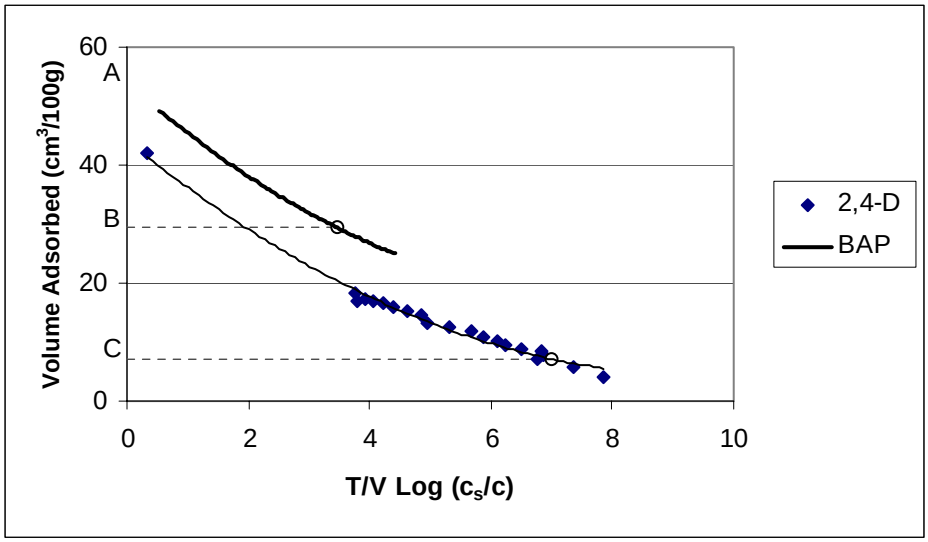

Figure 8.38. Polanyi plot of 2,4-D and BAP isotherm data for sorption onto T1. The BAP trace was produced from the Freundlich equation for BAP sorption onto T1 (Figure 8.10). The 2,4-D trace was based on the isotherm data of Figure 8.11. Points B and C correspond to the occupied adsorption volumes at the desired equilibrium concentrations of 1ppm and 2ppm for BAP and 2,4-D, respectively.

The data show a y-intercept well below the specific adsorption volume of T1. This anomaly has been noted previously (Rosene and Manes, 1976) and was attributed to "sponginess", the analogy being with poorly packed precipitated solute. Manes (1980)

applied an empirical correction factor to bring the data into agreement with the N_2 pore volume data. This approach would not change the result shown in Figure 8.38. The Polanyi approach did succeed in predicting that the adsorption of BAP would be unaffected by the presence of 2,4-D at the levels used here, but failed to predict the observed adsorption of 2,4-D when competing against BAP.

Multi-component Langmuir

An intriguing result occurs when the Langmuir equation is extended to multiple solutes (Ruthven 1997):

$$\frac{V_1}{V_{m1}} = \frac{b_1 p_1}{1 + b_1 p_1 + b_2 p_2 + \ldots} \; ; \; \frac{V_2}{V_{m2}} = \frac{b_2 p_2}{1 + b_1 p_1 + b_2 p_2 + \ldots} \tag{8.4}$$

To be rigorously applied, equation 8.4 requires that the monolayer capacities for each of the sorbates be equal, i.e. $V_{m1}=V_{m2}$. If solute 1 is present at significantly higher concentration than the others, the denominator of the equation may be reduced, giving:

$$\frac{V_i}{V_{mi}} = \frac{b_i p_i}{1 + b_1 p_1} \tag{8.5}$$

Similarly, if solute 1 demonstrates higher affinity than the others, i.e. b_1 is significantly larger than b_i, then the same equation results. The expression for solute 2 may be written as:

$$V_2 = \left(\frac{b_2 V_{m2}}{1 + b_1 p_1} \right) p_2 \tag{8.6}$$

Each component within the parenthesis is constant: equation 8.6 is simply Henry's law (Equation 4.10). *This result indicates that the sorption isotherm for the less competitive component will be linear*. The general practice has been to extend the Langmuir analysis to adsorption from solution by replacing the pressure terms with concentration terms, replacing *V* with adsorption (mass solute/mass sorbent), and to assume that *b* is still related to the energy of interaction between solute and sorbent. The case where 2,4-D

adsorption occurred in the presence of a large excess of BAP (Figure 8.12) agreed with the analysis above. However, in that case the initial assumption of the model was violated: the monolayer capacities for the two hormones were significantly different at pH 5.8 based on the plateau of their isotherms (Figure 8.10). Additionally, the Langmuir equation did not fit the data very well. Both of these findings would be consistent with the proposed multi-site model: each type of site would exhibit a different isotherm for a particular sorbate.

Anionic adsorption to charged sites has often been fit with the Langmuir isotherm at low coverages (Hingston 1981). It would logically follow that the multi-solute Langmuir equation could be applied to sorption of organic ions at these sites. However, in this case, the more strongly sorbed species would be the 2,4-D: the BAP would be expected to adsorb to these polar sites in a linear fashion, rather than the 2,4-D!

An alternate interpretation of the linear 2,4-D response is based on partitioning concepts. The observed behavior may be consistent with the formation of a hormone-rich organic phase between the adsorbed BAP layer and the bulk aqueous solution, a plausible phenomenon suggested in other literature (Schwarzenbach et al. 1993, Weber et al. 1991). Partitioning is a linear relationship. However, this partitioning response would require an abrupt transition between the liquid phases: without an inter*face* there would be no driving force for accumulation (the Gibbs isotherm concept). On a favorable surface, such a phase (*hemimicelle* or *admicelle*) could form from micelle-forming compounds, such as sodium dodecyl sulfate (SDS), well below their critical micelle concentration (Ko et al. 1998).

The most plausible component(s) of the medium for micelle formation are the casamino acids due to the colloidal nature of the source material (casein) and the relatively high concentration present in the tissue culture medium, 500 ppm. Experiments were conducted to see if visibly distinct phases would form when elevating the concentration of casamino acids both in pure aqueous solution and in sucrose solutions. However, multiphase behavior was not observed.

The linear response exhibited by 2,4-D when competing against BAP when both were present in large excess is difficult to reconcile with existing theory. The evidence supports the conclusion that 2,4-D was adsorbing to polar sites, where it out-competed BAP. More work is needed in order to understand the mechanisms of these phenomena.

Target Hormone Levels and Porosity

The purpose of this research project was to identify a measurable AC parameter(s) that would correlate with the degree of hormone adsorption, and subsequently with success in a plant tissue culture system. A confounding factor was the definition of *hormone adsorption*. The common practice is to define adsorption in terms of monolayer coverage. However, such a definition is complicated by the ambiguities of interpreting the isotherms consistently. The approach taken in this work was to quantify adsorption in terms of the desired equilibrium concentration or *target hormone level*. This distinction was more critical in this case due to the fact that neither hormone was present at sufficient concentration for complete monolayer coverage. As shown in Figures 8.16 and 8.17, a strong correlation was present for each hormone for adsorption-to-target vs. either BET surface area or total pore volume. The follow-up to this work revealed that normalizing the mass of AC based on its total pore volume, with no adjustment of the initial hormone levels, resulted in target hormone levels for seven different AC's (Figure 8.18), in very good agreement with the total pore volume relationship.

Though the total pore volume relationship worked extremely well, and better than what would have been achieved with BET, the difference between them was not great. There was a very good linear correlation for these carbons between BET and total pore volume (Figure 8.39). This correlation would not have been as good if the carbons were of higher microporosity due to the limitations of the BET model.

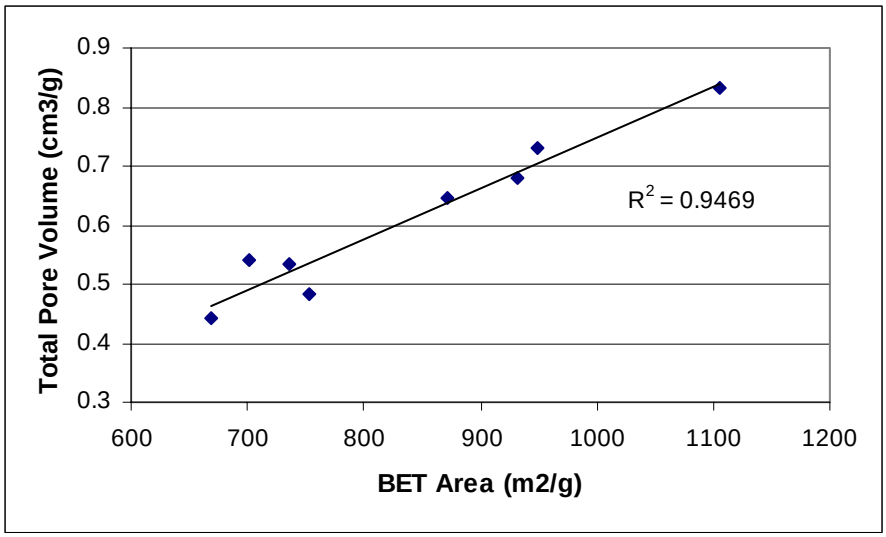

Figure 8.39 Total pore volume and BET correlation.

Changing the Hormone Target Levels

The target hormone levels could be sub-optimal in terms of culture success. However, a new target could be readily achieved for BAP using the single-solute isotherm, as the presence of 2,4-D had very little impact on BAP adsorption. For 2,4-D, as a first approximation, probably the best approach would be to assume linearity based on previous levels. Once initial concentrations were established for one carbon, however, the linear relationship with porosity would apply when using different activated carbons.

Changing the Hormones: NAA, Kinetin

A qualitative idea of how these hormones would compete for sorption onto activated carbon could be derived from the same principles of partitioning which help to explain the behavior of BAP and 2,4-D. A value for the partitioning coefficient for kinetin was unavailable from the literature. One method of estimating the effective partitioning coefficient, K_p, of a compound is to compare the elution times for unknown substances with those for known compounds using a reversed phase HPLC system (Schwarzenbach et al. 1993). The equation is given below in terms of K_{ow}:

$$\log K_{ow} = a \log t + b \qquad (8.7)$$

Given two known compounds, the constants may be determined.

An HPLC separation of the four hormones (NAA, 2,4-D, kinetin, BAP) from complete media is depicted in Figure 8.40. Note that for this particular chromatogram the flow rate was higher than presented earlier and the buffer was phosphate instead of acetate: these differences resulted in shorter retention times for 2,4-D (8.3 min) and BAP (19.1 min). The kinetin peak appeared at 10.6 min and the NAA elution appeared as a split peak (230 nm) at 6.6 and 7.0 minutes. From the retention times for BAP and 2,4-D, and using log K_p values for dissociated 2,4-D (mobile phase pH 6.0), 0.65, and nondissociated BAP, 1.56 , the constants may be determined. These were found to be: a=2.524; b=(-)1.675. Using these values, the log K_p value for NAA was calculated as 0.43 and that for kinetin was approximated as 0.90. Shafer (1990) reported the log K_p for NAA at pH 6.0 as 0.693 (calculated from data given in the article).

The NAA, with a pK_a reported as 4.2, would be more sensitive to pH decreases than 2,4-D. Kinetin would likely behave in a manner intermediate to BAP and 2,4-D, but without a pH dependence. One would anticipate similar sorptive capacities for kinetin and BAP; and also for the pair of auxins. However, in a successful system comprised of kinetin and NAA, and using the same target levels previously described, the initial concentrations would be more similar than the initial levels for a system with 2,4-D and BAP. A first approximation would place initial kinetin levels between 35 and 65 ppm, corresponding to different levels of competition noted for BAP and 2,4-D. NAA levels would be somewhat lower, near 25ppm.

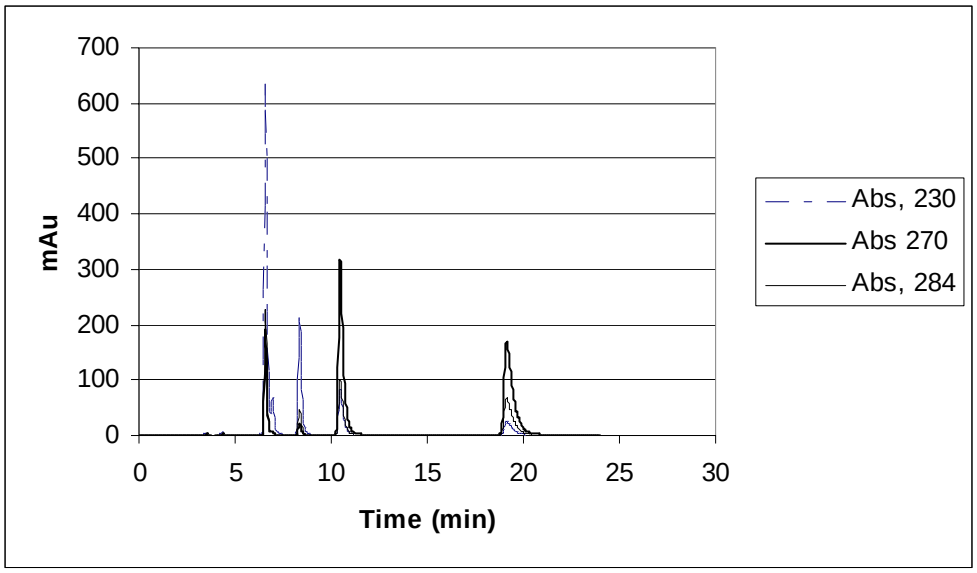

Figure 8.40. HPLC separation of four hormones (NAA, 2,4-D, kinetin, BAP). A separation of the hormones from aqueous solution was achieved using reversed phase (Sigma-Aldrich Spherisorb ODS-2 5μm, 250mm x 4.6mm) and isocratic elution: mobile phase 50% methanol/water with acetate/KOH buffer 0.01M, pH 6.0, flow rate 0.6 mL/min, injection volume 250μL. Three wavelengths were monitored (230nm, 270nm, 284nm). NAA eluted as a split peak at 6.6 and 7.0 minutes, 2,4-D eluted near 8.3 minutes, kintin eluted near 10.6 minutes and BAP eluted near 19.1 minutes.

D. Conclusions

For eight different activated carbons, five of them commonly referenced in the plant tissue culture literature (steam-activated, acid-washed carbons) a linear correlation was established between porosity (as characterized by total pore volume and BET surface area) and the adsorption of the plant growth regulators, BAP and 2,4-D. The adsorption capacity for BAP was approximately twice that for 2,4-D on the different activated carbons at pH 5.8. Target hormone levels in media with different activated carbons could be achieved simply by adjusting the mass of AC based on porosity, coupled with careful control of medium pH.

The data indicated that relatively small amounts of 2,4-D would adsorb on carbon preloaded with BAP. When the pH of the system was adjusted to 3.0, near the pKa of each compound, 2,4-D was adsorbed to a greater extent than BAP. These facts, coupled with additional pH-response data and the slower equilibration of 2,4-D relative to BAP,

suggest that charged sites play a role in adsorption of 2,4-D (dissociated) perhaps to the extent of regulating access to porosity, but are unimportant for BAP.

A number of the experimental results, including the role of temperature, background solute concentrations, and pH, were consistent with organic-aqueous partitioning which is most influenced by the activity of the solute in aqueous phase.

The solubility limit of BAP (165 ppm) imposed an experimental limitation on the mass of AC (0.66 g/L): precipitation confounds adsorption calculations. A percentage of the BAP was adsorbed reversibly. This reversibility confounded efforts to preload AC with BAP.

BAP obeyed a single-hormone adsorption isotherm in the presence of 2,4-D, but the reverse was not true. 2,4-D adsorption was reduced to a much lower level when BAP was present in large excess. For this system, the IAST and Polanyi models for competitive adsorption from solution were inappropriate, though Polanyi did predict BAP behavior.

IX. BIOASSAY

A. Results

Development of Successful Liquid Culture Media

The problem of developing a successful liquid initiation medium for Norway spruce containing AC was separated into three parts. The first task was to realize a successful liquid version of an existing non-AC medium. The next phase was to incorporate AC (T1) into an existing semi-solid medium. The final phase involved introducing the AC into the liquid medium. The partial results from two experiments have been combined and are tabulated in Table 9.1. A successful culture is shown in Figure 9.1.

The semi-solid control medium (first column) was ½ BLG medium as given in Table 6.11. The overall average success rate of 25% for the control was lower than the 30+% reported previously by Verhagen and Wann (1987) using the same medium. This difference in success may have been seed-related or possibly the result of using different production lots for the stock chemicals: agar and casein hydrolysate are two reagents expected to vary in composition.

Table 9.1. Norway spruce initiation success (number of successes per 10 plates per replication), after 9 weeks. Comparison of liquid vs. semi-solid media.

Rep #	Semi-solid[1] (Agar)	Liquid w/ filter, polyester[1]	Semi-solid w/ filter[1] (Agar)	Semi-solid w/ AC 1.25g/L[2] (Agar)	Semi-solid w/ AC 2.5 g/L[2] (Agar)	AC 2.5 g/L 125:62.5[3] Gelrite 2g/L
1	1	3	0	3	0	3
2	4	6	2	5	0	3
3	3	6	2	4	1	1
4	1	5				
5	4	4				
6	2	3				
Mean	2.5	4.5	1.3	4.0	0.3	2.3

1. Media include auxin (NAA) and cytokinin (BAP), 2 ppm and 1 ppm, respectively.
2. Media include 2,4-D and BAP at 100 ppm:50 ppm
3. 2,4-D to BAP: 125 ppm:62.5 ppm

It may be seen from Table 9.1 that the liquid medium, using the filter/polyester support, gave significantly higher success than did the semi-solid control. This success could not

be attributed simply to the filter, as semi-solid media with a filter placed on top of the gelled media performed relatively poorly.

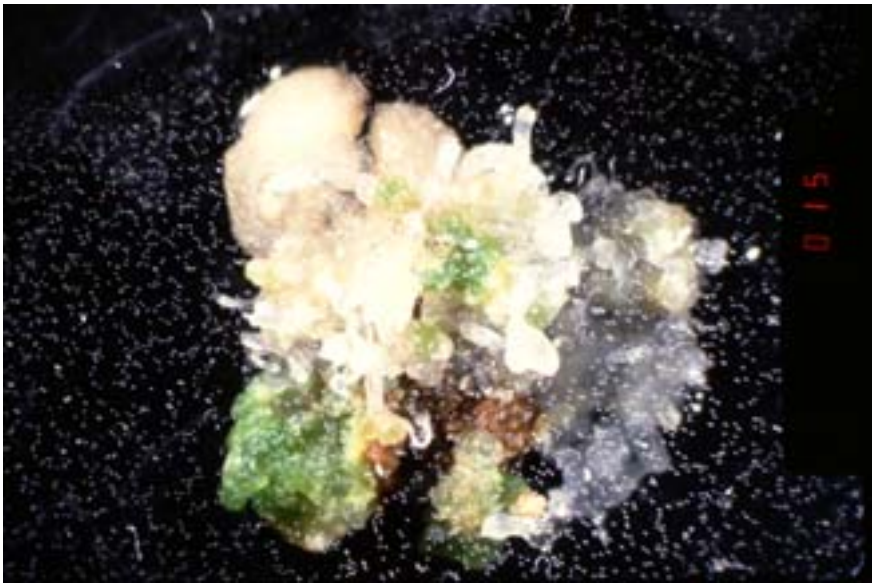

Figure 9.1 A successful initiation of ESM on growth media containing 10 ppm activated carbon (T1). Note that the cotyledons are undeveloped, no radical is present and there is a minimum of green tissue. Somatic embryos are present in the translucent growth and appear as finger-like projections.

The 1.25 g/L level of AC gave high success in the gelled medium (40%). The same media with AC at 2.5 g/L did not perform well at all (3.3% success). Subsequently, greater hormone levels (125 ppm 2,4-D and 62.5 ppm BAP) were tried in media with AC at 2.5 g/L, resulting in significantly improved success. Part of this improvement may have been due to the substitution of Gelrite for agar. Several other treatments with higher AC gave significantly lower success rates than those for the 1.25 g/L level. The major findings from these two experiments were that a liquid medium without AC could give high success rates and that gelled media with AC could also give acceptable rates of success.

The liquid medium with hormones NAA and BAP at 2 ppm and 1 ppm, respectively, and no activated carbon was chosen as the control for each experiment that followed. This control medium was replicated in more than fifty trials (typically, there were ten plates per experimental replication). These data were used to generate a reliable estimate of the mean and standard deviation.

Mean and Standard Deviation for the Liquid Control

Discrete data resulted from the tissue culture experiments, i.e. for each culture plate there were only two possible outcomes: success or no success. The assumption was made that the discrete distribution of data produced by each replication of ten plates could be modeled using a continuous distribution: i.e. that the standard normal curve could be applied to the binomial data generated. This assumption is valid for large numbers of replications, ten replications admittedly being on or below the lower limit for rigorous analysis (Walpole, Myers 1989).

Data for the control treatment (media without activated carbon) from twenty experiments were pooled. The mean number of successes for 48 experimental replications was 4.1 plates out of ten or a 41% success rate. The standard deviation was 1.4 successes. The coefficient of variation, COV, was therefore 34% (standard deviation / mean).

Most often, experiments were replicated three times. A confidence interval based on three experimental replications may be calculated:

$$½ Conf.Interval = \frac{(COV)(t_{½})}{\sqrt{n}} \qquad (9.1)$$

A ninety percent confidence interval was deemed adequate for this research, and α was specified as 0.1, where α represents the probability of rejecting the null hypothesis when it is true (type 1 error). For 3 replications there were 2 degrees of freedom with $\alpha/2$ of 0.05 (two-tailed test): the *t* statistic was found to be 2.92. Using the standard deviation estimated from the 48 control replications, the 90% confidence interval was calculated as the *mean value* $\pm$ *57%*.

The statistically significant, minimum difference between two means (least significant difference) may be approximated by using a pooled, two-tailed t-test on the difference between the means (Ott, 1988).

$$t = \frac{y_1 - y_2}{s_p \sqrt{1/n_1 + 1/n_2}}$$

$$H_0 : \mu_1 - \mu_2 = 0 \qquad (9.2)$$

$$reject\ H_0\ if\ t > t_{\alpha/2};\ or\ if\ \ t<(-)\ t_{\alpha/2}$$

where y_1 and y_2 are experimental mean values, n_1 and n_2 designate the number of values used in calculating the experimental means; and, s_p designates the average standard deviation. Using the standard deviation from the control data and 4 degrees of freedom ($n_1 + n_2 - 2$, where each $n = 3$) at the $\alpha = 0.1$ level resulted in a least significant difference of 1.9 successful cultures. Based on the preceding analysis, several comparisons in Table 9.1 gave differences that were statistically insignificant.

Introducing AC into Liquid Media

Results from an experiment exploring the effect of different levels of AC on the liquid medium are given in Table 9.2. For this experiment, the different AC levels were simply added to the control media with no adjustment of nutrient composition, i.e. the hormone levels were 2 ppm NAA and 1 ppm BAP. Note how low the AC levels were, compared to the levels used in semi-solid media (1.25 g/L or greater). Yet, even at the low level of 100 ppm (0.1 g/L) with normal hormone levels, initiation was completely inhibited in liquid medium.

Table 9.2. Norway spruce initiation success, after 9 weeks for liquid media with varying levels of AC. *

Rep #	Control	10 ppm	50 ppm	100 ppm	250 ppm
1	3	5	4	0	0
2	6	3	1	0	0
3	5	5	5	0	0
Mean	4.7	4.3	3.3	0.0	0.0

* ppm (mg/L) refers to AC level. Liquid media were formulated with 2 ppm NAA, 1 ppm BAP and standard vitamin levels

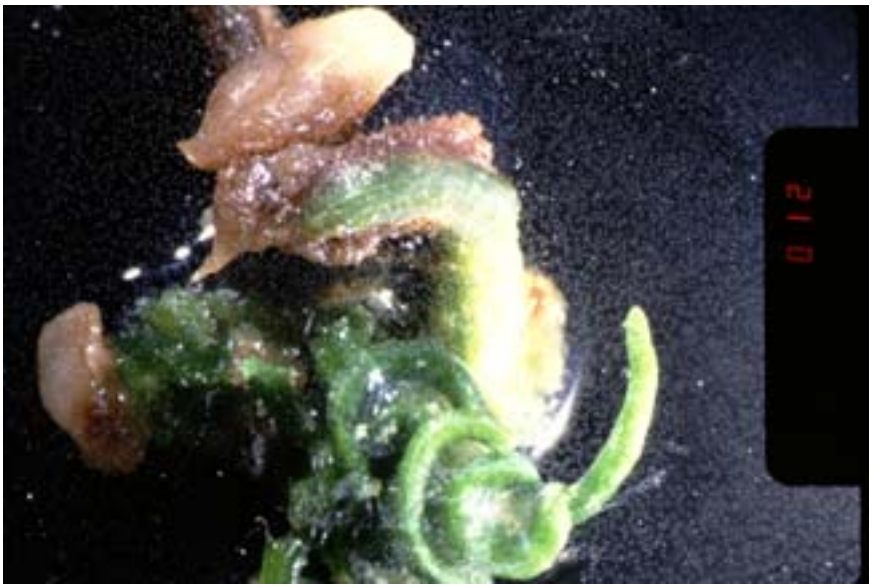

Figure 9.2. A germination tendency was observed on media with AC (T1) at 100 ppm. Cotyledons were clearly visible and a poorly defined radical was evident.

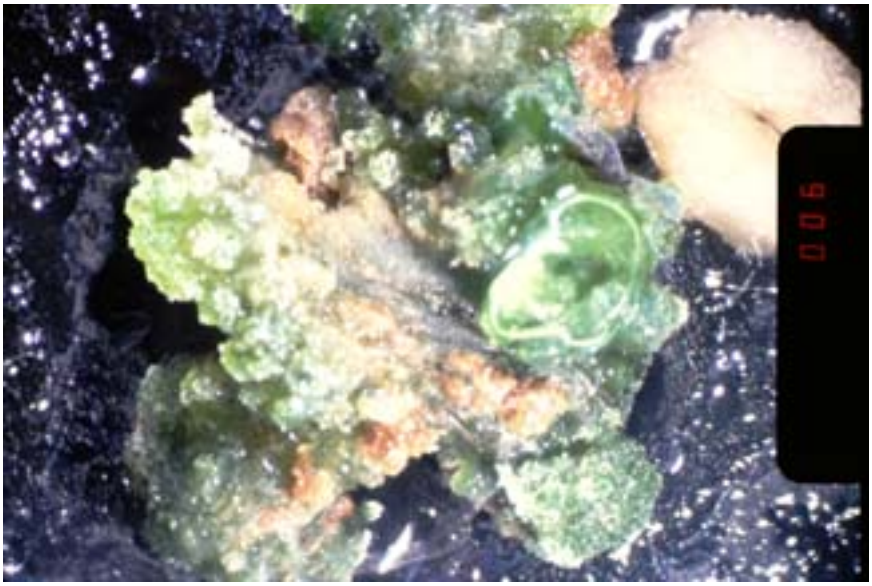

Figure 9.3 Aberrant growth occurred when AC (T1) was included in the media at the level of 50 ppm. This morphology was intermediate to that when AC was present at 10ppm and 100 ppm. A significant number of cultures with this level of AC produced somatic embryos.

A transition in culture response occurred at the AC level of 50 ppm. Above this level, the cultures tended towards germination, producing a radical, and green cotyledons (Figure 9.2). Below 50 ppm, the cultures resembled the expected embryogenic tissue, indistinguishable from the control. At 50 ppm, the cultures grew in an aberrant fashion with disorganized leafy growths along with callus, and embryogenic tissue at significant frequency (Figure 9.3).

Liquid Media: AC Target of 1.25 g/L

The results with liquid medium which included AC at 10 ppm were encouraging, but at this low level of addition, it was felt that AC variability would be amplified while the effect of using different AC would be minimized. A target AC level of 1.25 g/L was chosen.

Successful Douglas-fir initiation media with AC (2.5 g/L) included higher vitamin levels than those used in the Norway spruce medium (Pullman, Gupta, 1991). Based on the difference in AC level between the Douglas-fir and Norway spruce media (2.5 vs. 1.25 g/L), the target level for the vitamins was chosen as one half the level present in the Douglas-fir media. Trebling the vitamin level in the Norway spruce control resulted in a total vitamin level similar to that of using one half the Douglas-fir levels.

An experiment was conducted using media with elevated vitamin (3 x WB, Table 6.11) and hormone levels (2,4-D at 100 ppm and BAP at 90 ppm) and two different AC's (1.25 g/L). The results of this experiment are presented in Table 9.3.

Contrary to the earlier result with semi-solid media (Table 9.1), the 1.25 g/L level of AC in the modified liquid medium gave relatively low success. The difference in success between media with the different AC's was not statistically significant. In a separate experiment using media without AC it was found that increased hormone levels had no impact on the rate of success.

Table 9.3. Norway spruce initiation success after 9 weeks in liquid medium with two different AC's

Rep #	Control*	T1*	N*
1	3.3	1.8	3.1
2	3.3	1.7	2.0
3	5.0	0.9	0.8
Mean	3.9	1.5	2.0

* Liquid control media were formulated with 2 ppm 2,4-D, 1 ppm BAP and standard WB vitamins. Media with AC (1.25 g/L) were formulated with 100ppm 2,4-D, 90ppm BAP and 3 x WB vitamins. For this experiment the number of plates per rep varied but in each case exceeded 10: the number of successes are given based on ten plates per rep.

This result was unexpected. The hormone levels of the medium with N1 and T1 were determined by HPLC (Section VIII). It was found that the available BAP levels were very low for each carbon type after 2.5 days, 0.025 ppm and 0.003 ppm for N1 and T1, respectively. The 2,4-D levels were measured as 13 ppm and 1.2 ppm for N1 and T1, respectively. Media without AC were formulated with those hormone levels and tested with the Norway spruce bioassay. The results from this experiment are given in Table 9.4.

Table 9.4. Norway spruce initiation success for non-AC liquid media formulated with measured hormone levels, total success after 9 weeks.

Rep #	Control[1]	N1 Hormones[2]	T1 Hormones[3]
1	4.5	0.0	0.0
2	3.6	0.9	0.0
3	7.3	0.0	0.0
Mean	5.2	0.3	0.0

1. Standard WB vitamins, 2 ppm 2,4-D, 1 ppm BAP
2. Control media formulated with measured hormone levels for media with N1 after 2.5 days: 13 ppm 2,4-D, 0.025 ppm BAP
3. Control media with measured hormone levels for media with T1 after 2.5 days: 1.2 ppm 2,4-D, 0.003 ppm BAP.

The T1 formulation resulted in no successes whereas the N1 formulation gave 1 success. Tendencies towards germination were observed for cultures grown on media with the T1

hormone levels. A culture morphology that was very difficult to distinguish from a true early stage initiation was prevalent when using the N1 medium. This morphology resembled embryos inhibited from developing further.

Tissue were composed of two distinct cell types: a round cell lacking in polarity, which has been observed previously in non-embryogenic callus (von Arnold 1987) and a tissue

A.

B.

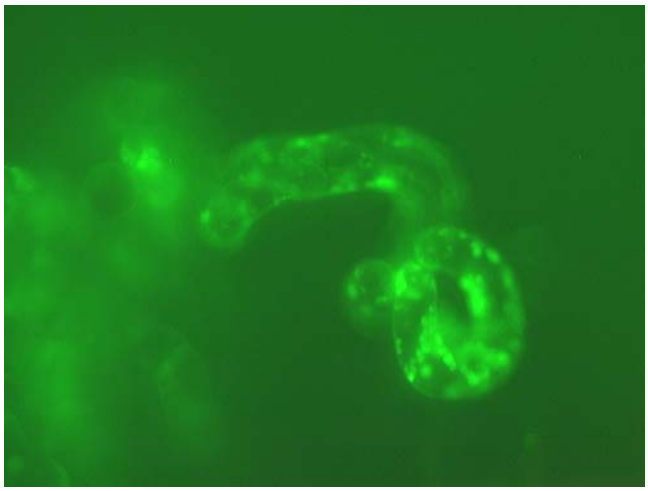

Figure 9.4 a,b.A. Image of an early stage embryo; B. cell with elongated morphology but lacking the nucleic organization of an embryo. Cells were stained with FDA fluorescing stain.

with elongated cells which may or may not have been embryogenic. Using a fluorescing stain, it was found that these elongated cells lacked the "signature" typical of an early stage embryo. This may be seen in Figure 9.4. Note the concentration of nuclear material in the true early stage embryo: the other cell type lacked this nuclear organization.

Reducing the Level of AC

It was believed that the inhibition of success observed in the previous experiments was due to low levels of BAP. Adsorption experiments revealed that BAP was preferentially adsorbed onto AC (Section VIII). Based on the success of the control medium, a target level of 1 ppm BAP was chosen. To achieve this level of residual hormone when using T1 at 1.25 g/L, it was found that more than 200 ppm of BAP would be required initially. However, the solubility limit for BAP in liquid medium was found to be 165 ppm.

As a result of these considerations, the level of the AC was reduced from 1.25 g/L to 0.3 g/L. Target hormone levels were chosen based on hormone levels in the successful control medium, 2 ppm 2,4-D and 1 ppm BAP. These levels were achieved with T1 by reducing the initial hormone concentrations to 12 ppm 2,4-D and 66 ppm BAP. The target levels were also achieved using a second AC, Norit Sx4. However, for Sx4 the initial hormone levels were reduced to 32 ppm 2,4-D and 8 ppm BAP. This difference in initial hormone levels was related primarily to differences in total pore volume between the two carbons (Section VIII).

Media were formulated with two different carbons (0.3 g/L) and with the appropriate hormone levels. The results are presented in Table 9.5. From the table it may be seen that successful initiation was achieved with AC present at a significantly higher level than had previously given acceptable levels of success (0.05 g/L). Though media with Sx4 were found to have a higher average than the control and T1 media, the difference was not statistically significant.

Table 9.5. Norway spruce initiation success after nine weeks for media with two different activated carbons.

Rep #	Control	T1	SX4
1	5	8	5
2	7	3	8
3	7	5	7
Mean	6.3	5.3	6.7

*Media with AC (0.3 g/L) were formulated with initial hormone levels (T1: 65 ppm BAP, 12ppm 2,4-D; Sx4: 32ppm BAP, 8ppm 2,4-D) that resulted in levels similar to the control (approx. 2ppm 2,4-D, 1ppm BAP) after 2.5 days. AC-containing media were formulated with elevated vitamin levels (3 x WB).

Support/AC Interaction

In a previous tissue culture experiment (results not shown) a different production lot of the black filters had been inadvertently substituted for the first production lot. When these new filters were used, the control gave zero success in three replications. For the original production lot of filters, the pH of the medium was found to decline to pH 4.8 as the media were poured. The second production lot gave pH 4.4.

Control media, i.e. media without activated carbon (Table 6.11), were treated with the different filters. Liquid media samples were collected after 2 days and analyzed for hormone levels (Figure 9.5). Different levels were measured when using the different filter production lots. Both 2,4-D and BAP were significantly reduced in availability when the 2nd production lot was used, indicating that adsorption had occurred.

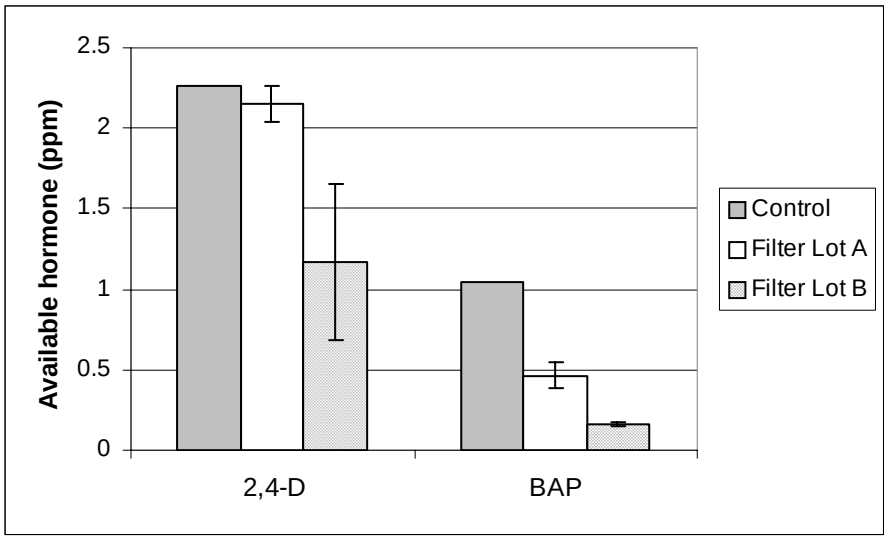

Figure 9.5. Control media (no AC present, 2 ppm 2,4-D, 1 ppm BAP) were treated with black filters from two different production lots (10 mL medium per filter). Media were equilibrated 2 days prior to addition of the filters. Measurements were made within four hours of adding paper. Error bars depict 90% confidence limits based on three replications.

The same experiment was repeated for media containing AC (Figure 9.6). For each filter production lot, the level of BAP was significantly greater than the control containing AC. The 2,4-D levels agreed well with the control values for media with filter production lot A. Media with Lot B gave significantly reduced levels of 2,4-D.

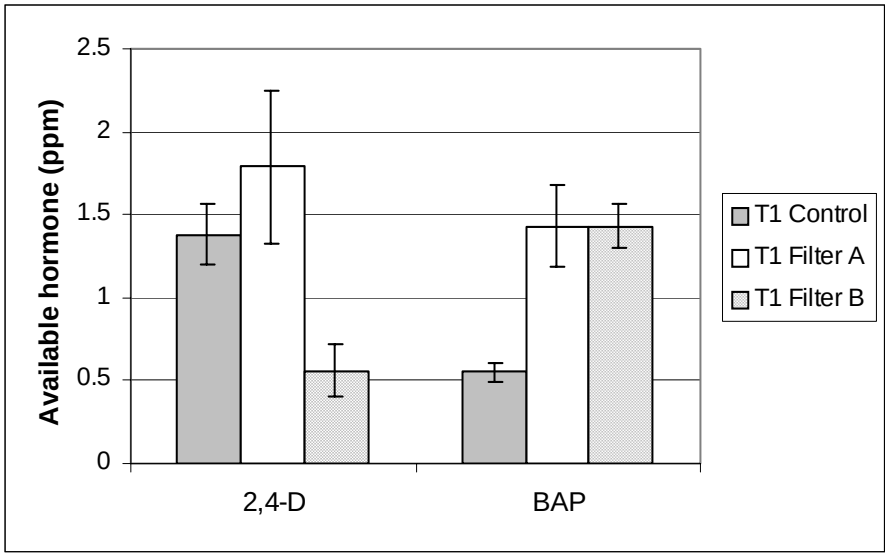

Figure 9.6. Media with AC (0.3 g/L) were treated with black filters from two different production lots (10 mL medium per filter). The media were equilibrated two days prior to adding the filter papers. Samples were taken within 2 hours. Error bars depict the 90% confidence interval based on three replications.

Sample filter papers from each production lot were imaged and are shown in Figure 9.7. They were clearly different in color. In fact, different dyes were used in their manufacture (personal correspondence with Ahlstrom). A primary component of a pigmented dye is the dispersant for the pigment. A commonly used dispersant is sodium dodecyl sulfate (SDS). It was estimated that a filter paper could contain ca. 5 mg SDS based on the difference in weight between a Whatman #1 filter and the black Ahlstrom filters. When this amount of SDS was added to media with AC that had been stored thirty days, the hormone levels increased immediately by a factor of three (Figure 9.8).

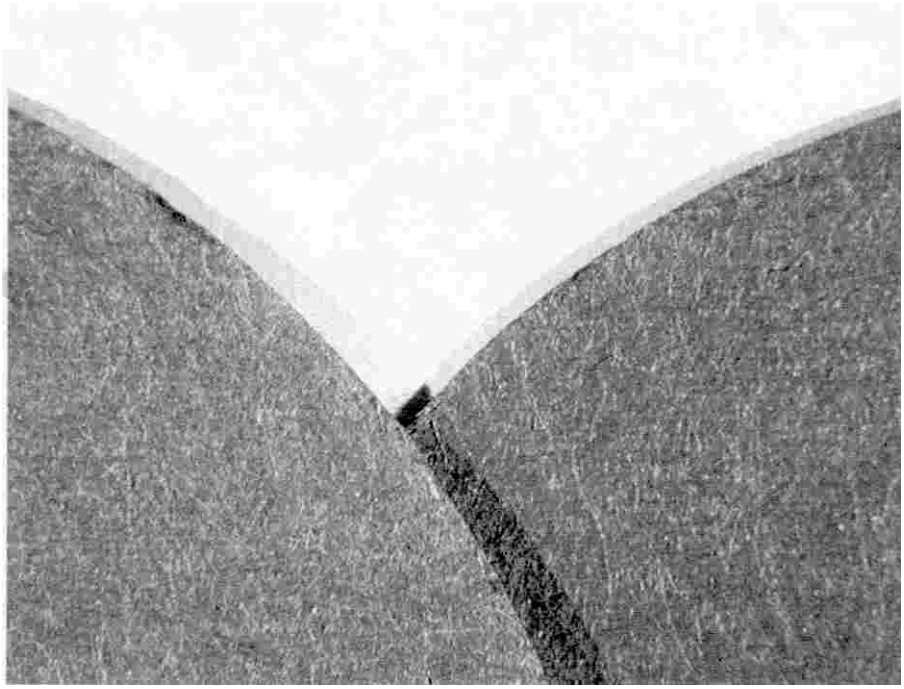

Figure 9.7 Image of black filters from two different production lots. A filter from lot A is shown on the left. Th e difference in color resulted from different dyes used in the production process. These dyes differed in chemistry and led to different medium compositions.

The black filter paper was originally chosen based on its color, which greatly facilitated the identification of successful initiations. Black cellulose ester membranes were tried as

a substitute, but were found to give no initiations for the control medium, instead resulting in the proliferation of necrotic tissue. Therefore, white filters were tried.

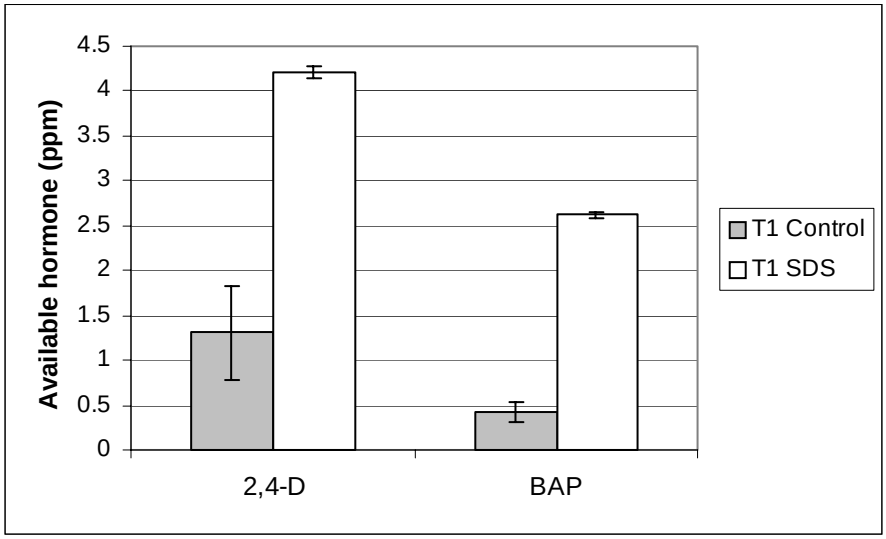

Figure 9.8. Media were formulated with AC (0.3 g/L) and equilibrated thirty days. SDS, 0.5mg per mL of media, was added to each of three replicates. Samples were taken within one hour of SDS addition. Error bars depict the 90% confidence interval based on three reps.

The results from a tissue culture experiment in which the control medium was dispensed to three different support combinations are given in Table 9.6. The difference between Whatman #1 and the black Ahlstrom filters was statistically significant, whereas the difference between Whatman #5 and the Ahlstrom filters was not.

Table 9.6. Norway spruce initiation success after 9 weeks. Comparison of different filters*

Rep #	Control	Whatman #1	Whatman #5
1	4.0	2.0	5.0
2	7.0	2.0	3.0
3	3.0	1.0	1.1
4	4.0	2.0	5.0
5	2.0		
6	5.0		
Mean	4.2	1.8	3.5

* None of these media contained AC: initial hormone levels of 1 ppm BAP, 2 ppm NAA, standard WB vitamins.

It is expected that the release of substance by the black filters in the absence of activated carbon had no impact on the hormone levels.

Results from Ion Experiment

An initiation experiment was conducted to evaluate whether or not the ionic differences given for media with N1 and T1 (Table 7.2) were significant to a growing culture. For this experiment AC was not included in the media.

The initial concentrations of phosphorus, magnesium, iron and manganese were adjusted to reflect the levels present in media with N1. The other ions were left at normal ½ BLG levels. The manganese and iron were reduced to 45% of their calculated ½ BLG concentrations. Phosphate was reduced to 83% of its normal value and magnesium was increased by 70%, to reflect the large amount released from N1 into the medium as the pH dropped. Though silicon was also released into the medium by N1, this element was not deemed important to metabolism. Control media were formulated as previously. Hormone levels were 1 ppm BAP and 2 ppm NAA. All media were adjusted to pH 5.8 prior to autoclaving.

Table 9.7. Norway spruce initiation after 9 weeks, effect of reduced ion levels

Trial	Control (%)*	Ion treatment (%)*
A	45.5	36.4
B	36.3	18.2
C	72.7	45.5
Mean	**51.5**	**33.4**

* Media were formulated with 2 ppm NAA and 1 ppm BAP with standard WB vitamins. *Ion treatment* reflects ion composition at pH 6.5, when using N1.

The percentages in Table 9.7 are the number of successful initiations out of eleven plates per experimental replication. The three replications of the experiment, designated A, B, and C, displayed a wide range in success rates; however, for each trial the ion treatment resulted in lower success.

B. Discussion

The low success for liquid medium with AC at 1.25 g/L was unexpected given that high success for the same level of AC had been achieved using semi-solid media. This difference in success was attributed to a higher rate of adsorption of the hormones in liquid media than in semi-solid media. The difference in rates of hormone adsorption between gelled and liquid media have been noted previously by Ebert and Taylor (1990). They reported that the level of 2,4-D present in gelled media after 5 days could be more than three times the amount present in liquid media of the same initial composition. Similar effects have been noted for adsorption of abscisic acid, an important component of other media (Gupta, Pullman 1991).

The decline of the hormone levels over time (Figures 8.3, 8.4) did not inhibit initiation for media which included AC at 0.3 g/L. These results, when considered together, indicate that the constant hormone levels expected to be present in media without AC were not required for success. In fact, a gradual decline in hormone level might even be beneficial. The cultures seemed to be responding to the hormone levels present at the start of the experiments. This observation agreed with results that were reported by von Arnold (1986), who noted that a pretreatment of the explants in a hormone solution subsequently enabled successful initiation on media without hormones. No initiation occurred on hormone-free medium without the pretreatment of the explant.

The depletion of nutrients necessary to supress germination could account for the germination response of the culture and the lower rates of success with increasing AC (Table 9.2): the culture produced green tissue to synthesize needed compounds. It was believed that the depletion of hormones or vitamins was responsible as they are known to have the greatest impact on cell organization and culture morphology.

Thiamine is synthesized in the green tissue of the culture. Previous research found that thiamine could be adsorbed from solution (Weatherhead et al. 1979), but these measurements were made in the absence of competing sorbates. The results reported in Section VIII have shown that even a compound completely miscible in aqueous solution,

sucrose, will adsorb onto activated carbon in the absence of competing sorbates. The aqueous solubility of thiamine (1g/mL) is so great that it is not expected to compete with either of the hormones. A more likely candidate is nicotinic acid; however, it is also far more soluble than either of the hormones (60mL H_2O per gram of solute, log K_{ow} –0.65 ; pK_a 4.85).

In Section VIII it was shown that the sorption of BAP occurred preferentially to 2,4-D. It is expected that 2,4-D was next adsorbed in preference to the remaining medium components. By extension, these remaining compounds would generally adsorb in order of hydrophobicity. A similar ranking of compounds has been applied to reversed-phase liquid chromatographic separations (Ladisch 1997).

For media with 1.25 g/L AC, increasing the vitamin levels to three times the control level resulted in less green tissue, better morphology overall, and increased initiation success, suggesting that the depletion of vitamin may be a concern when using AC in culture media. Control media (no AC), when formulated with 3 x WB showed no improvement compared to the control with normal vitamin levels. However at 1.25 g/L, the sorptive potential of the AC was significantly greater than that satisfied by the available hormone, hence the low BAP levels. The vitamins may have been depleted to inhibitory levels as a result of insufficient hormone.

The different interactions between the medium and the AC were further complicated through the effect of the black filter. The filter support had a significant impact on the medium, reducing its pH to 4.8 for production lot A and altering its chemical composition. The pH effect was instantaneous: the pH dropped as soon as the medium contacted the filter papers. The findings presented in Sections VII and VIII, showed that a reduction in pH led to greater adsorption of 2,4-D. Additionally, the precipitate that formed at higher pH, with the exception of a portion of the iron, redissolved as pH fell. The adsorption of zinc and copper was relatively insensitive to pH over the range of interest. A second production lot of black filters gave a significantly lower pH level, below 4.5. As pH declined further due to the second filter production lot, it was expected

that 2,4-D levels would decline due to increased adsorption onto the AC. BAP adsorption, however, was expected to be minimally affected by pH over this range. The first production lot of filters gave high initiation success despite the pH effect in both control and AC-containing media. This result showed that the initial pH of 5.8 was not critical to initiation success. However, the difference in pH due to the different production lots of the black filters may have been significant, as no success was observed for the second production lot, implying a pH threshold for inhibition of about pH 4.5.

According to the chemiosmotic theory, the uptake of auxin by the cell results in the secretion of H+ (Rubery 1980). At pH below 4.5 there is an excess of protons in the medium which inhibits this "proton pump." Egertsdotter et al. (1993) identified different strains of culture cells. The embryogenic cultures were unable to produce embryos at pH levels of 4.5 and below.

Further analysis would consider the different hormone levels present when using the different filters. When AC was absent from the medium, the BAP was adsorbed by both filters, with Lot B adsorbing BAP to a greater extent. From the results given in Section VIII, it is known that this is not a pH effect. Based on the tissue culture results for the controls (no AC), the BAP concentration with filter lot A was high enough to allow successful initiation. This level was about 0.5 ppm. Filter lot B gave low or no success in control media with about half that level of BAP. The level of 2,4-D was also reduced, but not to the point where initiation was completely inhibited. These results suggest that there is a threshold BAP concentration, below which initiation cannot occur.

An interaction was indicated between activated carbon and the black filter paper used to support the culture. This interaction led to an increase in the BAP level of the medium; that is, hormone was displaced from the AC surface. The two different production lots of the black filters were found to perform differently regarding their interaction with AC. This was attributed to the use of different dyes in their manufacture. The black dyes of the filters incorporate a dispersant for the pigment particles. Surfactants, such as sodium

dodecyl sulfate, SDS, are commonly used as dispersants. The addition of SDS to media with AC resulted in an instantaneous increase in hormone levels.

It is proposed that a three-factor mechanism accounted for the filter effect on the hormone composition in the presence of AC. A surfactant was released which displaced hormone from the surface of the activated carbon, and the pH was lowered which caused more of the 2,4-D to be adsorbed. Additionally, the sorption of the hormones was regulated by the surface area of the carbon black pigment: the different dyes used different pigments and surfactants. The combined surfactant, sorptive and pH effects led to an increase in available BAP and a decrease in available 2,4-D.

A similar displacement starts when metabolites are released into the medium by a growing culture. It has been reported that proteins are secreted from growing Norway spruce cultures (Egertsdotter et al. 1993). Proteins are large molecules with hydrophobic and hydrophilic regions and are commonly separated based on their hydrophobicity using electrophoretic and chromatographic techniques. The secretion of phenolic by-products by living cultures has also been noted. These were found to be readily removed by AC (Weatherhead et al. 1979; Fridborg et al. 1978; Johansson 1983). The adsorption of these various metabolites could result in the displacement of hormone, as with the adsorption of SDS.

The possible use of surfactants in combination with AC to produce novel hormone concentration profiles could lead to improvements in culturing techniques.

The bioassay, when using the second production lot of filters gave no success for either the control or media with AC. According to the analysis presented, the low success in the case of the control may be attributed to the low BAP level, whereas the low success in the case of media with AC may be attributed to low 2,4-D levels.

Relative to the impact of the different hormone levels, the impact of the different ionic compositions was minor. The ionic compositions were “worst case”: that is, they were

formulated to match the measured ion levels at elevated pH. Therefore, as the pH declined due to culture growth, the available ion concentration never exceeded that present at elevated pH. This would not have been the case in the complete medium at elevated pH. In the actual medium, the growing culture would force the pH of the medium below pH 5.6, resulting in the dissolution of the precipitate. The surplus of calcium and magnesium were not inhibitory based on tissue culture results for an experiment where the medium was formulated from extract from N1. The extract may actually have increased the rate of success. Therefore, the primary ionic effect of concern was the reduction of Fe and Mn availability as pH increased. The impact of reduced Fe-EDTA levels on culture success has been noted previously for anther cultures (Johannson et al. 1990). It was found that lowering the Fe-EDTA level could completely inhibit embryogenesis. It is therefore expected that the lower success due to the ion treatment was attributed to the lower iron levels present.

C. Conclusions

A successful liquid Norway spruce bioassay has been developed which incorporates activated carbon at levels up to about 0.5 g/L, the level being limited by BAP solubility. Based on three experimental replications and ten individual culture plates per replication (ten different zygotic embryos), a difference in average success of 1.9 (out of ten) is required to attain statistical significance. This level of resolution imposes restrictions on the interpretation of bioassay results.

The bioassay was applied using two different activated carbons. The initial hormone levels had been modified to compensate for the differences in sorption between the two AC's. The media with the two activated carbons were found to give success rates that exceeded the success rate of the non-AC control. Though one AC did give higher success than the other, the differences were not statistically significant. This result suggests that media can be compensated to ensure success when using different activated carbons.

The variation in ionic composition that resulted from elevated pH gave significantly lower initiation success. This result was attributed to the reduction in available iron. However, the bioassay proved to be more sensitive to the hormonal composition of the medium: improper hormone levels completely inhibited the bioassay. This inhibition was attributed primarily to low BAP levels. The initial hormone levels were more important to success than levels at later stages of culture.

The bioassay was affected by the variability between production lots of the black filters used to support the growing culture. These differences in performance were attributed to the different dyes used. It was shown that a common dispersant, SDS, could displace adsorbed hormone. Although the AC was already “loaded”, this result indicated that compounds could adsorb to the AC and displace previously adsorbed compounds. Even though the initial hormone level is thought to be more critical than subsequent levels, the release of hormone by a displacement mechanism over the duration of the experiment warrants further investigation, as it is a plausible explanation for how AC improves the performance of tissue cultures.

X. THESIS CONCLUSIONS

The physical characteristics of activated carbon were correlated with the available, non-adsorbed elemental content, available 2,4-dichlorophenoxyacetic acid and 6-benzylaminopurine content, and biological success of AC-containing tissue culture media.

Eight different activated carbon products were studied. The activated carbons were selectively characterized using commonly referenced techniques: including Boehm titration, oxygen content by difference (CHNSO), FTIR, isoelectric point (zeta potential), ash content (qualitative composition by SEM-EDS), moisture content, apparent density, point of zero charge (mass titration), acid titration, and BET area and porosity (nitrogen adsorption, density functional theory). Oxygen functionality characterization proved problematic.

Single-solute isotherm data for adsorption of each hormone onto three different activated carbons, measured by HPLC and UV, revealed that BAP adsorbed to about twice the level of 2,4-D. The adsorption of hormones was strongly correlated with BET surface area and total pore volume. Hormone adsorption correlated well with BET surface area and total pore volume.

Target levels of available hormone, 1ppm BAP and 2ppm 2,4-D measured after 2.5 days, were achieved in media with three different activated carbons present at 0.3 g/L. The presence of 2,4-D did not impact the adsorption of BAP. However, the adsorption of 2,4-D was greatly diminished when competing against BAP. Once a successful combination of initial hormone and activated carbon levels had been achieved for a particular AC, similar available hormone levels were attained with seven other activated carbons simply by adjusting the mass of carbon added to the medium. Activated-carbon mass adjustments based on the total pore volume or BET surface area resulted in mass levels that were within 6% of the final successful level for each of the seven activated carbons.

Non-acid-washed activated carbons were found to have a strong influence on the pH of the medium, increasing it from 5.8 to 6.5. Acid-washed carbons commonly used in plant tissue culture media were found to have minimal impact on the pH of the medium. The carbon characteristics most pertinent to the system pH were the point-of-zero charge and the buffering strength at pH 5.8.

During normal culture growth, the pH of medium without AC decreased from 5.8 to 4.8 over a period of 21 days. Experiments with AC-containing media, in the absence of growing tissue, formulated to pH 6.5, 5.8 and 4.8, revealed increased adsorption of 2,4-D as pH declined (measurements were made after equilibration of 2.5 days). Media that were equilibrated 2.5 days at pH 5.8 and then reduced to pH 4.8 in a single step-wise addition of HCl resulted in the same 2,4-D levels as when the media were initially formulated to pH 4.8. A small percentage of the total adsorbed 2,4-D was found to adsorb reversibly. Increasing the pH after adsorption had occurred resulted in the release of adsorbed 2,4-D. The adsorption of BAP was insensitive to pH over the same range. The pH-sensitivity for 2,4-D adsorption was attributed to the dissociated acid group, resulting in like-charge repulsion at pH above the pKa of 2,4-D (ca. 2.8).

A common surfactant, sodium dodecyl sulfate (SDS), was capable of displacing adsorbed hormone, resulting in increased hormone levels for both 2,4-D and BAP. Further, BAP reversibility was demonstrated for activated carbon which had been preloaded with BAP and introduced into a second medium.

The competitive sorptive behavior of 2,4-D was not predicted by three common models for competitive adsorption, the Polanyi potential model as adapted by Manes and Hofer (1969) the ideal adsorbed solution theory (IAST), or the multi-solute Langmuir model. However, the Polanyi model successfully predicted that the BAP adsorption would not be affected by 2,4-D at the levels used in tissue culture media. The adsorption of 2,4-D occurred to a limited extent even in the presence of BAP. Additionally, the 2,4-D was found to adsorb to AC preloaded with BAP. Finally, the 2,4-D exhibited pH-dependent

behavior. These findings indicated that the 2,4-D was adsorbing to sites unavailable to BAP.

The influence of temperature, background solute concentrations, and pH on hormone adsorption were consistent with similar organic-aqueous (e.g. octanol-water) partitioning behavior.

Of the quantifiable (ICP) elements in the growth medium that could be quantified using ICP-AES, copper and zinc were the only ones adsorbed onto activated carbon, 90% and 50%, respectively. This adsorption per gram of AC was relatively insensitive to changes in carbon type or changes in AC mass levels over the range from 1.25 g/L to 2.5 g/L. Adsorption was consistent with selective surface complexation of the free ions.

Several ions demonstrated a pH-dependent precipitation (Fe, Mn, Zn, Ca, P, and Mg). Iron and manganese were depleted by the greatest percentage in response to increasing pH from 5.8 to 6.5, 51% and 41% depletion, respectively. This pH-driven precipitation was reversible except for a percentage of iron (18 %). The evidence suggested that hydroxides were forming.

The precipitation of iron at elevated pH was compensated by increasing Fe-EDTA, increasing EDTA alone, filter sterilization, or adding potassium citrate. These strategies also resulted in higher Mn levels. The samples that included citrate were the only ones in the entire study to attain target Fe concentrations.

A successful Norway spruce initiation medium with AC was achieved based on the hormone adsorption isotherm data and the ion availability data. Successful media were demonstrated with two different activated carbons. Less successful media were explained by inadequate hormone levels and variation in ionic composition.

The variation in ionic composition that resulted from elevated pH gave significantly lower initiation success. This result was attributed to the reduction in available iron. The

bioassay proved to be more sensitive to the hormonal composition of the medium. Improper hormone levels completely inhibited the bioassay.

Therefore, the difference in tissue culture success that results when using different tissue-culture-grade activated carbons is plausibly related to the adsorption of hormones (or other poorly soluble organics), and this difference is directly related to the BET surface area or the total pore volume.

XI. RECOMMENDATIONS FOR FURTHER RESEARCH

Displacement/Reversibility

Protein secretion in plant cell suspension cultures is a well-known phenomenon. Inhibitory benzoic acid derivatives and phenolic compounds are also released by growing tissue into culture media. The present study has shown that pre-adsorbed glutamine in no way inhibited the adsorption of hormones. It was also shown that a percentage of the adsorbed hormones were displaced by surfactants, long-chain amphiphilic molecules. These observations suggest that hormones may be displaced from the surface of AC by proteins or other poorly soluble molecules released by the growing culture, resulting in increasing hormone levels over time. This response is a plausible explanation for the improvements noted in the literature for media with AC compared to media without AC. Novel hormone profiles could be produced in aged media simply by introducing small quantities of surfactant. These possibilities warrant further research.

pH Buffering

The study of the impact of pH on tissue culture has been confounded by the difficulty of identifying a pH buffer that doesn't ultimately accumulate in the cells. As shown in this study, growing cultures influence the pH of poorly buffered media. This poses problems when trying to assess the importance of pH to the growing tissue. Non acid-washed activated carbon may potentially be utilized as a non-metabolized buffer.

To gain the maximum benefit, the level of AC in the medium would have to be increased substantially above the 0.3 g/L level used in this study. The adsorption capacity of such a dose could be nullified with preloading of AC with a poorly soluble nutrient or non-nutrient. A better understanding of reversible adsorption is needed. Additionally, a better understanding of the pH drift of non-acid washed-carbons is required. Perhaps a feasible alternative would be to introduce a resin with desired buffering properties combined with activated carbon to gain the sorptive benefits of AC.

Sorption Phenomena

The adsorption of the two hormones showed a time dependence and also an adsorptive component which was irreversible over the time scale of the tissue culture experiments. In experiments examining the effect of shaker speed on equilibration, BAP was sensitive to shaking, however, BAP equilibrated more rapidly when competing against 2,4-D in a shaken flask. It was hypothesized that the ionic interactions of 2,4-D were responsible. These different phenomena indicate complex kinetic behavior which may be controlled by relative diffusion rates within the activated carbon particles as well as interactions with a surface containing a small percentage of unoccupied, possibly polar, sites. A kinetic study could help to clarify these phenomena, and could be based on a model system using substrates with controllable/quantifiable surface chemistry.

The adsorption of zinc and copper as opposed to other divalent ions that were present at higher relative concentrations may have been related to the oxygen functionality present on the surface of the carbon. Mossbauer spectroscopy may be a worthwhile technique for investigating the adsorbed state of these elements. Modifying the carbon using heavy isotopes of oxygen could enable the use of Nmr techniques to determine the nature of the oxygen groups involved. O^{17}-labelled activated carbon could also be used in pH studies to determine what role they might play in the repulsion of dissociated 2,4-D. The difficulty with O^{17} solid-state Nmr is in the interpretation of the resulting spectra. Model substrates would have to be examined as part of the study.

XII. ACKNOWLEDGEMENTS

This work would not have been possible without the generous support of IPST and its member companies. Special thanks are directed to Dr. Fred Baker for his support and Westvaco Corporation for their generosity in characterizing the activated carbons used in this study.

Committee members, Dr. Jeffrey Dean and Dr.Peter Pfromm, were instrumental in challenging me to improve this study at each opportunity. A very special word of thanks is in order for Dr.Pullman, who not only guided the research but also provided much needed encouragement and “moral” support.

Warm thanks go to Tabassum Shaw, Kathleen Poll, Mike Buchannon, Dave Roth, and Dr. David Rothbard of IPST’s Analytical and Microscopy services. Cathy Welder, a post-doc in IPST’s Wood Chemistry group, was also quite helpful with HPLC.

A word of thanks to all those students (Vincent Ciavatta, Andy Toering, Jim Seely, Troy Runge, Fadi Chakar, Brian Boyer, Dave Loebker, Eric Watkins, Joel Panek, Doug Eames, and Patricia Wild immediately come to mind) and staff (including but not limited to Teresa Vales, Cindy Bowden, Dani Denton, Lavon Harper, Marcos Abazeri, Bob Davies and Barry Crouse) who tolerated, even encouraged the miscellaneous ramblings of a mad man. Much needed inspiration came from various personalities including Helga, KSW, Nell, Hendrikje, PW, and the Empress.

Special thanks also to Shirley Whitfield who started every morning with a joyous greeting and promised me a job. And delivered. And a beer is in order for Major White.

I dedicate this work to my long-suffering spouse, Na.

XIII. REFERENCES

Adams M.D. (1991) The mechanisms of adsorption of $Hg(CN)_2$ and $HgCl_2$ onto activated carbon. *Hydrometallurgy* 26(1991) 201-210.

Adamson, A.W. (1967) *Physical Chemistry of Surfaces*. New York, Interscience.

Amerson HV et al. (1985) Loblolly pine tissue culture. In: *Tissue Culture in Forestry and Agriculture*. Basic Series 32(19) pp.271-287. Plenum press, New York.

Antipova, A.S.; Semenova, M.G. (1995) Effect of sucrose on the thermodynamic incompatibility of different biopolymers. *Carbohydrate Polymers* 28 359-365

Baker, F.S.; Miller, C.E.; Tolles, D.E. (1992) Activated carbon. *Kirk-Othmer Encyclopedia of Chemical Technology, 4th Edition, Volume No. 4* p. 1015. New York Wiley & Sons.

Baker, F.S. (1999) personal communication Westvaco research.

Barrett, E.P.; Joyner, L.G.; Halenda, P.H. (1951) J. Am. Chem. Soc. (73) 373.

Bautista-Toledo, I.; Rivera-Utrilla, J.; Ferro-Garcia, A.; Moreno-Castilla, C. (1994) Influence of the oxygen surface complexes of activated carbons on the adsorption of chromium ions from aqueous solutions: effect of sodium chloride and humic acid. *Carbon* 32(1) 93-100.

Becwar, M.R., Noland, T.L., Wann, S.R. (1987) A method for quantification of the level of somatic embryogenesis among Norway spruce callus lines. *Plant Cell Reports* No. 6 pp.35-38.

Becwar, M.R.; Pullman, G.S. (1994) Somatic embryogenesis in loblolly pine (*Pinus teada*). In: *Somatic Embryogenesis in Woody Plants, Vol. 3- Gymnosperms*. Eds. S. Mohan Jain, P.K. Gupta, and R.J. Newton. The Netherlands, Kluwer. pp. 287-301.

Biniak, S.; Kazmierczak, J.; Swiatkowski, A. (1990) Adsorption of phenol from aqueous solutions on activated carbons with different oxygen contents. *Polish J. Chem.* (64) 182-191.

Bokros, J. (1969) Deposition, structure and properties of pyrolytic carbon. In: *Chemistry and Physics of Carbon, vol. 5*. Ed. P.C. Walker. New York, Marcel Dekker pp.1-118.

Boehm, H.P. (1994) Some aspects of the surface chemistry of carbon blacks and other carbons. *Carbon* 32(5): 759-769.

Bonga,J.M. (1982) Tissue culture techniques. In: *Tissue Culture and Forestry*. Boston, Nijhoff & Junk.: 4-35.

Brunauer, S. (1945) *The Adsorption of Gases and Vapors, Vol.1: Physical Adsorption*. Princeton. Princeton University Press.

Chang, C.; Ku, Y. (1994) Adsorption kinetics of cadmium chelates on activated carbon. *J. Hazardous Materials* 38(1994)439-451.

Chang, C.; Ku, Y. (1995) The adsorption and desorption characteristics of EDTA-chelated copper ion by activated carbon. *Separation Science and Technology* 30(6) 899-915.

Chang,R. *Physical Chemistry with Applications to Biological Systems*. New York, Macmillan, 1981.

Corapcioglu, M.O.; Huang, C.P. (1987) The adsorption of heavy metals onto hydrous activated carbon. *Wat. Res.* 21(9) 1031-1044.

Cotton, F.A.; Wilkinson, G. (1976) *Basic Inorganic Chemistry*. New York, Wiley.

Difco Laborotories (1953) *Difco Manual, 9th Edition*. Difco Labs, Detroit.

Dalton, C.C., Iqbal, K., Turner, D.A. (1983) Iron precipitation in Murashige and Skoog media. *Physiol. Plant*. 57: 472-476.

Druart, P.H., Wulf, O.D. (1993) Activated carbon catalyzes sucrose hydrolysis during autoclaving. *Plant Cell Tissue and Organ Culture*. Vol. 32 pp. 97-99.

Ebert, A.; Taylor, F. (1990) Assessment of the changes of 2,4-dichlorophenoxyacetic acid concentrations in plant tissue culture media in the presence of activated charcoal. *Plant Cell, Tissue and Organ Culture* 20: 165-172.

Ebert, A., Taylor, F., Blake, J. (1993) Changes of 6-benzylaminopurine and 2,4-dichlorophenoxyacetic acid concentrations in plant tissue culture media in the presence of activated charcoal. *Plant Cell, Tissue and Organ Culture* 33 157-162.

Egertsdotter, U.; Mo, L.H.; von Arnold, S. (1993) Extracellular proteins in embryogenic suspension cultures of Norway spruce (*Picea abies*). *Physio. Plant*. 88 315-321.

Elliott, J.C. (1994) *Studies in Organic Chemistry 18. Structure and Chemistry of the Apatites and other Calcium Orthophosphates*. Elesevier New York.

Engelsen, S.B.; Perez, S. (1997) Internal motions and hydration of sucrose in a distilled water solution. *J. Molecular Graphics and Modelling* 15(April) 122-131.

Ferro-Garcia, M.A.; Rivera-Utrillo, J.; Rodriguez-Gordillo, J.; Bautista-Toledo, I. (1988) Adsorption of zinc, cadmium, and copper on activated carbons obtained from agricultural by-products. *Carbon* 26(3)363-373.

Fridborg, G.; Eriksson, T. (1975) Effects of activated carbon on growth and morphogenesis in cell cultures. *Physiol. Plant.* 34 306-308

Fridborg, G.; Pederson, M.; Landstrom, L-E.; Eriksson, T. (1978) The effect of activated charcoal on tissue cultures: adsorption of metabolites inhibiting morphogenesis. *Phsiol. Plant*. 43 194-106.

Gabaldon, C., Marzal, P., Ferrer, J., Seco, A. (1996) Single and competitive adsorption of Cd and Zn onto a granular activated carbon. *Wat. Res.* vol. 30, No. 12 3050-3060.

Garrett, R.H.; Grisham, C.M. (1995) *Biochemistry*. Philadelphia. Saunders College Publishing.

Gautheret, R.J. (1983) Plant tissue culture: a history. *Bot Mag Tokyo* 96: 393-410.

George, E.F.; Puttock, D.J.M.; George, H.F. (1987) *Plant Culture Media*, Exergetics, London.

George, E.F., Sherington, P.D. (1984) *Plant Propagation by Tissue Culture*. Exergetics, Ltd. Hants, England. pp. 324, 357, 365.

Gerloch, M., Constable, E.C. (1994) *Transition Metal Chemistry: The Valence Shell in d-Block Chemistry*. VCH Publishers, New York.

Giles, C.H.; Smith, D.; Huitson, A. (1974) A general treatment and classification of the solute adsorption isotherm, I. Theoretical. *J. Colloid and Interface Sci*. 47(3) 755-765.

Gubbins, K.E. (1997) Theory and simulation of adsorption in micropores. In: *Physical Adsorption: Experiment, Theory and Applications*, ed. J.Fraissard. pp.65-103.

Gupta,P.K.; G.S.Pullman. U.S. pat. # 5,036,007. Jul. 30, 1991.

Haberle-Bors, E. (1980) Interaction of activated charcoal and iron chelates in anther cultures of Nicotiana and Atropa belladonna. *Z. Pflanzenphysiol* Vol. 99 pp.339-346.

Hansch, C.; Leo, A.; Hoekman, D. (1995) *Exploring QSAR, Hydrophobic, Electronic, and Steric Constants*. Washington, D.C. ACS.

Haugland,R.P. 1992 *Molecular Probes: Handbook of Fluorescent Probes and Research Chemicals*. Molecular Probes, Eugene, Oregon pp. 172-180.

Hingston, F.J. (1981) A review of anion adsorption. In: *Adsorption of Inorganics at Solid-Liquid Interfaces*, eds. Anderson, M.A. ; Rubin, A.J. Ann Arbor Science, Ann Arbor.

Holl, W.H.; Horst, J. (1997) Description of sorption equilibrium for ions onto activated carbon using the surface complexation theory. *Wat. Sci. Tech*. 35(7) 287-294.

Horner, M.; McComb, J.A.; McComb, A.J.; Street, H.E. (1977) Ethylene production and plantlet formation by *Nicotiana* anthers cultured in the presence and absence of activated charcoal. *J. Exp. Bot*. 28 (107) 1365-1372.

Houghton,F.R.; J.Wildman. (1971) Manufacture and uses of active carbon. *Chem. Proc. Eng*. May:61-64, 1971.

Howard, D.G. (1988) Mossbauer study of cobalt ions adsorbed from solution onto activated carbon. *Carbon* Vol. 26, No. 4, pp. 559-563.

Immal, S.; Lichtenthaler, F.W. (1995) Molecular modeling of saccharides. 7. The conformation of sucrose in water – a molecular-dynamics approach. *Liebigs Annalen* (11) 1925-1937.

Jagiello, J. (1994) Stable numerical solution of the adsorption integral equation using splines. *Langmuir* 10(8)2778-2785.

Jagiello, J.; Bandosz, T.J.; Putyra, K.; Schwarz, J.A. (1995) Determination of proton affinity distributions for chemical systems in aqueous environments using a stable numerical solution of the adsorption integral equation. *J. Colloid and Interface Science* (172) 341-346.

Jagiello, J.; Tolles, D (1998) Calculation of pore size distribution of activated carbons based on densiy functional theory (DFT) data. *6th Internationl Conference on the Fundamentals of Adsorption*, Presqu'ile de Giens, France, May 24-28, 1998.

Jaycock, M.J.; Parfitt, G.D. (1986) *Chemistry of Interfaces*. New York. John Wiley and Sons.

Johansson, L.; Andersson, B.; Eriksson, T. (1982) Improvement of anther culture technique: AC bound in agar medium in combo w/liquid medium and elevated CO_2 conc. *Physiol.Plant*. 54:24-30.

Johannson, L. (1983) Effects of activated carbon in anther cultures. *Physiol. Plant*., Vol. 59: 397-403.

Johannson, L.; Calleberg, E.; Gedin, A. (1990) Correlations between activated carbon, Fe-EDTA and other organic media ingredients in cultured anthers of *Anemone canadensis*. *Physiol. Plant.* 80 243-249.

Kato-Naguchi, H. (1997) Effects of citrate on respiratory gas exchange and metabolism in carrot root tissues. *Phytochemistry* Vol. 45 no. 2 pp. 225-227

Ko,S-OH; Schlautman, M.A.; Carraway, E.R. (1998) Partitioning of hydrophobic organic compounds to sorbed surfactants. 1. Experimental studies. *Environ. Sci. Technol*. 32 2769-2775.

Kohlenbach, H.W., Wernicke, W.Z. (1978) Investigations on the inhibitory effect of agar and the function of activated carbon in anther culture. *Z. Pflanzenphysiol* Vol. 86.S: 463-472.

Kongolo, K.; Kinabo, C.; Bahr, A. (1997) Electrophoretic studies of the adsorption of gold and silver from aqueous cyanide solutions onto activated carbon. *Hydrometallurgy* 44(1997)191-200.

Ladisch, M.R. (1997) Bioseparations, in: *Encyclopedia of Separation Technology*, ed. D.M. Ruthven. John Wiley & Sons, New York.

Lastoskie, C; Gubbins, K.E.; Quirke, N. (1993) Pore size distribution analysis of microporous carbons: a density functional theory approach. *J.Phys.Chem*. 97(18) 4786-4796.

Lastoskie, C; Gubbins, K.E.; Quirke, N. (1994) Pore size distribution analysis and networking: studies of microporous sorbents. In: *Characterization of Porous Solids III*. Eds: J. Rouquerol, F.Rodriguez-Reinoso, K.S.W. Sing, K.K. Unger. Elsevier Science B.V.

Lazzeri, P.A.; D.F.Hildebrand; G.B.Collins. (1987) Soybean somatic embryogenesis: effects of nutritional, physical and chemical factors. *Plant Cell, Tissue and Organ Culture* 10: 209-220.

Leo, A., Hansch,C., Elkins, D. (1971) Partition coefficients and their uses. *Chemical Reviews*. Vol.71, No.6 pp.525-554.

Leon y Leon, C.E.; Radovic, L.R. (1994) Interfacial chemistry and electrochemistry of carbon surfaces. In: *Chemistry and Physics of Carbon, vol. 24*, ed. P.A Thrower. New York, Marcel Dekker.

Leon Y Leon, C.E., Solar, J.M., Calemma, V., Radovic, L.R. (1992) Evidence for the protonation of basal plane sites on carbon. *Carbon* Vol. 30, No.5, pp. 797-811.

Lesham, Y. (1973) *The Molecular and Hormonal Basis of Plant Growth Regulation*. New York, Pergamon Press.

Lowell, S.; Shields, J.E. (1991) *Powder Surface Area and Porosity, 3rd ed*. Chapman and Hall, New York. p. 41.

Maltseva, O.; McGowan, C.; Fulthorpe, R.; Oriel, P. (1996) Degradation of 2,4-dichlorophenoxyacetic acid by haloalkaliphilic bacteria. *Microbiology* 142(5) 1115-1122.

Manes, M.; Hofer, L. (1969) Application of the Polanyi adsorption potential theory to adsorption from solution on activated carbon. *J.Phys Chem* 73(3) 584-590.

Mattson, J.S.; Mark, H.B. (1971) *Activated carbon, surface chemistry and adsorption from solution*. New York. Marcel Dekker, Inc.

Menzuali-Sodi,A.; M. Panizza; G. Serra; F. Tognoni. Involvement of AC in the modulation of abiotic and biotic ethylene levels in tissue culture. *Sci. Hort.* (AMST) 54(1):49-57, 1993.

Merck Index (1989). Ed. Susan Budavari. Merck & Co. Rhaway, New Jersey.

Minocha, S.C. (1987) pH of the medium and the growth and metabolism of cells in culture. In: *Cell and Tissue Culture in Forestry, Vol.1*, eds. Bonga, J.M., Durzan, D.J. Martinus Nifhoff Publishers, Boston.

Montgomery, J.M. (1985) *Water Treatment and Design*. John Wiley & Sons, New York.

Morel, F.M.M., Hering, J.G. (1993) *Principles and Applications of Aquatic Chemistry*. John Wiley and Sons, Inc. New York.

Muller, G.; Radke, C.J.; Prausnitz, J.M. (1985) Adsorption of weak organic electrolytes from dilute aqueous solution onto activated carbon. *J.Colloid and Interface Science* 103(2) 466-483.

Murashige, T.; Skoog, F. (1962) A revised medium for rapid growth and bioassays with tobacco tissue cultures. *Physiol. Plantarum* 15: 473-497.

Nissen, S.J.; Sutter, E.G. (1990) Stability of IAA and IBA in nutrient medium to several tissue culture procedures. *HortScience* 25(7):800-802.

Noh, J.S., Schwarz, J.A. (1990) Effect of HNO3 tretament on the surface acidity of activated carbons. *Carbon* Vol. 28, No.5, pp. 675-682.

Norris, R.F.; Bukovac, M.J. (1972) Effect of pH on penetration of naphthaleneacetic acid and naphthaleneacetamide through isolated pear leaf cuticle. *Plant Phsyiol*. 49: 615-618.

Ott, L. (1988) *An Introduction to Statistical Methods and Data Analysis, 3rd Edition*. PWS-Kent publishing Company, Boston.

Owen,H.R. ; D.Wengerd, A.R.Miller. (1991) Culture medium pH is influenced by basal medium, carbohydrate source, gelling agent, activated charcoal, and medium storage method. *Plant Cell Reports*, 10: 583-586.

Parfitt,G.D.; C.H.Rochester. (1983) *Adsorption from Solution at the Solid/Liquid Interface*. New York, Academic Press.

Petersen, F.W.; Van Deventer, J.S. (1997) Competitive adsorption of gold cyanide and organic compounds onto porous adsrobents. *Separation Science and Technology* 32(13)2087-2103.

Pignatello, J.J.; Baehr, K. (1994) Ferric complexes as catalysts for "Fenton" degradation of 2,4-D and metachlor in soil. *J. Environ. Qual*. 23(March-April) 365-370.

Proskauer, J., Berman, R. (1970) Agar culture medium modified to approximate soil conditions. *Nature*. Vol. 227, Sept. pp. 1161.

Pullman, G.S., Gupta, P.K. U.S. Patent #5,034,326 (July 23, 1991).

Pullman, G.S., Johnson, S., Toering, A., (1995) Activated carbon adsorbs essential micronutrients: implications for somatic embryo initiation in loblolly pine (Pinus teada) *Proceedings Conifer Biotechnology Working Group, 7th International Conference*, June 26-30, 1995, p.27.

Pullman, G.S., Webb, D.T. (1994) An embryo staging system for comparison of zygotic and somatic embryo development. *TAPPI R&D Division Biological Sciences Symposium, October 3-6, 1994*, Minneapolis. pp. 31-34.

Radke, M.R.; Prausnitz, J.M. (1972) Thermodynamics of multisolute adsorption from dilute aqueous solutions. *A.I.Ch.E. J.* 18, 761-768.

Reed, B.E.; Nonavinakere, S.K. (1992) Metal adsorption by activated carbon: effect of complexing ligands, competing adsorbates, ionic strength, and background electrolyte. *Separation Science and Technology* 27(14)1985-2000.

Reuveni, O., Lilien-Kipnis, H. (1974) *Studies of the in-vitro culture of Date palm (Phoenix dactylifera L.) tissue and organs. Pamphlet No. 145*, the Volcani Institute of Agriculture Research, Isreal.

Roberts,L.W.; P.B.Gahan; R.Aloni. *Vascular Differentiation and Plant Growth Regulators*. Springer-Verlag. New York. 1988.

Rodriguez-Reinoso, F.; Linares-Solano (1989) Microporous structure of activated carbon. In: *Chemistry and Physics of Carbon, vol. 21*, ed. P.A.Thrower. New York Marcel Dekker, 1989, pp. 1-146.

Rodriguez-Reinoso, F., Molina-Sabio, M., Munecas, M.A. (1991) Effect of microporosity and oxygen surface groups of activated carbon in the adsorption of molecules of different polarity. *J. Phys. Chem*. Vol. 96 No.6, pp.2707-2713.

Rosene, M.; Manes, M. (1976) Application of the Polanyi adsorption potential theory to adsorption from solution on activated carbon. VII.Competitive adsorption of solids from water solution. *J. Phys Chem* 80(9) 953-959.

Rosene, M.; Manes, M. (1977) Application of the Polanyi adsorption potential theory to adsorption from solution on activated carbon. 9.Competitive adsorption of ternary solid solutes from water solution. *J. Phys Chem* 81(17) 1646.

Rubery, P.H. (1980) The mechanism of transmembrane auxin transport and its relation to the chemiosmotic hypotheis of the polar transport of auxin. *Plant Growth Substances 1979: Proceedings of the 10th International Conference on Plant Growth Substances,* Madison, Wisconsin. New York. Springer-Verlag. p.50-60.

Rubin, A.J.; Mercer, D.L. (1987) Effect of complexation on the adsorption of cadmium by activated carbon. *Separation Science and Technology* 22(5) 1359-1381.

Ruthven, D.M. (1997) Fundamentals of diffusion in porous and microporous solids. In: *Physical Adsorption: Experiment, Theory and Applications*, ed. J. Fraissard. Netherlands, Kluwer Academic, pp. 241-259..

Sangster,J. *Octanol-Water Partition Coefficients: Fundamentals and Physical Chemistry*. John Wiley and Sons, Inc, New York (1997).

Schwarzenbach, R.P.; Gschwend, P.M.; Imboden, D.M. (1993) *Environmental Organic Chemistry*. New York. John Wiley and Sons.

Seeley,S.B. Natural graphite. In: *Kirk-Othmer Encyclopedia of Chemical Technology. 3rd ed*. New York, John Wiley, 1978(vol.4): 689-693.

Shafer, W.E. (1990) Sorption of cytokinin N6-benzyladenine by leaf cuticles: prediction from n-octanol:water partition coefficients. *Phys.Plant*. 78: 43-50.

Shaw, D.J. (1992) *Colloid and Surface Chemistry*. Boston. Butterworth Heinemann.

Shoh, A. (1988) *Industrial applications of ultrasound in Ultrasound, Its Chemical, Physical, and Biological Effects*, ed K.S.Suslick pp.97.

Sircar, S. (1995) Influence of adsorbent size and adsorbent heterogeneity on IAST. *AIChE J.* 41(5) 1135.

Skoog, F.; Miller, C.O. (1956) Chemical regulation of growth and organ formation in plant tissue cultures in vitro. *Symp. Soc. Exp. Biol*. 9: 118-131.

Smith, D.L.; A.D.Krikorian. (1991) Growth and maintenance of an embryogenic cell culture of daylily (hemerocallis) on hormone-free medium. *Annals of Bot*. 67: 443-449.

Smith, D.L.; A.D.Krikorian. (1992) Low external pH prevents cell elongation but not multiplication of embryogenic carrot cells. *Physiologia Plantarum* 84: 495-501.

Soffel,R.W. (1978) Activated carbon. In*: Kirk-Othmer Encyclopedia of Chemical Technology. 3rd ed*. New York, John Wiley, 1978(vol.4): 561-576.

Sorial, G.A.; Suidan, M.T.; Vidic, R.D.; Maloney, S.W. (1993) Competitive adsorption of phenols on GAC. I: Adsorption equilibrium. *J. Env. Eng*. Vol 119, No. 6, pp.1027-1043.

Stumm, W., Morgan, J.J. (1996) *Aquatic Chemistry, Chemical Equilibria and Rates in Natural Waters, 3rd ed*. John Wiley and Sons, Inc., New York.

Sutherland, J.W. (1967) The usefulness of measurements of the physical adsorption of gases in characterizing carbons. In: *Porous Carbon Solids*, ed. R.L. Bond, Academic Press, New York. pp. 1-60.

Tan, T.C., Teo, W.K. (1987) Combined effect of carbon dosage and initial adsorbate concentration on the adsorption isotherm of heavy metals on activated carbon. *Wat. Res.* vol 21., No. 10 pp. 1183-1188.

Teasdale, R.D. (1987) 3. Micronutrients. In: *Cell and Tissue Culture in Forestry, Vol 1*. eds. Bonga, J.M., Durzan, D.J. Martinus Nifhoff Publishers , Boston. Pp. 17-49.

Teasdale, R.D.; Dawson, P.A.; Woolhouse, H.W. (1986) Mineral nutrient requirements of a loblolly pine (Pinus teada) cell suspension culture. *Plant. Physiol*. 82: 942-945.

Verhagen, S.A., Wann, S.R. (1989) Norway spruce somatic embryogenesis: high-frequency initiation from light-cultured mature embryos. *Plant Cell Tissue Organ Culture* 16, pp.103-111

von Arnold, S. (1987) Improved efficiency of somatic embryogenesis in mature embryos of Pices abies (L.) Karst. *J. Plant. Physiol*. Vol. 128, 233-244.

Walpole,R.E.; Myers, R.H. (1989) *Probability and Statistics for Engineers and Scientists, 4th Edition*. Macmillan Publishing Company, New York.

Wang, P-J., Huang, L-C. (1976) Beneficial effects of activated charcoal on plant tissue and organ cultures. *In Vitro*, 12(3) 260-262.

Weatherhead, M.A., Bourdon, L. Henshaw, G.G. (1978) Some effects of activated charcoal as an additive to plant tissue culture media. *Z. Pflanzenphysiol*. Vol. 89 pp.141-147.

Weatherhead, M.A., Bourdon, L. Henshaw, G.G. (1979) Effects of activated charcoal as an additive to plant tissue culture media. Part 2. *Z.Pflanzenphysiol*. Vol. 94, pp. 399-405.

Weber, W.J.; McGinley, P.M.; Katz, L.E. (1991) Sorption phenomena in subsurface systems: concepts, models and effects on contaminant fate and transport. *Wat.Res*. 25(5)499-528.

Wilczak,A.; Keinath, T.M. (1993) Kinetics of sorption and desorption of copper (II) and lead (II) on activated carbon. *Water Environment Research* 65(3) 238-244.

Williams, R.R.; A.M.Taji; J.A.Bolton. (1985) Specificity and interaction among auxins, light, and pH in rooting of Australian woody species in vitro. *Hort Science* 20(6): 1052-1053

Wohlebar, D.; Manes, M. (1971) Application of the Polanyi adsorption potential theory to adsorption on activated carbon. III. Adsorption of miscible organic liquids from water solution. *J. Phys. Chem.* **75**(24) 3720-3723.

Xue, H.; Sigg, L.; Kari, F.G. (1995) Speciation of EDTA in natural waters: exchange kinetics of Fe-EDTA in river water. *Environ. Sci. Technol*. 29(1) 59-68.

Yonge, D.; Keinath, T.. (1986) The effects of non-ideal competition on multi-component adsorption equilibria. *J. WPCF* 59(1) 78-81.

Zaghmout, O.M.F.; Torello, W.A. (1988) Enhanced regeneration inlongterm callus cultures of red fescue by pretreatment with activated carbon. *HortScience* Vol. 23, pp. 615-616.

Zawadzki, J; (1989) Infrared spectroscopy in surface chemistry of carbons. In*: Chemistry and Physics of Carbon, vol. 21*, ed. P.A.Thrower. New York Marcel Dekker, pp. 147-380.